TRANSPORT AND FATE OF NITROGEN FROM EARTHEN MANURE STORAGE EFFLUENT SEEPAGE

A Thesis Submitted to the College of

Graduate Studies and Research

in Partial Fulfillment of the Requirements

for the Degree of Doctor of Philosophy

in the Department of Civil and Geological Engineering

University of Saskatchewan

Saskatoon, Saskatchewan

By

Terrance Alden Fonstad

August 2004

PERMISSION TO USE

In presenting this thesis in partial fulfillment of the requirements for a Postgraduate degree from the University of Saskatchewan, I agree that the Libraries of the University may make it freely available for inspection. I further agree that permission for copying this thesis in any manner, in whole or in part, for scholarly purposes may be granted by the professor or professors who supervised my thesis work or, in their absence, by the Head of the Department or the Dean of the College in which my thesis work was done. It is understood that any copying or publication or use of this thesis or parts thereof for financial gain shall not be allowed without my written permission. It is also understood that due recognition shall be given to me and the University of Saskatchewan in any scholarly use which may be made of any material in my thesis.

Requests for permission to copy or to make use of material in this thesis in whole or part should be addressed to:

Head of the Department of Civil and Geological Engineering
University of Saskatchewan
Saskatoon, Saskatchewan S7N 5A9

ABSTRACT

The primary focus of this project was determination of the potential for nitrogen transport and mobility from earthen manure storage (EMS) facilities – the key issue in regulations, guidelines, and management practices. Specific objectives, addressed through an integrated set of laboratory, column and batch test experiments and detailed field monitoring, were to:

1. Measure effluent source chemistry within EMS used in pork production operations and interpret this chemistry in light of the potential for contaminant transport and groundwater contamination;
2. Characterize geochemical conditions within an EMS effluent plume and summarize factors controlling mobility of species of concern; and
3. Develop a method of establishing nitrogen mobility based on effluent and/or soil characteristics.

EMS solutions contained, on a molar basis, 36% ammonium, 36% bicarbonate, 8% potassium, 6% chloride, 5% sodium plus sulphate, calcium, magnesium and other nutrients. Additionally, the solution contained ~6,000 and 9,000 mg/L organic and inorganic carbon, respectively, and had a near neutral pH. The high biological demand results in a solution with a low Eh causing nitrogen to remain in the ammonium form.

Conditions within the effluent plume were slightly reducing due to naturally low oxygen concentrations and the chemistry of the EMS effluent. Ammonium and potassium transport in the effluent plume was attenuated by ion exchange; the release of magnesium and calcium from the soil exchange complex produced concentrations in excess of 29 and 7 times their concentration respectively in the background groundwater. This hard water front or "hardness halo" offers a method to provide early indications of EMS plume advance. Organic carbon transport was similar to chloride (assumed to be non reactive) and further promoted reducing conditions. Nitrogen remained as ammonium with the

exception of the leading edge and upper fringe of the plume where both oxidation and reduction of nitrogen occurred depending on chemical conditions and time of year.

The variability of the retardation of cations during contaminant transport may be caused by variations in ion adsorption due to variability in their selectivity by the soil exchange complex. Preliminary modeling of EMS effluent transport using varying selectivity coefficients illustrates the potential for enhancement of current models by incorporation of subroutines to accommodate variable selectivity. Selectivity coefficients for ammonium, as referenced to sodium, varied from 0.23 to 2.2 and distribution coefficients for ammonium varied from 0.03 to 0.8L/kg. The ability of ammonium to replace ions on the exchange sites was a function of the ratio of monovalent to divalent cations in solution rather than the concentration of only the ammonium in solution. The ability of ammonium to replace ions on the exchange sites increased with an increasing ratio of monovalent to divalent cations in solution, and became significant above a ratio of 0.9. The retardation factor for ammonium was determined to be less than 3, an order of magnitude less than assumed in previous studies; nitrogen transport in EMS effluent plumes may therefore be much greater than originally assumed by some regulators, developers and engineers. Furthermore, sorbed ammonium will likely release into solution once the source is removed and natural waters begins to leach the contaminated soil.

ACKNOWLEDGEMENTS

I would first like to thank my wife and family for their support and encouragement during my graduate studies.

I would like to acknowledge the guidance and encouragement offered by the members of my advisory committee and in particular my co-supervisors Dr. S.L. Barbour and Dr. M.D. Haug of the Department of Civil and Geological Engineering. I would also like to acknowledge the encouragement and support received from the faculty and staff of the Department of Agricultural and Bioresource Engineering. In particular I would like to thank research engineers Laura Ingram and Denise Meier for their efforts during the laboratory and field portions of this project.

This thesis would not have been possible without the financial support of Sask Pork and Saskatchewan Agriculture Food and Rural Development and the in-kind contributions of test drilling, laboratory testing and technical advice of the Geotechnical Division of the Prairie Farm Rehabilitation Administration of Agriculture and Agri-Food Canada.

TABLE OF CONTENTS

PERMISSION TO USE i
ABSTRACT ii
ACKNOWLEDGEMENTS iv
TABLE OF CONTENTS v
LIST OF TABLES x
LIST OF FIGURES xii
LIST OF SYMBOLS xxiii

1 INTRODUCTION 1

2 LITERATURE REVIEW 6

2.1 Nitrogen in Groundwater 6
2.1.1 Nitrogen Sources 7
2.1.2 Fate of Ammonium 7
2.1.3 Fate of Nitrate 8
2.1.4 Denitrification 9
2.2 EMS Seepage Research 12
2.2.1 Source Chemistry 13
2.2.2 Sealing or Clogging of Soil 14
2.2.3 Characterization of EMS Effluent Plumes 15
2.2.3.1 Studies Using Soil Samples from Beneath an EMS 16
2.2.3.2 Studies Using Monitoring Wells Adjacent to EMS 22
2.2.3.3 Use of Remote Sensing to Delineate EMS Effluent Plumes 25
2.2.4 Conclusion of EMS Research to date 25
2.3 Characterization of Contaminant Plumes from other sources 27
2.3.1 Landfill Leachate 27
2.3.2 Sewage Treatment/Disposal 29
2.4 Impact of Redox Zoning and Ion Exchange on Attenuation 30
2.4.1 Oxidation-Reduction Zoning 31
2.4.1.1 Measurement of Redox Potential 31

2.4.1.2 Interpretation of Redox Measurements 34
2.4.2 Ion Exchange in Clay Minerals 36
2.4.2.1 Source of Ion Exchange in Clayey Soils 36
2.4.2.2 Cation Ion Attraction 38
2.4.2.3 Partitioning of Ions on Exchange Sites 39
2.4.2.4 Use of Exchange as a Retardation Factor in Transport 47
2.4.2.5 Use of Ion Exchange in Modeling of Transport 51
2.5 Representative Groundwater Sampling 52
3 METHODS AND MATERIALS 54
3.1 Source Chemistry 54
3.1.1 Instrument Design 54
3.1.2 Sampling Procedure 55
3.1.3 Sample Handling and Analysis 56
3.2 Column Study 56
3.2.1 Column Design 57
3.2.2 Column Setup and Commissioning 58
3.2.3 Sampling and Instrumentation Reading 58
3.2.4 Column Decommissioning and Soil Sampling 60
3.2.5 Soil Laboratory Analysis 60
3.2.6 Short Term Batch Test 60
3.3 Field Investigation 62
3.3.1 Previous Investigations at the Site 63
3.3.2 Instrumentation Design and Materials 63
3.3.2.1 Piezometers 65
3.3.2.2 Thermocouples 65
3.3.2.3 ORP Probes 66
3.3.2.4 Soil Gas Samplers 67
3.3.3 Instrumentation Installation 67
3.3.3.1 Piezometers 69
3.3.3.2 Thermocouples 71
3.3.3.3 ORP Electrodes 71

3.3.3.4 Soil Gas Samplers 72
3.3.4 Water Sampling 72
3.3.5 Instrumentation Reading 73
3.3.5.1 Piezometric Head 73
3.3.5.2 Thermocouples 74
3.3.5.3 ORP Electrodes 74
3.3.5.4 Soil Gas Samplers 74
3.3.6 Sampling and Analysis for Microbial Populations 75

4 PRESENTATION OF RESULTS 79

4.1 EMS Effluent Chemistry 79
4.1.1 Eh, EC, DO, pH, Temperature and TS Profiles 79
4.1.2 Filtered Sample Analysis 79
4.1.3 Source Chemistry Conclusions 96
4.2 Column and Batch Test Studies 96
4.2.1 Soil Characteristics 97
4.2.2 Column Study Bulk Density and Moisture Content 99
4.2.3 Column Study Specific Discharge 99
4.2.4 Column Study Oxidation- Reduction Potential (ORP) 105
4.2.5 Column Effluent Chemistry 105
4.2.6 Column Study Soil Extraction Results 111
4.2.7 Ion exchange 125
4.2.8 Batch Tests 129
4.2.9 Sorption Isotherm Analysis 136
4.2.9.1 Calcium 138
4.2.9.2 Magnesium 140
4.2.9.3 Sodium 140
4.2.9.4 Potassium 143
4.2.9.5 Ammonium 146
4.2.10 Langmuir Distribution Coefficient 150
4.2.11 Transport modeling of Column No. 1 155
4.2.12 Exchange Coefficients 158

4.2.13 Estimation of distribution coefficients from selectivity coefficients... 191
4.2.14 Laboratory study conclusions 198
4.3 Field Investigation 199
4.3.1 Site Geology and Hydrogeology 199
4.3.2 Site Layout 200
4.3.3 Soils Analysis Results 200
4.3.4 Results of N(5) and N(-3) 2MKCl Extraction from Soil Cores 200
4.3.5 Water Table, ORP, and Soil Gas Field Readings 206
4.3.6 Water Sampling Results 206
4.3.7 Microbial Sampling Results 231
4.3.8 Analysis of Field Data for ADF Research Site No 1 235
4.3.9 Summary of field findings 248
4.4 Simulation of Column No. 1 248

5 CONCLUSIONS AND IMPLICATIONS 259

5.1 Implications 261
5.2 Recommendations for further research 262

6 LIST OF REFERENCES 263

Appendices

A- Water And Soil Analysis - Operating Procedure Summary

B- Statistical significance of correlation coefficients for the column and batch tests data analysis

LIST OF TABLES **Page**

Table 2.1: Typical ranges of concentrations of various constituents in landfill leachate 28

Table 3.1: Testing methods for soil physical properties. 68

Table 4.1: Laboratory analysis results for filtered manure samples (mg/L) 82

Table 4.2: Laboratory analysis results for filtered manure samples (meq/L) 84

Table 4.3: Raw data of various EMS samples 86

Table 4.4: Concentrations of select ion species from analysis of seven manure samples. 91

Table 4.5: Concentration of the most abundant ions in EMS effluent from seven sites in Saskatchewan. Values are average percentage of the total and (standard deviation of the average) 91

Table 4.6: Soil characteristics of soils used in column study 98

Table 4.7: Column No. 1 (Clearfield Site Soils) saturated paste extraction results 116

Table 4.8: Column No. 1 extractable cations 118

Table 4.9: Column No. 2 (Site No. 1 Soils) saturated paste results 121

Table 4.10: Column No. 2 extractable cations 127

Table 4.11 - Concentration of ions in solution at the end of the batch test for the Kelvington soil. 133

Table 4.12 - Concentration of exchangeable ions at the end of the batch test for the Kelvington soil. 133

Table 4.13 - Concentration of ions in solution at the end of the batch test for the Site No. 1 soil. 134

Table 4.14 - Concentration of exchangeable ions at the end of the batch test for the Site No. 1 soil. 134

Table 4.15: Retardation factors for ammonium and potassium. 155

Table 4.16: Selectivity coefficients for $K_{Na/I}$ 162

Table 4.17: Selectivity coefficients for $K_{Ca/I}$ 162

Table 4.18: Water analysis results for piezometers located within the plume at Site No. 1- Feb. 2000 (mg/L) 218

Table 4.19: Water analysis results for piezometers located within the plume at Site No. 1- Feb. 2000 (meq/L) 219

Table 4.20 Water analysis results for piezometers located within the plume at Site No. 1- May 2004 (mg/L) 220

Table 4.21: Water analysis results for piezometers located within the plume at Site No. 1- May 2004 (meq/L) 221

Table 4.22: Results of NETPATH (Plummer et al. 1994) modeling of mixing of raw effluent and background water. 239

Table 4.23: Site No. 1 Saturation Indices 246

LIST OF FIGURES **Page**

Figure 2.1 Oxidation of organic carbon in the saturated zone with the sequence of electron acceptors and the resulting inorganic compounds. Values in ellipses are Gibbs free energy released (if < 0) or consumed (if > 0) by the electron-acceptor half reactions (Korum, 1992) 10

Figure 2.2: Concentration profiles for Site No. 1 from Miller et al. (1976). EMS was constructed in calcareous clay till and was in use for 2 years. Concentrations are from core samples. 16

Figure 2.3: Concentration profiles for Site No. 2 from Miller et al. (1976). EMS was constructed in lacustrine clay and was in use for 2 years. Concentrations are from core samples. 17

Figure 2.4: Concentration profiles for Site No. 3 from Miller et al. (1976). EMS was constructed in sandy till and was in use for 10 years. Concentrations are from core samples 17

Figure 2.5: Concentration profiles for Site No. 4 from Miller et al. (1976). EMS was constructed in layered sands, silts and clays and was in use for 8 years. Concentrations are from core samples. 18

Figure 2.6: Ion concentrations from Saturated paste extraction from cores beneath the EMS at Research Site No. 1 (Fonstad and Maule, 1996). The EMS was constructed in layered sands, silts and clays and had been in use for 10 years. 19

Figure 2.7: Ion concentrations from saturated paste extraction from cores beneath the EMS at Research Site No. 3 (Fonstad and Maule, 1996). The EMS was constructed in 9% clay content clay till and had been in use for 3 years. 20

Figure 2.8: Ion concentrations from saturated paste extraction from cores beneath the EMS at Research Site No. 7 (Fonstad and Maule, 1996). The EMS was constructed in clay till and had been in use for 10 years. 20

Figure 2.9: Ion concentrations from saturated paste extraction from cores beneath the EMS at Research Site No. 15 (Fonstad and Maule, 1996). The EMS was constructed in sandy clay till and had been in use for 7 years. 21

Figure 2.10: Concentration profiles below the EMS at Research Site No. 21 from Fonstad and Maule (1996). The EMS was constructed in layered sands, silts and clays with a 600 mm clay till liner which was allowed to freeze and was in use for 12 years. Concentrations are from saturated paste extractions of core samples. 21

Figure 2.11: Concentration profiles below the EMS at Site No. 22 from Fonstad and Maule 1996. EMS was constructed in clay till and was in intermittent use for 17 years. Concentrations are from saturated paste extractions from core samples. 22

Figure 2.12: C/Cmax for data from Ciravolo et al. 1979. TRACE EMS was report to have been constructed in sandy clay soils at a research farm and had been in use for 1.5 years at the time of final sampling. Cmax for Cl-, NH4+ and NO3- were taken as 264 mg/L, 18.8 mg/L and 30.7 mg/L respectively. 23

Figure 2.13: C/Cmax for data from Ciravolo et al. 1979. The private farm EMS is reported to have been constructed in sandy soils and had been in use for over 8 years. Cmax for Cl-, NH4+ and NO3- were taken as 256 mg/L, 63.8 mg/L and 68.1 mg/L respectively. High levels away from the EMS were attributed to EMS overflows. 24

Figure 2.14: Breakthrough curves for major ions for Soil No. 7 (Fonstad 1996; Maule and Fonstad, 2000). Soil was obtained from Research Site No. 1 during test drilling. 27

Figure 2.15: Sequence of important redox processes at pH 7 in natural waters (Stumm and Morgan, 1981). 32

Figure 2.16: The sequence of reduction processes as reflected by groundwater composition. At the right is shown classification of redox environments together with solids which are expected to form in each zone (after Appelo and Postma, 1996). 35

Figure 2.17: Schematic development of redox zones downstream of a landfill (after Appelo and Postma, 1996). 36

Figure 3.1: EMS Sampling Apparatus 55

Figure 3.2: Column set-up for large column study conducted at PAMI, Humboldt, Saskatchewan. 59

Figure 3.3: ADF Research Site No. Site Plan. 64

Figure 3.4: Piezometer installation detail. 70

Figure 3.5: Installation bundle for inaccessible monitoring locations. 71

Figure 3.6: Suction sampler apparatus. 76

Figure 4.1: Characteristics with depth for Clearfield Feeder Unit Cell No. 1. 80

Figure 4.2: Characteristics with depth for the EMS at ADF Research Site No. 1. 81

Figure 4.3: Select EMS Effluent Chemistry (mg/L) (liquid fraction only). 83

Figure 4.4: Select EMS Effluent Chemistry (moles/kg H20) (liquid fraction only). 85

Figure 4.5: EMS source chemistry results of seven samples from various sites. Raw data plotted as molality. 87

Figure 4.6: Relative concentration of species in seven EMS effluent samples. 89

Figure 4.7: Activity of the most abundant species found in seven EMS effluent samples. 90

Figure 4.8: EMS source chemistry percentage of the total molarity. Values are analytical results from filtered samples and speciation using PHREEQC. 92

Figure 4.9: EMS source chemistry percentage of the total activity. Values are analytical results from filtered samples speciated using PHREEQC. 93

Figure 410: Comparison of hog manure chemistry and several landfill leachates (mg/L). 94

Figure 4.11: Comparison of hog manure chemistry and several landfill leachates (meq/L). 95

Figure 4.12: Dry density versus moisture content data for Columns No. 1 and 2 at the start and end of column testing conducted at PAMI. 100

Figure 4.13: Specific discharge for Column No. 1 (Clearfield Feeder Unit soil) versus number of days since start of test. 101

Figure 4.14: Specific discharge for Column No. 2 (Site No. 1 soil) versus number of days since start of test. 102

Figure 4.15: Specific discharge for Column No. 1 (Clearfield Feeder Unit soil) versus pore volumes of solution passing through the column. 103

Figure 4.16: Specific discharge for Column No. 2 (Site No. 1 soil) versus pore volumes of solution passing through the column. 104

Figure 4.17: ORP readings with depth for Column No. 1 with water and after manure addition to the column. 106

Figure 4.18: ORP readings with depth for Column No. 2 with water and after manure addition to the column. 107

Figure 4.19: Effluent chemistry for chloride, ammonium and potassium for the top 75 mm of Column No. 1. 108

Figure 4.20: Effluent chemistry for chloride and select ions for the top 75 mm of Column No. 1. 109

Figure 4.21: Effluent chemistry changes for chloride and select cations for the top 228 mm of Column No. 1. 110

Figure 4.22: Effluent chemistry changes for selected ions for Column No.2. 112

Figure 4.23: Column No. 1 concentration of ions in solution with depth within the soil column. 113

Figure 4.24: Column No. 1 concentration of anions in solution with depth within the soil column. 114

Figure 4.25: Column No. 1 concentration of cations in solution with depth within the soil column. 115

Figure 4.26: Column No. 1 distribution of ions on exchange sites as a function of the depth below the surface of the soil column. 119

Figure 4.27: Column No. 1 TOC, CEC and pH vs depth within the column. 120

Figure 4.28: Column No. 2 saturated paste extractions results of ions in solution at end of column test. 122

Figure 4.29: Column No. 2 saturated paste extractions results of anions in solution at end of column test. 123

Figure 4.30: Column No. 2 saturated paste extractions results of cations in solution at end of column test. 124

Figure 4.31: Column No. 2 quantities of ions on the exchange sites as a function of depth below the soil surface. 126

Figure 4.32: Column No. 2 TOC, CEC and pH vs depth within the column 128

Figure 4.33: Column No. 1 change in equivalent fraction adsorbed as a function of depth in the column. 130

Figure 4.34: Column No. 1 cation exchange capacity increase as a function of the total organic carbon. 131

Figure 4.35: Column No. 2 change in equivalent fraction adsorbed as a function of depth in the column. 132

Figure 4.36: Quantities of ions on the exchange sites for the batch test results for the Kelvington soil. 135

Figure 4.37: Quantities of ions on the exchange sites for the batch test results for the Site No. 1 soil. 137

Figure 4.38: Langmuir isotherm plots for Calcium. 139

Figure 4.39: Langmuir isotherm plots for Magnesium. 141

Figure 4.40: Langmuir isotherm plots for Sodium. 142

Figure 4.41: Langmuir isotherm plots for Potassium. 144

Figure 4.42: Potassium sorption isotherm for Column No.1 and the Kelvington soil batch test. 145

Figure 4.43: Potassium sorption isotherm for Column No.2 and the Site No. 1 soil batch test. 147

Figure 4.44: Langmuir isotherm plots for ammonium. 148

Figure 4.45: Ammonium sorption isotherm for Column No.1 and the Kelvington soil batch test. 149

Figure 4.46: Ammonium sorption isotherm for Column No.2 and the Site No. 1 soil batch test. 151

Figure 4.47: Potassium distribution coefficients calculated from the Langmuir isotherms for the column and batch tests. 152

Figure 4.48: Ammonium distribution coefficients calculated from the Langmuir isotherms for the batch tests. 154

Figure 4.49: Column No. 1 POLLUTE model of chloride transport. 156

Figure 4.50: Column No. 1 POLLUTE model of potassium transport. 157

Figure 4.51: Column No. 1 POLLUTE model of ammonium transport. 159

Figure 4.52: Column No. 1 modeled exchange coefficients and experimental values as a function of the fraction of monovalent cations in solution. 165

Figure 4.53: Column No. 1 calculated and modeled selectivity coefficients (calcium and magnesium). 166

Figure 4.54: Column No.1 experimental and modeled selectivity coefficients for potassium and ammonium. 167

Figure 4.55: Column No. 1 comparison of experimental and calculated equivalent fractions on soil exchange sites. 169

Figure 4.56: Column No. 1 selectivity coefficients with respect to sodium as a function of the ratio of monovalent to divalent cations in solution. 170

Figure 4.57: Column No. 1 selectivity coefficients with respect to calcium as a function of the ratio of monovalent to divalent cations in solution. 171

Figure 4.58: Column No. 2 selectivity coefficients with respect to sodium as a function of calcium absorbed on exchange sites. 173

Figure 4.59: Column No. 2 proposed (modeled) exchange coefficients with respect to sodium as a function of calcium absorbed. 174

Figure 4.60: Column No. 2 experimental and estimated selectivity coefficients for calcium and magnesium. 176

Figure 4.61: Column No. 2 experimental and estimated selectivity coefficients for potassium and ammonium. 177

Figure 4.62: Column No. 2 equivalent fraction of adsorbed divalent ions; experimental versus calculated values. 178

Figure 4.63: Column No. 2 equivalent fraction of adsorbed monovalent ions; experimental versus calculated values. 179

Figure 4.64: Column No. 2 equivalent fraction of absorbed divalent ions: experimental selectivity coefficients versus default selectivity coefficients. 180

Figure 4.65: Column No. 2 equivalent fraction of absorbed monovalent ions: experimental selectivity coefficients versus default selectivity coefficients. 181

Figure 4.66: Kelvington soil batch test selectivity coefficients referenced to sodium versus the ratio of monovalent to divalent cations in solution. 182

Figure 4.67: Site No. 1 soil batch test selectivity coefficients referenced to sodium versus the ratio of monovalent to divalent cations in solution. 183

Figure 4.68: Column No. 1 quantity of ions released or adsorbed as a function of depth in the column. 185

Figure 4.69: Column No. 1 percentage change in the amount of each ion adsorbed. 186

Figure 4.70: Column No. 2 quantity of ions released or adsorbed as a function of depth in the column. 188

Figure 4.71: Column No. 2 percentage change in the amount of each ion adsorbed at various depths within the column. 189

Figure 4.72: Column No. 1 Saturation Indices as a function of depth within the column. 190

Figure 4.73: Column No. 2 Saturation Indices as a function of depth within the column. 192

Figure 4.74: Column No. 1 PHREEQC modeling results of breakthrough curves. 200 mm soil column modeled using default selectivity coefficients after Appelo and Postma (1996). 193

Figure 4.75: Distribution coefficients calculated from estimated selectivity coefficients. (K and NH4) 194

Figure 4.76: Distribution coefficients for ammonium calculated using estimated selectivity coefficients as a function of the ratio of monovalent to divalent cations in solution. 196

Figure 4.77: Distribution coefficients for potassium calculated using estimated selectivity coefficients as a function of the ratio of monovalent to divalent cations in solution. 197

Figure 4.78: Site No. 1 2MKCl extraction results for test hole C29 on north side of EMS. 201

Figure 4.79: Site No. 1 2MKCl extraction results for ammonium and nitrate for test hole C14 12 meters south of the EMS. 202

Figure 4.80: Site No. 1 2MKCl extraction results for ammonium and nitrate for test hole C17 22 meters south of the EMS. 203

Figure 4.81: Site No. 1 2MKCl extraction results for ammonium and nitrate for test hole C22 33 meters south of the EMS. 204

Figure 4.82: ADF Research Site No. 1 north-south cross section of the south side of the EMS showing test hole logs with ammonium concentrations determined from soil samples using 2MKCl extraction. 205

Figure 4.83: Site No. 1 groundwater elevations and locations of piezometer tips. 207

Figure 4.84: Water level contours at Site No. 1 October 2000 208

Figure 4.85: Water level contours at Site No. 1 May 2004 209

Figure 4.86: Site No. 1ORP (Eh) readings 12 meters south of the EMS 210

Figure 4.87: Site No. 1ORP (Eh) readings 22 meters south of the EMS 211

Figure 4.88: Site No. 1ORP (Eh) readings 33 meters south of the EMS 212

Figure 4.89: Site No. 1 Electrical conductivity of groundwater at piezometer nest 20 meters north of the EMS (C29 and C30). 213

Figure 4.90: Site No. 1 Electrical conductivity of groundwater directly below the EMS. 214

Figure 4.91: Site No. 1 Electrical conductivity of groundwater at piezometer location 12 meters south of the EMS (C14 through C16) 215

Figure 4.92: Site No. 1 Electrical conductivity of groundwater at piezometer location 23 meters south of the EMS (C17 through C19). 216

Figure 4.93: Concentrations of selected ions at various distances from the EMS through and assumed transect of the seepage plume. 223

Figure 4.94: Concentrations of selected ions at various distances from the EMS through and assumed transect of the seepage plume. 224

Figure 4.95: Site No. 1 chloride and alkalinity concentrations in the plume May 2004. 225

Figure 4.96: Site No. 1 ammonium-N and potassium concentrations in the plume May 2004. 226

Figure 4.97: Site No. 1 sodium and sulphate concentrations in the plume May 2004. 227

Figure 4.98: Site No. 1 magnesium and calcium concentrations in the plume May 2004. 228

Figure 4.99: Site No. 1 pH and nitrate concentrations in the plume May 2004. 229

Figure 4.100: Site No. 1 electrical conductivity and organic carbon concentrations in the plume May 2004. 230

Figure 4.101: Site No. 1 microbial sampling results for Spring 2001. Locations directly below the EMS. 232

Figure 4.102: Site No. 1 microbial sampling results for Spring 2001. Piezometers C13 through C16 (12 meters south of the EMS). 233

Figure 4.103: Site No. 1 microbial sampling results for Spring 2001. Piezometers C20 through C22 (33 meters south of the EMS). 234

Figure 4.104: Groundwater chemistry of a transect through the plume at Site No. 1. 236

Figure 4.105: Groundwater chemistry of a transect through the plume at Site No. 1. (without alkalinity or ammonium) 237

Figure 4.106: Relative ion concentrations as a function of distance from the EMS determined using a source concentration of 56% effluent and 44% groundwater as determined by NETPATH. 240

Figure 4.107: Relative ion concentrations as a function of distance from the EMS determined using a source concentration of 56% effluent and 44% groundwater as determined by NETPATH. (without magnesium, reduced scale) 241

Figure 4.108: Relative ion concentrations for chloride, ammonium and potassium as determined using a source concentration of 56% effluent and 44% groundwater (NETPATH results) versus the distance from the EMS. 242

Figure 4.109: Ion concentrations relative to background water concentrations versus the distance from the EMS. 244

Figure 4.110: Saturation Indices of select mineral phases as a function of distance from the EMS. 245

Figure 4.111: Column No. 1 PHREEQC model of breakthrough curves for a 200mm soil sample using selectivity coefficients determined for a ratio of monovalent to divalent cations in solution of 0.73. (near the front of the plume)(Mg, Ca, and S(-6)) 249

Figure 4.112: Column No. 1 PHREEQC model of breakthrough curves for a 200mm soil sample using selectivity coefficients determined for a ratio of monovalent to divalent cations in solution of 0.73. (near the front of the plume)(C(4), Cl, Na, K and NH4) 250

Figure 4.113: Column No. 1 PHREEQC model of breakthrough curves for a 200mm soil sample using selectivity coefficients determined for a ratio of monovalent to divalent cations in solution of 0.90. (Mg, Ca, and S(-6)) 251

Figure 4.114: Column No. 1 PHREEQC model of breakthrough curves for a 200mm soil sample using selectivity coefficients determined for a ratio of monovalent to divalent cations in solution of 0.90. (C(4), Cl, Na, K and NH4) 252

Figure 4.115: Column No. 1 PHREEQC model of breakthrough curves for a 200mm soil sample using selectivity coefficients determined for a ratio of monovalent to divalent cations in solution of 0.96. (near the back of the plume)(Mg, Ca, and S(-6)) 253

Figure 4.116: Column No. 1 PHREEQC model of breakthrough curves for a 200mm soil sample using selectivity coefficients determined for a ratio of monovalent to divalent cations in solution of 0.96. (near the back of the plume)(C(4), Cl, Na, K and NH4) 254

Figure 4.117: Column No. 1 PHREEQC simulation of breakthrough curves for a fully contaminated 200mm thick soil sample subjected to background water using selectivity coefficients determined for the back of the plume.(C(4), Cl, Na, K and NH4) 257

Figure 4.118: Column No. 1 PHREEQC simulation of breakthrough curves for a fully contaminated 200mm thick soil sample subjected to background water using selectivity coefficients determined for the back of the plume.(C(4), Cl, Na, S(-6), Ca, and Mg) 258

List of Symbols

n = the number of electrons
R = universal gas constant (0.001987 kcal/mol °F or 8.314 J/K mol)
T = absolute temperature (K)
F = Faraday's constant (23.061 kcal/volt g equivalent)
N_S = surface site density (sites/m^2)
S_A = surface area per weight of sorbent (m^2/g)
C_S = weight of sorbent in contact with a liter of solution (g/L)
N_A = Avogadro's number (6.022 x 10^{23} sites/mol of sites)
K_{eq} = equilibrium constant
K_C= distribution coefficient
n = is an exponent
$[A^+]$ = activity of ion A in solution
$[B^+]$ = activity of ion B in solution
(AX) = "activity" of ion A on the exchange sites
(BX) = "activity" of ion B on the exchange sites
λ_A= the rational activity coefficient for the solid phase
β_A = the equivalent fraction of ion A
CEC = the cation exchange of the exchanger (cmol/kg, meq/100g)
V^{α} = volume of homogeneous phase per equivalent of charge (m^3/keq)

$\bar{u}$ = the Boltzman accumulation factor
ε = dielectric constant (for water 7.08x10^{-10} F/m at 25 °C)
N_a = Avogadro's number (6x10^{23}/mol),
q_e = is the charge of the electron (1.6x10^{-19} C), and
I = ionic strength (mol/L).
S = absorbed concentration (mg/kg, meq/100g)
C = solution concentration (mg/L, meq/L)
$K_{A/B}$ = selectivity coefficient of B with respect to A
Eh = oxidation reduction potential (mV)
K_d' = distribution coefficient (L/kg).
ρ_b = bulk density (kg/m^3)
η = porosity (L/ m^3)
β = the maximum amount of solute that can be absorbed by the solid (Smax) (mg/kg)
α = an absorption constant related to the binding energy
R_L = retardation factor for the Langmuir isotherm
ρ = bulk density (kg/ m^3)
ε = porosity

1 INTRODUCTION

Rapid expansion of the intensive livestock industry in Western Canada over the past 15 years has focused public attention on the potential impact of earthen manure storages (EMS) on groundwater quality. In the early 1990's Saskatchewan Agriculture, Food and Rural Revitalization (SAFRR) issued approximately 10 to 20 permits per year for the development of intensive livestock operations. That number grew to between 80 and 90 permits per year by the late 1990's (Farrer, 1997), but has decreased somewhat in the early 2000's to approximately 40 to 60 permits per year (McKnight, 2003). Approximately 40-50% of permits issued over the past 15 years were for hog production facilities with EMS. Similar expansion occurred in Manitoba and Alberta during this same period.

Increasing size of production facilities has compounded the issue of expansion. A typical large pork production facility prior to 1990 was a 200 sow farrow to finish facility housing approximately 2,000 animals of various age and size. These facilities produce approximately 5,000 m^3 of effluent per year. Storage to accommodate 200 to 400 days of storage translates to a minimum EMS volume of 3,000-6,000 m^3 depending on management practices. Current industry trends are to construct 1,200 sow farrow to finish facilities requiring six times the effluent storage. Another common method of hog production is 5,000 sow segregated early weaning units where sows and nursery animals are housed at individual sites with three additional sites being developed as finishing facilities. The largest finishing facilities house approximately 14,400 finisher pigs and produce approximately 45,000 m^3 of effluent per year. Current permitting requires these facilities to accommodate 400 days of effluent storage, with a minimum EMS volume of 50,000 m^3.

Hog manure is essentially a dilute liquid fertilizer with a typical N-P-K-S content (% by weight) of 0.30-0.10-0.13-0.03 (Bayne 1997) as compared to a commercial liquid fertilizer with an N-P-K-S content of 20-7-7-6. In addition to the liquid fraction, there is 4 to 6% solid material made up of undigested feed and hair. Earthen manure storages are typically constructed with 3:1 to 4:1 side slopes and are 4 to 5 m in depth. The larger EMS require an area of 1 to 2 ha depending on berm widths, side slopes and topography. EMS are generally constructed using conventional earth moving equipment and in-situ soil materials. Earthen storages are cost effective relative to concrete or steel, and provide an environmentally feasible way of holding manure until field application, as long as proper design consideration is given to seepage control.

The news media has heightened public awareness of potential mismanagement of hog manure, increasing the pressure on SAFRR and other regulators in Western Canada to ensure protection of surface and groundwater when permitting intensive livestock facilities. The Saskatchewan government replaced the Pollution (By Livestock) Control Act (1985) by the Agricultural Operations Act (1995). The new act requires developers of livestock facilities to provide sufficient information ensuring they will not degrade surface or groundwater resources. Two parts are usually required: a nutrient management plan for utilization of the manure on local crop land, and submission of a detailed site investigation and EMS design drawings prepared by a professional engineer. Nutrient management plans and EMS design of smaller facilities may be completed with the assistance of SAFRR extension specialists.

The requirement for a detailed site investigation and EMS design drawings has meant considerable effort is taken to locate sites with low risk of contaminant transport. Studies from the 1970's and 1980's (Davis et al. 1973; Chang et al. 1974; Culley and Phillips 1982; Rowsell et al. 1985; Barrington et al. 1987) indicated manure particulate matter and microbial by-products clog soil pores. This clogging may inhibit effluent seepage from EMS facilities. In the early 1990's SAFRR reviewed these works to determine if soil clogging would contribute to protection of groundwater resources at EMS sites, hoping to characterize sites with natural conditions which limit contaminant

transport. In 1994 SAFRR facilitated a study by UMA Engineering Ltd. of Saskatoon, Saskatchewan to conduct a preliminary investigation of the groundwater chemistry near approximately 20 existing EMS and to conduct a laboratory study of the effect of soil clogging on the hydraulic conductivity of seven Saskatchewan soils. The clogged layer affecting the quantity of effluent passing through the soil sample was found to be approximately 5 mm thick and exhibited a hydraulic conductivity of $5x10^{-11}$ m/s (Fonstad 1996; Maule and Fonstad 2000). Soil clogging was limited to the soil surface, and no change in the hydraulic conductivity of the soil samples was evident after two years of manure ponding. Additionally, changes in temperature and even slight agitation of the manure soil interface disturbed the clogged layer sufficiently to increase the hydraulic conductivity to values equal to the soil. The study concluded the layer was too thin and unstable to be considered a design factor for EMS facilities.

In 1997, Sask Pork and the Agricultural Development Fund of SAFRR initiated a study to evaluate the long term safety of EMS in Saskatchewan. This study was led by the Department of Agricultural and Bioresource Engineering at the University of Saskatchewan with geotechnical drilling and laboratory support provided by the Geotechnical Division of the Prairie Farm Rehabilitation Administration of Agriculture and Agri-Food Canada. The study objectives were to install monitoring equipment beneath and adjacent to several new EMS to monitor for 10 to 20 years, investigate the effluent plume at two existing EMS sites near Saskatoon, and to conduct laboratory work to determine factors controlling seepage from EMS and contaminant transport within soils adjacent to EMS.

Concurrently, a 1999 study was commissioned by a tri-provincial committee addressing site characterization to develop siting guidelines for EMS facilities. This study, contracted to GEONET Consulting Ltd. of Saskatoon, Saskatchewan, consisted of two parts: a literature review and a modeling study. The literature review synthesized known case studies of solute migration from EMS or other similar facilities and contained a preliminary characterization of the chemistry of EMS effluent. The modeling study provided results of sensitivity modeling of one dimensional solute

transport through a clay aquitard, and considered transport through both fractured and non-fractured porous media under steady state seepage. Both the literature review and the sensitivity modeling indicated potential for a non-reactive species at 10% of the source concentration to transport to depths of approximately 10 m, within the lifespan of an EMS.

The 1997 Department of Agricultural and Bioresource Engineering and 1999 GEONET Consulting Ltd. studies identified several key areas requiring further study. Definition of source chemistry was required to establish concentrations of species of particular concern due to potential mobility and/or toxicity. Determination of geochemical conditions within an EMS, in the solute plume, and in uncontaminated soils adjacent to an EMS were required to assist in detailed characterization of geochemistry of solute plumes in the vicinity of EMS facilities and mobility of reactive ions. Of reactive ions, ammonium was of particular concern; although concentrations could be attenuated by both natural biodegradation and adsorption, typical values for its adsorption were required to evaluate the risk of nitrogen contamination of groundwater resources in the vicinity of EMS facilities.

The research reported in this thesis was conducted in conjunction with the 1997 study by the Department of Agricultural and Bioresource Engineering. The primary focus of is determining the potential for nitrogen transport and mobility from EMS facilities – the key issue in regulations, guidelines, and management practices. Research published to date has focused on transport of selected tracer or conservative species or on transport of total dissolved solids away from EMS. Studies have also determined viability of particulate clogging as a means of seepage reduction. Minimal research has attempted to define detailed chemistry of EMS effluent or the effluent plume. In addition, factors influencing mobility of nitrogen within the effluent plume have not been quantified. This thesis addresses these issues for EMS servicing pork production facilities in Saskatchewan, Canada.

Specific objectives of this research are to:

1. Measure effluent source chemistry within EMS used in pork production operations and interpret this chemistry in light of the potential for contaminant transport and groundwater contamination;
2. Characterize geochemical conditions within an EMS effluent plume and summarize factors controlling mobility of species of concern; and
3. Develop a method of establishing nitrogen mobility based on effluent and/or soil characteristics.

These objectives were addressed through an integrated set of laboratory column and batch test experiments and detailed field monitoring.

2 LITERATURE REVIEW

Earthen manure storages are a potential source of nitrogen contamination. Elevated levels of nitrate in groundwater are a known threat to both human and animal health, and therefore concerns regarding potential groundwater contamination as a result of seepage from EMS have been the primary motivator for monitoring.

The focus of many early investigations was simply on controlling seepage losses. Research to date has focused on quantification of seepage losses as defined by delineation of the extent of existing effluent plumes, using a variety of methods including soil cores, water sampling from shallow monitoring wells, and remote sensing. These investigations have generally focused on detecting increases in total dissolved solids (TDS) or specific tracer ions such as chloride or nitrate. Chloride and nitrate-nitrogen have been assumed to be suitable tracer ions. A further assumption has been that since both are anions, they are conservative tracers and any increase in chloride or nitrate is representative of the maximum contaminant transport distance. To date, the specific mobility of nitrogen in light of the species available for transport or any factors affecting attenuation has not been considered.

2.1 Nitrogen in Groundwater

Nitrogen found in groundwater near an EMS could result from transport from the EMS or fertilizer application, be present as a component of the parent material, or be derived from a number of other potential sources. Nitrogen is also subject to many possible transformations depending on conditions at the site, and could be absorbed onto or adsorbed into the soil matrix, oxidized or reduced, or even assimilated into the soil biomass.

Studies as early as 1945 demonstrated nitrate (NO_3^-) present in groundwater was responsible for methemoglobinemia (cyanosis or "blue baby syndrome") in infants (Korom, 1992). Methemoglobinemia is caused when nitrate is ingested and reduced to nitrite (NO_2^-); nitrite is then absorbed into the blood stream where it oxidizes oxyhemoglobin to methemoglobin, blocking oxygen transport. Nitrates can also form carcinogenic nitrosamines by reaction with other nitrogenous compounds in the body (Paul and Clark, 1996). Kreitler and Jones (1975) mention discovery of nitrate in groundwater of Runnels County, Texas following the death of several cattle from anoxia in 1968. The water ingested contained > 250 mg/L nitrate and was the result of nitrogen release from cultivated grassland. Most jurisdictions have set the safe drinking water limit for infants at 10 mg/L nitrate as nitrogen (45 mg/L as nitrate; Korom 1992). Recommendations for mature livestock are commonly < 100 mg/L as nitrate with recommendations for young animals similar to those for infants. Groundwater supplies of most concern are those in unconfined aquifers below intensive agriculture areas.

2.1.1 Nitrogen Sources

Nitrogen can occur in oxidation states from –3 (NH_3 and NH_4^+) to +5 (NO_3^-); many transformations are carried out by microorganisms at normal temperatures and pressures (Paul and Clark, 1996). For example, nitrogen is present in anaerobic waste storages, on exchange sites in the clay lattice, and in many fertilizers in the ammonia (NH_3) or ammonium (NH_4^+ or N(-3)) state while nitrate (N(5)) is present in the aerobic zone of surface soils and in some fertilizers.

2.1.2 Fate of Ammonium

The positive charge on the ammonium ion leads to ammonium adsorption to clays and organic matter. NH_4^+ is held on the exchange complex where it can be replaced by cations from the soil solution. NH_4^+ is approximately the same size as K^+ and readily enters the interlayer portion of clays. Drying then collapses the clays, fixing the N so it

cannot be removed by exchange reactions. As much as 50% of the total N in subsurface horizons is fixed within interlayer portions of clays.

NH_4^+ can be oxidized to NO_3^- by chemoautotropic bacteria if oxygen levels are sufficient. Ammonium oxidation yields low amounts of energy but will proceed spontaneously. Ammonium can also be oxidized by heterotrophs which use organic carbon as their energy source. This oxidation process is assumed most often when investigating groundwater nitrate sources; a sufficient amount of organic carbon exists in most sub-surface soils to support heterotrophic nitrification (Korom, 1992). These organisms can produce nitrate from both inorganic sources and organic sources with the following intermediates and associated oxidation states (Paul and Clark, 1996):

$$\underset{-3}{NH_4^+} \longrightarrow \underset{-1}{NH_2OH} \longrightarrow \underset{+1}{NOH} \longrightarrow \underset{+3}{NO_2^-} \longrightarrow \underset{+5}{NO_3^-} \qquad [2.1]$$

Nitrification is an aerobic process and therefore factors which limit oxygen diffusion, such as moisture conditions and soil structure, will control the rate. Because nitrification is biological, temperature also affects nitrification rates (30 to 35°C is optimum). Nitrification, although slow below 5°C, still occurs under snow cover in many soils (Paul and Clark, 1996). Hendry et al. (1984) used ion and Eh measurements to show nitrate could exist in isolated aerobic enclaves below the current water table in weathered till deposits of southern Alberta. Nitrification rates are also dependent on pH with optimum values occurring between 6.6 and 8.0; rates typically decrease below pH 6.0 and become negligible below 4.5. High pH values inhibit the transformations of nitrite to nitrate (Paul and Clark, 1996).

2.1.3 Fate of Nitrate

Nitrate present in porous media is subject to several fates including leaching, transport, and reduction by micro-organisms to gaseous forms of N and N_2 (denitrification) and loss to the atmosphere (Paul and Clark, 1996; Korum, 1992). Nitrate is a negatively charged ion and thus will not easily be adsorbed to soil organic matter or clays, tending

to travel at the center of macro pores. Excessive amounts of nitrate can be leached to lower areas or the water table. Intermediates of nitrate reduction, like nitrite, are sometimes found in groundwater in low concentrations, and are good indicators of ongoing nitrate reduction. Under natural conditions nitrite is only an intermediate state in a process (denitrification) to a final end product of nitrogen gas (N_2; Appelo and Postma 1996); denitrification and migratation of N_2 out of the water table offers the best hope for nitrate removal from groundwater Nitrate can be assimilated to biomass but the dominant product of nitrate reduction appears to be N_2 gas; N_2 is stable over a wide range of Eh values and for pH values between 6 and 9, typical of most groundwater (Appelo and Postma, 1996). The ammonium produced from dissimilatory nitrate reduction to ammonium (DNRA) can be nitrified if Eh conditions change (Korum, 1992).

2.1.4 Denitrification

Denitrification is the process whereby nitrate is reduced through several oxidation states to nitrogen gas through the following sequence:

$$\overset{(+5)}{NO_3^-} \rightarrow \overset{(+3)}{NO_2^-} \rightarrow \overset{(+2)}{NO} \rightarrow \overset{(+1)}{N_2O} \rightarrow \overset{(0)}{N_2} \qquad [2.2]$$

Denitrification results in the eventual loss of nitrogen from the system as nitrogen gas diffuses to the unsaturated zone or the atmosphere; the solubility of nitrogen gas is approximately 4 mg/L at standard temperature and pressure (STP), about half that of oxygen. Rates of denitrification in groundwater from lab and field studies was reported by Korum (1992) with a range of 0.12 to 3.1 mg-N/L per day (44 to 1132 mg-N/L/year) with an average value of 0.86 mg-N/L per day.

Denitrification can be accomplished through the oxidation of organic matter as an electron donor (heterotrophic denitrification) or through oxidation of inorganic compounds of Fe^{2+}, HS^- and Mn^{2+} which serve as electron donors (autotrophic denitrification; Stumm and Morgan, 1981; Korum, 1992; Appelo and Postma, 1996). Nitrate is a strong oxidant and is preferentially used by micro-organisms when

dissolved oxygen levels drop below 0.2 mg/L (Trudell et al., 1986). Figure 2.1 shows organic carbon oxidation in the saturated zone with the sequence of electron acceptors and the resulting inorganic compounds. The oxidation of graphite (C) and reduction to nitrate in solution yields nitrogen gas, bicarbonate and carbon dioxide and releases 458.06 kJ per mole of nitrate; oxidation of pyrite (FeS_2) and reduction of nitrate yields nitrogen gas, ferric hydroxide, sulfate and hydrogen and releases 415.84 kJ per mole of nitrate. Organic matter should be the preferred electron donor as it yields more energy (Appelo and Postma, 1996).

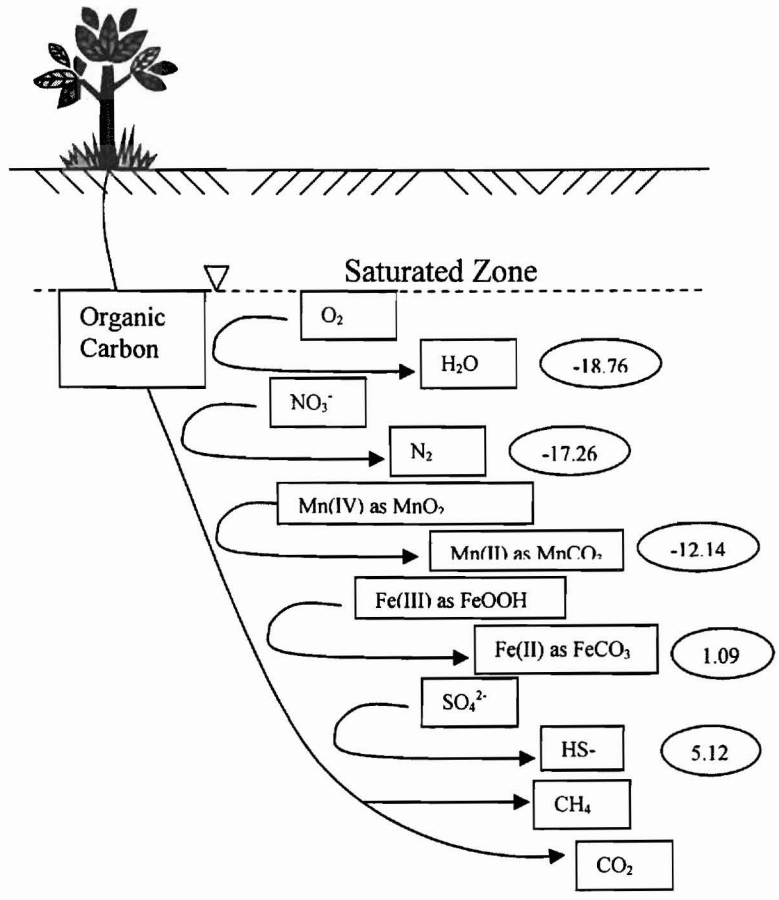

Figure 2.1: Oxidation of organic carbon in the saturated zone with the sequence of electron acceptors and the resulting inorganic compounds. Values in ellipses are Gibbs free energy released (if < 0) or consumed (if > 0) by the electron-acceptor half reactions (after Korum, 1992).

Heterotropohic denitrification, oxidizing organic carbon as an electron donor for nitrate reduction, is accomplished through:

$$5CH_2O + 4NO_3^- \rightarrow 2N_2 + 4HCO_3^- + CO_2 + 3H_2O \quad [2.3]$$

or for glucose

$$4NO_3^- + 5/6C_6H_{12}O_6 + 5CaCO_3 + 4H^+ \quad [2.4]$$
$$= 2N_2 + 10HCO_3^- + 5Ca^{2+} + 2H_2O$$

Trudell et al. (1986) used the increase in HCO_3^- to estimate the rate of denitrification in a shallow aquifer. As long as organic carbon concentrations are sufficient, denitrification should proceed; organic carbon should not be limiting in effluent plumes from sewage lagoons or animal manure storages. Inducement of heterotrophic denitrification can be accomplished by injection of sucrose and methanol into contaminated groundwater plumes (Korum, 1992).

Autotrophic denitrification can be of significant importance in the removal of nitrate from groundwater sources and is often not fully examined in many groundwater studies (Korum, 1992). An example of autotrophic denitrification is nitrate reduction by pyrite oxidation is described by:

$$5FeS_2 + 14NO_3^- + 4H^+ \rightarrow 7N_2 + 5Fe^{2+} + 10SO_4^{2-} + 2H_2O \quad [2.5]$$

and

$$10Fe^{2+} + 2NO_3^- + 14H_2O \rightarrow 10FeOOH + N_2 + 18H^+ \quad [2.6]$$

The energy yield from sulfide oxidation is larger than from Fe (II) oxidation, so incomplete pyrite oxidation yields Fe^{2+} rich environments (Appelo and Postma, 1996). Other interesting oxidation reactions involve elemental sulfur and partially reduced sulfur compounds (Paul and Clark, 1996):

$$5S + 6KNO_3 + 2H_20 = 3N_2 + K_2SO_4 + 4KHSO_4 \quad [2.7]$$

$$5K_2S_2O_3 + 8\ KNO_3 + H_20 = 4\ N_2 + 9\ K_2SO_4 + H_2SO_4 \quad [2.8]$$

Denitrification can occur without microbial conversion but is exceedingly slow. Most denitrifying bacteria grow best at pH 6 to 8; denitrification becomes slow below pH 5

although can still be significant. Temperature affects denitrification exponentially above 15 to 20°C and linearly below these values (Paul and Clark, 1996).

2.2 EMS Seepage Research

Seepage losses from EMS have been a concern in North America since at least the early 1960's. Initial studies focused on quantifying seepage losses so appropriate regulations could be developed for new EMS (Hart and Turner, 1965; Davis et al. 1973; Chang et al. 1974; Lo, 1977; DeTar, 1977). During these investigations clogging of soil pores by particulate matter was found to significantly reduce the quantity of effluent leaving an EMS by seepage. Studies into the mechanisms of soil clogging and the ability to rely on soil clogging to permanently reduce seepage losses continued until the late 1990's (Fonstad, 1996; Maule and Fonstad, 2000). Other research has focused on delineating leachate plumes at livestock production sites. Soil coring, monitor well installations and remote sensing have all been utilized to attempt to determine the extent of plumes.

A critical component missing from EMS research is the source chemistry for evaluating the potential for contaminant transport, determined by the chemistry (beyond tracer elements) of the pore fluid at the soil-manure interface. Studies of EMS effluent have to date focused on determination of the spatial differences in nutrient and solids concentration within the vertical profile of an EMS. Chemistry of manure effluent from livestock operations (primarily swine) is typically conducted after chemical digestion of the samples; data reported are either as excreted or as totals within a non-filtered sample. This methodology results from a prevailing interest in the nutrient content or "fertilizer" value of the manure, which can vary significantly with solids content. For investigations of seepage and transport of effluent from an EMS, the complete chemistry of the mobile portion (i.e., a filtered sample) is required. No reference was found to provide complete EMS effluent chemistry from filtered samples analyzed using the same methods which would be conducted for a ground water sample. This "source" chemistry is critical to our understanding of the transport mechanisms involved in EMS seepage.

2.2.1 Source Chemistry

SAFRR (1997), MidWest Plan Service (MWPS, 2000) and other organizations give values for major nutrient concentrations of manure. Their average values are useful as general guidelines since nutrient values may vary widely, depending on factors such as animal age, animal diet, type of storage, and manure handling system (Reick-Hinz et al., 1996; Bayne 1997; Campbell et. al., 1997). The literature contains information regarding concentrations of macronutrients (N, P, K, and S) and micronutrients (Cu, Mn, and Z); values cited are generally for the total effluent mix of solids and liquids or as mass excreted per kilogram of animal weight.

Studies attempting to characterize hog manure storages have reported significant differences in dry matter, as well as nutrient content with depth and among storages. A recent study conducted by Campbell et al. (1997) in Prince Edward Island involved determination of the variation of solids content and chemistry with depth. The results may not reflect true solids content as the sampler used was fitted with a 7 mm screen. Concentrations of various ions were comparable to earlier studies in Canada, the United States and Europe; no carbonate chemistry was reported and only the liquid fraction was analyzed for ammonium. Iowa State University conducted a study of 183 swine manure pits that entailed retrieving samples using a 12 ft long plastic tube or as grab samples during agitation while emptying the storage (Lorimor et al., 1997). Dry matter contents ranged substantially within and across the two studies, from 1.8-5.4% (Campbell et al. 1997) to 1.2-18.1% (Lorimor et al. 1997). Campbell et al. (1997) reported ammonium and potassium concentrations in ranges from 1450-5670 mg/L and 690-2970 mg/L respectively; corresponding values from Lorimor et al. (1997) were 2300-16,000 mg/L and 370-3100 mg/L respectively. The large variation in ammonium may result from variations in solids content or animal diet. American hog producers market hogs at a higher finished weight. Older animals also tend be less efficient at feed conversion which is reflected in higher nutrient levels in the manure. No studies

reported filtering of samples prior to the analysis and/or analysis of both major cations and anions.

The literature highlights the difficulty of obtaining a representative sample from an EMS pond. In order to obtain accurate field information regarding the characteristics of the manure and how they change with depth, a sampler should be able to retrieve distinct samples at any depth. Samplers used by researchers for this purpose vary widely in configuration and operation. Lorimor et al. (1997) used a PVC tube with a manually operated ball valve on the bottom. Booram et al. (1975) used a Plexiglass tube pushed through to the bottom of the lagoon. These samplers collect an integrated sample of the vertical profile. Campbell et al. (1997) used a peristaltic pump attached to a sampling line which contained a 175 mm long strainer with 7 mm inlets. This sampler would not retrieve representative samples in dense manure with high solids content, and difficulty was reported in obtaining a representative sample at various depths in the storage. The Kroes-Barth-Dodd sampler (Kroes et al., 1987) takes distinct samples at any lagoon depth and worked well at solids concentrations of up to 21% (Barth et al., 1985).

2.2.2 Sealing or Clogging of Soil

Studies of sealing or clogging of soils were prevalent in the late 1940's and early 1950s when groundwater recharge by surface infiltration ponds was used to rejuvenate depleted surficial aquifers. Researchers speculated earthen manure storages may be good candidates for infiltration rate reduction due to soil clogging. Field and laboratory research on clogging by manure has been conducted by numerous researchers under differing environmental conditions (Hart and Turner, 1965; Davis et al. 1973; Chang et al. 1974; Lo, 1977; DeTar, 1977; Culley and Phillips, 1982; Rowsell et al. 1985; Barrington et al. 1987; Barrington and Madramootoo, 1989; Gangbazo et al. 1989, Fonstad, 1996). All agree initial clogging occurred at the soil manure interface and clogging was on total solids content of the manure (Davis et al. 1973). Although clogging occurred in all tested soils resulting in similar long-term infiltration rates, the

time required to achieve this lower steady infiltration was dependent on soil texture (Lo, 1977; Rowsell et al. 1985; Fonstad 1996). The clogged surface interface layer ranged in thickness from 3 to 15 mm (Laak, 1970; Rowsell et al. 1985). Maule and Fonstad (2000) reported this interface grew into the soil matrix at a rate of 0.3 mm/month and demonstrated a hydraulic conductivity of approximately $5x10^{-11}$ m/s.

Barrington and Madramootoo (1989) and Fonstad (1996) reported clogging was limited to the surface and any reduction in hydraulic conductivity with depth was inconsistent and very secondary to the surface clogging. Maule and Fonstad (2000) found no evidence of hydraulic conductivity reduction with depth when the manure and clogged layer were removed and the columns retested with water of similar ionic strength to the manure. They also reported breakthrough curves and visual inspection of the exfiltrate from their columns showed considerable concentrations of solutes passing through 200 mm depth of all soils tested within 1 yr of manure ponding. Soils tested ranged in clay content from 9-33% and contained 25-80% fines (< 0.075 mm) respectively. Soils with the highest clay contents (24 and 33%) were effective in attenuating the movement of ammonium and potassium, but the breakthrough of C/Co= 0.50 at 1 pore volume for other ions tested occurred close to the same time for all soils (6 to 12 months).

2.2.3 Characterization of EMS Effluent Plumes

Studies in the late 1960's and early 1970's indicated significant amounts of effluent could seep into groundwater from EMS constructed in granular soils. Consequently, several studies attempted to determine the potential transport distance or seepage depth, and ranged from placing soil cores in the base of an EMS (Chang et al., 1974) to placing a drilling rig on the ice during winter months and retrieving cores from below the EMS (Fonstad and Maule, 1996). Results demonstrated the development of effluent plumes and led to further studies involving coring adjacent to EMS and installation of monitoring wells to retrieve groundwater samples. Costs associated with coring or drilling testholes and laboratory analysis of soil samples prompted attempts to use remote sensing to determine extent of effluent plumes at EMS sites. The objective of

studies to date has been to determine the potential for contaminant transport from EMS by establishing the geochemical extent of EMS effluent plumes.

2.2.3.1 Studies Using Soil Samples from Beneath an EMS

Miller et al. (1976) extracted disturbed samples with a hand auger from the bottom of four hog manure storages in Ontario. No significant phosphorus or nitrate transport was detected below any of the four storages (Figures 2.2 to 2.5). Ammonium transport was limited to within 0.3 m of the storage floor below EMS constructed in calcareous clay till and lacustrine clay (Figures 2.2 and 2.3). Significant ammonium transport was reported to depths of at least 1.5 m below a storage constructed in sandy till and in use for 10 years, as well as to depths of at least 4 m below a storage constructed in layered sand, silts and clays and in use for 8 years (Figures 2.4 and 2.5).

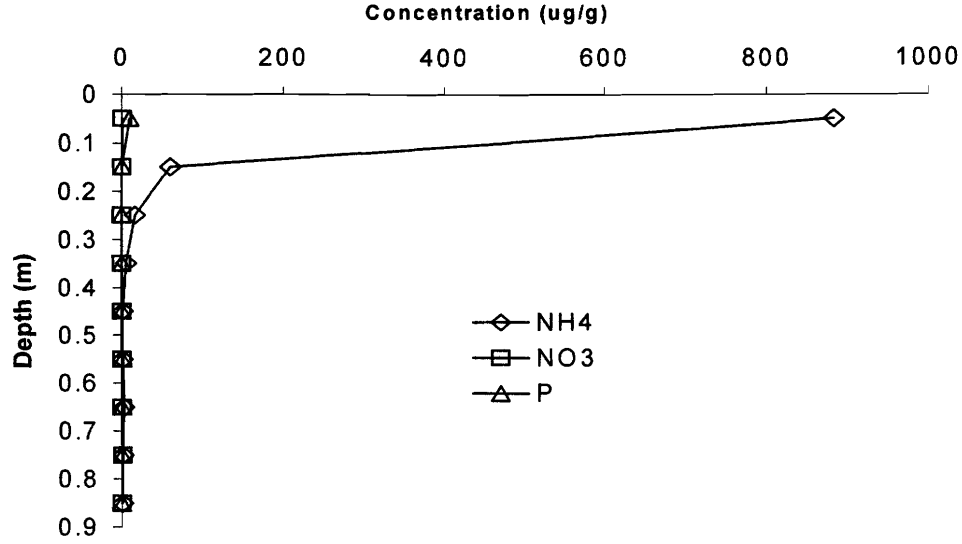

Figure 2.2: Concentration profiles for Site No. 1 from Miller et al. (1976). EMS was constructed in calcareous clay till and was in use for two years. Concentrations are from core samples.

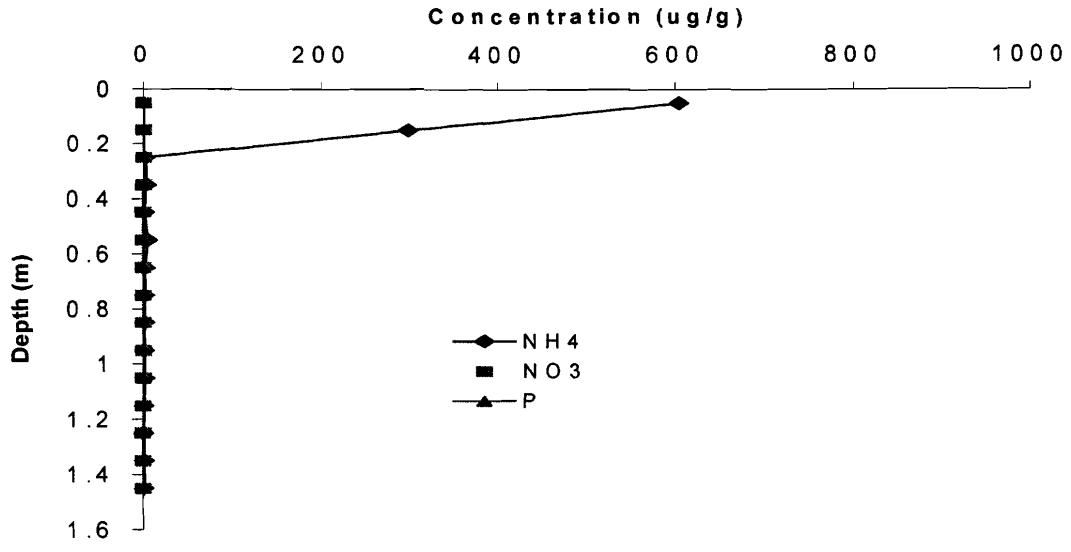

Figure 2.3: Concentration profiles for Site No. 2 from Miller et al. (1976). EMS was constructed in lacustrine clay and was in use for two years. Concentrations are from core samples.

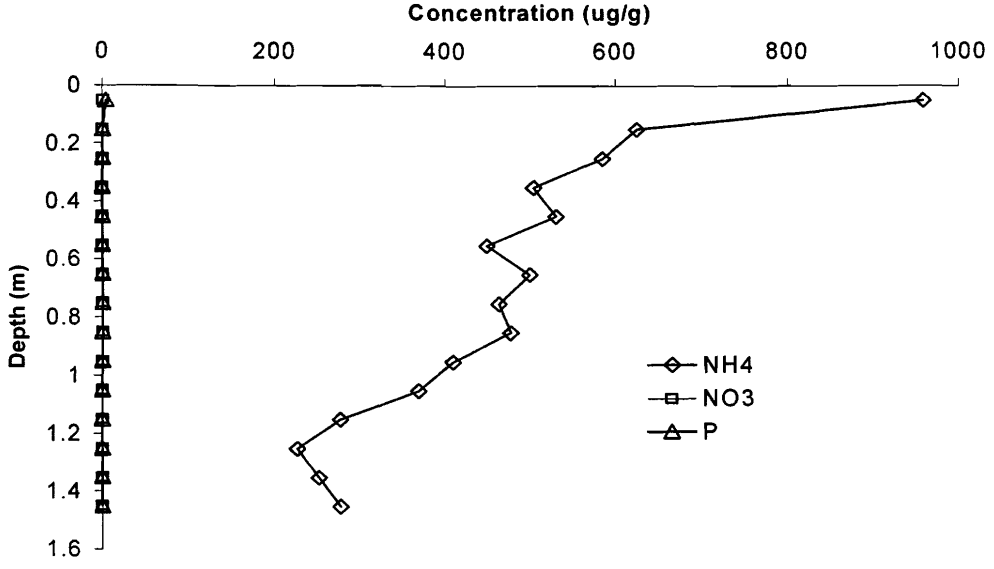

Figure 2.4: Concentration profiles for Site No. 3 from Miller et al. (1976). EMS was constructed in sandy till and was in use for ten years. Concentrations are from core samples.

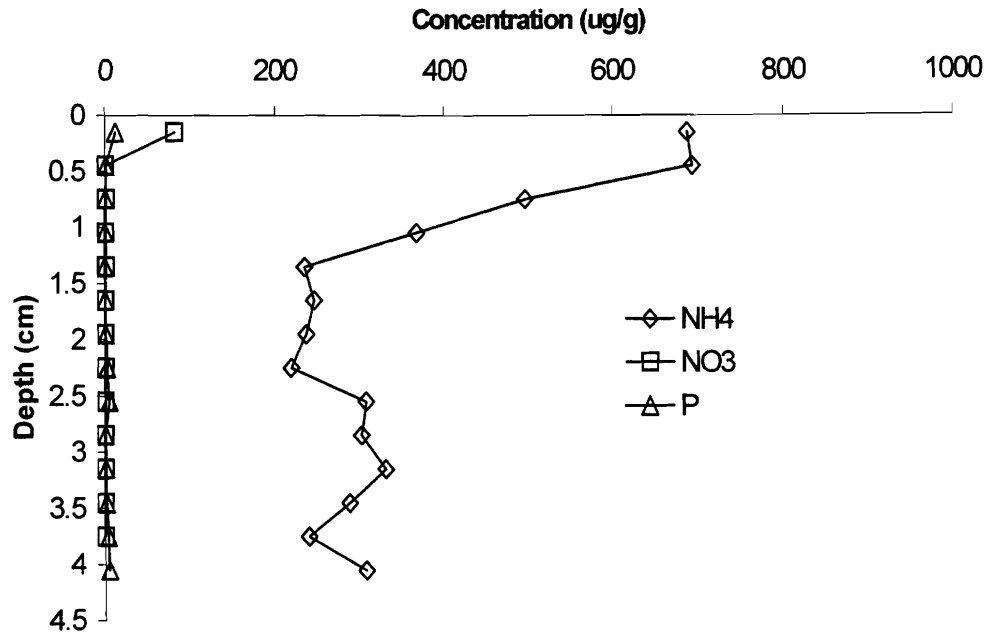

Figure 2.5: Concentration profiles for Site No. 4 from Miller et al. (1976). EMS was constructed in layered sands, silts and clays and was in use for eight years. Concentrations are from core samples.

Twenty years later, Fonstad and Maule (1996) reported similar results from below 6 hog manure storages in Saskatchewan. Samples were collected in the winter by drilling through the ice and then using split spoons and/or Shelby Tubes to collect samples at depths ranging from 1.8-10 m below the bottom of the storage. Ammonium transport was similar to Miller et al. (1976). Ammonium and potassium transport was less than 0.5 m below two storages constructed in clay till and in use for 3 and 7 years, respectively (Figures 2.7 and 2.8); storages constructed in a layered lacustrine deposit (Figures 2.6), sandy till (Figure 2.9), and layered alluvial deposit (Figure 2.10) showed elevated ammonium and potassium levels to depths of 1.4, 0.8, and 5 m, respectively. Although ammonium and potassium transport were limited at several sites, chloride transport was evident at all sites in use for more than 3 years; vertical transport depths ranged from 1.6 m (Figures 2.6, 2.8 and 2.9) to at least 8 m (Figure 2.10). Both Miller et al. (1976) and Fonstad and Maule (1996) reported low to negligible nitrate levels below all storages with the exception of Site No. 22 (Figure 2.11) which had been

empty for several years. The prevailing lack of nitrate nitrogen indicates nitrogen within the EMS is still in the ammonium state, and conditions below the storages either do not allow nitrification or the rate of nitrification and subsequent denitrification exceeds the rate of nitrogen increase as a result of groundwater transport.

Coring of soils beneath EMS has indicated some ion transport. Ten to 20 year old storages demonstrate transport of effluent to depths of at least 2 to 4 m in clayey soils and 5 to 10 m in layered or sandy soils. This indicates EMS might require sampling to depths of 10 m or more below their floor, depending on the hydrogeological setting and the nature of the subsoils.

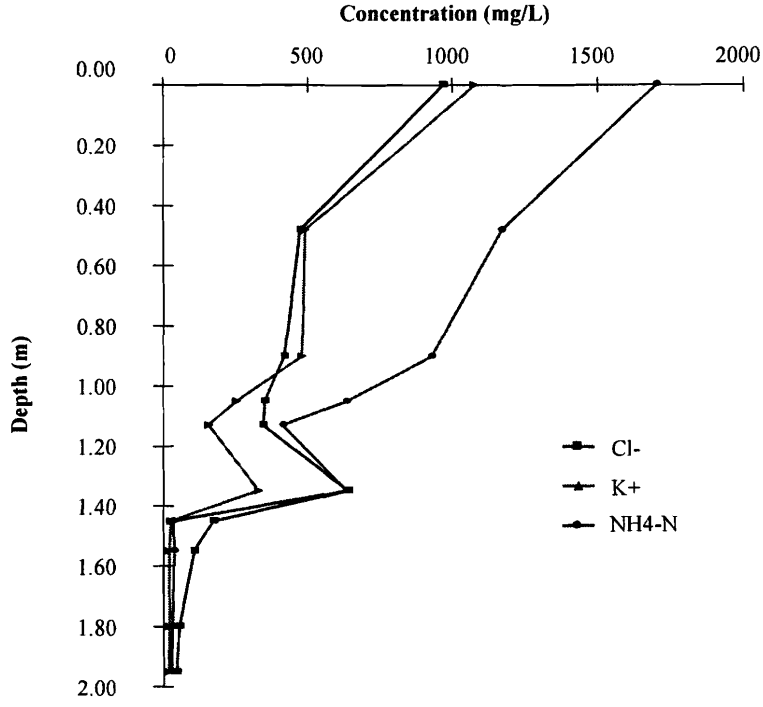

Figure 2.6: Ion concentrations from Saturated paste extraction from cores beneath the EMS at Research Site No. 1 (Fonstad and Maule, 1996). The EMS was constructed in layered lacustrine sands, silts and clays and had been in use for ten years.

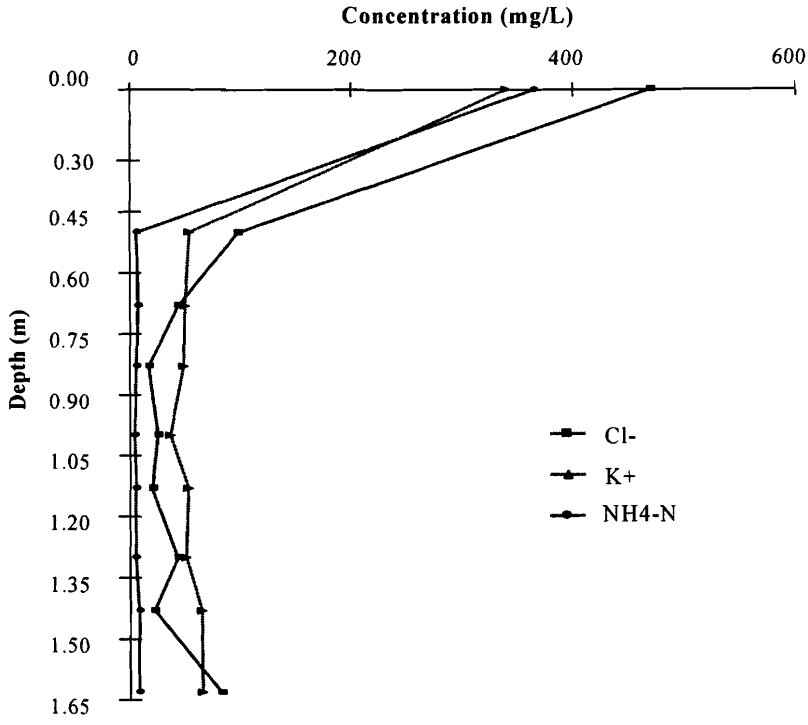

Figure 2.7: Ion concentrations from saturated paste extraction from cores beneath the EMS at Research Site No. 3 (Fonstad and Maule, 1996). The EMS was constructed in 9% clay content clay till and had been in use for three years.

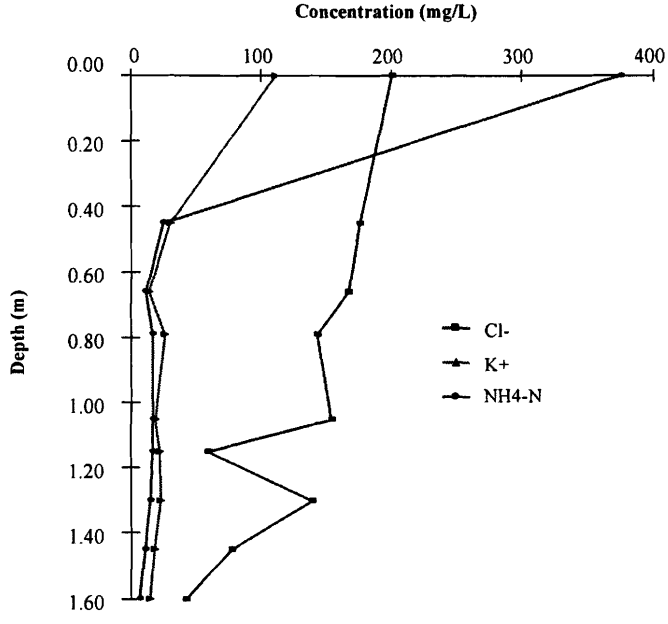

Figure 2.8: Ion concentrations from saturated paste extraction from cores beneath the EMS at Research Site No. 7 (Fonstad and Maule, 1996). The EMS was constructed in clay till and had been in use for ten years.

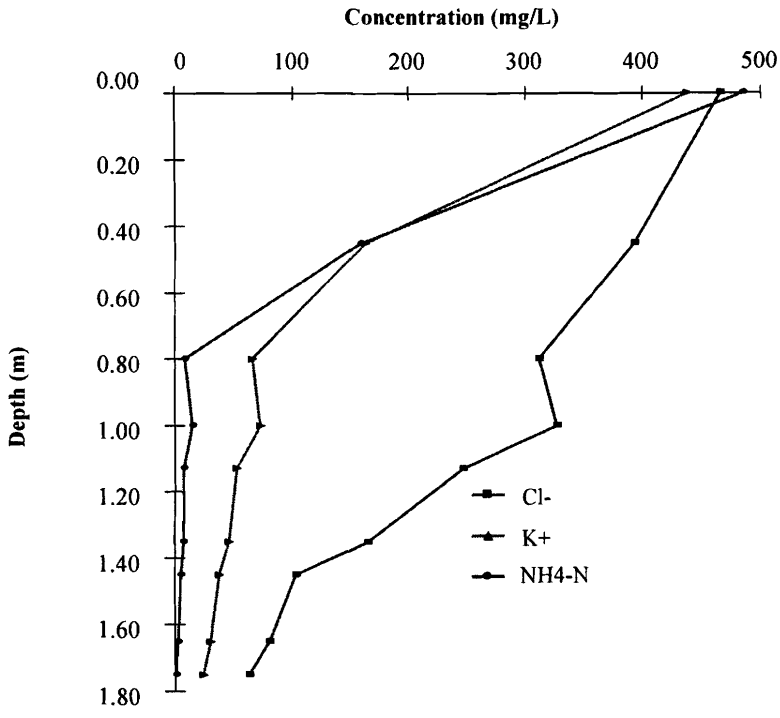

Figure 2.9: Ion concentrations from saturated paste extraction from cores beneath the EMS at Research Site No. 15 (Fonstad and Maule, 1996). The EMS was constructed in sandy clay till and had been in use for seven years.

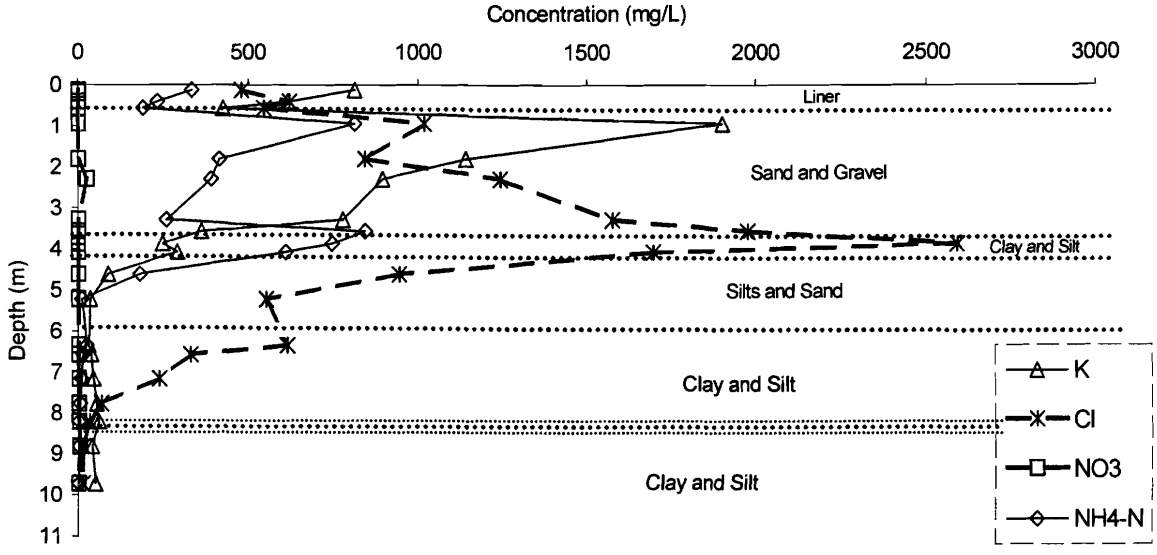

Figure 2.10: Concentration profiles below the EMS at Research Site No. 21 from Fonstad and Maule (1996). The EMS was constructed in a layered alluvial deposit with a 600 mm clay till liner which was allowed to freeze and was in use for twelve years. Concentrations are from saturated paste extractions of core samples.

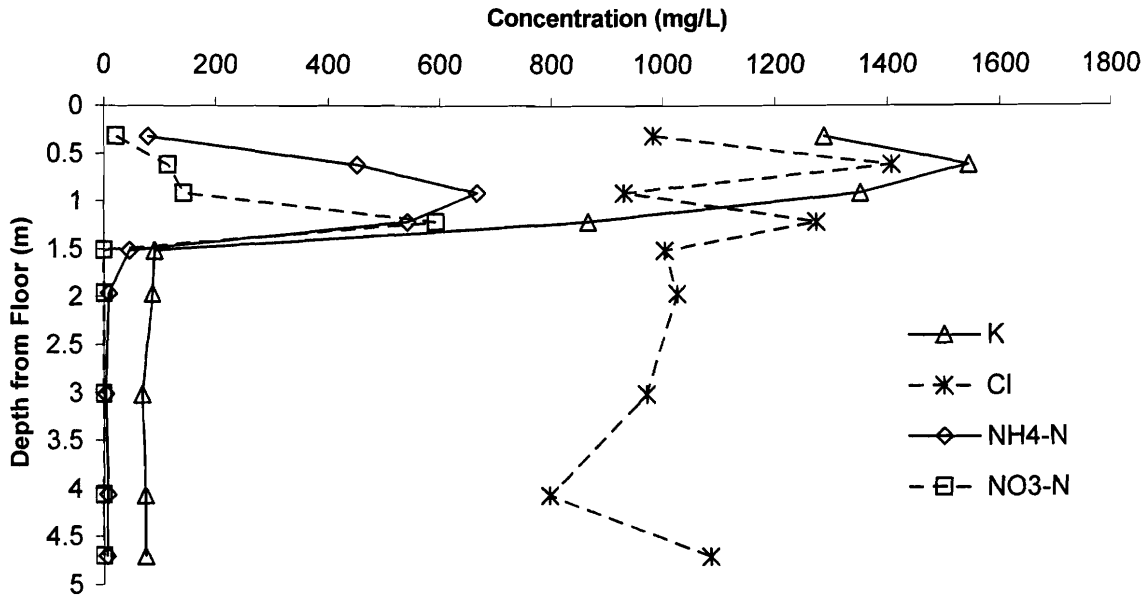

Figure 2.11: Concentration profiles below the EMS at Site No. 22 from Fonstad and Maule (1996). EMS was constructed in clay till and was in intermittent use for seventeen years. Concentrations are from saturated paste extractions from core samples.

2.2.3.2 Studies Using Monitoring Wells Adjacent to EMS

Plume definition through installation of shallow monitoring wells has been undertaken in various locations in the US and Canada. Westerman et al. (1993) reported nitrogen within the manure storage present as ammonium. Effluent samples from the plume indicated as much as 50% of the nitrogen was present as nitrate; this prevalence is expected as ground waters of the surficial sands in the North Carolina site have warm temperatures (near 20°C) and contain high levels of dissolved oxygen, both of which promote microbial conversion of ammonium to nitrate. Ciravolo et al. (1979) recorded ammonium and nitrate near the EMS and nitrification near the front of the plume at both locations they studied. These results may be due to warm temperatures and high dissolved oxygen levels in the shallow groundwaters of the Mid-Eastern United States where the study took place. Data from Ciravolo et al. (1979) are plotted in Figures 2.12 and 2.13 as C/Cmax (concentration at the well divided by the highest reported concentration within the plume) versus distance. Chloride transport distances ranged

from 1.3 times that of nitrogen at C/Cmax of 0.50 to 20 times that of nitrogen at C/Cmax of 0.10 (Figure 2.12). Figure 2.13 suggests the effluent plume may be generated as a series of solute pulses, thought to result from removal of the clogged layer during cleanout operations or soil desiccation when the storage is emptied annually or bi-annually. Ciravolo et al. (1979) suggest these pulses result from several overflow events at the site.

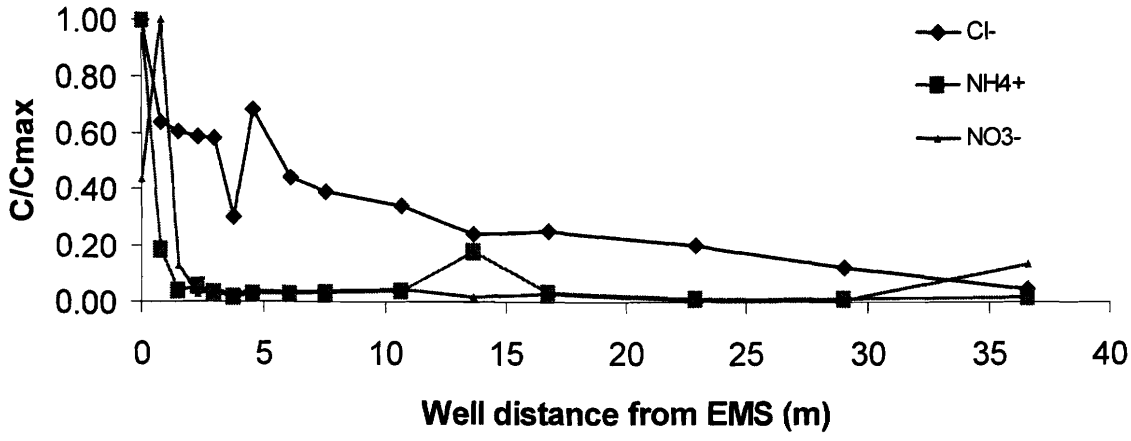

Figure 2.12: C/Cmax for data from Ciravolo et al. (1979). TRACE EMS was report to have been constructed in sandy clay soils at a research farm and had been in use for one and a half years at the time of final sampling. Cmax for Cl-, NH4+ and NO3- were taken as the highest reported values which were 264 mg/L, 18.8 mg/L and 30.7 mg/L respectively.

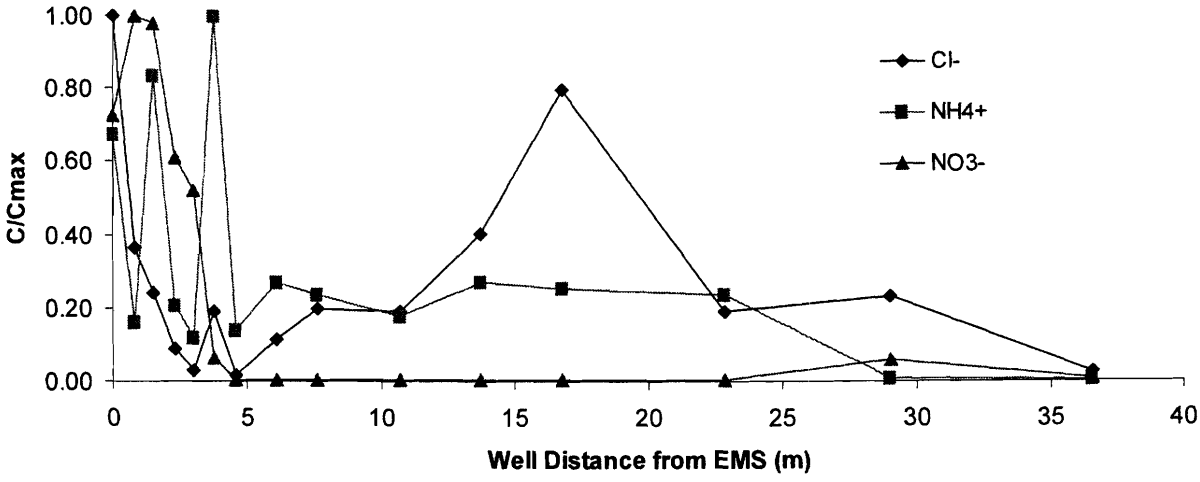

Figure 2.13: C/Cmax for data from Ciravolo et al. (1979). The private farm EMS is reported to have been constructed in sandy soils and had been in use for over eight years. Cmax for Cl-, NH4+ and NO3- were taken as the highest reported values which were 256 mg/L, 63.8 mg/L and 68.1 mg/L respectively. High reported concentrations away from the EMS were attributed to EMS overflows.

Plumes from EMS in the Canadian Prairies do not appear to have nitrogen present as nitrate, possibly due to lower groundwater temperatures (6° C) and low dissolved oxygen levels inhibiting microbial conversion. Any nitrate formed would likely be reduced to $N_2(aq)$ through oxidation-reduction with carbon or iron and manganese in the soil (Korom, 1992).

All monitoring well studies to date demonstrate ammonium is attenuated relative to a conservative species such as chloride. Ciravolo et al. (1979) and Fonstad and Maule (1996) suggest ammonium ions can be preferentially taken up on exchange sites of clays within the soil matrix. This ion exchange will then release into solution the ions originally on the exchange sites, including magnesium, calcium and sodium. This ion exchange is similar to seawater intrusion into fresh groundwater (Appelo and Postma, 1996), or the backwashing of a water softener where NH^{4+} and K^{+} are the brine stripping Na^{+}, Mg^{2+}, Ca^{2+}, and Fe^{2+} from the exchange resin (clay).

2.2.3.3 Use of Remote Sensing to Delineate EMS Effluent Plumes

Several researchers have attempted to determine the extent of solute migration from EMS through remote sensing, primarily electromagnetic (EM) surveys. Many studies started out as drilling and sampling studies that switched to or were in combination with EM surveys for plume tracing. These studies have had varying success.

An EM survey can provide insight to aid in delineation of shallow groundwater plumes. EM instruments send out an electrical signal which generates a secondary magnetic field. The amplitude of this field can then be related to the bulk electrical conductivity of the soil, which can be related to *in situ* soil conditions and used to determine contamination.

Moffitt et al. (1993) attempted to use EM surveys to determine the extent of effluent plumes at several EMS sites in Texas and North Carolina, but results were inconclusive. Huffman and Westerman (1995) estimated nitrogen export from an EMS using groundwater quality (3 to 4 wells) with plume tracing using EM surveys. The results showed promise as the survey results correlated with groundwater results. Drommerhausen et al. (1995) also found good results using EM surveys near EMS and loafing areas for dairies. EM surveys are difficult to interpret unless done in conjunction with drilling and sampling to determine site geology, stratigraphy, and background water characteristics, and can be very hard to interpret in soils with high electrical conductivity. The best results have been obtained in deep surficial sands with plumes a few hundred meters in length.

2.2.4 Conclusion of EMS Research to date

This review demonstrates the need for investigations to determine EMS effluent chemistry, transport mechanisms and plume characterization. Evidence suggests that nitrate may not be present in EMS effluent plumes, that chloride, potassium and ammonium are likely the ions of major concern, and organic carbon may move at a rate

similar to chloride. The presence of organic carbon and ammonium and the lack of nitrate suggests reducing conditions exist, at least within the plume.

The attenuation of major cations was observed in almost every study reviewed, suggesting ion exchange, precipitation or absorption is taking place. Both potassium and ammonium would be expected to exist as single charged ions at the concentrations and conditions reported. Adsorption may account for some attenuation but likely is not significant given the concentrations reported within the plume and the sandy materials investigated in several studies. These factors suggest ion exchange is the dominant mechanism responsible for the attenuation of EMS effluent.

Breakthrough curves of Fonstad (1996) and Maule and Fonstad (2000) support the hypothesis that ion exchange is a significant factor. They used laboratory columns to study the effects of manure on soil hydraulic properties and to study ion transport. Manure was ponded at a depth of 600 mm over a 200 mm thick recompacted sample of soil for a period of approximately 2 years. Exfiltrate quality was analyzed periodically during this period. Figure 2.14 shows evidence of ion exchange forcing magnesium and calcium into solution at concentrations far exceeding those present either in the source or background pore fluid. The breakthrough of total carbon (initial concentration 16,000 mg/L) was similar to chloride (Maule and Fonstad 2000).

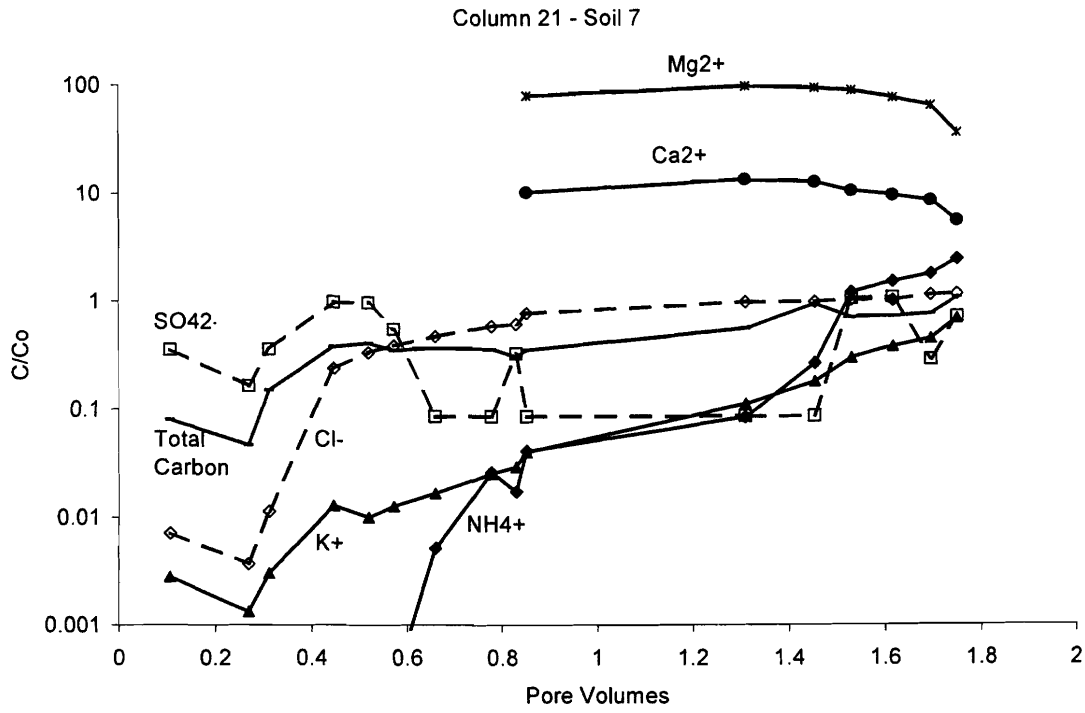

Figure 2.14: Breakthrough curves for major ions for Soil 7 (Fonstad, 1996; Maule and Fonstad, 2000). The concentration is presented as a percentage of the concentration of the species in the source effluent (C/Co).

2.3 Characterization of Contaminant Plumes from other sources

Little research has been published regarding the chemistry within EMS effluent. However, other situations exist in which comparable chemistry can occur, and any similarities with EMS may assist in interpretation of data generated during this study. Two such examples are landfill leachate which can contain relatively high quantities of inorganic ions, and municipal sewage infiltration fields which generally contain similar ions but at much lower concentrations. Both have been studied in regards to inorganic ion transport and, in particular, cation attenuation during transport.

2.3.1 Landfill Leachate

Landfill leachate tends to contain relatively high concentrations of inorganic ions as a result of anaerobic degradation of household and construction wastes (Table 2.1).

Relatively high concentrations of chloride, ammonium and potassium are similar to those reported for animal manures, suggesting similar contaminant transport concerns.

Table 2.1: Typical ranges of concentration of various constituents in landfill leachate.

Reference		Freeze and Cherry (1979)	Kjeldsen (1993)	Erskine (2000)	Thornton et al. (2001)
pH		4-8	6.7-6.9		7.2
Alkalinity	mg/L	500-10000			4600
Chloride	mg/L	300-3000	420-1200	2000	1965
Sulphate	mg/L	10-1000	<5	70	52
Calcium	mg/L	100-3000	240-330	155	125
Magnesium	mg/L	100-1500	50-80	250	135
Sodium	mg/L	200-1200	380-680	700	1340
Potassium	mg/L	200-1000	70-360	780	490
Ammonium	mg/L	10-1000	140-450	800	1029
Nitrate	mg/L	0.1-10		3	
Iron	mg/L	1-1000	0.5-86	540	13.9

Goodall and Quigley (1977) reported results of ions extracted from core samples taken below two sanitary landfill sites near Sarnia, Ontario. Both sites exhibited high concentrations of calcium and magnesium, released from *in situ* soils due to ion exchange with the landfill leachate.

In 1983, the Journal of Hydrology published Volume 63 as a special edition dedicated to results of a study of a plume of contamination in a sandy aquifer near the abandoned landfill at the Canadian Forces Base, Borden, Ontario. These research studies were headed by the Department of Earth Sciences, University of Waterloo, Waterloo, Ontario. An injection experiment into the aquifer at the site identified retardation factors for potassium of approximately 2 and coefficients relating to the relative replacability of one ion for another (selectivity coefficients) for Ca↔Mg ($K_{Ca/Mg}$), Ca↔Na ($K_{Ca/Na}$) and Ca↔K ($K_{Ca/K}$) exchange of 1.27, 2.6 and 0.0014 respectively, which agreed with previous laboratory work reported by Reardon et al. (1983). Results of this study were used to develop mixing cell models to simulate results from an injection well experiment.

Similar investigations of landfill leachate transport and large scale field experiments were reported by a group from the Technical University of Denmark (Bjerg and Christensen 1993, Kjeldsen 1993, Bjerg et al. 1993, and Bjerg et al. 1995) concerning studies of a contaminated aquifer at a landfill site near Vejen, Denmark and a leachate plume extending 300 m down gradient from the Grinstead Landfill (Denmark). These studies identified a retardation factor for potassium of approximately 10 and selectivity coefficients for Ca↔Mg ($K_{Ca/Mg}$), Ca↔Na ($K_{Ca/Na}$) and Ca↔K ($K_{Ca/K}$) exchange of 0.5-1, 26 and 0.009; these correspond with those determined at the Borden site with the exception of Ca↔Na selectivity coefficient which was an order of magnitude higher.

Recent investigations from the United Kingdom have determined attenuation of cations in landfill leachate. Erskine (2000) was concerned the use of large distribution coefficients for ammonium (25 L/kg) by regulatory agencies conflicted with values of 0.08 to 0.4 L/kg reported by Thornton et al. (2000). Thornton et al. (2001) reported results of 14 batch tests, conducted on 100% quartz sand and various soil liner mixtures with as much as 15% clay content, to determine distribution coefficients for sodium, potassium and ammonium. Results indicate distribution coefficients (slope of a line relating the concentration of an ion in solution to the quantity of that ion absorbed to the solid phase) for sodium, potassium and ammonium of 0 to 0.054 L/kg, 0.014 to 0.163 L/kg, and 0.016 to 0.224 L/kg respectively. These studies suggest a distribution coefficient for ammonium of less than 0.5 L/kg.

2.3.2 Sewage Treatment/Disposal

Other studies have investigated the injection of municipal sewage into aquifer material as a means of treatment and groundwater recharge. Valocchi et al. (1981) proposed a numerical model to simulate ion exchange during advective-diffusive movement of municipal wastewater used for groundwater recharge in the Palo Alto Bay lands region of California. They based their model on the assumptions that ion activity coefficients could be ignored and selectivity coefficients were constant, conceding these assumptions were required to simplify the model. Selectivity coefficients of 3.0 meq/L

for $K_{Ca/Na}$ and 1.7 meq/L for $K_{Mg/Na}$ were determined during Valocchi's Ph.D. work (1980, Stanford University) and used in the model. Of particular interest were peaks and plateaus of calcium and magnesium in monitoring wells caused by ion exchange with the influent water. Valocchi et al. (1981) also reported selectivity coefficients: $K_{K/Na}$ of 13.0 and $K_{NH4/Na}$ of 3. Converting all selectivity coefficients to $K_{Na/I}$ and to the Gaines Thomas convention (Appelo and Postma, 1996) yields $K_{Na/NH4}$ of 0.33, $K_{Na/K}$ of 0.077, $K_{Na/Mg}$ of 0.36 and $K_{Na/Ca}$ of 0.11. Valocchi's results were later simulated using a mixing cell model by Van Omen (1985).

The U.S. Geologic Survey investigated a nitrogen-rich municipal sewage effluent plume in southwestern Cape Code, Massachusetts (Desimone et al. 1996). Retardation of ammonium and potassium at the site was reported by Ceazan et al. (1989). Distribution coefficients for ammonium ranged from 0.34 L/kg to 0.87 L/kg, similar to studies by Erskine (2000) and Thornton et al. (2000) mentioned previously.

Desimone et al. (1996) reported much higher distribution coefficients for ammonium, approximately 3-6 L/kg, when using low ionic strength solutions and concentrations of NH4-N less than 22 mg/L. These high distribution values were also mentioned by Bjerg et al. (1993) and were explained as the result of an enhanced affinity for ammonium when present in only trace concentrations.

2.4 Impact of Redox Zoning and Ion Exchange on Attenuation

The issues of concern when storing animal manure in EMS are large quantities of organic matter and relatively high concentrations of nitrogen. If we assume EMS effluent will behave similar to landfill leachate, any plume which develops will likely experience reducing conditions and ion exchange; both factors are significant in regards to the transport of nitrogen in the effluent plume. If ammonium seeps from the EMS into a reducing environment, it will tend to stay as ammonium and be subject to ion exchange. This will lead to attenuation of nitrogen in the effluent plume and may provide for some protection against nitrogen contamination of nearby aquifers. An

understanding of redox zoning and adsorption processes will aid in the interpretation of investigations of transport mechanisms of EMS effluent.

2.4.1 Oxidation-Reduction Zoning

The oxidation-reduction (redox) state of groundwater has been used as a method of determining the distribution of dissolved species such as O_2, Fe, Mn, SO_4^{2-}, H_2S, and CH_4. Eh is an indirect measure of the level and type of biological activity, which affects both organic and inorganic contaminant transport. These measurements can therefore be related to certain redox processes (Figure 2.15) and used to qualitatively monitor the geochemical conditions within a waste plume.

2.4.1.1 Measurement of Redox Potential

The potential of a solution to be either reducing or oxidizing can be expressed in three ways. Gibb's free energy, the sum of the free energies of the compounds in solution, can be determined for a solution if the ion species and concentrations of the solution are known. pE value, the negative log of the concentrations of electrons in a solution, is a theoretical value of free electrons in water and must be calculated. Eh, the energy gained in the transfer of electrons in an electrochemical cell, is a value for a given system expressed in volts. Eh can be theoretically calculated given the concentrations of the species involved, or directly measured and used to calculate the concentrations of the involved species.

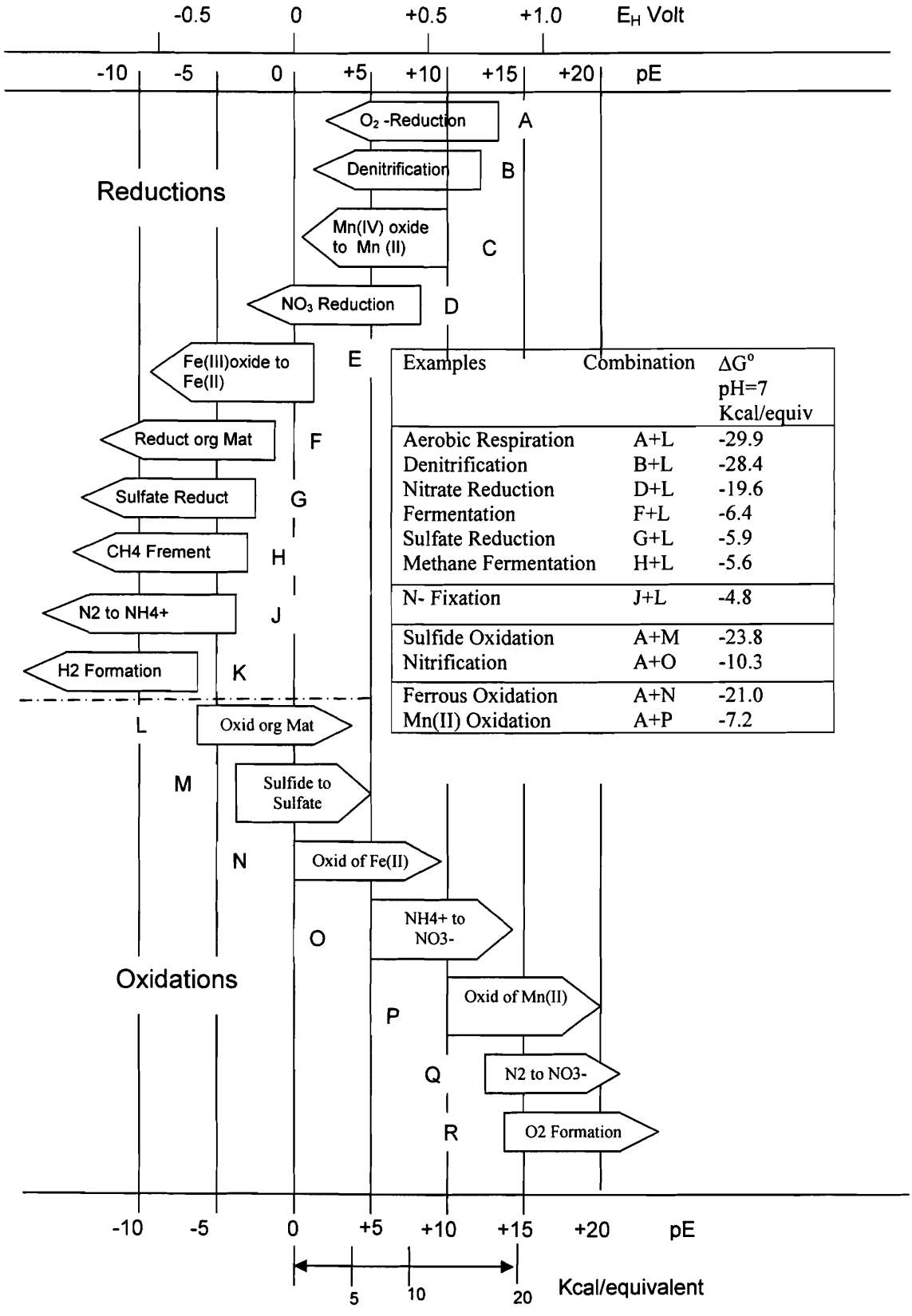

Examples	Combination	ΔG^o pH=7 Kcal/equiv
Aerobic Respiration	A+L	-29.9
Denitrification	B+L	-28.4
Nitrate Reduction	D+L	-19.6
Fermentation	F+L	-6.4
Sulfate Reduction	G+L	-5.9
Methane Fermentation	H+L	-5.6
N- Fixation	J+L	-4.8
Sulfide Oxidation	A+M	-23.8
Nitrification	A+O	-10.3
Ferrous Oxidation	A+N	-21.0
Mn(II) Oxidation	A+P	-7.2

Figure 2.15: Sequence of important redox processes at pH 7 in natural waters (after Stumm and Morgan, 1981).

The Eh of a reaction can be calculated using the Nernst equation:

$$Eh = E^0 + \frac{RT}{nF} \ln \frac{(A)^a (B)^b}{(C)^c (D)^d} \qquad [2.9]$$

where: $E^0 = \frac{-\Delta G_r^0}{nF}$ ($-\Delta G_r^0$ is the Gibb's free energy of the reaction)

the standard potential of the half reaction in volts

n = the number of electrons

R = 0.001987 kcal/mol deg

T = absolute temperature

F (Faraday's constant) = 23.061 kcal/volt g eq.

The uppercase and lowercase letters are the species involved and their stoichiometric coefficients.

For example, a redox reaction involving the reduction of nitrate can be expressed as:

$$NO_3^- + 6H^+ + 5e^- = \frac{1}{2} N_{2(aq)} + 3H_2O \qquad [2.10]$$

The equation for the Eh of this system is:

$$Eh = 0.734 + 0.118 \log \frac{[NO_3^-]}{[N_2]^{0.5}} \qquad [2.11]$$

The Eh of a solution can be determined by measuring the voltage between a platinum electrode and a reference cell. The platinum electrode and reference cell must have an electrical connection; for groundwater studies, this connection is provided by the electrical conductance of the groundwater. Using this method, redox potential can be measured *in situ*. However, practical problems may exist with the electrode and interpretation of results. Reaction with the surrounding environment or formation of a coating on the platinum electrode (e.g., adsorption of dissolved oxygen in aerobic environments) may inhibit performance over time and make measurements unreliable (Bohn, 1969; Bailey and Beauchamp, 1971, Nicholson et al., 1983, Rickman et al., 1968). Eh measurements are most reliable in anaerobic environments such as where denitrification occurs (Farrel et al., 1991).

Eh is referenced to the standard hydrogen electrode. Because hydrogen electrodes are impractical for routine measurement, another reference electrode of known potential is often used. Common reference cells are silver-silver chloride (Farrel et.al., 1991; Campbell, 1980; Blackwell, 1983; Bornstein and McGurik, 1978; Dirasian, 1968) and calomel electrodes (Grable et al., 1968; Bohn, 1969; Meek et al., 1975; Whistler et al., 1974; Farrel et al, 1991; Austin and Huddleson, 1999; Bailey and Beachamp, 1971; Faulkner et al., 1989; Patrick and Henderson, 1981; Cogger et al., 1992; Dirasian, 1968). Bockris and Oldfield (1955) use a saturated mercury chloride and Clay et al. (1990) mention copper constantin. The measurement taken with one of these electrodes is then corrected so the reading is referenced to the standard hydrogen electrode.

$$Eh = E_{measured} - E_{reference\ electrode} \qquad [2.12]$$

2.4.1.2 Interpretation of Redox Measurements

Redox potentials are typically evaluated using equilibrium thermodynamics. However, reactions occurring in natural aquatic environments are sometimes sluggish or can be essentially irreversible (i.e., the oxidation of organic matter by oxygen). Therefore in most natural environments, the measured Eh value is of a non-equilibrium system; despite this, stable values can often be measured. A constant Eh value exists when the concentration of one redox couple is much greater than any others. Thus, the measured Eh may be dominated by one couple, although mixed potentials are the rule (Stumm and Morgan, 1981). Different redox couples may dominate a natural system (Figure 2.15). In natural systems, measured values of Eh cannot be related to quantitative values of chemical species but are indicative of the relative concentration of the redox pair. "Equilibrium redox potentials of Eh of real systems should not be over interpreted and should be viewed only as providing general guidance for: 1) where any system is headed, and 2) what types of concentrations are feasible in the system." (Langmuir, 1997).

Berner (1980) defines a series of environments–oxic, post-oxic, sulfidic, and methanic–based on the presence or absence of dissolved species (see Figure 2.16). Oxic

environments contain dissolved O_2. The post-oxic classification includes waters with high concentrations of iron and manganese but no dissolved oxygen, C as CO_2, or S as SO_4^{2-}. Further classifications include "post-oxic I" and "post-oxic II" environments, based on the N species present. In post-oxic I, N is found primarily as nitrate; post-oxic II contains mainly ammonia. Sulphidic environments contain sulphides, C as CO_2, and low Fe and Mn concentrations. Methanogenic environments are the most reducing and contain C mainly as methane; S should be very low or present as dissolved sulphides, N should be in ammonia form, and dissolved Fe and Mn concentrations are dependant on the relative amount of S in the system. Moving from conditions of oxidation to increasing reduction (higher to lower Eh), first oxygen is reduced, followed by nitrate, sulfate, and finally the formation of methane. Figure 2.17 shows how these different redox zones relate to landfill plume migration.

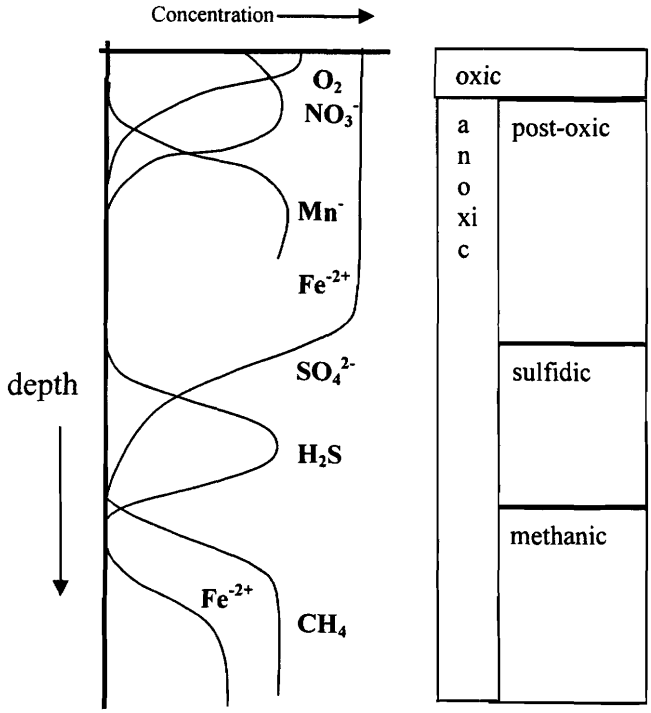

Figure 2.16: The sequence of reduction processes as reflected by groundwater composition. At the right is shown classification of redox environments is shown together with solids that are expected to form in each zone (after Appelo and Postma, 1996).

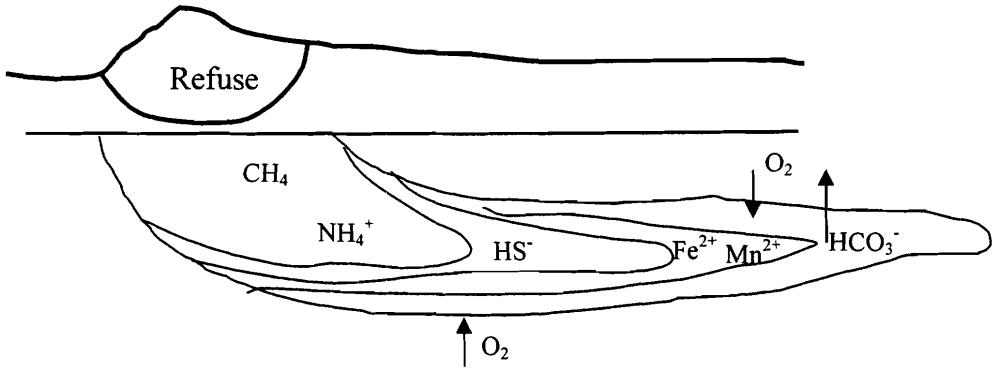

Figure 2.17: Schematic development of redox zones downstream of a landfill (after Appelo and Postma, 1996.)

2.4.2 Ion Exchange in Clay Minerals

One focus of this study is determining the effects of ion exchange on plume geochemistry. Manure seepage has relatively high ion levels; as these ions transport through soils, exchange occurs with ions on charged particles within the soil matrix.

2.4.2.1 Source of Ion Exchange in Clayey Soils

Clay minerals are constructed of alumino-silicate sheets (McBride 1994). These sheets can be either tetrahedral or octahedral. Tetrahedral sheets (⊢) consist of a cation (usually silicon) surrounded by four oxygen atoms; octahedral sheets (O) consist of a cation (usually aluminum) surrounded by six oxygen atoms (or hydroxyls). Clay minerals consist of stacks of these layers held together by shared oxygen. The stacking of the layers determines the type of clay mineral:

- Kaolinite: A repeating pattern of ⊢O ⊢O held together by oxygens of the octahedral sharing protons with the tetrahedral of the next layer.
- Smectite: A repeating pattern of ⊢O⊣ ⊢O⊣ held together by interlayer cations.
- Chlorite: Similar to smectite but held together by an additional octahedral layer giving a repeating pattern of ⊢O⊣ O ⊢O⊣ O.

Surface charges (usually negative) on clay minerals may be considered constant for such minerals as smectite and vermiculite clays and zeolites. Kaolinite clay and metal oxyhydroxides tend to have variable charge depending on solution composition: net positive charge at low pH, and net negative charge at high pH. The difference in charge potential is the source of the charge imbalance, including:

1. *Isomorphous Substitution*

   Isomorphous substitution occurs when insufficient silicon (Si^{4+}) is available during formation of the tetrahedral layer and aluminum (Al^{3+}) is substituted in the structure. Similarly, aluminum (Al^{3+}) can be substituted by magnesium (Mg^{2+}), iron ($Fe^{2+,3+}$), manganese (Mn^{2+}) or even calcium (Ca^{2+}), sodium (Na^{+}) or potassium (K^{+}) in the octahedral layer. The lower charge of the substituting ion results in a net negative charge.

2. *Lattice Imperfections or Defects*

   Lattice imperfections or defects occur when insufficient aluminum (Al^{3+}) in the octahedral layer or a deficit of interlayer cations results in a net negative charge.

3. *Broken or Unsatisfied Bonds*

   Broken or unsatisfied bonds occur at crystal plate corners and edges leading to the ionization of surface groups, usually resulting in a pH dependent net negative charge due to exposed oxygen (O^{2-}) and hydroxyl groups (OH^{-}).

Both isomorphous substitution and lattice imperfections result in permanent charges in clay minerals. Permanent negative charges of illites, smectites and vermiculites range from 1.9-2.8, 0.7-1.7, and 1.6-2.5 mol sites/kg respectively (Sposito 1979). Broken or unsatisfied bonds are important in all clays but significantly affect the charge on large particle clays such as kaolinite. At low pH values, hydrogen (H+) ions can compete for exposed oxygen (O^{2-}) and hydroxyl (OH^{-}) sites and at very low pH values can result in a net positive charge.

Several models used for calculating the absorption of ions in natural waters (e.g. MINTEQA2) use a quantitative value for the number of surface absorbing sites (Γ_s) as a concentration of sorbing surface sites in units of moles of monovalent sites exposed to a liter of solution (Langmuir 1997).

$$\Gamma_s(molesites/L) = \frac{N_s(sites/m^2) \times S_A(m^2/g) \times C_S(g/L)}{N_A(site/molsites)} \quad [2.13]$$

Where:

N_S = surface site density (sites/m^2),

S_A = surface area per weight of sorbent (m^2/g),

C_S = weight of sorbent in contact with a liter of solution (g/L), and

N_A = Avogadro's number (6.022 x 10^{23} sites/mol of sites)

Dividing the result by the weight of sorbent in contact with a liter of solution (C_S), gives the concentration of sorbing surface sites in units of moles of monovalent sites per gram of sorbent. This convention is preferred by soil scientists and is termed cation exchange capacity (CEC) given as milli-equivalents per 100 grams of dry soil (sorbent) (meq/100 g) or as centimoles per kg of soil (sorbent) (cmol/kg). Langmuir (1997) gives the following relation between the above mentioned variables and CEC:

$$CEC\,(meq/100\,g) = N_s(site/nm^2) \times S_A(m^2/g) \times 0.1661 \quad [2.14]$$

2.4.2.2 Cation Ion Attraction

The force of attraction between an ion (A+) and the surface of a negatively charged clay particle is inversely proportional to the distance between the two charges. The distance is the sum of the effective distance or radius of the surface charge (r_S) and the radius of the cation ion (r_A). The force, or electrostatic attraction, is proportional to the square of the electronic charge over the distance between the two charges given by:

$$E_{attraction} \propto \left[\frac{e^2}{r_s + r_A}\right] \quad [2.15]$$

where e is the electronic charge.

If an ion (A+) moves from solution to the surface, dehydration of both the ion and surface must occur. Similarly, if an ion (A+) is absorbed on the surface, then ion (B+) must desorb from the surface to solution. The total energy change is proportional to the change in electrostatic attraction energy and the change in hydration energy giving:

$$\Delta E_{Total} \propto \left[\left(\frac{e^2}{r_s + r_B} - \frac{e^2}{r_s + r_A} \right) - (E_B - E_A) \right] \qquad [2.16]$$

where E_A and E_B are the energy of hydration of ions A and B respectively.

From this we can see that:

i. if $r_s >> r_A$ and r_B, then the total energy change is dependent on the hydration energies of the ions. This situation, termed a weak field bond, is the case for clays with charge deficits in the octahedral layer such as smectite where weakly hydrated ions can displace strongly hydrated ions.
ii. if $r_s << r_A$ and r_B, then the total energy change is dependent on the electrostatic term. This situation is termed a strong field bond. An example would be cation absorption on Fe oxides. No permanent charge clays have been shown to have this behaviour.

2.4.2.3 Partitioning of Ions on Exchange Sites

For solutions in contact with an exchanger, ions tend to leave the solution and sorb to exchange sites. At the same time, an equal "activity" of ions leaves the exchange sites and goes into solution. This exchange is affected by many factors including:

- the charge of the ions;
- the size of the ion or hydrated radius;
- the properties of the exchanger (e.g. clay mineral);
- quantity and ratios of the various valence of ions present; and
- the total solution concentration.

If an exchanger with all sites occupied by a monovalent cation is placed in a solution with ions of only one different monovalent cation, exchange will take place. For the Law of Mass Action this exchange takes the form:

$$A^+ + BX = B^+ + AX \qquad [2.17]$$

where A+ and B+ represent ions in solution and BX and AX represent absorbed ions.

Then:

$$K_{eq} = \frac{[B^+]}{[A^+]}\left(\frac{(AX)}{(BX)}\right)^n \qquad [2.18]$$

For the assumption of thermodynamic equilibrium:

$$\frac{[A^+]}{[B^+]} K_C = \frac{(AX)}{(BX)} \qquad [2.19]$$

if the quantity of each ion on the exchange sites is proportional to the ratio of the ions in solution (White and Zelazny 1986), where:

K_{eq} = the equilibrium constant or K_C= the distribution coefficient,

n = is an exponent,

$[A^+]$ = activity of ion A in solution,

$[B^+]$ = activity of ion B in solution,

(AX) = "activity" of ion A on the exchange sites, and

(BX) = "activity" of ion B on the exchange sites.

Activities for each ion in solution can generally be calculated using the Debije-Huckel equations but there is no agreed way to calculate ion activities on exchange sites. One can write the "activities" of the ions as functions of the fraction of the total number of exchange sites the ion occupies multiplied by a "rational activity coefficient" giving the value of:

$$(AX) = \lambda_A \beta_A CEC \qquad [2.20]$$

where:

λ_A= the rational activity coefficient for the solid phase,

β_A = the equivalent fraction of ion A, and

CEC = the cation exchange of the exchanger.

Substituting this into Equation [2.18] and canceling the CEC gives:

$$K_{eq} = \frac{[B^+]}{[A^+]}\left(\frac{(\lambda_A \beta_A)}{(\lambda_B \beta_B)}\right)^n \qquad [2.21]$$

One shortcoming of this approach is if K_{eq} is by definition a constant, then changes in selectivity need to be accounted for in changes in the rational activity coefficients for the solid phase (λ_A and λ_B). Changes in these coefficients are similar to that observed in solution activities as ionic strength increases. At high ionic strengths, the surface activity for certain ions may be negligible (McBride 1994), due to reasons including:

- increased entropy associated with the more hydrated (and more mobile) ion causes a decrease in the exchanger preference for the less hydrated (and less mobile) ion as the exchange sites become more occupied with the more hydrated ion;
- solutions of higher ionic strength altering the chemical potential of water to decrease the size of the hydration shell of strongly hydrated ions, thus reducing the distance between the charge sources and increasing the attraction between the charges;
- cation-cation repulsion forces; or
- changes in clay site geometry.

This phenomenon has been explained by assuming the absorbent charge exists as a uniform surface volume or density of charge (Bolt 1982). This approach indicates the absorbent charge is either changing with distance from the center of the absorbent particle or constant throughout this charged volume around the particle. The selectivity coefficient (K_N) is written in terms of:

$$K_N = \sqrt{\frac{2}{V^{\alpha}}} \frac{\sqrt{(1-1/\bar{u}^3}}{\sqrt{(1-1/\bar{u}^2}} \qquad [2.22]$$

where:

V^{α} = volume of homogeneous phase per equivalent of charge (m^3/keq), and

$\bar{u}$ = the Boltzman accumulation factor for counterions in a diffuse double layer in a phase with a constant electrical potential. (This accumulation factor is proportional to the electrical potential and inversely proportional to the kinetic energy per molecule).

Therefore, an increase in concentration of the solution results in a decrease in the Boltzman accumulation factor and causes an increase in the selectivity coefficient. For a given ratio of monovalent cations to divalent cations, the amount of absorbed divalent cations will increase with increasing ionic strength or electrolyte concentration. For adsorbents with a constant charge density, the surface potential vanishes at very high electrolyte concentrations (Bolt 1982).

A further explanation considers the decrease in size of the hydration shell due to the collapse of the diffuse double layer (DDL) on hydrated ions and surfaces. Debije-Huckel theory for ion activities uses a parameter $1/\kappa$ termed the Debije length. This parameter can be given with ionic strength as a variable giving:

$$\frac{1}{\kappa} = \sqrt{\frac{\varepsilon \cdot RT}{2(N_a q_e)^2} \cdot \frac{1}{1000I}} \qquad [2.23]$$

where, ε = dielectric constant (for water 7.08×10^{-10} F/m at 25 °C)

R = 8.314 J/K.mol,

T = absolute temperature (K),

N_a = Avogadro's number (6×10^{23}/mol),

q_e = is the charge of the electron (1.6×10^{-19} C), and

I = ionic strength (mol/L).

This equation indicates that at 25 °C, $1/\kappa = 3.085x\text{-}10/\sqrt{I}$. The thickness of the diffuse double layer is considered the distance away from the ion where the potential (ψ) is equal to the potential at the ion surface divided by e (Appelo and Postma 1996). This is the position where the thickness of the DDL (x) is equal to $1/\kappa$; therefore, the thickness of the DDL at 25 °C can be given by $x = 3.085x\text{-}10/\sqrt{I}$. As the ionic strength increases, the thickness of the DDL decreases exponentially. This collapse of the DDL will affect the ability for ions to compete for exchange sites and thus cause variability in $K_{A/B}$.

Compounding the use of activity coefficients for the solid phase is the lack of experimental data. McBride (1994), however, lists three "General Rules of Cation Exchange":

i. Adsorption of high-charge ions is associated with increases in entropy and enthalpy of the clay–water system.
ii. An increase in solution concentration of low-charge ion causes the selectivity coefficient to increase, suggesting a greater preference for the high-charge ion.
iii. Increased loading of exchange sites with high-charge ions generally shifts the value of the selectivity coefficient in favor of the high-charge ion.

Thirty years earlier, Wiklander (1964) explained several observations from experiments involving ion exchange. These included:

i. Dilute solutions tend to favour adsorption of divalent cations.
ii. K, Mg, and Ca are more firmly adsorbed than NH_4 which is more firmly adsorbed than Na.
iii. The more Ca that is removed from the exchanger, the more difficult it is to remove more.
iv. The more Na that is removed from the exchanger, the easier it is to remove more.
v. There is no single universal order of the replacing power of cations.

In order to overcome the inability to determine ion activities on the solid phase, a more common method of calculating ion partitioning assumes the exchange ions form an ideal solution. When the "rational activity coefficients" (λ_A ad λ_B) are equal to one (1), Equation [2.21] reduces to:

$$K_{eq}' = \frac{[B^+]}{[A^+]}\left(\frac{(\beta_A)}{(\beta_B)}\right)^x \qquad [2.24]$$

where x is a function of "n" or an adjusted "n" and therefore $K_{eq}'=K_{eq}= K_{A/B}$.

This implies the adsorbed concentration of the ion on the exchanger can be calculated as:

$$meq_A = \beta_A \cdot CEC \qquad [2.25]$$

Application of the above theory to the exchange of a monovalent cation for a divalent cation can be written as:

$$A^+ + 0.5BX_2 = 0.5B^{2+} + AX \qquad [2.26]$$

and

$$K_{A/B} = \frac{[B^{2+}]^{0.5}}{[A]} \frac{(AX)}{(BX_2)^{0.5}} \qquad [2.27]$$

and for calculation using equivalent fractions:

$$K_{A/B} = \frac{[B^{2+}]^{0.5}}{[A^+]} \frac{\beta_A}{\beta_B{}^{0.5}} \qquad [2.28]$$

Values of $K_{A/B}$ have been published by numerous researchers for various ions and many of these results compiled by Bruggenwert and Kamphorst (1982). The published values appear to be useful for some situations depending on exchanger and solution concentrations.

The exchange of various ions in solution is easier if written with respect to only one ion for all ions in solution. The chosen ion is usually sodium as values of $K_{Na/I}$ are available without further calculation (Appelo and Postma 1996). For example if we have Na, Ca, Mg, K, and NH_4 in a solution in contact with an exchanger, we can write the following equations:

$$\beta_{Ca} = \frac{\beta_{Na}{}^2}{K^2{}_{Na/Ca}} \frac{[Ca^{2+}]}{[Na^+]^2} \qquad [2.29]$$

$$\beta_{Mg} = \frac{\beta_{Na}{}^2}{K^2{}_{Na/Mg}} \frac{[Mg^{2+}]}{[Na^+]^2} \qquad [2.30]$$

$$\beta_K = \frac{\beta_{Na}}{K_{Na/K}} \frac{[K^+]}{[Na^+]} \qquad [2.31]$$

$$\beta_{NH4} = \frac{\beta_{Na}}{K_{Na/NH4}} \frac{[NH_4^+]}{[Na^+]} \quad [2.32]$$

and $$\beta_{Ca} + \beta_{Mg} + \beta_{Na} + \beta_K + \beta_{NH4} = 1 \quad [2.33]$$

This gives a quadratic equation that can be solved for β_{Na} and then the remainder can be solved through substitution. Knowing the values of $K_{Na/I}$, we can calculate the fraction of each ion on the exchanger for every point in the system for which we know the concentrations of the ions in solution. Bruggenwert and Kamphorst (1982) and Appelo and Postma (1996) give values and ranges for various exchange coefficients for numerous ions with respect to Na^+ (i.e. $K_{Na/I}$). These values have been used by several researchers and yielded successful results (Beekman and Appelo 1990; Parkhurst and Appelo 1999) but may not be valid for all solutions and concentrations.

If sufficient data is available, we can write Equation [2.19] as:

$$\frac{[A^+]}{[B^+]} = K_C \left(\frac{(AX)}{(BX)} \right)^n \quad [2.34]$$

which leads to:

$$\log \frac{[A^+]}{[B^+]} = \log K_C + n \log \frac{(AX)}{(BX)} \quad [2.35]$$

Plotting the logarithm of the ratio of the ion activities in solution against the logarithm of the ratio of the quantity (concentration) of the ions on exchanger yields a slope of "n" and an intercept equal to log K_C (log $K_{A/B}$). $K_{A/B}$ is affected by solution concentration, the ratio of the divalent to monovalent ions, and various other factors; thus $K_{A/B}$ is not actually a reaction constant but rather a variable.

Several researchers have modified Equation [2.19] to reflect a best fit to experimental data and to satisfy assumptions regarding ion exchange made by other researchers. The first was Kerr (1928) who proposed:

$$K_K = \frac{[B^{n+}]^m}{[A^{m+}]^n} \frac{\left(A^{m+}\right)^n}{\left(B^{n+}\right)^m} \quad [2.36]$$

where all quantities are in molar units for the reaction:

$$nA^{m+} + mBX_n = mB^{n+} + nAX_m \qquad [2.37]$$

Vanselow (1932) conducted experiments with ammonium and calcium and proposed a modification of the Kerr equation, not accepting the idea that activity of the solid phase was unity. He modified the Kerr equation by using solution ion activities and a correction factor based on the absorbed ions expressed as:

$$K_V = \frac{[B^{n+}]^m}{[A^{m+}]^n}\frac{(A^{m+})^n}{(B^{n+})^m}\cdot[A^{m+} + B^{n+}]^{m-n} \qquad [2.38]$$

which, for monovalent-divalent exchange becomes:

$$K_V = \frac{[B^{2+}]}{[A^{+}]^2}\frac{(AX)^2}{(BX)}\cdot\frac{1}{[(BX)+(AX)]} \qquad [2.39]$$

where solution phase quantities are in activity and absorbed phase are molar.

Both Krishnamoorthy and Overstreet (1949) and Gaines and Thomas (1953) felt the Vanselow correction factor was somewhat over simplified and added a factor to account for the charge of the ions on the absorbed phase within the correction factor term. The Krishnamoorthy and Overstreet equation can be represented by:

$$K_{KO} = \frac{[B^{n+}]^m}{[A^{m+}]^n}\frac{(A^{m+})^n}{(B^{n+})^m}\cdot[aA^{m+} + aB^{n+}]^{m-n} \qquad [2.40]$$

where "a" is 1 for monovalent ions, 1.5 for divalent ions and 2 for trivalent ions. The Gaines and Thomas equation can be represented by:

$$K_{GT} = \frac{[B^{n+}]^m}{[A^{m+}]^n}\frac{(A^{m+})^n}{(B^{n+})^m}\cdot\frac{n}{m}[mA^{m+} + nB^{n+}]^{m-n} \qquad [2.41]$$

where solution quantities are expressed as activities and solid phase quantities are molar. A more extensive review of the various exchange equations can be found in White and Zelazny (1986).

Soil scientists commonly prefer the Vanselow method of calculating exchange coefficients while geochemists tend toward use of the Gaines and Thomas equation (Parkhurst and Appelo 1999). With the lack of exhaustive experimental data for exchange of numerous ions with numerous absorbents, there is still work to be done to determine appropriate correction factors for use in reactive transport modeling of solutes involving ion exchange. With data for both the absorbed and solution phases, one could calculate a partitioning coefficient ($K_{A/B}$) and then using a best-fit method determine a correction factor. These values may only be valid for the absorbent and solution used, but could possibly be used to predict equivalent fractions for each ion given or predicting solution chemistry at an individual location.

2.4.2.4 Use of Exchange as a Retardation Factor in Transport

The use of equivalent fractions, while helpful for visual representation of ion fractions on exchangers, may not be particularly useful in calculating the transport of reactive ions through a porous medium. For this we need the function of how absorbed concentration (S in mg/kg dry soil) changes with the solution concentration (C mg/L). The ratio of S to C is termed the distribution coefficient (K_d').

$$\frac{S}{C} = K_d' \qquad [2.42]$$

$$S = K_d \cdot C^n \qquad [2.43]$$

Equation 2.43 gives the more common form of this relation where "n" is simply an exponent. If we plot log C versus log S, and a straight line results (a Freundlich isotherm), then the slope is equal to the exponent "n" and the intercept to log K_d. The Freundlich isotherm assumes an unlimited amount of unreacted sorption sites. Using K_F for the Freundlich distribution coefficient we get:

$$\log S = \log K_F + n \log C \qquad [2.44]$$

The Langmuir isotherm assumes a finite number of sorption sites (S_{max}) and can be written as follows using K_L as the Langmuir distribution coefficient:

$$S = \frac{S_{max} K_L C}{(1 + K_L C)} \qquad [2.45]$$

For exchange with trace elements where the major ion on the exchange site is not affected, the value of K_d can also be obtained by multiplying the equivalent fraction of the ion exchanging from the solution to the solids by CEC divided by 100 to give mille-equivalents per gram, and multiplying the activity of the ion by the charge of the ion. Thus for:

$$1/mA^{m+} + 0.5BX_2 = 0.5B^{2+} + 1/mAX_m \qquad [2.46]$$

gives:

$$K_d = \frac{\frac{CEC}{m} \cdot 10}{\left(K_{B/A} \frac{\beta_B^{0.5}}{[B^{2+}]} \right)^m} \qquad [2.47]$$

K_d thus far has been in units of $\frac{\frac{mg}{kgdrysoil}}{\frac{mg}{Lofsolution}}$ or L/kg. K_d can be converted to a dimensionless number by expressing both the amount sorbed per kg sorbant and the solution concentration on a total volume basis. The easiest way is to multiply the sorbant concentration by the bulk density (kg or dry soil per total volume) and multiply the solution concentration by porosity (volume of pores per total volume). For saturated conditions the volume of pores is equal to the volume of solution and this gives:

$$Kd = Kd' \frac{\rho_b}{\eta} = \frac{S\rho_b}{C\eta} \qquad [2.48]$$

where:

ρ_b = bulk density (kg/m^3), and

η = porosity (L/ m^3)

The equation for one-dimensional advection-dispersion can be modified to include sorption and decay (Fetter 1992) giving:

$$\left(\frac{\partial C}{\partial t}\right) = D_L\left(\frac{\partial^2 C}{\partial t^2}\right) - v_x\left(\frac{\partial C}{\partial x}\right) - \frac{\rho}{\eta}\left(\frac{\partial S}{\partial t}\right) + \left(\frac{\partial C}{\partial t}\right)_{rxn} \qquad [2.49]$$

(dispersion) (advection) (sorption) (reaction)

where

C = concentration of the solute in the liquid phase

t = time

D_L = longitudinal dispersion coefficient

v_x = average linear groundwater velocity

ρ = bulk density

η = porosity of the saturated media (volumetric moisture content if saturated)

S = amount of solute sorbed per unit weight of solid

rxn = subscript indicating a biological or chemical reaction of the solute other than sorption.

The decay term can be ignored for most ions associated with EMS seepage given some indication that nitrogen stays in the ammonium state. Recognizing this and substituting the distribution coefficient for S (Eq 2.42) yields:

$$\left(\frac{\partial C}{\partial t}\right) = D_L\left(\frac{\partial^2 C}{\partial t^2}\right) - v_x\left(\frac{\partial C}{\partial x}\right) - \frac{\rho}{\eta}\left(\frac{\partial S}{\partial t}\right) \qquad [2.50]$$

This equation can be reorganized to:

$$\frac{\partial C}{\partial t}(1+\frac{\rho}{\eta}Kd') = D_L\frac{\partial^2 C}{\partial x^2} - v_x\frac{\partial C}{\partial x} \qquad [2.51]$$

$(1+\frac{\rho}{\eta}Kd')$ is termed the retardation factor (R) and Kd' is considered constant for the range of concentration of interest.

R indicates the relative transport of an ion to a nonretarded ion. This is also equal to the difference between the average linear groundwater velocity (v) and the velocity of the solute where the concentration of the solute is one-half the original (v_c). That is to say:

$$R = \frac{v}{v_c} \qquad [2.52]$$

where $R = 1+\frac{\rho}{\eta}Kd'$

A limitation for the use of the $R=1+\frac{\rho}{\eta}Kd'$ for calculation or prediction of solute transport is a constant Kd' implies no limit to the amount of solute that can be absorbed to the solids phase. This, of course, is not always the case, especially at higher solute concentrations where the quantity of solute in solution exceeds the quantity of exchange sites available. Kd' for a particular species can also be affected by factors such as competition with other ions for exchange sites.

If an ion adsorption isotherm is a straight line, Freundlich isotherm (Eq 2.43), then equation 2.50 can be written:

$$\left(\frac{\partial C}{\partial t}\right)=D_L\left(\frac{\partial^2 C}{\partial t^2}\right)-v_x\left(\frac{\partial C}{\partial x}\right)-\frac{\rho}{\eta}\left(\frac{\partial(KdC^n)}{\partial t}\right) \qquad [2.53]$$

and after differentiation and reorganization Equation 2.53 becomes:

$$\frac{\partial C}{\partial t}(1+\frac{\rho}{\eta}Kd'nC^{n-1})=D_L\frac{\partial^2 C}{\partial x^2}-v_x\frac{\partial C}{\partial x} \qquad [2.54]$$

where $1+\frac{\rho}{\eta}Kd'nC^{n-1}=1+KdnC^{n-1}=R_F$ and if n is greater than 1 equation 2.54 leads to a spreading front and if n is less than one the front will be sharpening. If n is equal to 1 then Freundlich sorption isotherm becomes the linear isotherm and R_F=R.

For many situations the sorption isotherm is not linear and tends to a maximum amount of solute on the solids phase (S_{max}). Substituting Equation 2.45 for the Langmuir isotherm, equation 2.50 can be written:

$$\left(\frac{\partial C}{\partial t}\right)=D_L\left(\frac{\partial^2 C}{\partial t^2}\right)-v_x\left(\frac{\partial C}{\partial x}\right)-\frac{\rho}{\eta}\left(\frac{\partial\left(\frac{KdS_{max}C}{1+Kd'C}\right)}{\partial t}\right) \qquad [2.55]$$

and after differentiation and reorganization Equation 2.55 becomes:

$$\frac{\partial C}{\partial t}\left[1+\frac{\rho}{\eta}\left(\frac{KdS_{max}}{(1+KdC)^2}\right)\right]=D_L\frac{\partial^2 C}{\partial x^2}-v_x\frac{\partial C}{\partial x} \qquad [2.56]$$

where $1+\frac{\rho}{\eta}\left(\frac{KdS_{max}}{(1+KdC)^2}\right)=R_L$ the retardation factor for the Langmuir sorption isotherm. Several researchers have reported sorption isotherms with at least two distinct sections indicating two-types of sorption sites with differing bonding energy (Fetter, 1992). The Langmuir two-surface sorption isotherm is:

$$S=\frac{Kd_1S_{max\,1}C}{1+Kd_1C}+\frac{Kd_2S_{max\,2}C}{1+Kd_2C} \qquad [2.57]$$

which can also be substituted into Equation 2.50 and solved for the retardation factor.

2.4.2.5 Use of Ion Exchange in Modeling of Transport

Numerous models coupling advective-diffusive transport and ion exchange have been developed. Numerical models incorporating ion exchange can simulate laboratory results (Valocchi et al. 1981) while mixing cell models can simulate injection well studies in an aquifer (Dance and Reardon, 1983; Van Omen, 1985). Another modeling technique is the use of a finite-difference flow and solute transport model where solute transport is described by the traditional advection-dispersion equation and solved by a finite-difference technique (Bjerg et al., 1993).

Although most models use constant selectivity coefficients, Mansell et al. (1988) developed a model after the method used by Valocchi et al. (1981), and incorporated variable selectivity coefficients to account for non-linear exchange. The model required selectivity coefficients as a function of the concentration of each ion in solution and on the exchange sites. They concluded although the model yielded reasonable results, future consideration should be given to including additional chemical processes such as ion pairing, speciation, and chemical disequilibrium. One model developed to incorporate these factors is PHREEQC (Parkhurst and Appelo, 1999). This model is written in the C programming language and calculates a transport step first, then calculates all equilibrium and kinetically controlled reactions including ion exchange, precipitation, dissolution, and decay, and then calculates the diffusive component, and

again calculates all equilibrium and kinetically controlled reactions including ion exchange, precipitation, dissolution, and decay prior to transporting the next step.

2.5 Representative Groundwater Sampling

The most difficult task when using groundwater as an indicator of contaminant migration is obtaining a representative sample (U.S. EPA, 1995; U.S. EPA, 1991; Gosselin et al., 1994; Boulding 1993; Robbins and Martin-Hayden, 1991; Hartz, 1991). Hydrogeological variations in the aquifer may complicate well design and placement decisions (Gosselin et al., 1994; Robbins and Martin-Hayden, 1991). In addition, installation of the well may introduce new colloidal matter causing reactions with the contaminants, or the filter may remove naturally mobile colloids (U.S. EPA, 1991; Puls and Barcelona, 1989; Driscoll, 1986). Purging methods for sample acquisition may also introduce colloidal matter, cause degassing (change in pH), or precipitation of dissolved contaminants (Boulding, 1993; U.S. EPA, 1991; Puls and Barcelona, 1989; Driscoll, 1986). Finally, sample transportation, storage, and analysis may cause degassing, precipitation, pH changes, temperature changes and/or species alterations (U.S. EPA, 1991; Annon., 1987, Pohlmann et al., 1994). Parameters such as pH, gases and alkalinity should be determined in the field (Boulding, 1993). Samples for total dissolved solute analysis must be filtered with filter sizes less than or equal to 1.0 μm (U.S. EPA, 1995).

Methods of well purging to remove stagnant water in the casing have come under review in the last ten years. Traditionally, well purging involved the evacuation of 3 to 5 or 10 well volumes (U.S. EPA, 1991); this method is no longer recommended. Instead, the well is pumped until water indicators (pH, EC, Eh, temperature, and dissolved oxygen) have stabilized to +/- 10% over at least two well volumes (Bone, 1986; Boulding, 1993). Dedicated pumps with pumping rates of 0.1-1 L/min are now recommended rather than the traditional 11-20 L/min (Boulding, 1993; Puls and Barcelona, 1989, Shanklin et al., 1995). This low-flow sampling decreases the amount of wastewater, entrainment of immobile particles, chances of O_2 and CO_2 exchange,

and uncertainties in interpreting the source of the sampled water (U.S. EPA, 1995; Pohlmann et al., 1994; Puls and Barcelona, 1989). The U.S. EPA (1995) also suggests purge rates be kept at the point where well draw down is minimized so the removal rate matches the rate of the water entering the well bore under natural hydrological flow conditions.

3 METHODS AND MATERIALS

3.1 Source Chemistry

Detailed characterization of EMS effluent chemistry was identified as one of the deficiencies in the literature. Hog production facilities are of four general types: farrowing units, where mainly sows are housed; nursery units, where piglets from 10 to 60 days of age are housed; finishing units, where pigs from 60 to 180 days are housed; and farrow to finish units where all three are housed together. In order to characterize the source chemistry of a typical EMS, a number of different EMS ponds at hog production facilities in Saskatchewan were sampled, including two EMS servicing farrow to finish operations, two servicing farrow to wean operations and three servicing finishing operations.

3.1.1 Instrument Design

The sampler was constructed of a 0.3 m length of ABS pipe connected to two ABS gate valves (Figure 3.1). Lengths of stainless steel pipe acted as the handle of the sampler and more lengths were connected to reach the various sampling depths as required. A stainless steel rod connected to both valves and passing through the handle was used to actuate the valves.

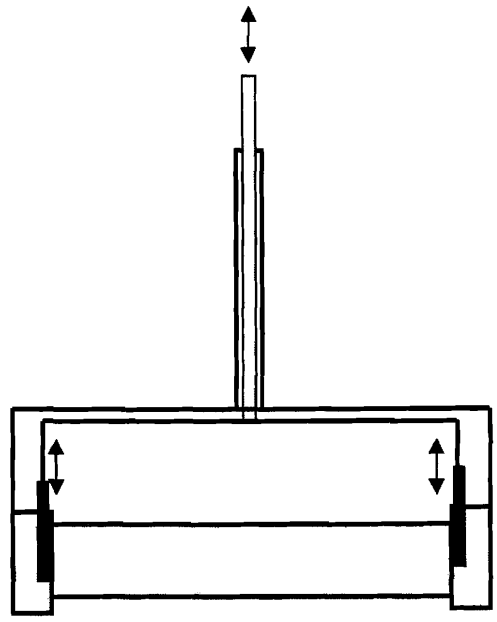

Figure 3.1: EMS sampling apparatus.

3.1.2 Sampling Procedure

Sampling was conducted from a boat on the EMS pond. The sampler was lowered to the desired depth with the gate valves closed. The valves were opened by pulling the inner handle rod and the sampler pulled sideways to get a representative sample at the selected depth. The gate valves were then closed and the sampler brought to the surface and emptied into a 1 L container. Each EMS was sampled at depths of 0.1 and 1.0 m, and each subsequent meter to depth. To ensure retrieval of representative samples with regards to solids content at the bottom of the storages, the sampler was left open at the bottom of the storage for up to 20 days; this procedure was conducted from the bank of the EMS. After all the samples were retrieved, the sectioned pipe was removed from the sampler and a dissolved oxygen probe with temperature measurement capabilities was taped to the pipe along with a platinum redox probe. These instruments were then lowered into the storage. Readings were taken at 0.1 m, 0.5 m and each subsequent 0.5 m interval in order to obtain a profile of the EMS pond.

3.1.3 Sample Handling and Analysis

Samples were placed in sealed plastic containers and transported to Saskatchewan Research Council Analytical Laboratory in Saskatoon, Saskatchewan where EC, pH, and Total Solids analysis on the mixed sample were measured. A portion of the sample was filtered through a 0.45 μm filter, then split for analysis of alkalinity, major ions, metals, total ammonium, nitrate, nitrite and sulphide. We assumed fluid passing a 0.45μm filter could potentially transport from the EMS to the surrounding groundwaters. Filtering samples to 0.45μm was assumed to remove a majority of colloids present (Puls and Barcelona, 1989). Major ions (Ca, Mg, Na, K and SO_4^{2-}) were analyzed by ICP-IRS, carbonates (HCO3-, CO3 and alkalinity) by acid titration, nitrogen and chloride by colorimetric method, sulphide and pH by electrode, organic carbon by Dohrman Pheonix carbon analyzer, and metals by ICP-AES. Analytical methods and detection limits are presented in Appendix A.

3.2 Column Study

Mechanisms governing leachate transport and attenuation of nitrogen were also identified as areas requiring study. A column experiment was conducted with large columns to simulate EMS conditions, and was part of a longer-term study into the performance of EMS being conducted by the Department of Agricultural and Bioresource Engineering. In addition to the laboratory studies, five EMS sites were monitored. Three two-cell EMS at sites in Saskatchewan were instrumented prior to commissioning of the EMS. The study sites included the Big Sky Farms' Clearfield Feeder Unit site near Kelvington, Genex Swine Bon Accord Nucleus Unit near Ituna, and the Prairie Swine Center PSC Elstow Research Farm near Elstow. Two older EMS sites were also investigated and piezometer nests installed in suspected plumes. These sites are referred to as ADF Research Site No. 1 (9.6 km south of Saskatoon) and ADF Research Site No. 9 (3.2 km south of Hepburn). Specific locations are not provided based on agreements with the landowner.

Large columns were constructed to study the transport of EMS effluent through soils. Soil for Column No. 1 was collected from the Clearfield Feeder Unit site near Kelvington during

construction of the EMS. This soil is a till with approximately 16% clay content and a CEC of 6 to 8 meq/100g. Soil for Column No. 2 was collected from ADF Research Site No. 1 by excavation of test holes. This soil is a silty-sand (SPSM) with approximately 8% smectite clay and a CEC of 8 meq/100g. Manure effluent for Column No. 1 was also collected from the Clearfield Feeder Unit site. Manure effluent for Column No. 2 was collected from Big Sky Farms' farrow to wean facility west of Burr, Saskatchewan; ADF Research Site No. 1 could not be accessed due to biosecurity concerns.

3.2.1 Column Design

The columns were fashioned in a similar manner to those used by both Barrington et al. (1987) and Fonstad (1996) although approximately five times larger. Two columns were constructed of 300 mm diameter PVC DR35 pipe placed vertically to form a 4 m column (Figure 3.2). The columns were instrumented to determine oxidation-reduction potentials, to collect samples from manometers at various levels with in the liquid and soil portions of the column, and to collect exfiltrate from the base of the column at various times during the experiment. Compacted soil was placed in the bottom 1 m of the column. Manure was ponded in the top 3 m of the columns. Six 50 mm PVC pipes and valves were installed for manure sampling within the top 3 m and four 19 mm PVC pipes and valves were installed within the soil in the lower 1 m of the column. Manometer tubing was attached to each pipe and extended up the side to allow head measurement. The manometer connection also allowed retrieval of a liquid sample at each location; sample volume was limited to the volume of the 19 mm diameter pipe. Eh or Redox probes were installed at each valve location to attempt to measure redox conditions and to verify the usefulness of the redox probes. A 19 mm PVC pipe and valve was placed in a gravel layer below the soil column for effluent collection. Each pipe was installed to the center of the column. All 19 mm diameter pipes were covered with soil filter cloth to ensure that plugging did not occur. The top 3 m of the column was constructed as a separate piece so that the soil column could be easily removed and sectioned at the end of the column test.

3.2.2 Column Setup and Commissioning

The columns were constructed in early 1999 and the soils compacted into the columns on March 15, 1999. The soils were compacted wet of Standard Proctor optimum moisture content to compaction levels less than Standard Proctor maximum dry density with a simulated Proctor hammer. Soils in Column No.1 were compacted at 3.2% above optimum moisture content to a dry density of 95% of maximum Standard Proctor. Soils in Column No. 2 were compacted at 7.8% above optimum moisture content to a dry density of 92% of maximum Standard Proctor. The hydraulic conductivity of each column was measured with fresh water to establish initial hydraulic conductivity. Column No. 2 was filled with manure on April 5, 1999 and Column No. 1 filled on April 8, 1999. Each column was then monitored for liquid levels, manometer levels, effluent volumes, and Eh (redox) readings with time. All exfiltrate was returned to the top of the column to maintain head with the exception of 50 mL required for sample analysis.

3.2.3 Sampling and Instrumentation Reading

Solution samples were taken periodically from each sampling point within the soil column and from the exfiltrate container. The samples were taken to the laboratory at the Department of Agricultural and Bioresource Engineering at the University of Saskatchewan for analysis of EC, ammonium, nitrate, chloride and potassium. Ion analysis was by ion selective electrode. Solution samples taken just prior to dismantling the columns as well as several selected earlier samples were analyzed by ion chromatography with a Dionex Ion Chromatograph in the Department of Geological Sciences at the University of Saskatchewan.

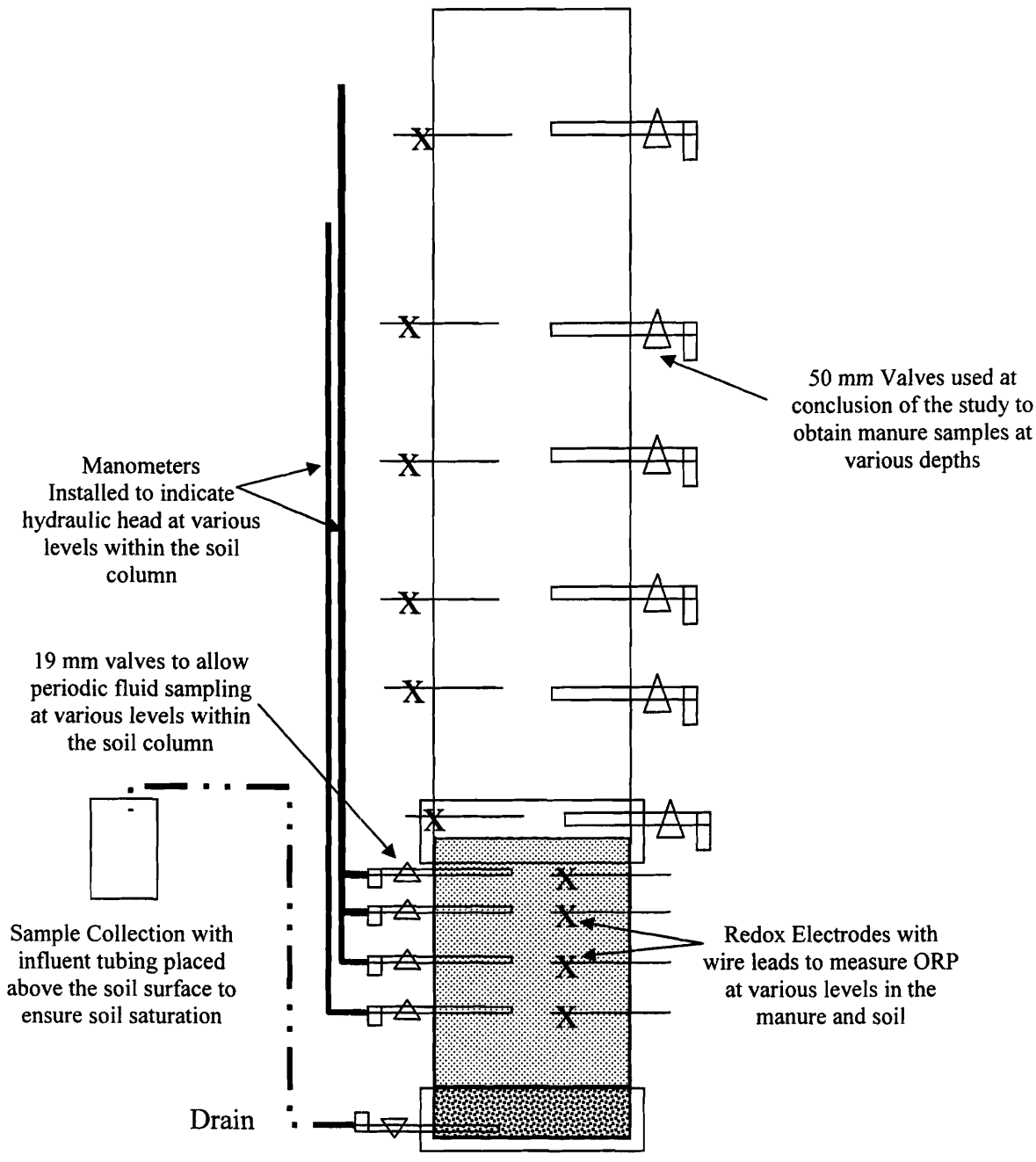

Figure 3.2 – Column set-up for large column study conducted at PAMI, Humboldt, Saskatchewan.

3.2.4 Column Decommissioning and Soil Sampling

The columns were dismantled on August 17, 1999, by first draining off the 3 m of manure, taking the top 3 m of the column off and then wrapping the bottom 1 m of the PVC column containing the soil with plastic for transport to the Department of Agricultural and Bioresource Engineering at the University of Saskatchewan. The columns were placed in a walk-in freezer and stored at –30°C until dissection. Column No. 1 was dissected on April 27 and Column No. 2 on April 28, 2000. The soil columns were sectioned into layers of maximum thickness of 50 mm. Each layer was split and one-half the sample was sent to the Soil Science laboratory at the University of Saskatchewan for analysis; the remaining half was stored frozen in case of sample loss or contamination.

3.2.5 Soil Laboratory Analysis

The samples sent to the Soil Science laboratory were split in half. One-half was used to determine the original water content by oven drying. The remaining portion was dried and ground, then processed for extractable ions by saturated paste extraction and exchangeable ions using ion removal by splitting the samples and subjecting them to 1N NH_4OAc or 1N $BaCl_2$. Extraction solutions were analyzed by atomic absorption spectrophotometry with exceptions of ammonium by reagent dilution, and anions by titration (bicarbonate) or calorimetric methods (chloride and sulfate). Xray diffraction analysis results were obtained from another study (Maule and Fonstad, 2000). Analytical methods and detection limits are outlined in Appendix A.

3.2.6 Short Term Batch Test

A short term batch test for determining distribution ratios (ASTM D4319-93) complemented the column study. The test was conducted using soil samples from the Clear Field Feeder Unit site (Kelvington soil) and from ADF Research Site No. 1 (Site

No.1 soil) following ASTM D4319-93 (2001) and Shackelford and Daniel (1991). Although care was taken to use similar soils to those in the large column study, site soil variability may have resulted in a significantly different soil being used for the batch test, particularly at the Clear Field site. Soils were sieved and air dried. For each soil, 200g of air dried soil was placed in each of 10 plastic containers. A liquid solution was added to each container (approximately 790 mL) to obtain a 4:1 solution to dry soil mixture by weight. The solution was a mixture of distilled water, ammonium bicarbonate, sodium chloride, sodium sulphate, magnesium carbonate and calcium carbonate in appropriate portions to simulate manure chemistry. No source of organic carbon was added to the solution and different results may have been produced if manure had been used. The 10 containers received solutions ranging from 10% to 100% of the manure solutions by substituting distilled water in the liquid added. The containers were placed on a shaker table in a controlled environment room at 5°C for 36 hours (Kelvington soil) to 48 hours (Site No. 1 soil). During this time the containers were inverted three times per day. The containers were then left to stand for 48 hours after which Eh, EC and pH readings were obtained from each sample. Approximately 30 mL of liquid was decanted from each container and used to determine alkalinity. All containers were then delivered to the Saskatchewan Research Council Analytical Laboratory in Saskatoon, Saskatchewan for further analysis.

Each sample was thoroughly agitated and 50 mL of soil-solution mixture decanted to a centrifuge tube. Samples were centrifuged for 30 min and the highest setting and the liquid decanted for analysis. Care was taken not to remove clay particles. Deionized water was then added and the sample shaken for 10 min then centrifuged for 30 min. The resulting liquid was decanted and tested for electrical conductivity. The addition of deionized water, shaking and centrifuging procedure was repeated until the decanted liquid had an EC of less than 100 μS/cm. Each soil sample was then subjected to 1N $BaCl_2$ extraction and the resulting solution analyzed for ions removed from the soil. 1N NH_4OAc extraction was then completed on each sample and the resulting solution analyzed for barium to determine cation ion exchange capacity and check for any significant differences between extracted ions and extracted barium.

Total alkalinity, bicarbonate and carbonate analysis was by titration. Chloride, ammonium and nitrite plus nitrate were analyzed colorimetricly. Calcium, magnesium, potassium, sodium and sulphate were analyzed by ICP-IRS. Samples with relatively high concentrations were diluted prior to analysis.

3.3 Field Investigation

Investigation of an EMS leachate plume was conducted to characterize the geochemical conditions within an EMS plume and verify findings of the column study. A study of EMS plumes in Saskatchewan (UMA Engineering Ltd., 1995) indicated seepage from EMS constructed in glacial clay till deposits was limited to within 2 to 3 m of the EMS, unless transport occurred along fractures or granular lenses which intercepted the EMS. EMS constructed in granular deposits developed leachate plumes to horizontal distances of at least 30 m. ADF Research Site No. 1 was constructed in 1984 to service a 250-sow farrow to finish operation which produces approximately 7300 m^3 of effluent per year. The site was constructed in a lacustrine deposit; soils consist of approximately 6 to 8 m of sands (SM and SPSM) with lenses of silts (ML) and clays (CL and CI) over lying at least 4 to 6 m (maximum depth of investigation) of firm clay (CI) with lenses of sands (SM) and silts (ML).

The EMS at this site was constructed without a liner in the same fashion as construction of an earth borrow pit. Excavation equipment accessed the excavation from the ends during construction resulting in relatively steep side slopes (2:1) and gradual end slopes (4:1 to 5:1). Material from the excavation was used to construct the berms on the north, east and south sides. The top of the berm at the west end of the EMS is at original ground elevation. The storage was excavated until a clay layer was encountered at approximately 2-2.5 m below grade. No effort was made to compact the soils additional to the weight of the construction equipment during excavation.

The groundwater gradient at this site was determined to be almost perpendicular to the EMS sides and flow from north to south. The relatively steep side slopes perpendicular to the groundwater gradient and the granular upper soils with the underlying clay soils resulted in the development of a seepage plume extending at least 30 m from the storage. Due to the extent of this plume the EMS was chosen for further investigation.

3.3.1 Previous Investigations at the Site

Initial investigation of the site was conducted by the Geotechnical Division of the Prairie Farm Rehabilitation Administration of Agriculture and Agri-Food Canada. Test holes with piezometers were installed on March 3, 1994 on the west and south sides of the EMS (C1 and C2; Figure 3.3). An electro-magnetic (EM) survey was conducted at the site and two test holes with piezometers were installed in June 1994 by UMA Engineering Ltd. on the south and north sides of the storage (UMA2 and UMA3; Figure 3.3; UMA Engineering Ltd., 1995). The Geotechnical Division of the PFRA of Agriculture and Agri-Food Canada and the UMA Engineering Ltd. conducted further test drilling on January 31, 1995. Two test holes with piezometers were installed approximately 300 m west and southwest of the EMS (C4 and C5; Figure 3.3). These piezometers were used in conjunction with an unused shallow well east of the EMS to define groundwater flow directions in the unconfined aquifer. These piezometers and shallow well indicated the groundwater gradient at the site is to the south-southeast. Based on this information, eight more test holes with piezometers were installed February 1 to February 3, 1995 on the south side of the storage in an attempt to delineate the plume (C6 to C13). Results of this study were reported to the Agricultural Development Fund of SAFRR by UMA Engineering Ltd. (1995), and indicate the presence of a plume of contamination on the south side of the EMS.

3.3.2 Instrumentation Design and Materials

Instrumentation at the field site consisted of standard standpipe piezometers nested at various locations. At select piezometer nest locations, soil gas samplers, thermocouples

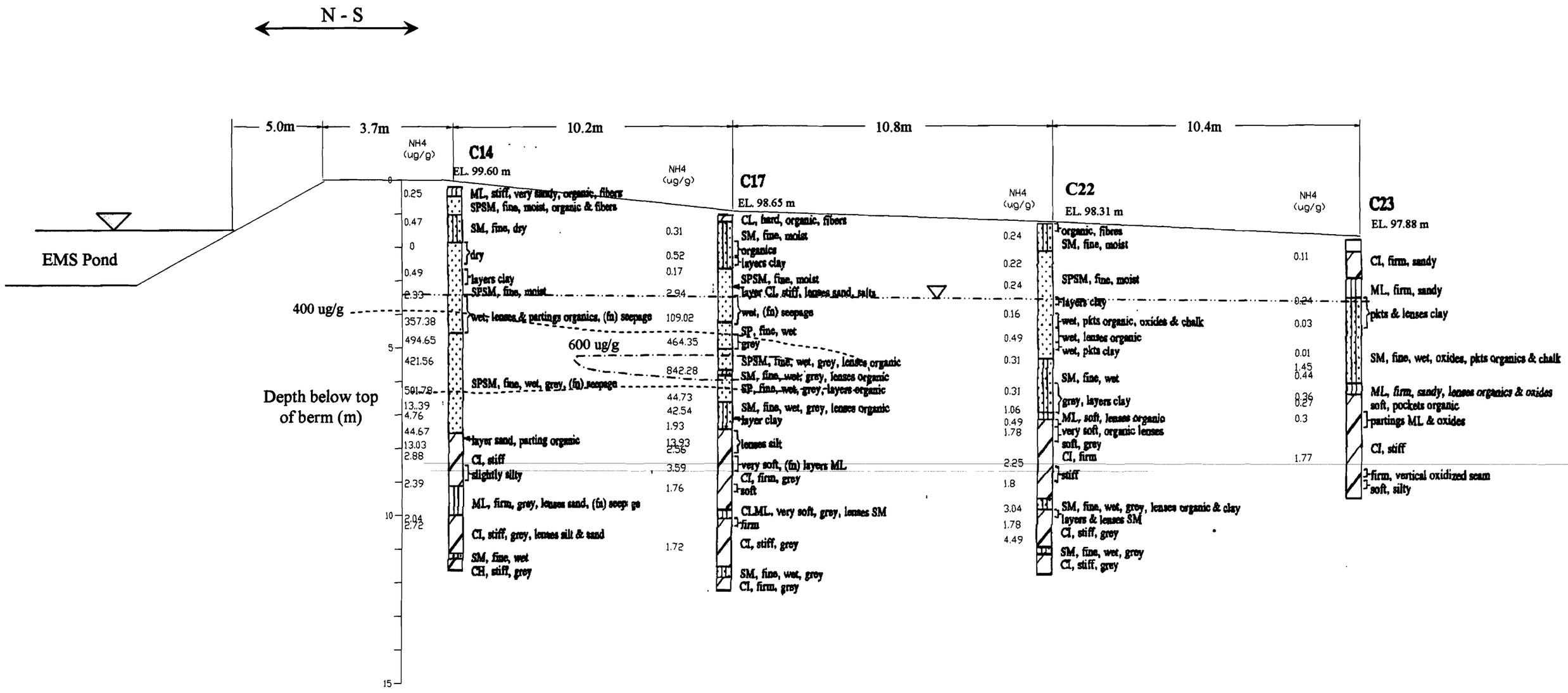

Figure 4.82 - ADF Research Site No.1 north-south cross section of the south side of the EMS showing test hole logs with ammonium concentrations determined from soil samples using 2M KCl extraction.

and ORP probes were installed. One installation was completed below the EMS by drilling through the ice of the EMS during winter months.

3.3.2.1 Piezometers

Standpipe piezometers were constructed using 50 mm diameter SCHD 40 PVC. Screened sections were also constructed with 50 mm diameter SCHD 40 PVC precut with 0.25 to 0.5 mm slots. This slotted pipe was cut into lengths, capped and fitted with a coupler to form a 500 mm long screen with approximately 450 mm of exposed slots. Screens installed in wet conditions or silty soils were fitted with a filter sock to reduce fines entering the screen. Solid SCHD 40 PVC pipe was installed from the top of the screen to approximately 1 m above grade. All piezometers were vented to the atmosphere and capped with SCHD 40 caps and threaded plugs forming a watertight seal.

Model P-100 minerature pneumatic piezometers were purchased from RST Instruments Ltd., Coquitlam, British Columbia. The model P-100 incorporates a 50 μm stainless steel screen and is capable of monitoring pore pressures from 0 to 13,000 kPa, and requires only 0.002 mL displacement allowing measurements to be made under essentially zero volume change conditions. The pneumatic piezometers were ordered with the appropriate length of access tubing, fittings and calibrated from 0 to 100 kPa. Reading was accomplished using a RST Instruments Ltd. Model C-106 Digital Pneumatic Readout instrument.

3.3.2.2 Thermocouples

Thermocouples to measure *in situ* groundwater temperatures were constructed of 20-gauge Type T thermocouple wire in the manner suggested by Culik et al. (1982). The wire was cut to the desired length and approximately 25 mm of one end was stripped. The stripped wires were twisted together by clamping the end with pliers and turning the pliers until the wires had been evenly twisted 3 times. The twisted wires were then fluxed and soldered liberally

with a 40% lead / 60% tin solder. The soldered portion was cleaned thoroughly and clipped off to a length of approximately 10 mm. A 25 mm length of heat-shrink tubing with an adhesive inner wall was cut and placed so that it extended over the soldered tip by about 5 mm. The tubing was heated using a heat gun until the adhesive appeared. The end of the tubing was then clamped using pliers. After cooling, the thermocouples were tested by measuring them at a known temperature.

3.3.2.3 ORP Probes

Oxidation-reduction potential (ORP) electrodes were constructed using a method similar to Farrell et al. (1991) for construction of platinum electrodes suitable for long-term field measurements. A 12.5 mm length of 20-gauge 99.99% pure platinum wire was cut and silver soldered to a pre-measured length of 18-gauge copper cable with PVC casing. A hole just large enough for the platinum wire was drilled through the bottom of a plastic syringe needle packing tube using a dental pick. Epoxy was mixed using 80 parts Glenmark GMI#80 hardener to 100 parts Glenmark GMI#1630 resin. The needle packing tube was filled with the epoxy using a 20 cc syringe with a 14-gauge needle. After filling the plastic tube with the epoxy, the platinum tip was placed into the open end of the tube and then threaded through the hole on the bottom of the tube until approximately 10 mm of platinum was exposed; this ensured that the only exposed wire was the platinum extending out of the end of the plastic needle tube. The platinum tip was cleansed of epoxy using a paper towel and left to dry for 24 h. At the end of the drying period, the dry tips were cleaned with a utility knife and rubbing alcohol, followed by a solution of 10% HCl and 10% detergent after procedures described by Bailey and Beachamp (1971). Tips were then rinsed with distilled water and capped with a temporary plastic needle tip held in place by electrical tape for protection from damage until installation.

The electrodes were checked by placing them in a standard redox solution (Zobell's solution) consisting of 3.33 mM potassium ferrocyanide, 3.33 mM potassium ferricyanide and 0.1 M KCl (Farrell et.al. 1991). A silver/silver-chloride (Ag-AgCl)

electrode was also placed in the solution to act as a reference. A voltmeter was used to check the potential between the reference electrode and the platinum electrode by connecting the terminals to the copper lead from the platinum electrode and the lead from the reference electrode. For consistency, the reference electrode lead was always connected to the common terminal of the voltage meter. With reference to an Ag/AgCl electrode, the voltmeter was expected to give a direct reading of +230 mV. All probes within ± 10 mV of this standard were rinsed with distilled water, recapped and packed for transport to the site. Those not reading within the specified range were cleaned and checked again and either packed (passed calibration) or discarded (failed calibration). The effect of differing lead lengths was also examined but had no affect on electrode performance.

3.3.2.4 Soil Gas Samplers

Gas sampling was accomplished using a brass filter with a stainless steel screen. The filters were fuel filters intended for use in small engines such as chainsaw motors. These filters were covered with nylon screen and connected to 3.2 mm ID poly tubing using barbed fittings and small hose clamps. The tubing extended from the filter to the ground surface and terminated in a PVC electrical box. A three-way valve was attached to the end of each line for sampling and to prevent contamination from atmospheric air.

3.3.3 Instrumentation Installation

The Geotechnical Division of the PFRA of Agriculture and Agri-Food Canada and the Department of Agricultural and Bioresource Engineering conducted further test drilling adjacent to the EMS in February 1999, October 2000 and September 2001. Drilling was accomplished using a Cyclone Model 36 churn rig mounted on a tandem axle three-ton truck. Piezometer nests were installed at approximately 10 m intervals on the south side of the EMS with one nest located on the north side of the EMS to record background water quality. The direction of groundwater flow in the unconfined aquifer had been determined previously to be south-southeast of the EMS and this was considered to be

the most likely location of a leachate plume at the site (Fonstad and Maule, 1995; UMA Engineeing Ltd. 1995).

Test holes C14 to C28 were installed in February 1999 at various locations on the south side (Figure 3.3). Piezometers C29 and C30 were also installed on the north side to determine background conditions. Piezometers C14 through C31 were installed with a screened length of no more than 0.5 m to delineate the plume in two dimensions. Two to four test holes were excavated at each nest location. Soil cores were taken in 60 mm diameter by 750 mm long brass liners at each nest location, then sealed and stored between 2°C and 6°C. Soil cores were extruded in the PFRA geotechnical laboratory in Regina on March 8 to 10, 1999. These samples were split and one set of samples was sent to the University of Saskatchewan Soil Science Laboratory for 2M KCl extractions to determine ammonium and nitrate concentrations. The remaining soil was analyzed by the PFRA soil laboratory for grain size, Atterberg Limits, density, specific gravity, water content and hydraulic conductivity (Table 3.1).

Table 3.1 - Testing Methods for Soil Physical Analysis

Physical Property	Method Used/Reference
Soil Drying and Preparation	ASTM D-421-85 (R93)
Particle-Size Analysis	ASTM D-422-63 (R90)
Atterberg Limits	ASTM D-4318-93
Proctor Analysis	ASTM D-698-91
Moisture Content (mass)	ASTM D-2216 -92
Unified Soil Classification	ASTM D-2487-93
Agricultural Soil Textural Class.	USDA Textural Classification Chart, (PCA, 1992)
Engineering Soil Textural Class.	US-FAA Textural Classification Chart, (PCA, 1992)

On March 22, 1999, drilling was completed through the ice on the EMS to retrieve soil samples and install monitoring equipment below the storage. Drilling was accomplished with a rotary drill rig mounted on a three-ton truck owned and operated

by P. Machibroda Engineering Ltd. The drill rig used hollow stem augers to excavate to the required depth in an attempt to prevent contamination of the samples. Sampling was accomplished using Shelby tubes pushed into the soil using the drill rig. The rig was parked on the ice surface of the EMS and the hollow stem auger drilled down to the soil surface. Shelby tube samples were then taken after which the auger drilled down to the sample depth. This procedure was repeated to a depth of 3 to 4 m. Samples were placed in cold storage until extrusion was possible. Soil samples obtained from this drilling were not analyzed as the silty-sand soils liquefied when disturbed and tended to be forced up the test hole excavation due to the hydraulic head difference between the test hole base and the water table which was higher than the test hole base. This same soil remained stiff, if not disturbed, and the test hole remained open during auger extraction long enough to allow installation of the instrument bundles, backfilling with sand and sealing with bentonite.

Gas samplers were installed on October 4, 2000. Stacked samplers were installed at five different locations designated C31 through C35. Sampling depths vary from 0.25 to 2.5 m below ground surface with all samplers above the water table. All samplers at each location were installed in the same 100 mm diameter borehole. ORP probes were installed at four locations within the plume on September 10, 2001, with probe depths ranging from 1 to 11 m below grade. ORP probes at each location were installed in a single 100 mm diameter borehole. Soil samples from test drilling were analyzed at the Regina Geotechnical Laboratory of the Geotechnical Division of the Prairie Farm Rehabilitation Administration of Agriculture and Agri-Food Canada.

3.3.3.1 Piezometers

Each standpipe piezometer was installed in a 100 to 150 mm diameter hole. Sand was placed to a height of 50 mm above the screened portion of the piezometer. Soil retrieved from the installation depth was compacted above the sand to form a 100 mm to 200 mm soil plug. The remainder of the hole was sealed to surface with bentonite chips (Figure 3.4).

The first piezometer nest was sited as close as practical to the EMS; test drilling proceeded at locations south away from the EMS until no obvious odour was detected in soils taken from the hole. Odour detection was determined by simple sniffing of the samples by a number of staff on site. The last nest site was installed 10 m past the location where odour could no longer be detected.

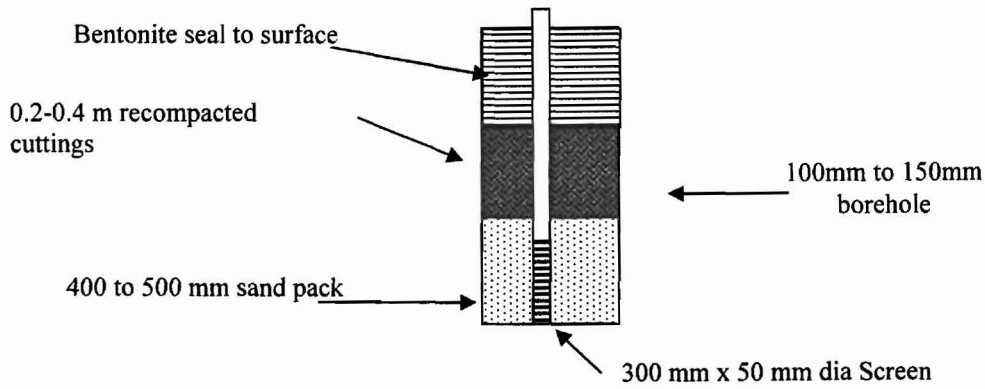

Figure 3.4 – Piezometer installation detail

Monitoring equipment below the EMS was installed within a 300 mm section of 50 mm diameter slotted SCDH 40 PVC screen fitted with a filter sock. The instrumentation consisted of a thermocouple, redox probe, pneumatic piezometer and two 3.18 mm diameter-sampling tubes. A 25 mm poly tubing was placed over the cables and attached to the screen section with a watertight seal (Figure 3.5). Silicone sealant was used to seal the tubing entrance to the PVC screen. Three piezometer tips were placed in the test hole: at the bottom, midpoint, and just below the soil surface. Each PVC screen and associated instrument bundle was sand packed and then sealed with bentonite up to the level of the next installation. After installation of all three piezometer tips, the 25 mm tubing containing the 3.18 mm sampling tubes, thermocouple and ORP leads were extended to the EMS bank for installation in a weatherproof panel. This instrumentation allows measurement of temperature, ORP and hydraulic head below the EMS and also provides the ability to obtain a water sample at the elevation of each of the piezometer tips. Sometime between the spring of 2000 and the spring 2001, the upper most

installation below the EMS was pulled from the ground; during the summer of 2001 this installation was anchored to the EMS floor with concrete blocks.

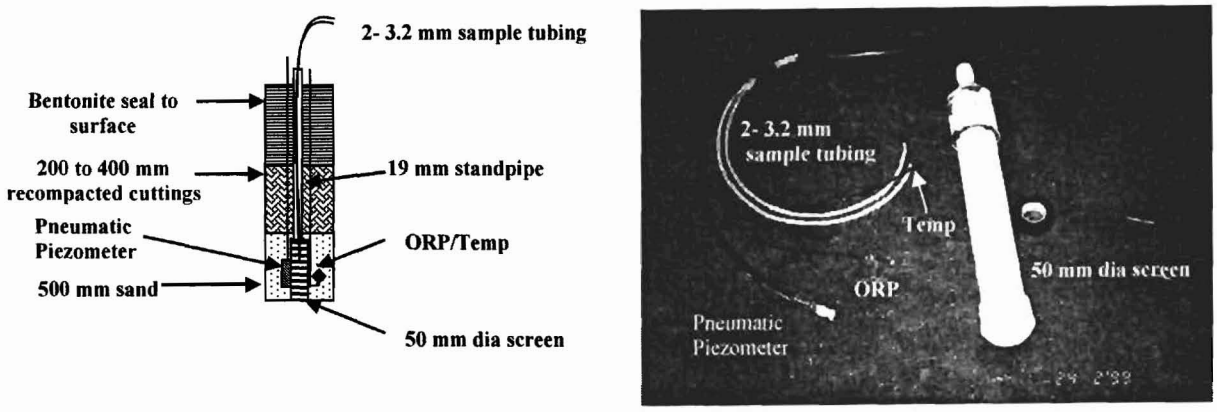

Figure 3.5 - Instrument bundle for inaccessible monitoring locations

3.3.3.2 Thermocouples

Thermocouples installed below the storage were secured to the sample tubes and pneumatic piezometers with PVC electrical tape and then installed as a bundle inside the 50 mm slotted pipe. Thermocouples installed with standpipe piezometers and with gas samplers were secured to the outside of the riser pipe with electrical tape and sand was placed over the tip at each location. Surface terminations were installed in a PVC electrical junction box with a protective cover to prevent weather damage.

3.3.3.3 ORP Electrodes

ORP electrodes were installed in the same manner and in the same PVC junction box as the thermocouples. At locations where only ORP electrodes were installed, electrodes were secured with electrical tape at the appropriate locations along a 19 mm diameter SCHD 40 PVC pipe. The assembly was then inserted at the appropriate elevation in the borehole and

sand placed over the lowest electrodes to a height of approximately 50 mm above the electrode. Bentonite chips were then placed over the sand to a level approximately 50 mm below the next electrode. Sand was then placed over the electrode to a height of approximately 50 mm above the electrode. This procedure was continued until the surface was reached. At several locations the wet silty-sand material would not allow the hole to remain open so that the bentonite seal could be placed between electrodes; at these locations the in-situ material was simply allowed to surround each electrode and then the borehole was sealed near the ground surface with bentonite chips.

3.3.3.4 Soil Gas Samplers

Soil gas samplers were installed at five piezometer nest locations: one on the north side of the EMS and four on the south side. These samplers were installed to determine oxygen gas concentrations within the vadose zone in the area of the plume. All samplers were installed within a single borehole, and secured with electrical tape at the appropriate locations along a 19 mm diameter SCHD 40 PVC pipe. The PVC pipe assembly was then installed at the appropriate elevation in the borehole. Each sampler was installed with 25 to 50 mm of sand above and below the sampler and bentonite between the sand layers. Bentonite was also used at the ground surface to seal the borehole to prevent surface water contamination.

3.3.4 Water Sampling

Water sampling at the site was accomplished by bailing each piezometer with a plastic 1 L bailing tube until approximately three piezometer volumes had been removed or the piezometer was empty. Piezometers were then allowed to recover for 1 to 3 h. A water sample was then retrieved using the tube, and placed in a 100 mL sterile plastic container and stored in a cooler for transport. A portion of each sample were passed through a 0.45 μm filter and analyzed in the field for pH and EC by electrode and alkalinity by titration. Samples were then taken to the laboratory at the Department of Geological Sciences at the University of Saskatchewan where they were diluted and

decanted into vials and then analyzed for Na, Ca, Mg, NH_4, K, Cl, NO_3, and SO_4 using a Dionex Ion Chromatograph.

Water samples were retrieved from piezometers C15, C18, C21, C24 and C29 in February 2000 and from C8 through C10, C14 through C24 and C27 through C29 in May 2004. These samples were field filtered to 0.45 μm and analyzed for pH, temperature and alkalinity. Filtered water samples from each piezometer were sent to the Saskatchewan Research Council for analysis of major ions, minor ions and metals. Special care was taken to ensure minimal air was introduced to the sample; samples were kept at temperatures between 1-5°C and samples were delivered to the laboratory for analysis within several hours of retrieval. Major ions (Ca, Mg, Na, K and SO_4^{2-}) were analyzed by ICP-IRS, carbonates (HCO3-, CO3 and alkalinity) by acid titration, nitrogen and chloride by colorimetric analysis, sulphide and pH by electrode, organic carbon by Dohrman Pheonix carbon analyzer, and metals by ICP-AES.

3.3.5 Instrumentation Reading

Wherever possible, all lines, leads or tubing were installed in steel panel boxes or PVC electrical junction boxes with weather resistant seals.

3.3.5.1 Piezometric Head

Pneumatic piezometers were read with an RSI Digital Pneumatic Piezometer Reader using Argon gas to pressurize the piezometer. Pressure readings were recorded in both kilopascals and pounds, then converted to a height of water using calibration curves supplied by the manufacturer. Standpipe piezometers were read by dropping a standard water level tape meter down each piezometer and recording the level at which the signal is activated.

3.3.5.2 Thermocouples

Thermocouples readings were taken with an Omega HH-25TC digital thermometer Type-T thermocouple reader. Thermocouples in this study were read individually but could be connected to a digital multi-reader.

3.3.5.3 ORP Electrodes

A silver/silver-chloride (Ag/AgCl) reference electrode (–222 mV at 20°C) was used to determine ORP readings at this site. The reference electrode was placed in the edge of the EMS or in a borehole adjacent to the electrodes being read to ensure electrical connectivity. The reference electrode was then connected to the common terminal of a standard multi-meter and the ORP electrode connected to the remaining terminal. Readings required time to stabilize, and were taken when the change in voltage was less than 0.1 mV for a period of 10 sec. This value was corrected by the voltage of the reference electrode to adjust the reading to the zero reference.

3.3.5.4 Soil Gas Samplers

Soil gas samplers were sampled using a Gastech GT Series portable gas monitor equipped with an internal pump. This unit contained sensors for oxygen, carbon dioxide, hydrocarbons and hydrogen sulfide; only oxygen was recorded for this study. Each soil gas sampling tube was fitted with a three-way valve and connected to the portable gas analyzer. The internal pump draws air through the stainless screen buried below grade. Soil gas passes through the poly tubing and past the sensor within the analyzer. Each tube was pumped until a steady reading is obtained. Data was recorded manually. The valve on the end of each tube was turned to seal the tube from ambient air entry after sampling but prior to disconnecting from the sampler.

3.3.6 Sampling and Analysis for Microbial Populations

Water samples from the piezometers at Site No. 1 were retrieved and analyzed for microbial populations in the fall of 2000 and again in the spring of 2001. Samples from standpipe piezometers were retrieved using a 3.18 mm diameter jerk line (3.18 mm diameter poly tubing with a brass checkvalve on the bottom). Purging was accomplished by bailing the water from the piezometer with a disposable bailer. A new bailer was used for each hole to avoid cross-contamination. The tip of the jerk line (checkvalve) was rinsed with 95% ethanol followed by repeated rinsing with deionized water between sampling of piezometers. New tubing was used for each piezometer. The tip of the jerk line was lowered to approximately 0.2 m above the standpipe bottom. By moving the line up and down in the water column (jerking), water was pumped up the line. Approximately 50 mL of the water was allowed to run onto the ground for rinsing. The line was then placed in the sample container that was allowed to fill from the bottom up. The container was overfilled and the lid closed expelling water to ensure minimal air was left in the sample container.

Water samples from below the EMS were retrieved using a suction apparatus connected to a sampling container (Figure 3.6). The sampling container consisted of a Nalgene reusable filter holder system (no.301-500) from Fisher Scientific. The suction source consisted of a small electric vacuum pump attached to an empty propane tank fitted with a pressure gauge and needle valve for suction control. The suction was used to draw water up the tubing and into the container.

After approximately 50 to 100 mL of water had been retrieved, the suction was stopped and the water in the container removed, and discarded. Suction was again applied to the container until approximately 300 mL of sample had accumulated. This water was then poured into sample containers that were then tightly capped, labeled, and placed in a cooler. These containers were overfilled with water to allow minimal oxygen contact; due to limited water available at some positions, this was not always possible. Sampling equipment was rinsed with 95% ethanol and deionized water between each sample. Handling of water

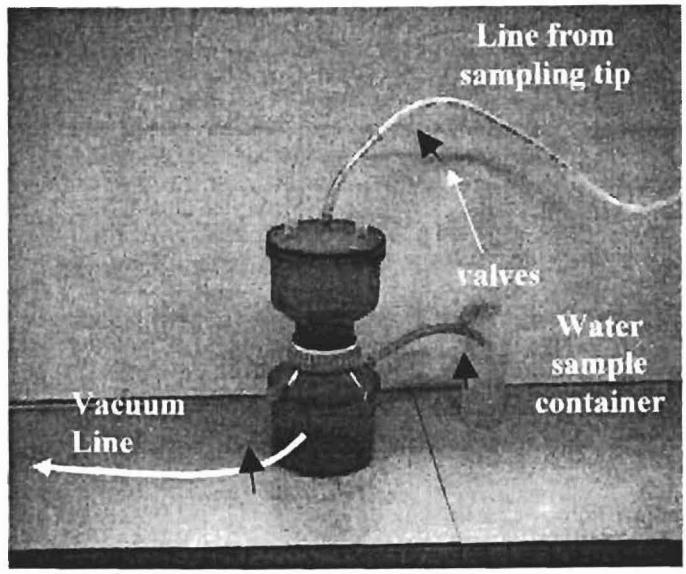

Figure 3.6 – Suction sampling apparatus

sampling equipment and sample protocol was developed under the guidance of Dr. J.R. de Freitas, microbiologist with the Department of Soil Science at the University of Saskatchewan and Sheila Blachford, M.Sc. B.Sc.(Hons), Manager of Microbiology, BDS Laboratories, BDS Microbial Services Inc., Qu'Appelle, Saskatchewan.

BDS Laboratories in Qu'Appelle, Saskatchewan completed sample analysis for the fall 2000 sampling. BDS Laboratories could not accommodate analysis of the spring 2001 samples so PBR Laboratories Inc., Edmonton, Alberta agreed to use the same methodology as BDS Laboratories. Analysis consisted of determination of standard plate count, anaerobic plate count, total coliforms, fecal coliforms, *E.Col* counts, *E*coli 0157 (presence or absence), iron reducing and denitrifying bacteria (presence or absence) and sulphate reducing and methanogenic bacteria counts. PBR Laboratories, Edmonton, Alberta and BDS Laboratories, BDS Microbial Services Inc., Qu'Appelle, Saskatchewan supplied the following analysis methodology:

1. **Standard Plate Count** (considered total aerobes and facultative anaerobes): Standard plate counts were determined by Pour Plate Method (APHA, AWWA, WEF 1998). Each sample was serially diluted to 10^{-1} to 10^{-4} sample dilutions. Three dilutions were plated for enumeration. One mL of

each of the three dilutions was plated in duplicate using pour plate technique. Standard plate count Agar (Oxoid) was used as the medium of choice. After autoclaving, the temperature of the medium was equilibrated to 45°C prior to placing. The plates were incubated at 35+/- 2 °C for 48 hours. At the end of incubation, plates producing countable colonies were scored.

2. **Anaerobic Plate Count** (total anaerobes): Anaerobic plate counts were determined by Pour Plate Method (Difco, 1984). Each sample was serially diluted to 10^{-1} to 10^{-4} sample dilutions. Three dilutions were plated for enumeration. One mL of each of the three dilutions was plated induplicate using pour plate technique. Brewer Anaerobic Agar (Merck) was used as the medium of choice. After autoclaving, the temperature of the medium was equilibrated to 45°C prior to placing. The plates were incubated at 35+/- 2 °C for 48 hours in anaerobic chambers using BBL™ Gas Pak *Plus*™ (Becton Dickinson). At the end of incubation, plates producing countable colonies were scored.
3. **Total Coliforms:** Total Coliform counts were determined by MPN method (APHA, AWWA, WEF 1998). Lauryl tryptose broth (Difco) was used for the three tube MNP technique. Four dilutions from 10^{-1} to 10^{-4} of the sample were used for enumeration. The tubes were incubated at 35+/- 2 °C for 48 hours. At the end of the incubation MPN index per mL was determined.
4. **Fecal Coliforms:** Fecal Coliforms were also determined by MPN method (APHA, AWWA, WEF 1998). BBL™ EC broth with MUG (Becton Dickinson) was used to determine the Fecal Coliform count. Four dilutions from 10^{-1} to 10^{-4} of the sample were used for enumeration. The tubes were incubated at 44.5+/- 0.2 °C for 48 hours. At the end of the incubation MPN index per mL was determined. Tubes with typical blue fluorescence at 366-nm were used to determine the *E.Coli* count.
5. ***E*coli Counts**: *E.Coli* Counts were also determined by MPN method (APHA, AWWA, WEF 1998). BBL™ EC broth with MUG (Becton Dickinson) was used to determine the *E.Coli* count. Four dilutions from 10^{-1} to 10^{-4} of the sample were used for enumeration. The tubes were incubated

at 44.5+/- 0.2 °C for 48 hours. At the end of the incubation MPN index per mL was determined. Tubes with typical blue fluorescence at 366-nm were used to determine the *E.Coli* count.

6. ***Ecoli* 0157 (presence or absence)**: *E.Coli 0157* counts were determined by Membrane Filtration Method (Gov. Canada, 1995). Samples which were positive for *E.Coli* were tested to detect the presence of *E.Coli 0157.* Sorbitol MaConkey agar (Oxoid) along with its selective supplement was used to detect the presence of *E.Coli 0157.* One mL of the sample was filtered through 0.45μm filter, the filter was then placed on the specified medium and incubated at 35+/- 2 °C for 24 hours. Typical *E.Coli 0157* colonies were scored after 24 hours.
7. **Iron Reducing and Denitrifying Bacteria** (presence or absence): Iron and denitrifying bacteria were determined for presence of absence using BART™ kits (Drycon Bioconcepts Inc.) supplied by HACH. Iron bacteria samples were inoculated and observed for 8 days at room temperature for typical brown color development. Denitrifying bacteria samples were inoculated and observed for 3 days at room temperature for typical foam development.
8. **Sulphate Reducing Bacteria Counts**: Sulphate Reducers were determined by Pour Plate Meethod (APHA, AWWA, WEF 1998). One mL of the undiluted sample and one mL of the 10-1 dilution of the sample were plated in duplicate. The plates were incubated anaerobically at 30°C for one week in anaerobic chambers using BBL™ Gas Pak *Plus*™ (Becton Dickinson) anaerobic system envelopes. At the end of the incubation, typical black colonies were counted as sulphate reducing bacteria.
9. **Methanogenic Bacteria Counts**: Methanogens were determined by Pour Plate Method (Atlas, 1997). Methanogen Enrichment Medium, Barker, was used to determine the Methanogens count. One mL of the undiluted sample and one mL of the 10-1 dilution of the sample were plated in duplicate. The plates were incubated anaerobically for one week in anaerobic chambers using BBL™ Gas Pak *Plus*™ (Becton Dickinson) anaerobic system envelopes. At the end of the incubation plates were scored for growth.

4 PRESENTATION OF RESULTS

4.1 EMS Effluent Chemistry

4.1.1 Eh, EC, DO, pH, Temperature and TS Profiles

Profiles were created for the two study sites (Figures 4.1 and 4.2). Fluid throughout the EMS had Eh readings of <-100mV and low DO levels, indicating reducing and anaerobic conditions. The Clearfield Feeder Unit EMS (Figure 4.1) DO concentrations ranged from 0.3 to 1.3 mg/L. Site No 1 EMS (Figure 4.2) DO concentrations ranged from 0.3 mg/L near the surface to the instrument detection limit of 0.1 mg/L at 0.5 m below the surface. pH of the Clearfield EMS ranged from 6.9 to 7.2; Site 1 EMS remained constant at 7.7 throughout the profile. The EC of both EMS was ~20 mS/cm in the upper portion above the settled solids and decreased within the solids to 8 and 13 mS/cm for the Clearfield and Site 1 EMS respectively. Total solids (TS) profiles for both EMS are similar with TS ranging between 2,000 (2%) and 5,000 mg/L (5%) in the upper two thirds of the storage, increasing to greater than 40,000 mg/L (40%) in the lower third.

4.1.2 Filtered Sample Analysis

Results of analyses of filtered raw manure samples are provided in units of mg/L (Table 4.1, Figure 4.3), meq/L (Table 4.2, Figure 4.4) and molality (mol/kg H_2O; Table 4.3, Figure 4.5) respectively. Eh values calculated using the S(-2)/S(-6) redox couple ranged between –197 and –270 mV (Table 4.3); these values were only slightly lower than Eh readings in the EMS ponds at the two sites (–150 to –250mV; Figures 4.1 and 4.2). Reducing conditions may result from organic matter in the EMS; organic matter contents ranged between ~5 and 40%. Figure 4.2 clearly shows the major cation and

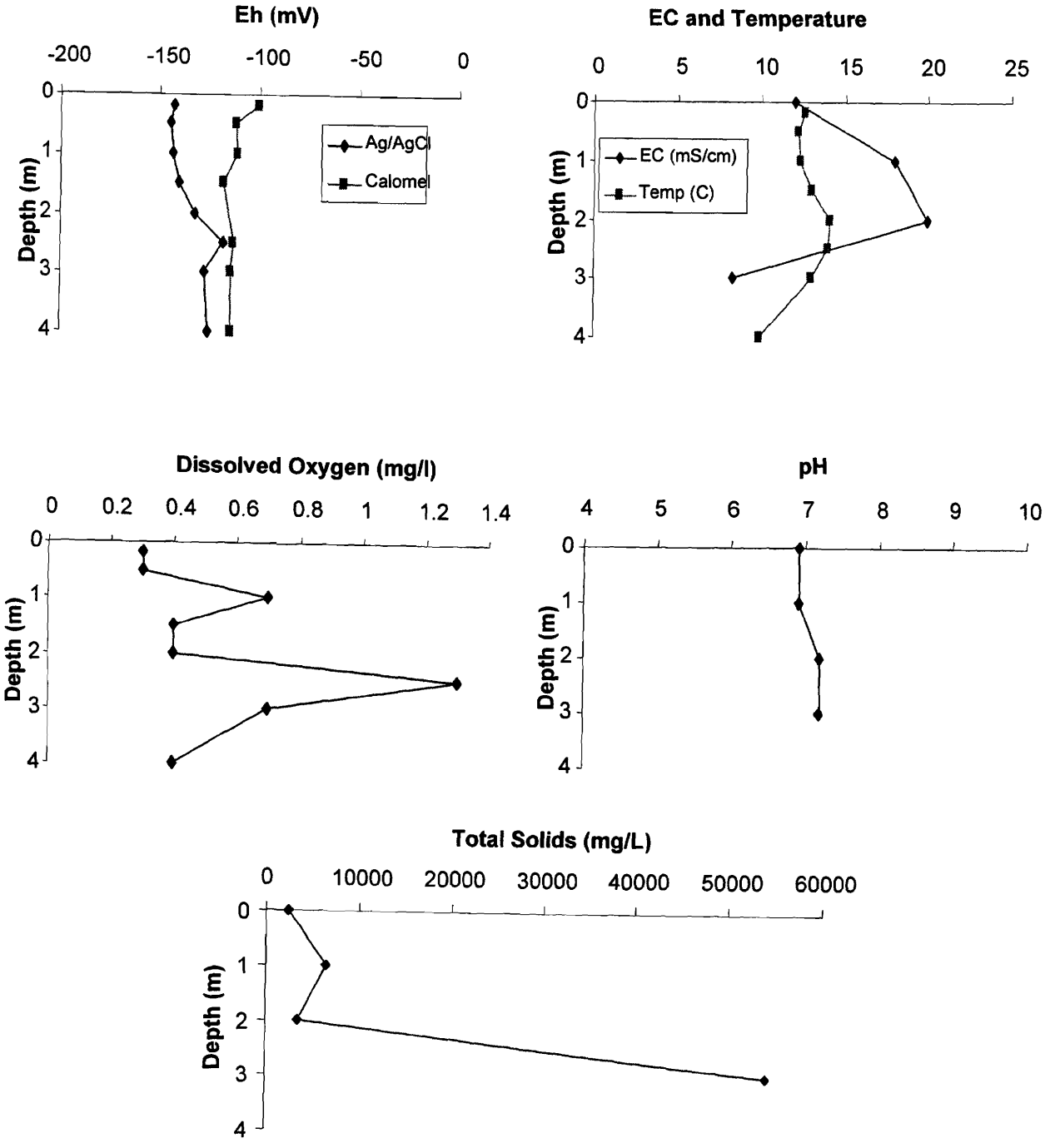

Figure 4.1: Characteristics with Depth for Clearfield Feeder Unit Cell No. 1

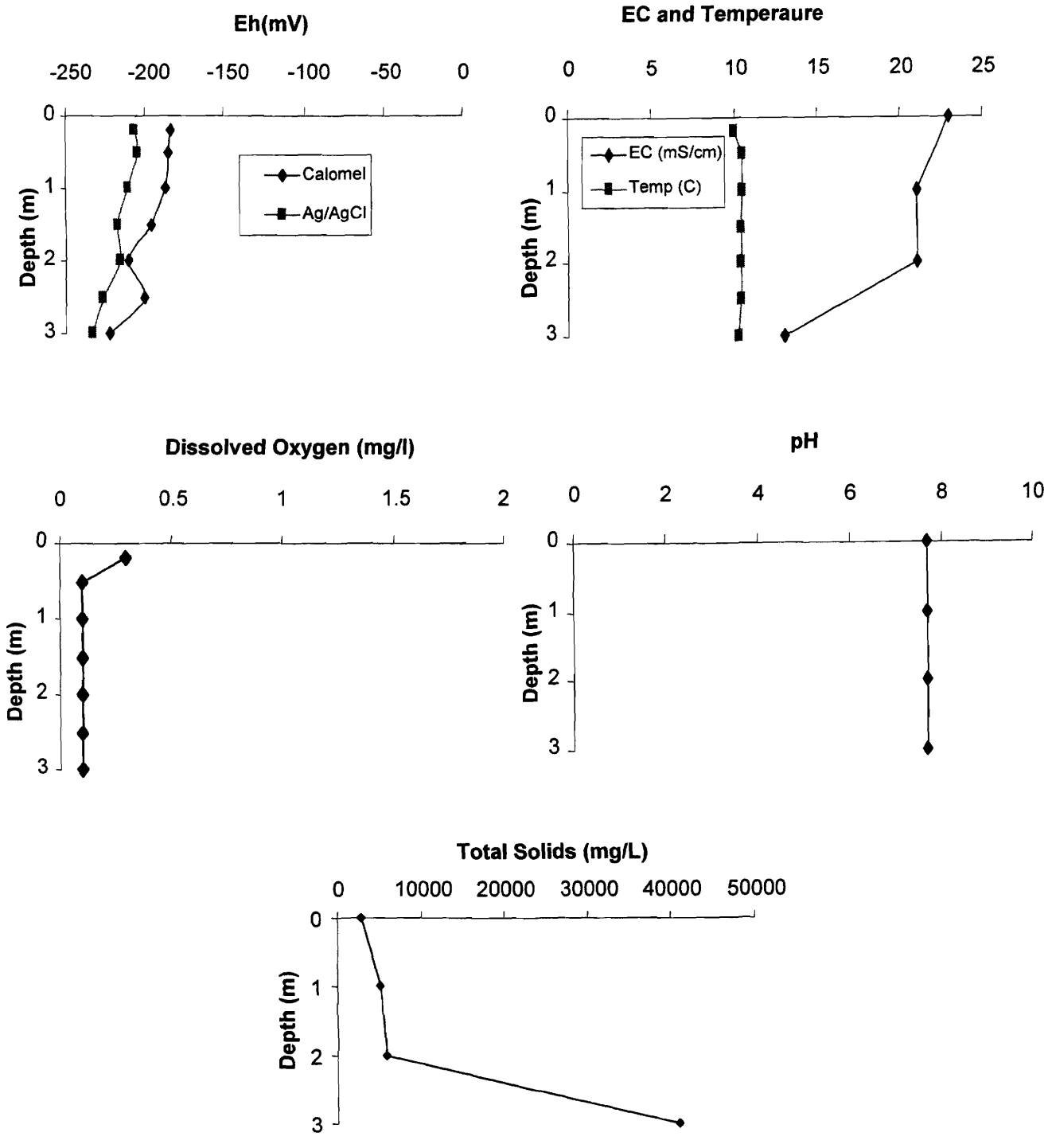

Figure 4.2: Characteristics with depth for the EMS at ADF Research Site No. 1

Table 4.1 - Laboratory analysis results for filtered manure samples (mg/L)

	Source		ADF Research Site 1	ADF Research Site 9	Big Sky 1 Farrowing Unit	Clearfield Feeder Unit	PSC Elstow Research Farm	Peterson	MacKay (Aerated)				
	Sample No.		1	2	3	4	5	6	7				
	PHREEQC annotation	units								Average	Standard Deviation	Minimum	Maximum
pH	pH		8.27	6.94	7.33	7.66	8.26	7.68	7.1	7.61	0.52	6.94	8.27
Ammonium N	Amm	mg/L	3716	2957	1903	3729	4147	3941	6763	3879	1483	1903	6763
Potassium	K	mg/L	2400	1230	740	1840	1720	2060	4170	2023	1092	740	4170
Sodium	Na	mg/L	529	330	490	1260	394		1400	734	469	330	1400
Calcium	Ca	mg/L	90	210	75	502	72		191	190	164	72	502
Magnesium	Mg	mg/L	2.7	13	250	301	0.8		9.4	96.2	139.9	0.8	301
Alkalinity	Alkalinity	mg/L $CaCO_3$	12200	7400	5810	12800	12700	11000	20000	11701	4565	5810	20000
Chloride	Cl	mg/L	1590	1030	575	1180	1300	1160	2620	1351	638	575	2620
Sulfate	S(6)	mg/L	357	1300	1150	933	316	78	761	699	461	78	1300
Sulfide	S(-2)	mg/L	0.02	27			0.04	36.7		15.9	18.8	0.02	36.7
Nitrate as N	N(5)	mg/L	2.3		1	1.5	12	0.32	4.7	3.6	4.4	0.32	12
Nitrite as N	N(3)	mg/L	2.2	0.03	0.05	0.17	5.9	0.02		1.40	2.37	0.02	5.9
Phosphorus	P	mg/L	350	110	4.8	8.1	120		93	114	126	4.8	350
Silicon	Si	mg/L	81	64	47	86	30			62	23	30	86
Iron	Fe	mg/L	0.79	4.5	4.3	6.7	0.11			3.28	2.76	0.11	6.7
Boron	B	mg/L	0.71	1.1	0.51	1.2	2.1			1.12	0.61	0.51	2.1
Strontium	Sr	mg/L	0.34	0.43	0.5	3.5	0.46			1.05	1.37	0.34	3.5
Zinc	Zn	mg/L	0.042	5.1	0.01	0.019	0.002			1.03	2.27	0.002	5.1
Manganese	Mn	mg/L	0.054	0.38	0.04	3.5	0.096			0.81	1.51	0.04	3.5
Barium	Ba	mg/L	0.087	0.064	0.028	0.54	0.02			0.15	0.22	0.02	0.54
Copper	Cu	mg/L	0.016	0.41	0.015	0.004	0.006			0.09	0.18	0.004	0.41
Lead	Pb	mg/L	0.2	0.007		0.002	0.002			0.05	0.10	0.002	0.2
Inorganuc Carbon		mg/L	9230										
Organic Carbon		mg/L	6300										

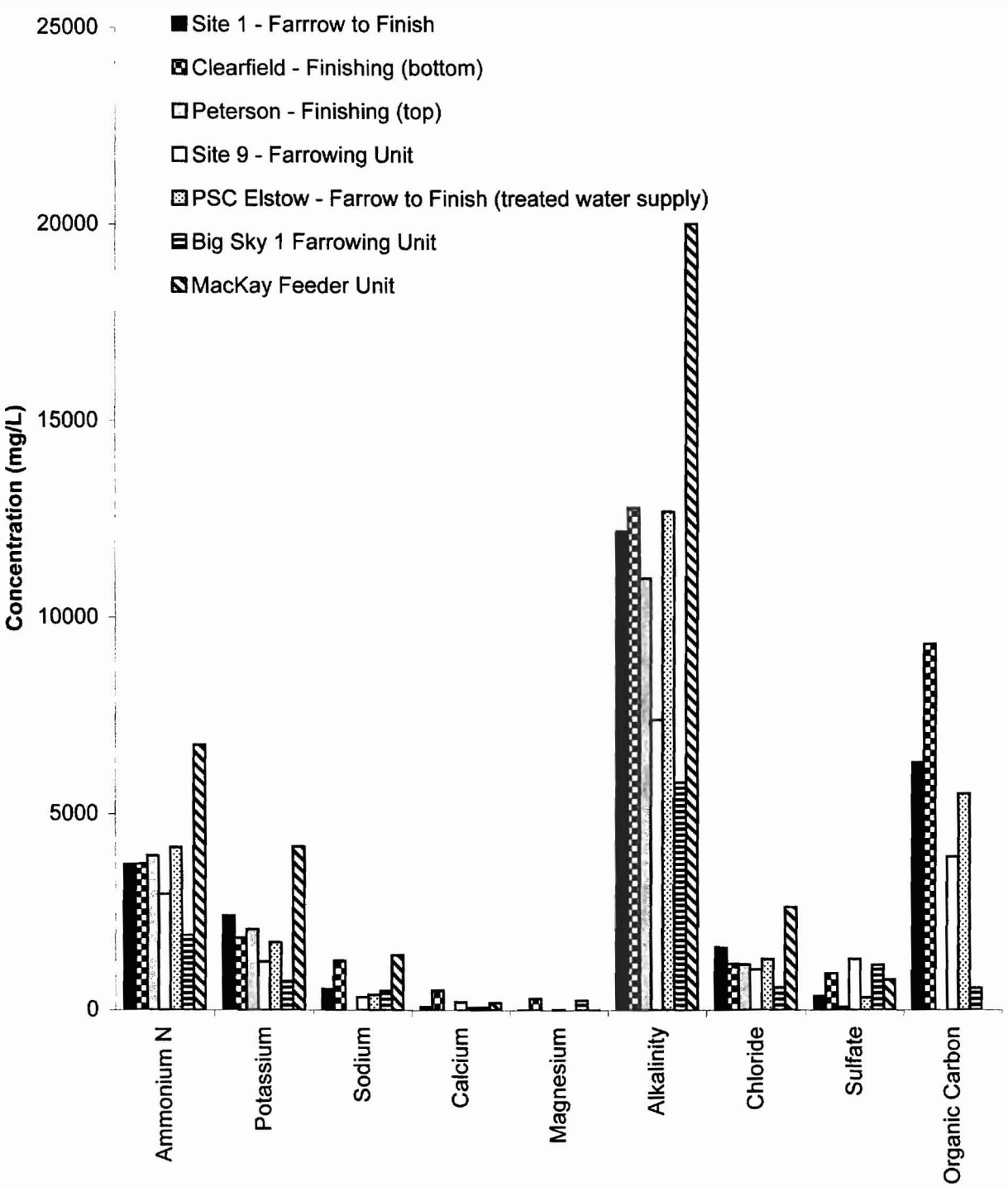

Figure 4.3: Select EMS Effluent Chemistry (raw data in mg/L) (liquid fraction only)

Table 4.2 - Laboratory analysis results for filtered manure samples (meq/L)

	Source		ADF Research Site 1	ADF Research Site 9	Big Sky 1 Farrowing Unit	Clearfield Feeder Unit	PSC Elstow Research Farm	Peterson	MacKay (Aerated)				
	Sample No.		1	2	3	4	5	6	7				
	PHREEQC annotation	units								Average	Standard Deviation	Minimum	Maximum
pH	pH		8.27	6.94	7.33	7.66	8.26	7.68	7.1	7.61	0.52	6.94	8.27
Ammonium N	Amm	meq/L	206	164	105	207	230	218	375	215	82	105	375
Potassium	K	meq/L	61	31	19	47	44	53	107	52	28	19	107
Sodium	Na	meq/L	23	14	21	55	17		61	32	20	14	61
Calcium	Ca	meq/L	4	10	4	25	4		10	9	8	4	25
Magnesium	Mg	meq/L	0.2	1.1	20.6	24.8	0.1		0.8	7.9	11.5	0.1	24.8
Alkalinity	Alkalinity	meq/L	244	148	116	256	254	220	400	234	91	116	400
Chloride	Cl	meq/L	45	29	16	33	37	33	74	38	18	16	74
Sulfate	S(6)	meq/L	7	27	24	19	7	2	16	15	10	2	27
Sulfide	S(-2)	meq/L	0.001	0.8			0.001	1.1		0.5	0.6	0.001	1.11
Nitrate as N	N(5)	meq/L	0.037		0.016	0.024	0.194	0.005	0.076	0.1	0.1	0.005	0.194
Nitrite as N	N(3)	meq/L	0.0478	0.0007	0.0011	0.0037	0.1283	0.0004		0.03	0.05	0.0004	0.128
Phosphorus	P	meq/L	11.3	3.6	0.2	0.3	3.9		3.0	4	4	0.2	11.3
Silicon	Si	meq/L	2.9	2.3	1.7	3.1	1.1			2	1	1	3
Iron	Fe	meq/L	0.014	0.081	0.077	0.120	0.002			0.06	0.05	0.002	0.120
Boron	B	meq/L	0.07	0.10	0.05	0.11	0.19			0.10	0.06	0.05	0.19
Strontium	Sr	meq/L	0.004	0.005	0.006	0.040	0.005			0.01	0.02	0.004	0.040
Zinc	Zn	meq/L	0.00064	0.07802	0.00015	0.00029	0.00003			0.02	0.03	0.00003	0.078
Manganese	Mn	meq/L	0.00098	0.00692	0.00073	0.06371	0.00175			0.01	0.03	0.0007	0.064
Barium	Ba	meq/L	0.00063	0.00047	0.00020	0.00393	0.00015			0.001	0.002	0.0001	0.004
Copper	Cu	meq/L	0.00025	0.00645	0.00024	0.00006	0.00009			0.001	0.003	0.00006	0.006
Lead	Pb	meq/L	0.00097	0.00003		0.00001	0.00001			0.0003	0.0005	0.00001	0.001

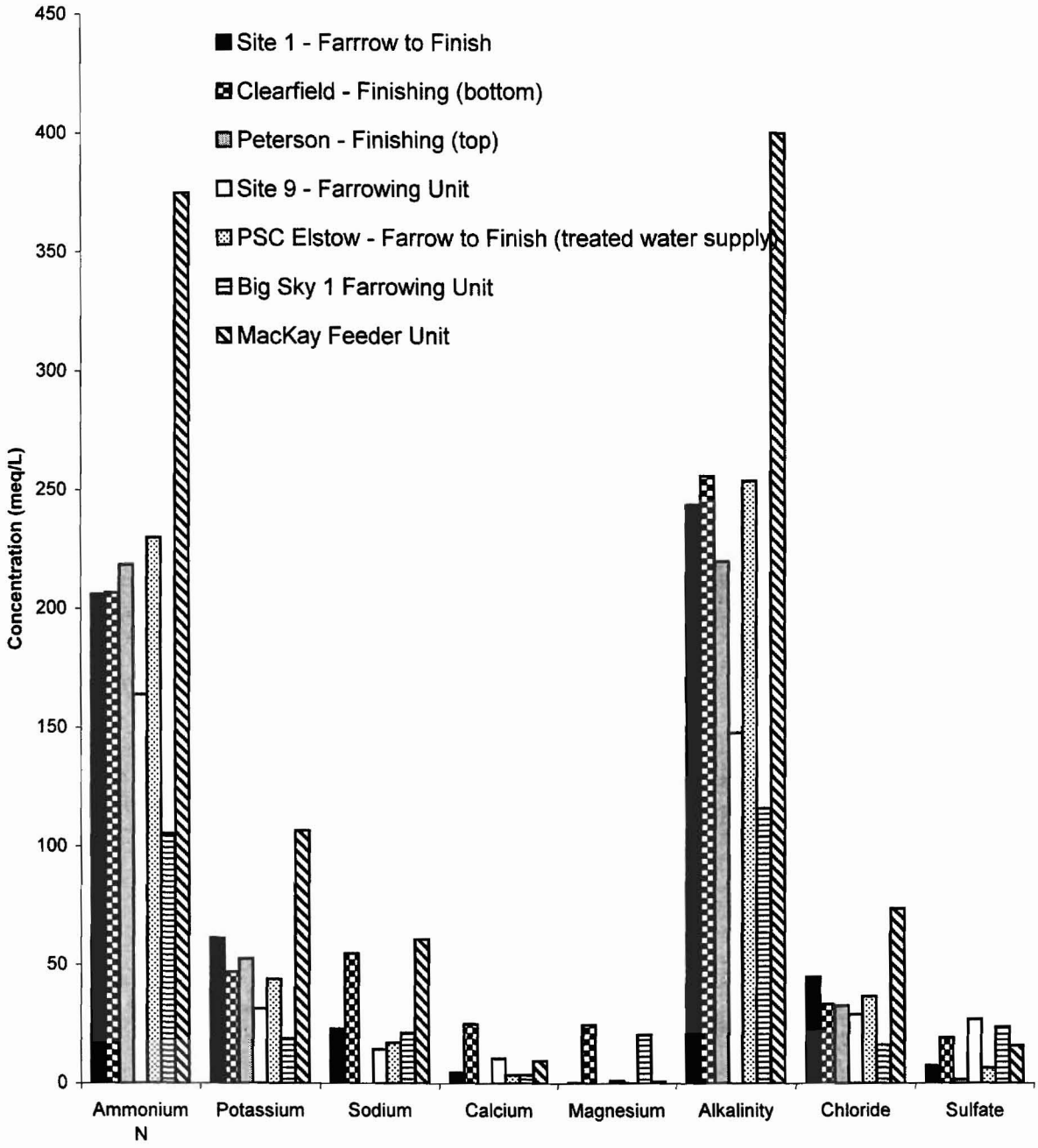

Figure 4.4: Select EMS effluent chemistry (raw data in meq/L)
(liquid fraction only)

Table 4.3 Raw data of various EMS samples

		Site 1	Site 9	Big Sky Farrowing Unit	Clearfield Feeder Unit	PSC Elstow	Peterson Feeder Uint	MacKay			
Type of Facility		Farrow to Finnish	Farrow to Wean	Farrow to Wean	Feeder	Farrow to Finnish	Feeder	Feeder			
Elements									Average	Stdev	Stdev/Ave
pH		8.3	6.94	7.33	7.66	8.26	7.68	7.1	7.61	0.53	7%
[1]pe	S(-2)/S(6)	-4.6	-3.4			-4.64	-4.53		-4.29	0.60	14%
[1]Eh (mV)	S(-2)/S(6)	-268	-197			-270	-268		-250.75	35.85	14%
[2]Ionic Strength		0.31	0.22	0.17	0.32	0.3	0.3	0.5	0.30	0.10	34%
Al	Molality	3.79E-06	5.27E-05						2.82E-05	3.46E-05	122%
Alkalinity	Molality	2.49E-01	1.50E-01	1.17E-01	2.20E-01	2.59E-01	2.45E-01	3.76E-01	2.31E-01	8.36E-02	36%
B	Molality	6.71E-05	1.03E-04	4.77E-05	1.13E-04	1.98E-04			1.06E-04	5.81E-05	55%
Ba	Molality	6.47E-07	4.73E-07	2.06E-07	4.02E-06	1.49E-07			1.10E-06	1.64E-06	150%
Ca	Molality	2.29E-03	5.32E-03	1.89E-03	1.28E-02	1.84E-03	2.55E-03	6.32E-03	4.71E-03	3.98E-03	84%
Cl	Molality	4.58E-02	2.95E-02	1.64E-02	3.40E-02	3.75E-02	3.34E-02	6.22E-02	3.70E-02	1.42E-02	38%
Cu	Molality	2.57E-07	6.55E-06	2.39E-07	6.43E-08	9.64E-08			1.44E-06	2.86E-06	198%
Fe	Molality	1.45E-05	8.18E-05	7.79E-05	1.23E-04	2.01E-06			5.97E-05	5.03E-05	84%
K	Molality	6.27E-02	3.19E-02	1.91E-02	4.81E-02	4.49E-02	5.38E-02	9.74E-02	5.11E-02	2.49E-02	49%
Mg	Molality	1.14E-04	5.43E-04	1.04E-02	1.26E-02	3.36E-05	2.10E-03	3.15E-04	3.73E-03	5.40E-03	145%
Mn	Molality	1.00E-06	7.02E-06	7.36E-07	6.51E-05	1.79E-06			1.51E-05	2.80E-05	185%
N(-3)	Molality	2.11E-01	1.67E-01	1.07E-01	2.11E-01	2.35E-01	2.23E-01	3.98E-01	2.22E-01	8.90E-02	40%
N(3)	Molality	1.61E-04	2.17E-06	3.61E-06	1.24E-05	4.30E-04	1.46E-06		1.02E-04	1.73E-04	170%
N(5)	Molality	1.68E-04		7.22E-05	1.09E-04	8.75E-04	2.33E-05		2.50E-04	3.54E-04	142%
Na	Molality	2.35E-02	1.46E-02	2.16E-02	5.60E-02	1.75E-02	2.22E-02	5.26E-02	2.97E-02	1.71E-02	58%
P	Molality	1.16E-02	3.60E-03	1.57E-04	2.67E-04	3.96E-03	2.50E-03	2.81E-03	3.55E-03	3.83E-03	108%
Pb	Molality	9.86E-07	3.43E-08		9.86E-09	9.86E-09			2.60E-07	4.84E-07	186%
S(-2)	Molality	6.37E-07	8.55E-04			1.27E-06	1.17E-03		5.06E-04	5.97E-04	118%
S(6)	Molality	3.80E-03	1.37E-02	1.21E-02	9.92E-03	3.36E-03	8.29E-04	9.10E-03	7.55E-03	4.89E-03	65%
Si	Molality	1.38E-03	1.08E-03	7.91E-04	1.46E-03	5.10E-04			1.04E-03	3.99E-04	38%
Sr	Molality	3.97E-06	4.98E-06	5.77E-06	4.08E-05	5.36E-06			1.22E-05	1.60E-05	132%
Zn	Molality	6.57E-07	7.92E-05	1.55E-07	2.97E-07	3.13E-08			1.61E-05	3.53E-05	220%

Notes: 1) Values are calculated from S(-2)/S(6) redox couple
2) Calculated using PHREEQC

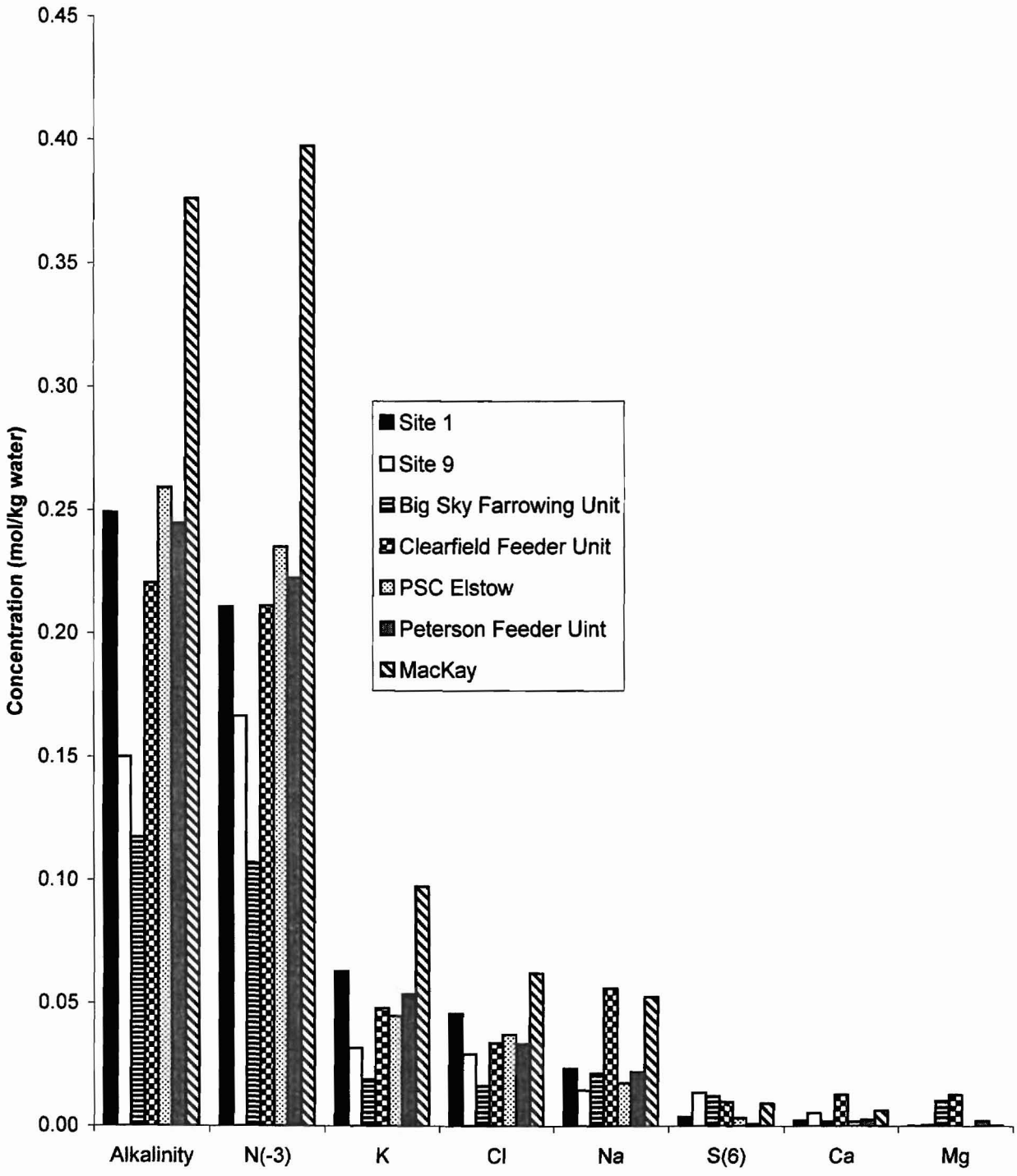

Figure 4.5: EMS source chemistry results of seven samples from various sites. Raw data plotted as molality.

anion are ammonium and bicarbonate (alkalinity) respectively for all samples analyzed. Potassium and chloride are also significant in all samples but are approximately one quarter the concentration of the two major ions. Sodium, calcium, magnesium and sulfate vary between samples, and may indicate these ions have a greater dependence on water and feed sources at the facilities. Organic carbon (Figure 4.5) transports similarly to chloride (Maule and Fonstad, 2000) and should reduce oxygen levels in a plume due to increased microbial activity. Variances in the measured data could be the result of differences in water source, feed mixes and animal age.

Variations in ammonium and bicarbonate influenced ionic strength of solutions (determined using PHREEQC; Parkhurst and Appelo, 1999) which ranged from 0.17 to 0.5 (Table 4.3). Figure 4.6 provides a bar graph of the concentration in molality for the seventeen most abundant species of ions. The eight most abundant ions as determined by PHREEQC were NH_4^+, HCO_3^-, K^+, Cl^-, Na^+, CO_2, SO_4^{2-}, and NH_3 (Figure 4.7). Bicarbonate (HCO_3^-) is the major anion and ammonium [NH_4^+ or N(-3)] the major cation for all samples. Potassium (K^+) and chloride (Cl-) are also significant with some sodium (Na^+) and sulfate [SO_4^{-2} or S(6)]. Ammonium and bicarbonate are rarely used in tracer studies or studies of EMS seepage transport modeling. Chloride is the most commonly used tracer ion in investigations of EMS seepage while potassium (K), an ion of similar activity, is rarely considered. Ion species order from most to least abundant was similar for all samples regardless of concentration variations (Figure 4.6 and Table 4.4); this consistency was expected as all samples had high bicarbonate and ammonium levels, low Eh and neutral pH conditions. Although calcium and magnesium are important in terms of molar concentrations (Figure 4.5), low activity coefficients at the ionic strengths indicated produce relatively low activities for these ions compared with major ions.

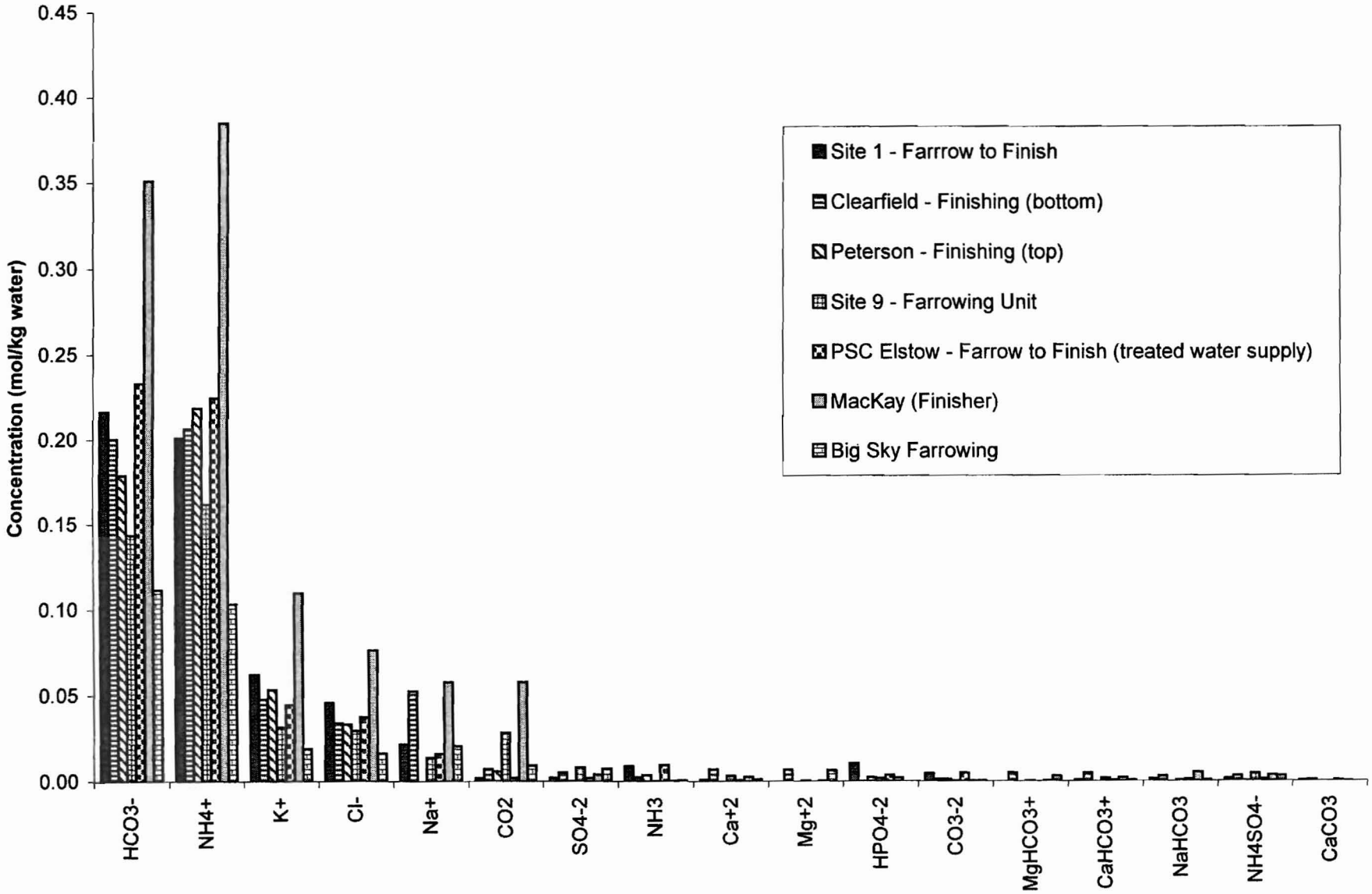

Figure 4.6: Relative concentration of species in seven EMS effluent samples as predicted by PHREEQC software.

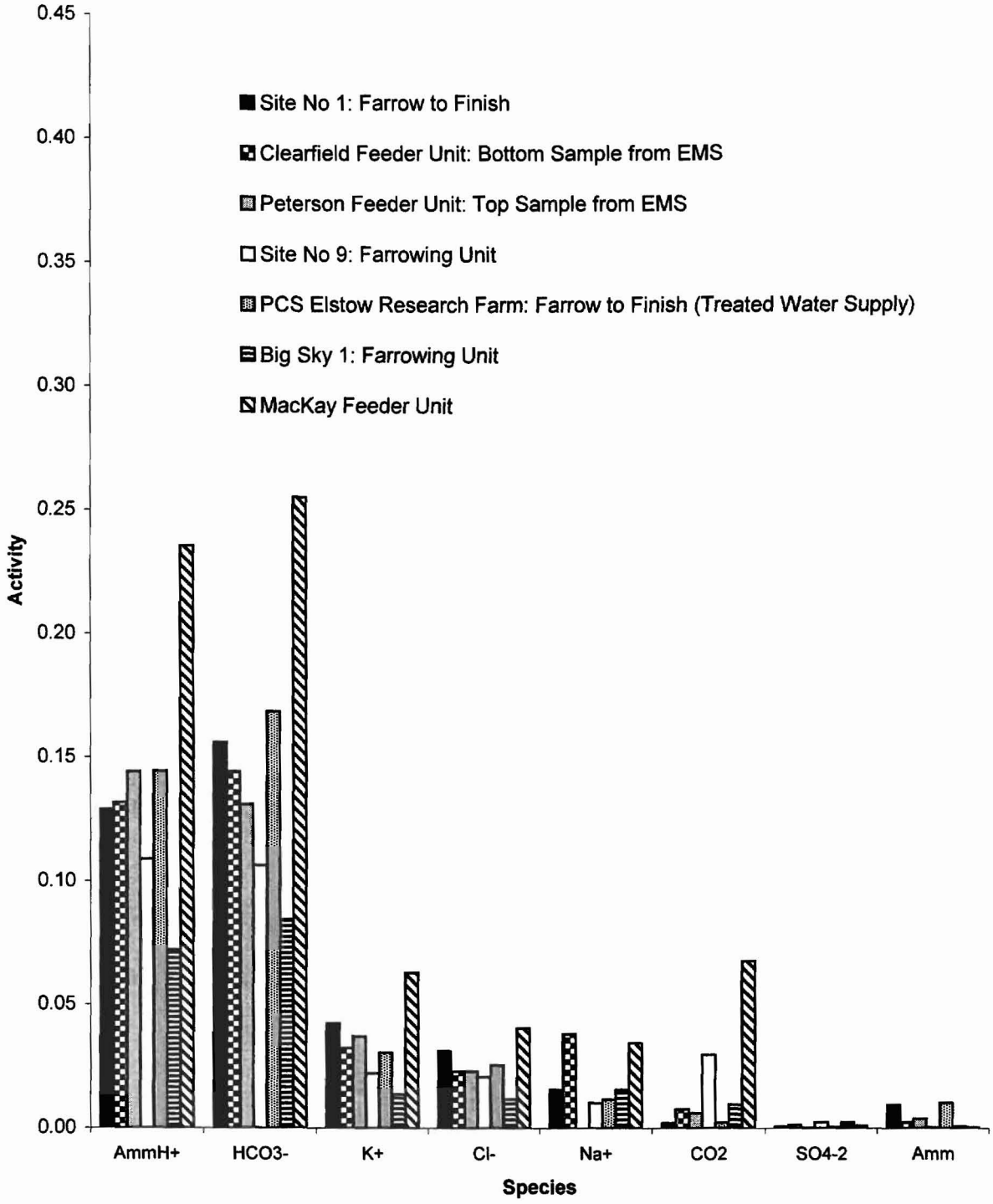

Figure 4.7: Activity of the most abundant species found in seven EMS effluent samples as predicted by PHREEQC software.

Table 4.4 – Concentration of select ion species from analysis of seven manure samples.

	Site 1	Clearfield	Peterson	Site 9	PCS	MacKay	Big Sky	
Species	Molality	Molality	Molality	Molality	Molality	Molality	Molality	Average
HCO3-	2.2E-01	2.0E-01	1.8E-01	1.4E-01	2.3E-01	3.5E-01	1.1E-01	2.03E-01
NH4+	2.0E-01	2.1E-01	2.2E-01	1.6E-01	2.2E-01	3.8E-01	1.0E-01	2.04E-01
K+	6.2E-02	4.8E-02	5.3E-02	3.1E-02	4.5E-02	1.1E-01	1.9E-02	4.03E-02
Cl-	4.6E-02	3.4E-02	3.3E-02	2.9E-02	3.7E-02	7.6E-02	1.6E-02	3.48E-02
Na+	2.2E-02	5.3E-02		1.4E-02	1.6E-02	5.8E-02	2.1E-02	1.53E-02
CO2	1.9E-03	7.1E-03	5.9E-03	2.8E-02	2.1E-03	5.8E-02	9.2E-03	1.08E-02
SO4-2	2.2E-03	5.2E-03	4.7E-04	8.2E-03	1.9E-03	4.0E-03	7.5E-03	4.04E-03
NH3	8.7E-03	2.2E-03	3.6E-03	3.5E-04	9.6E-03	3.2E-04	5.8E-04	6.50E-03
Ca+2	8.3E-04	6.9E-03		3.0E-03	7.2E-04	2.7E-03	1.2E-03	1.48E-03
Mg+2	4.0E-05	6.8E-03		2.9E-04	1.4E-05	1.8E-04	6.3E-03	1.07E-04

Note: Values determined using a speciation model – PHREEQC Parkhurst and Appelo (1999)

Individual ion concentrations from speciation of each solution (Table 4.4) were divided by total molality or activity to normalize data for all sites (Figures 4.8 and 4.9, Table 4.5). Relative concentration of the four most abundant ions in all seven samples was similar, suggesting an approximate concentration could be determined knowing the total concentration of ions in solution. Differences between samples could result from variation in animal age and feed and water chemistry.

Table 4.5 – Concentration of the most abundant ions in EMS effluent from seven sites in Saskatchewan. Values are average percent of total and (standard deviation).

Ion	Molality	Activity
Ammonium ($NH4^+$)	36% (2%)	34% (1%)
Bicarbonate (HCO3-)	36% (3%)	38% (3%)
Potassium (K^+)	8% (2%)	8% (1%)
Chloride (Cl-)	6% (1%)	6% (1%)
Sodium (Na+)	5% (2%)	5% (2%)
Suphate (SO4-2)	1% (1%)	< 1%
Carbon Dioxide (CO2)	3% (3%)	4% (4%)

Landfill leachate generally contains slightly lower ammonium, potassium and bicarbonate levels and slightly higher sodium, calcium, magnesium and chloride than hog manure (Figure 4.10 and 4.11). Landfill leachate can contain metals and organics

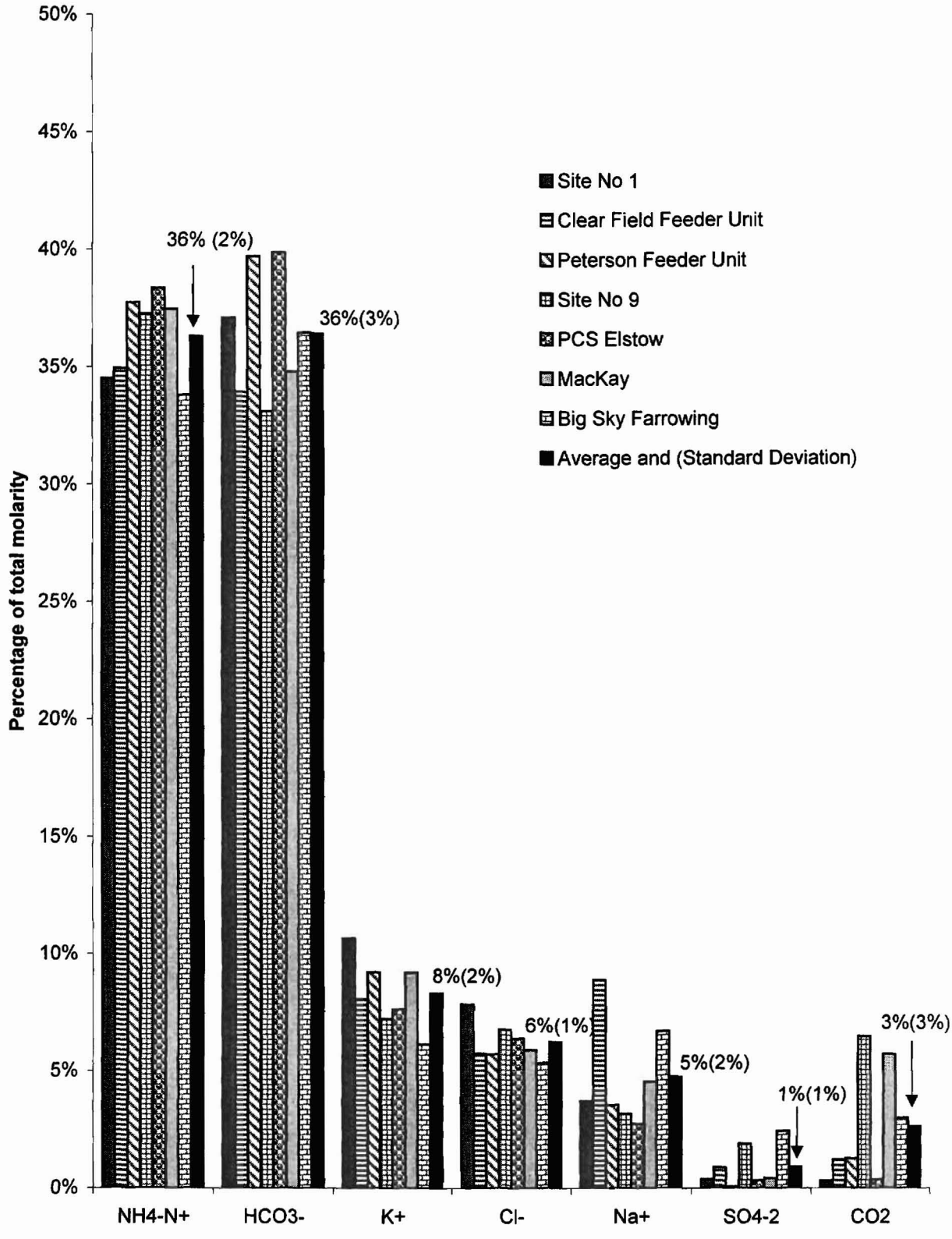

Figure 4.8: EMS source chemistry percentage of total molarity. Values are analytical results from filtered samples and speciation using PHREEQC software.

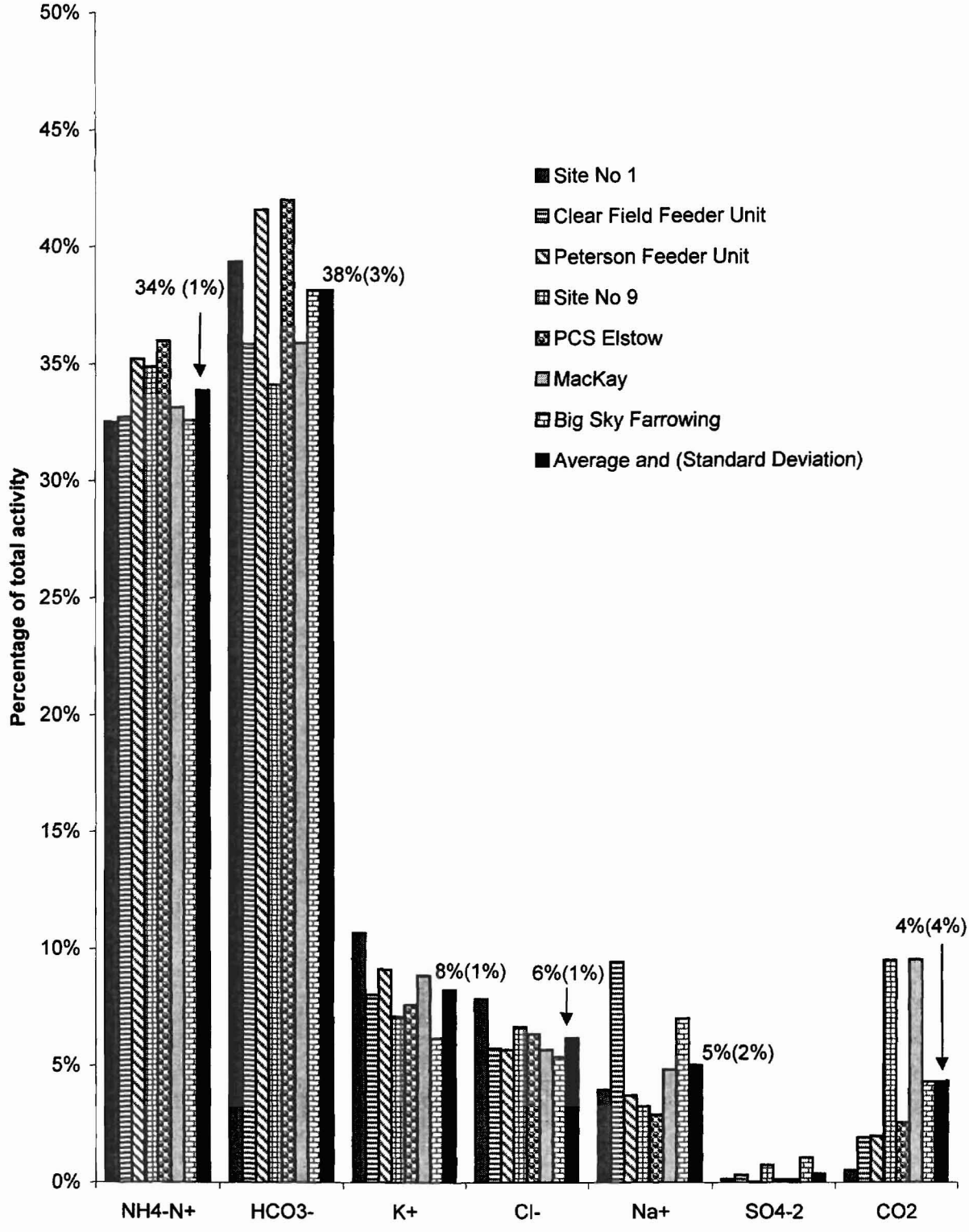

Figure 4.9: EMS source chemistry percentage of total activity. Values are analysis of filtered samples and then speciation using PHREEQC software.

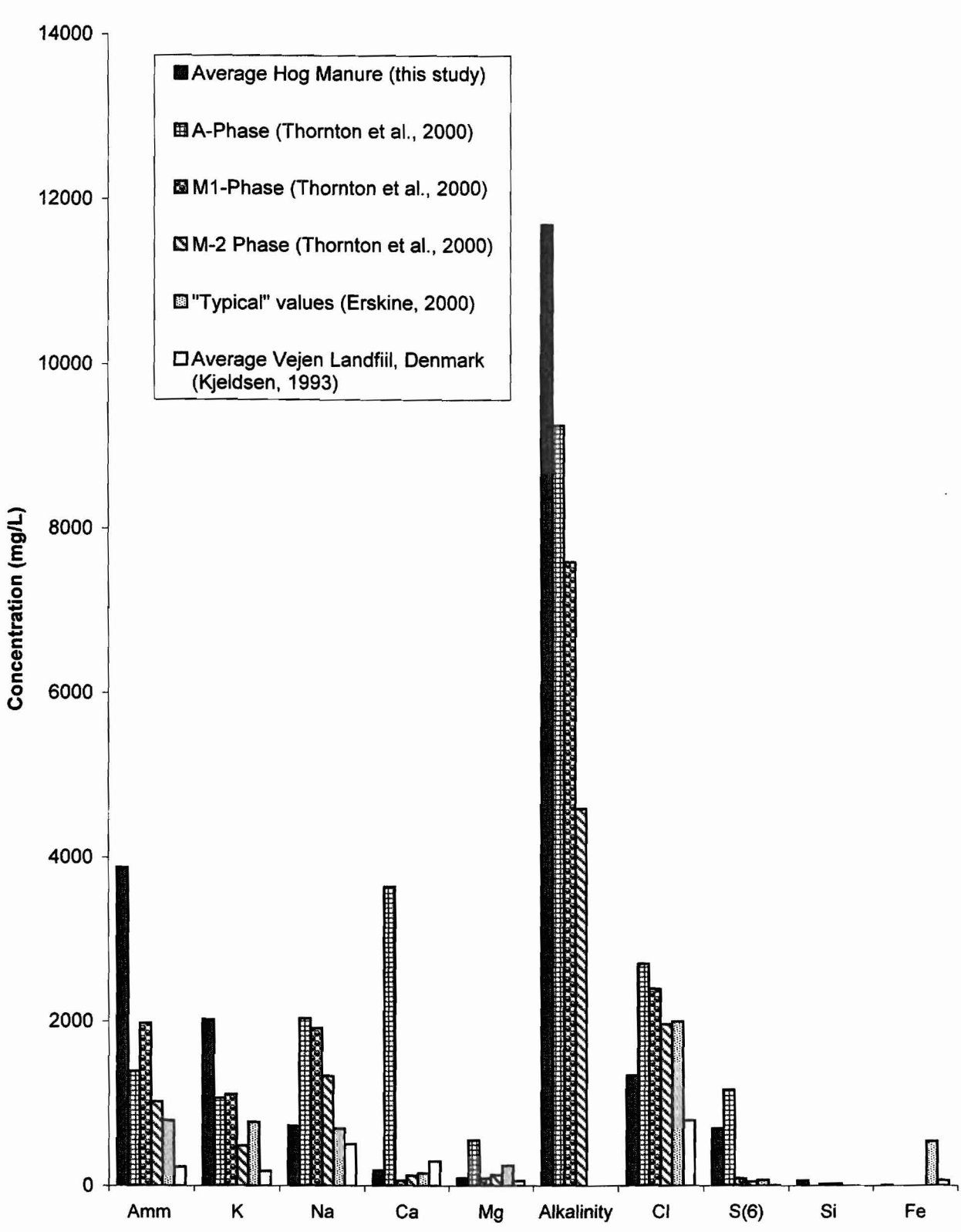

Figure 4.10: Comparison of hog manure chemistry and several landfill leachates

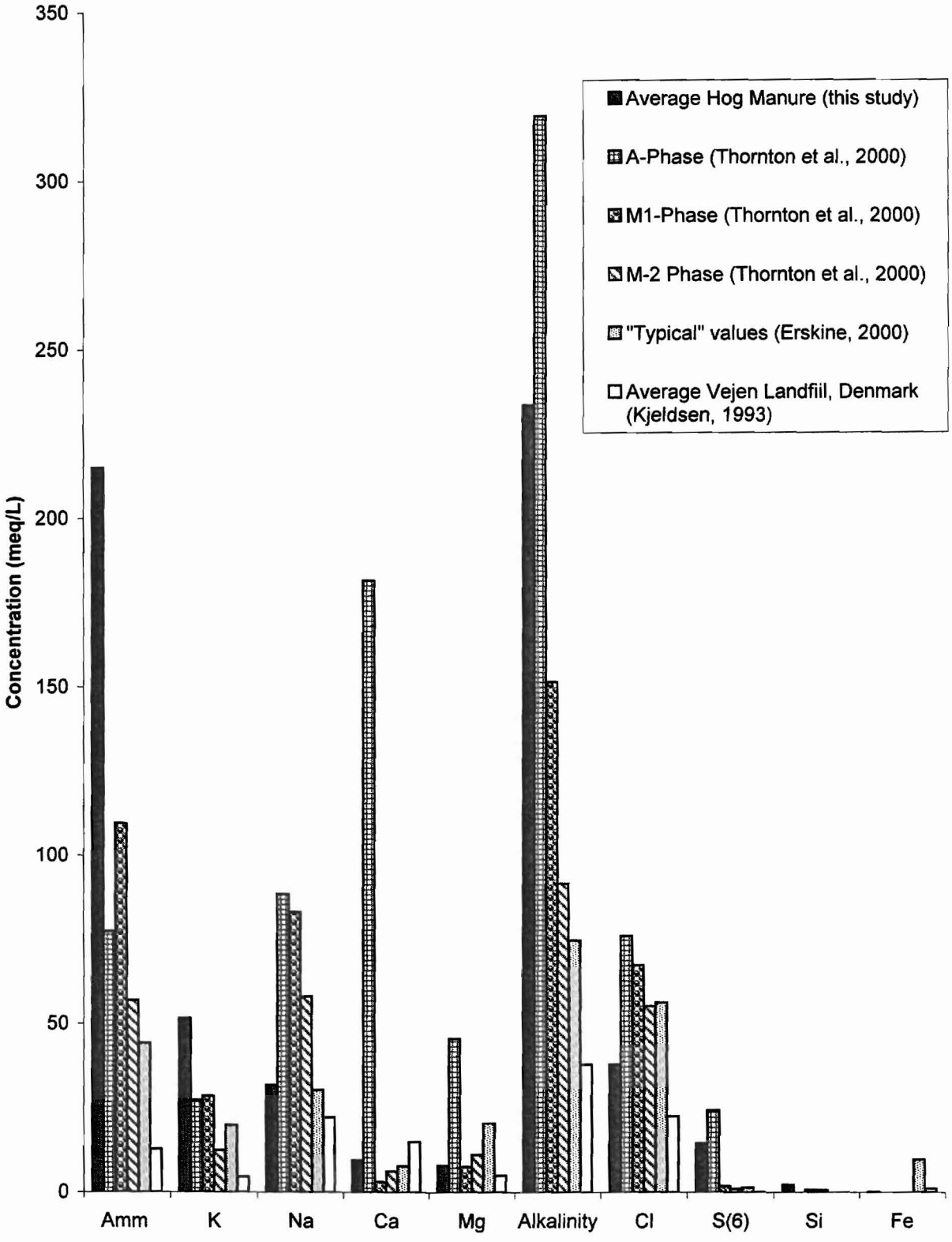

Figure 4.11: Comparison of hog manure chemistry and several landfill leachates

not normally found in hog manure but with respect to major ions they are similar. Calcium and sulphate levels in one landfill leachate sample were significantly higher than other samples, attributed to disposal of building materials in the area (Thornton et al., 2000).

4.1.3 Source Chemistry Conclusions

The species of most concern in EMS seepage is nitrogen. Ammonium nitrogen is the most abundant form of nitrogen and one of the most abundant ions in the EMS effluent studied. Potassium and sodium may be cations of concern as they will likely compete with ammonium for soil exchange sites, which in turn will affect attenuation of ammonium. Bicarbonate and chloride are the most abundant anions (bicarbonate >> chloride). High concentrations of bicarbonate will likely affect precipitation of carbonaceous minerals and may affect solution pH. Similarities between landfill leachate to EMS seepage provide the opportunity for comparison of transport mechanisms and selectivity and distribution coefficients.

4.2 Column and Batch Test Studies

Complementary column and batch test studies were conducted to determine attenuation processes which would limit transport of nitrogen in EMS seepage. Batch tests provide relatively easy to analyze data that may not reflect field conditions, while column test results may better reflect field conditions but large variations in solution chemistry complicate data analysis. Column tests rely on infiltration of a source of assumed constant concentration. As the solution passes through the soil, processes such as ion exchange, dissolution and precipitation can cause changes in chemistry of the pore water solution. We expect ammonium and potassium to remove calcium and magnesium from soil exchange sites, producing an area of low concentration of divalent cations and a high concentration of monovalent cations within the plume and an area of high concentration of divalent cations and a low concentration of monovalent

cations near the front of the plume. Batch studies do not allow relocation of the exchangeable ions as each sample is isolated from others.

4.2.1 Soil Characteristics

Soils from the Clearfield Feeder Unit Site (Table 4.6) are sandy-clay till material classified as clay (CL to CI) under the Unified Soil Classification System. Particle size analysis indicates 40% (average % by weight of particles) >75μm diameter (% sand and gravel), 60% <75 μm diameter (% fines), and 30 % <2 μm diameter (% clay). Atterberg Limits analysis indicates an average Plastic Limit of 18% and an average Liquid Limit of 33% resulting in an average Plasticity Index of 15%. Soil chemistry indicates an average soil pH of 7.5 and an average CEC of 11 cmol/kg (meq/100g). X-ray diffraction results of two till samples of soils from similar sites in the area indicate the clay fraction is composed of 20 to 30% smectite, 5 to 10% mica, 0 to 10% vermiculite, 0 to 5% chlorite, 10 to 20% kaolinite and 40 to 50% quartz and feldspars. The relatively high clay content and moderate CEC are consistent with the lower proportion of smectite relative to other clay minerals. Although the soils used in the column study did have some sand and silt lenses mixed with the till material, the x-ray diffraction analysis gives some indication of the relative distribution of clay material.

Soils from ADF Research Site No. 1 (Table 4.6) are clayey and silty-sand material of lacustrine origin classified as poorly graded silty-sand (SPSM) under the Unified Soil Classification System. Particle size analysis indicates 82% (average % by weight of particles) >75μm diameter (% sand and gravel), 18% <75 μm diameter (% fines), and 9 % <2 μm diameter (% clay) as determined by ASTM D-2487-93. 99% of the sand and gravel portion was fine sand, and Atterberg Limits analysis indicates this material is non-plastic. Soil chemistry indicates an average soil pH of 8.2 and an average CEC of 7 cmol/kg (meq/100g). X-ray diffraction analysis of this soil from a previous study (Fonstad, 1996) indicated the clay fraction was composed of 70% smectite, 10% mica, 5 to 10% vermiculite, and less than 5% each of chlorite, kaolinite and quartz and

Table 4.6 - Soil characteristics of soils used in column study

Column	Soil	USCS	%clay (< 2 μm)	%fines (< 75 μm)	PL	LL	pH	CEC
			%	%	%	%		meq/100g
1	Clearfield	Cl	30	60	18	33	7.5	11
2	Site No 1	SPSM	9	18	NA	NP	8.2	7

Note: All values are averages
LL = Liquid Limit
PL = Plasticity Limit
Unified Soil Classification - Sand is > 75 μm, Clay is > 2 μm, ASTM D-2487-93

Column	Soil	USCS	X-ray diffraction of clay minerals					
			Smectite	Mica	Vermiculite	Chlorite	Kaolinite	Quartz+ Feldspars
			%	%	%	%	%	%
1	Clearfield	Cl	20-30	5-10	0-10	0-5	10-20	40-50
2	Site No 1	SPSM	70	10	5-10	<5	<5	<5

Note: X-ray diffraction results for Clearfield soil are from tests of similar soils from other sites in the area

feldspars. The relatively high CEC for this low clay content soil is consistent with the higher proportion of smectite to other clay minerals.

4.2.2 Column Study Bulk Density and Moisture Content

Column compaction was conducted at relatively high moisture contents of 18.5 and 22.3% for Columns No. 1 and 2 respectively, resulting in corresponding dry densities of 1715 and 1579 kg/m^3. Cores taken during sectioning of the columns indicate soils consolidated to dry densities of 1766 and 1652 kg/m^3 with moisture contents of 19.1 and 23.9% respectively (Figure 4.12). Standard Proctor moisture content and dry density for Column No. 1 soils was 14.7% and 1840 kg/m^3 as determined by the average of four Standard Proctor tests preformed by P. Machibroda Engineering Ltd. in Saskatoon, Saskatchewan. Standard Proctor moisture content and dry density for Column No. 2 soils was 18% and 1710 kg/m^3 from Fonstad (1996).

4.2.3 Column Study Specific Discharge

Both columns experienced a reduction in hydraulic conductivity similar to reports by Barrington and Madramootoo (1989), Fonstad (1996) and Maule and Fonstad (2000). The specific discharge of Column No. 1 (Figure 4.13) decreased from 3.4×10^{-6} to 5×10^{-9} m^3/s/m^2 within 13 days of manure placement. Over the course of the column study, Column No.1 experienced a reduction in specific discharge of approximately three orders of magnitude and reached a minimum specific discharge within 0.04 to 0.06 pore volumes (Figure 4.15). The specific discharge of Column No. 2 (Figure 4.14) decreased from 1.2×10^{-5} to 1×10^{-7} m^3/s/m^2 within 30 days of manure placement. Column No. 2 experienced a reduction in specific discharge of approximately two orders of magnitude and reached a minimum specific discharge within 0.9 to 1.3 pore volumes (Figure 4.16). Column No 1 results are similar to Fonstad (1996) and Maule and Fonstad (2000) while Column No 2 results are up to 50% higher. Fonstad (1996) and Maule and Fonstad (2000) explain the reduction of specific discharge as the result of a thin

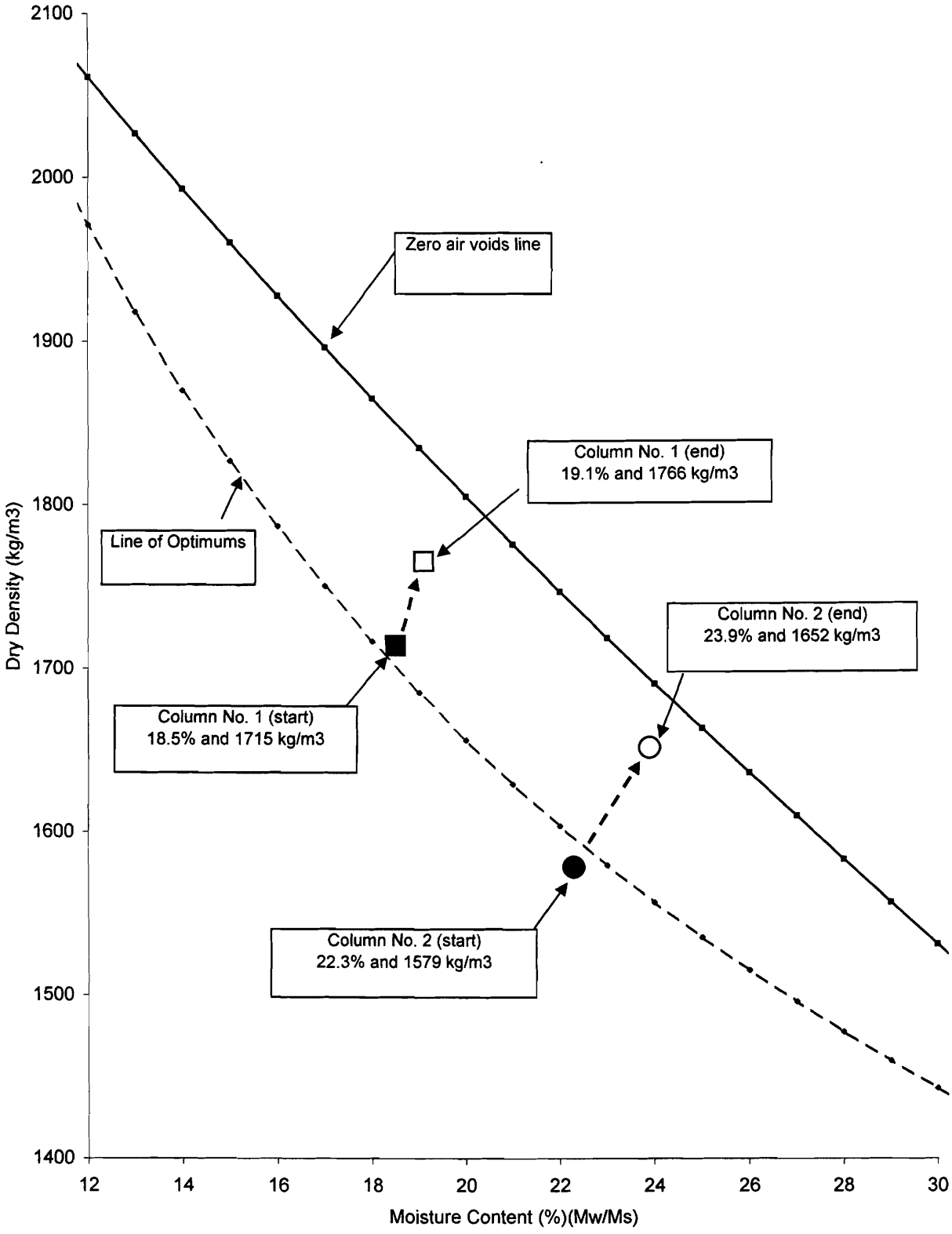

Figure 4.12 - Dry density versus moisture content data for Columns No. 1 and 2 at the start and end of column testing conducted at PAMI

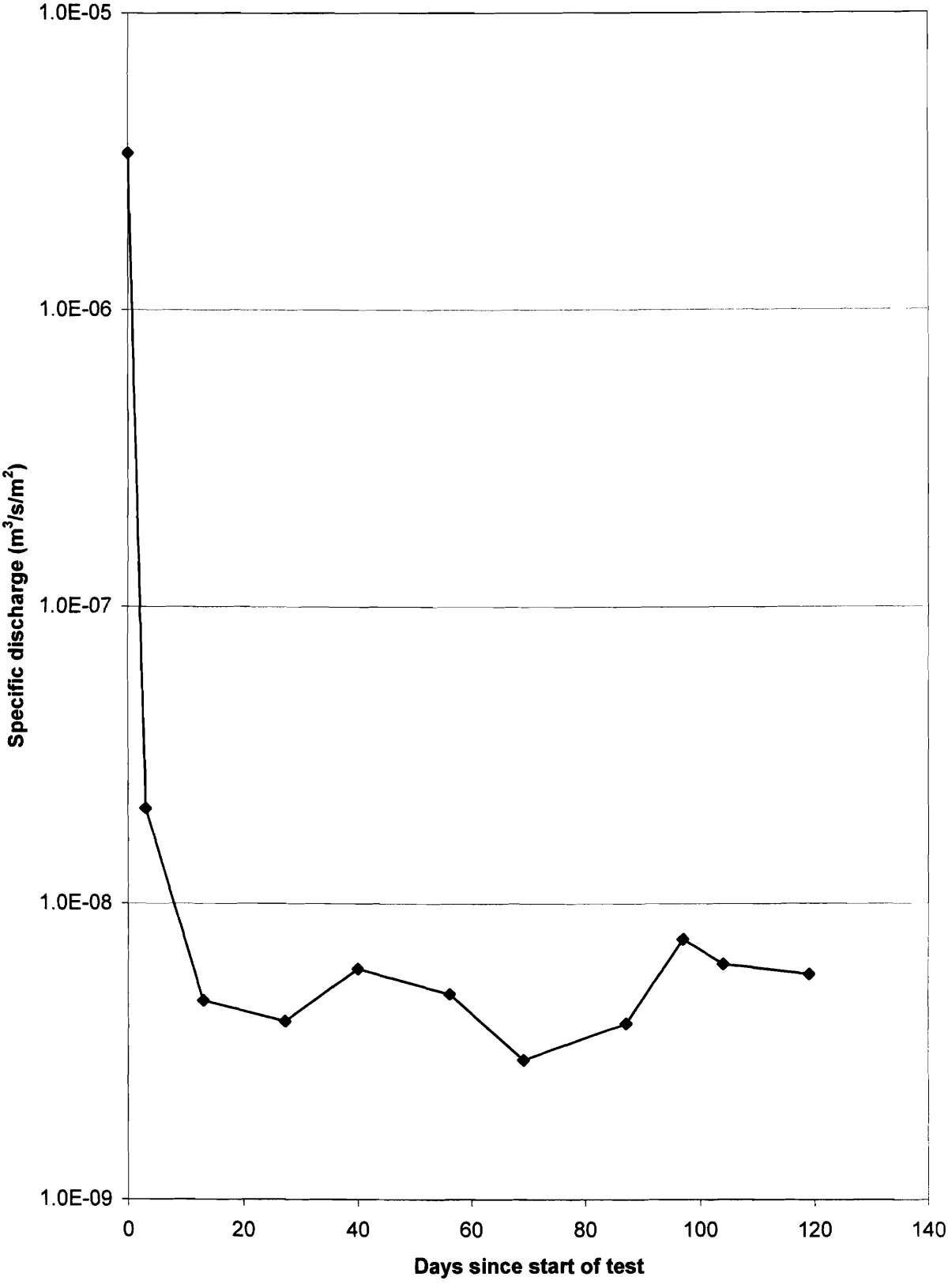

Figure 4.13 - Specific Discharge for Column No. 1 (Clearfield Feeder Unit soil) versus number of days since start of test

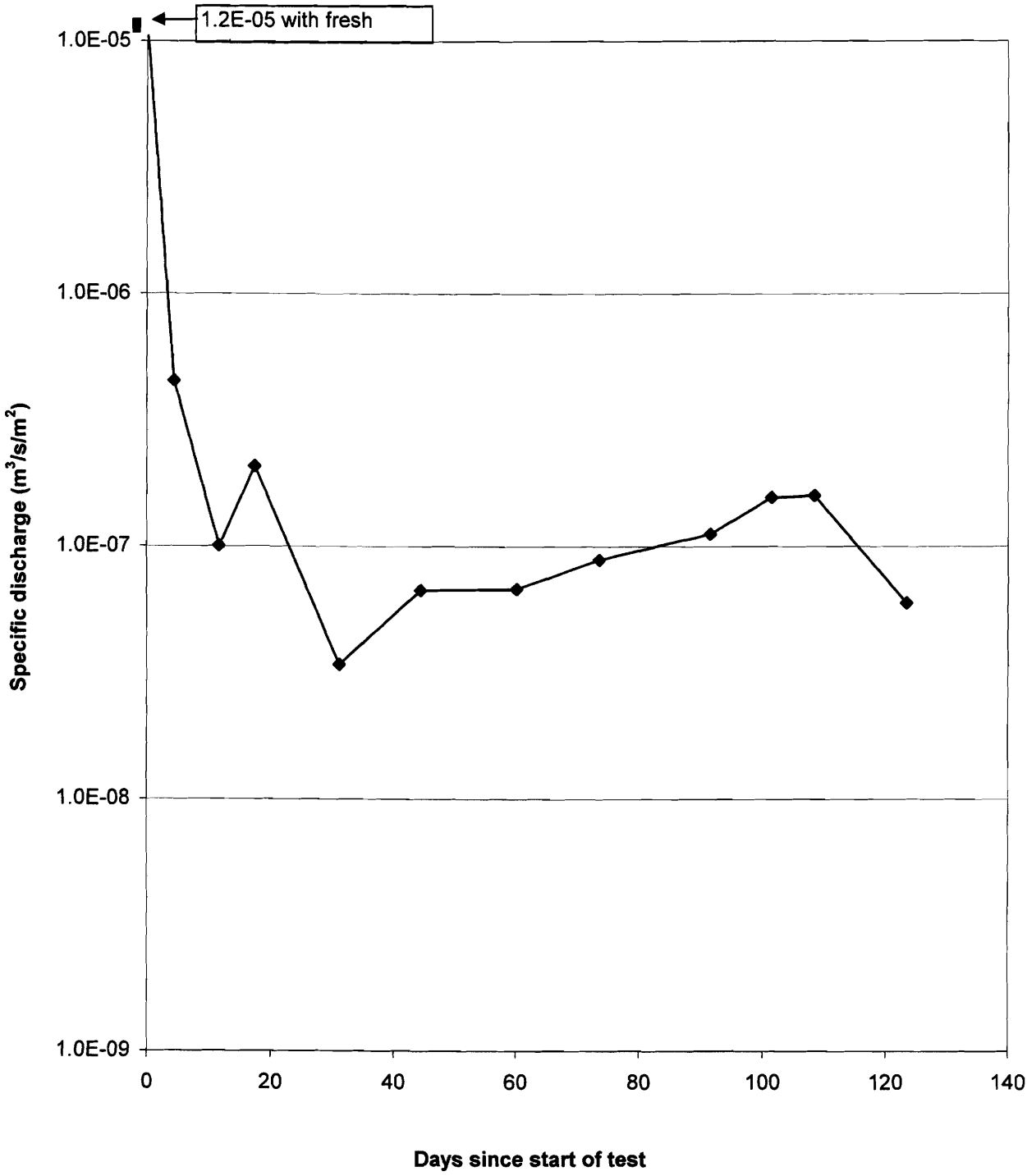

Figure 4.14 - Specific Discharge for Column No. 2 (Site 1 soil) versus number of days
since start of test

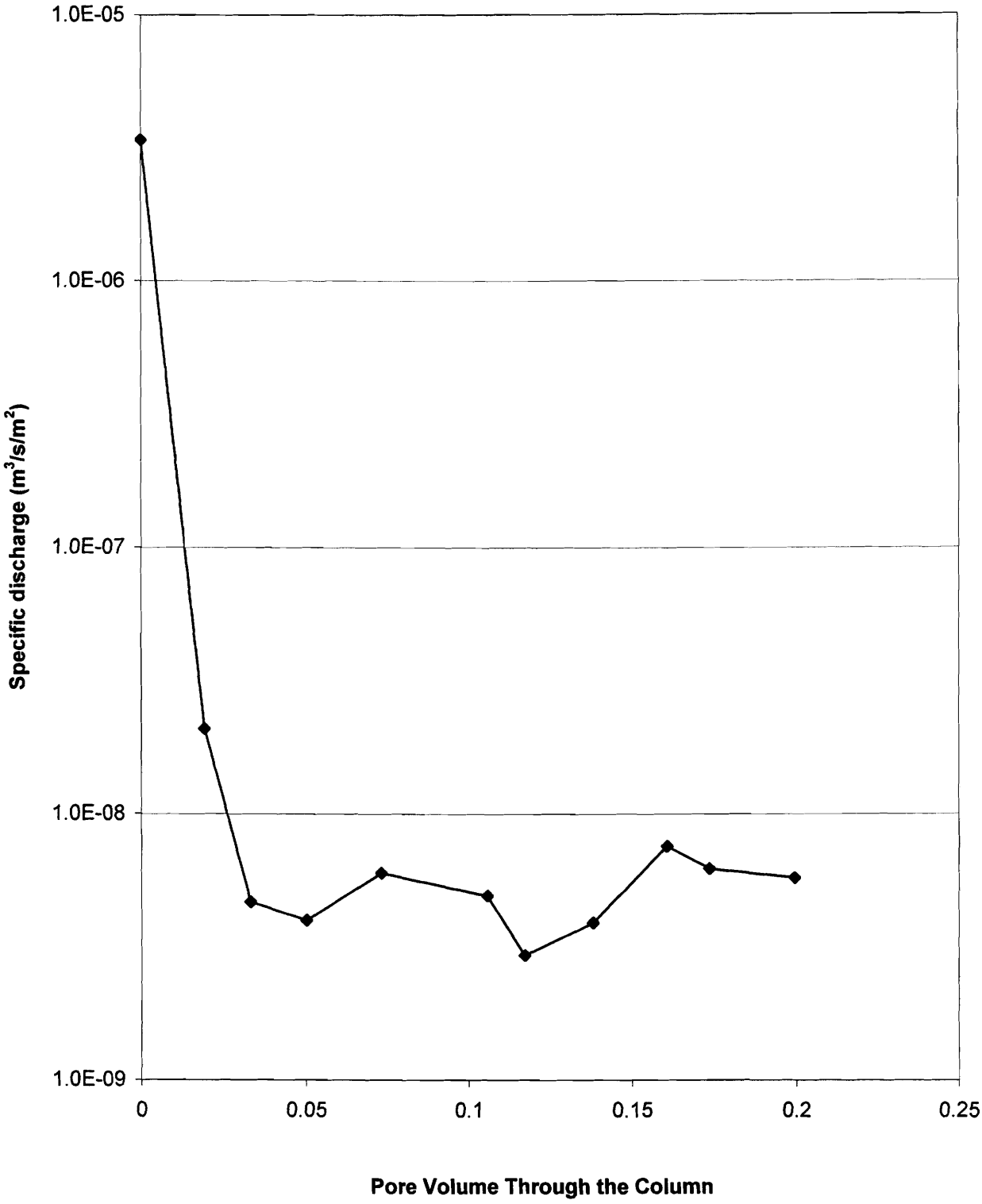

Figure 4.15 - Specific Discharge for Column No. 1 (Clearfield Feeder Unit soil) versus pore volumes of solution passing through the column

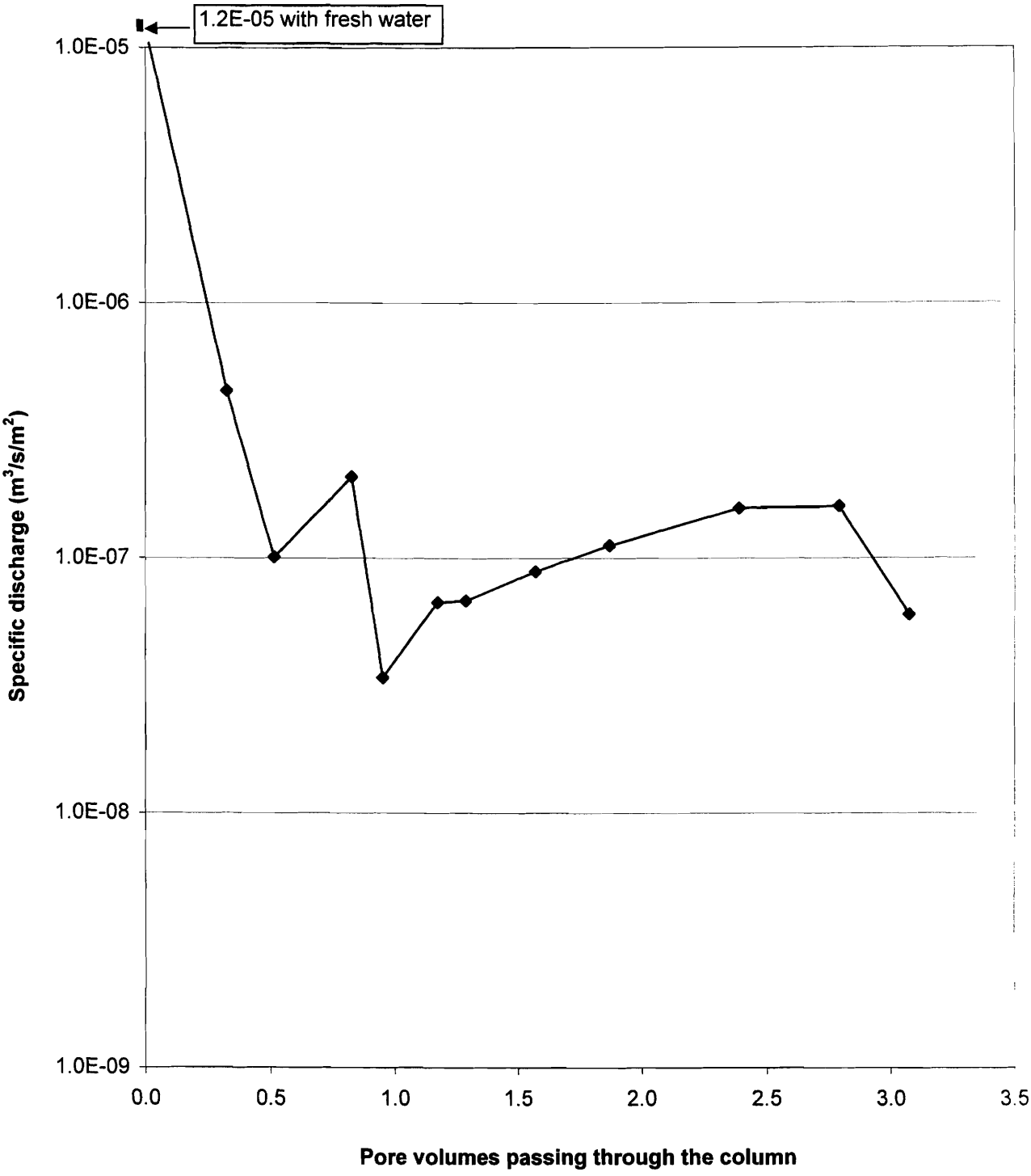

Figure 4.16 - Specific Discharge for Column No. 2 (Site 1 soil) versus pore volumes of solution passing through the column

clogged layer (hydraulic conductivity ~$5x10^{-11}$ m/s, thickness ~5 mm) at the manure-soil interface.

4.2.4 Column Study Oxidation- Reduction Potential (ORP)

ORP measurements were obtained during initial conductivity testing with water in the columns and periodically within the first 2 wks after manure ponding. Both columns experienced similar ORP (Eh) within the water column and the soil, with ORP (Eh) values ranging between +350 and +450 mV (Figures 4.17 and 4.18). Although manure placed in both columns was mixed significantly in the presence of air, the Eh within a few hours of placement was < –200 mV; within 13-17 days the Eh was reduced to –300 to –350 mV indicating progression to more anaerobic conditions. Eh values obtained within the soil column were initially aerobic (+350 mV to +450 mV) and reduced with depth and time over the first 2 weeks.

4.2.5 Column Effluent Chemistry

Effluent chemistry of Column No. 1 did not significantly change within the 4 month test period. At a column depth of 75 mm, the C/Co for chloride approached 1 prior to 1 pore volume while potassium and ammonium reached C/Co values of 0.35 and 0.5 respectively after 2.3 pore volumes (Figure 4.19). The early breakthrough of chloride could be due to irregularities in the soil surface caused by pumping manure effluent into the column, irregular compaction of the soil, and/or fracture flow. Calcium and magnesium reached C/Co concentrations of 1.1 and 1.6 after 2.3 pore volumes (Figure 4.20). At a depth of 228 mm below the top of the column, chloride reached a C/Co concentration of 0.75 after 0.8 pore volumes while ammonium and potassium did not significantly increase (Figure 4.21). Calcium and magnesium reached C/Co concentrations of 0.85 and 1.8 respectively after 0.8 pore volumes. Appelo and Postma (1996) and Beekman and Appelo (1990) explain magnesium C/Co concentrations greater than 1 as a result of ion exchange; magnesium and calcium on soil exchange sites are exchanged for ammonium or potassium, releasing magnesium and calcium into solution.

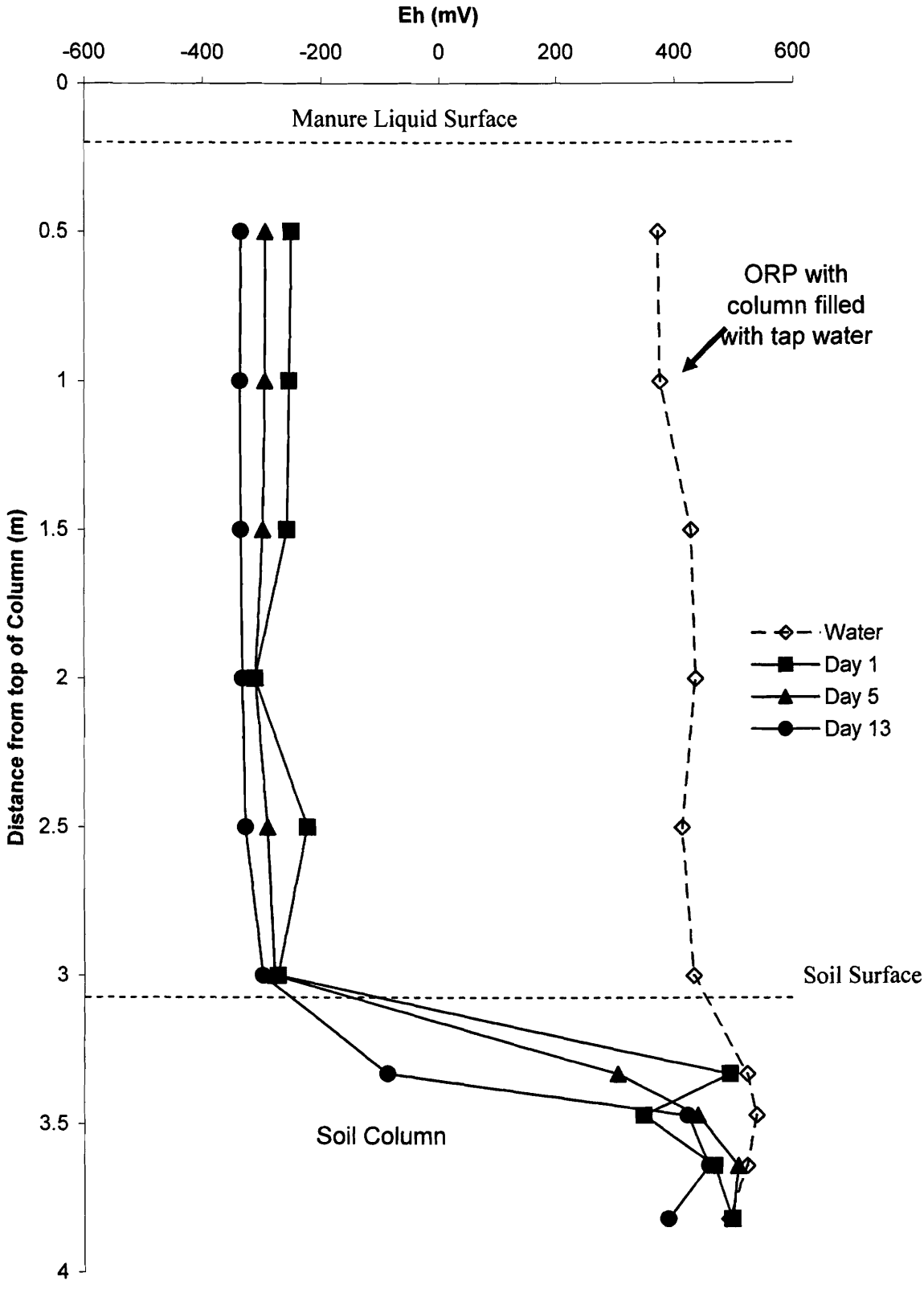

Figure 4.17 - ORP readings with depth for Column No. 1 with water and after manure addition to the column

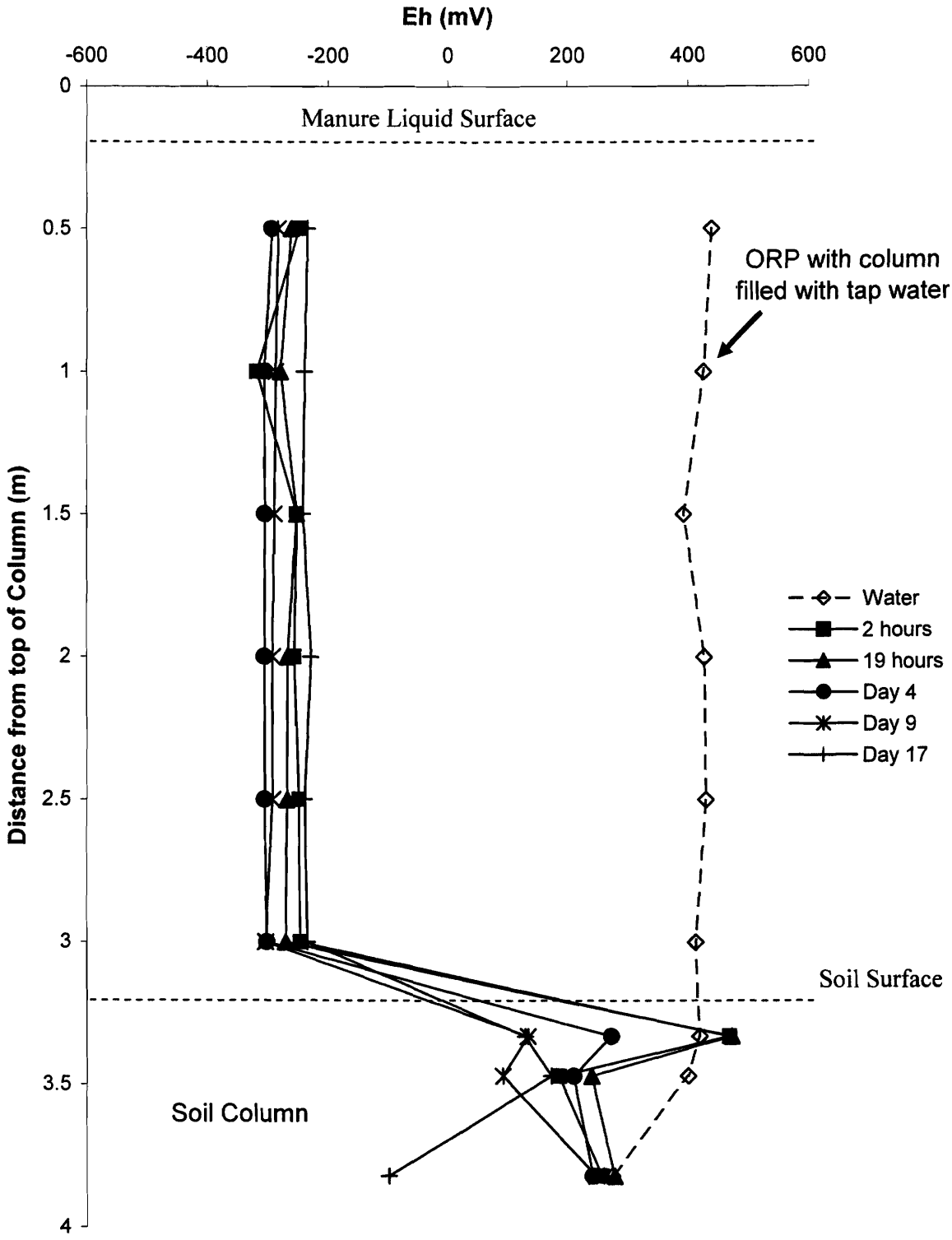

Figure 4.18 - ORP with depth within Column No. 2 with water and after manure addition to the column

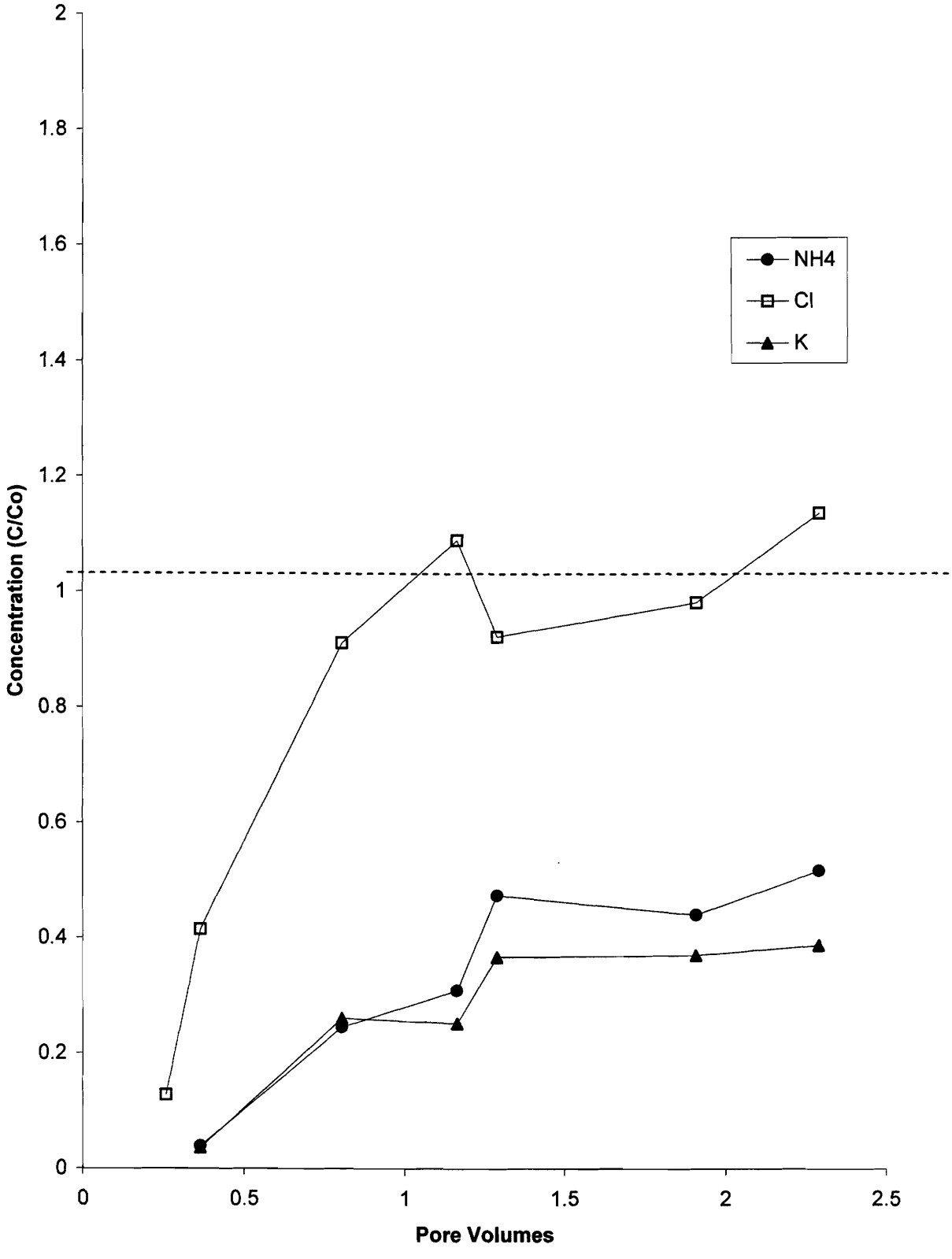

Figure 4.19- Effluent chemistry changes for Chloride, Ammonium and Potassium for the top 7.5 mm of Column No. 1

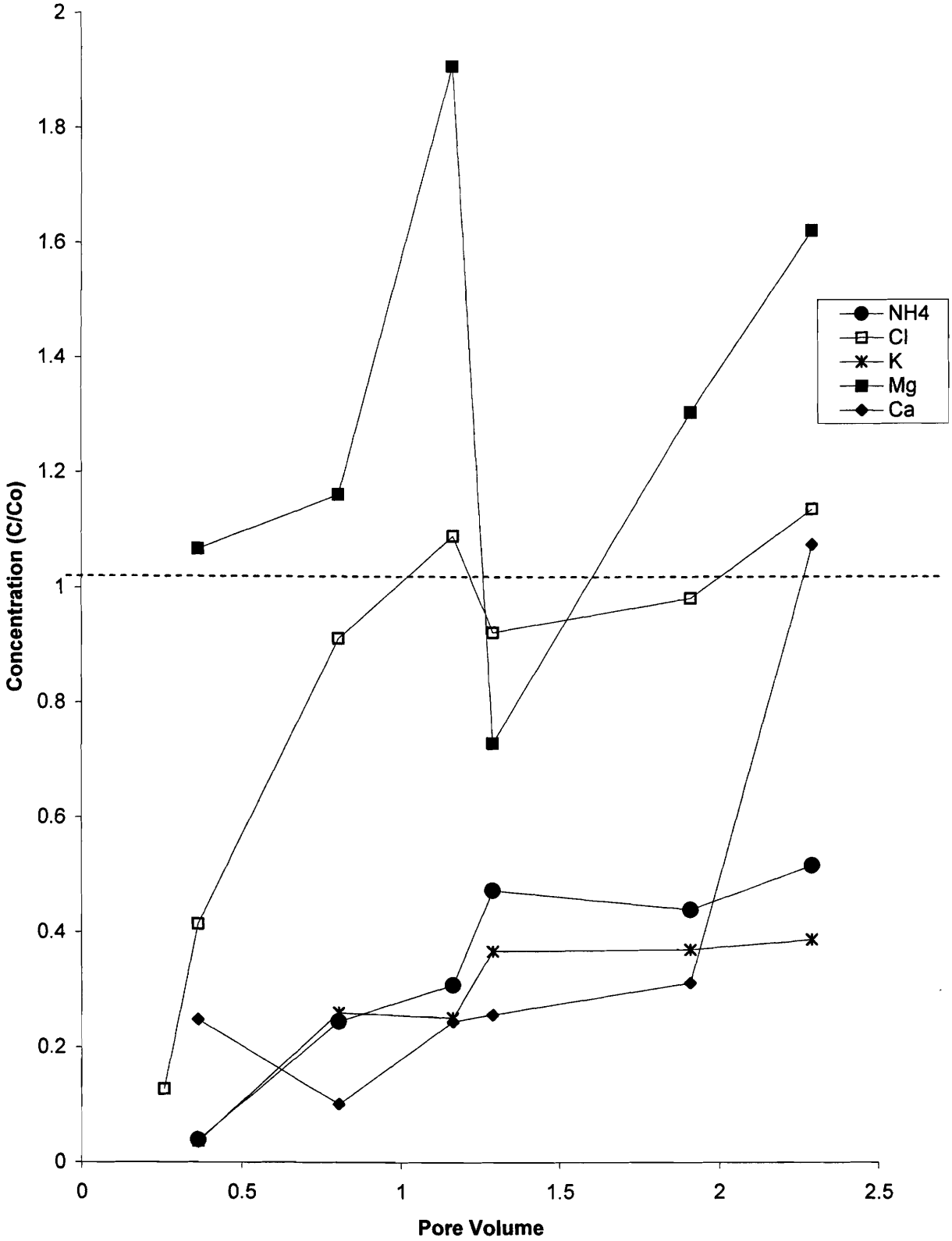

Figure 4.20 - Effluent chemistry changes for chloride and select anions for the top 75 mm of Column No. 1

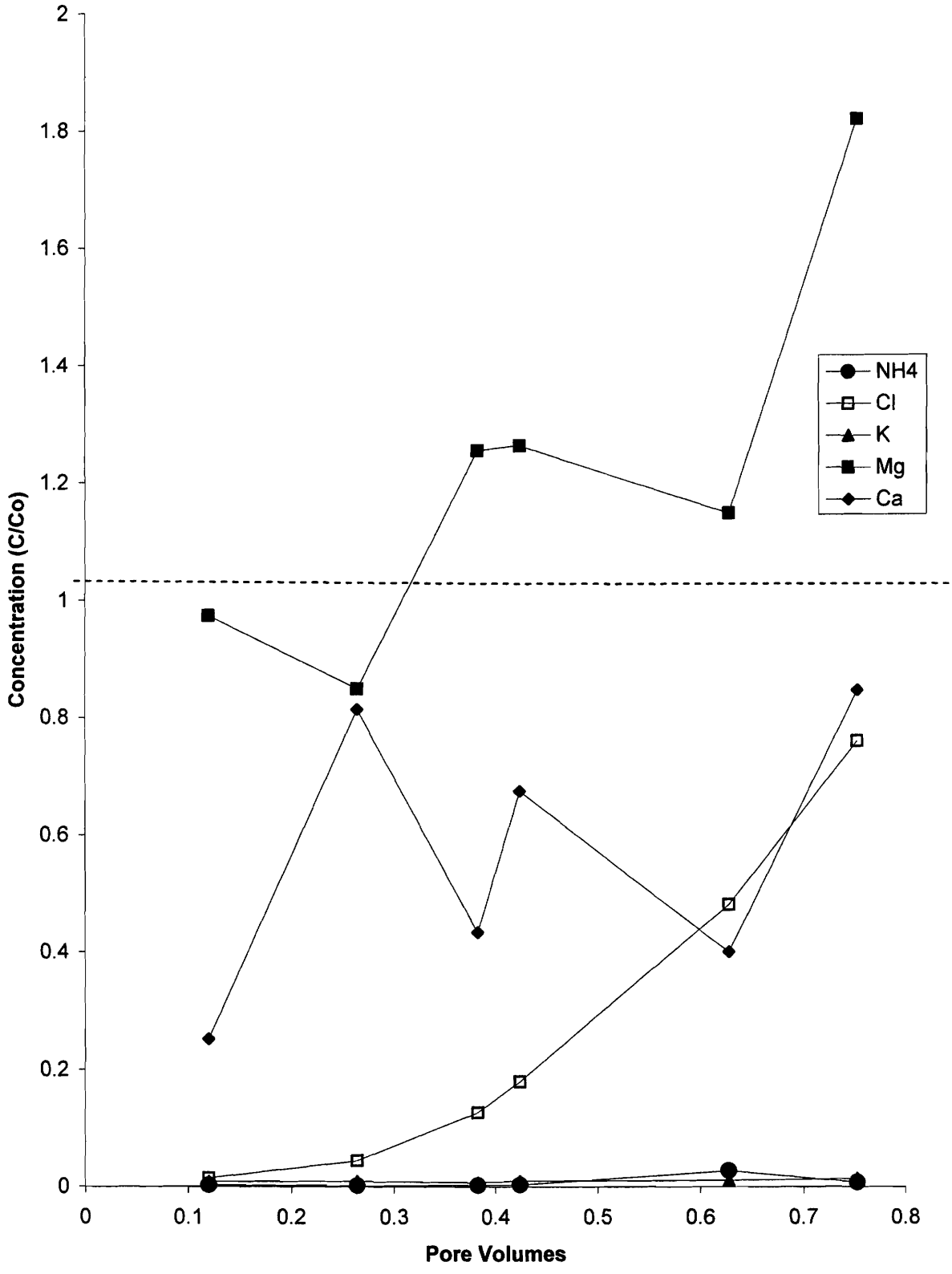

Figure 4.21 - Effluent chemistry changes for chloride and select cations for the top 228 mm of Column No. 1

Although a well-defined breakthrough curve was not found for Column No. 2 (Figure 4.22), results provide some indication of processes occurring during transport of manure through the column. Neither potassium, ammonium nor sodium reached a C/Co concentration of 1 after 3.9 pore volumes. Magnesium reached a C/Co concentration of 1.9 after 1.8 pore volumes then decreased to near 1 after 3.9 pore volumes. Calcium concentrations initially increased, similar to magnesium, but dropped slightly from 1 to 2.1 pore volumes while magnesium was increasing. When magnesium concentrations decreased from 1.9 to 3.9 pore volumes, calcium concentrations increased to a C/Co concentration of 0.6 after 3.9 pore volumes. These results are similar to Beekman and Appelo (1990) who used seawater (NaCl) to flush soil columns.

4.2.6 Column Study Soil Extraction Results

Column 1 soils experienced approximately 0.2 pore volumes of flow during the column study (Figure 4.15) and there was no indication of breakthrough of any ions at the column base. Saturate paste extraction indicated bicarbonate and chloride both increase with depth while sulfate decreases (Figure 4.23), particularly in the area behind the effluent front (Figure 4.24). Bicarbonate and chloride profiles resemble typical advection-dispersion profiles. Sulfate is almost a mirror image of the others, potentially indicating sulfate reduction within the seepage front. Nitrate levels determined by colorimetry were negligible. Cation profiles show ammonium, potassium and sodium decreasing with depth. Calcium and magnesium increase with depth to below the depth of the other three cations; they continue to decrease with depth to assumed background levels (Figure 4.25). Calcium and magnesium near the infiltration front exceed background concentrations; accumulation of cations at this location results from exchange with the infiltration ions ("hard water front"). Complete saturated paste extraction results are provided in Table 4.7.

Exchangeable cation analysis of Column No 1 soil sections (Table 4.8) are similar to saturate paste extraction results with two notable exceptions. While quantities of exchangeable ammonium and potassium are high near the soil-manure interface (top of

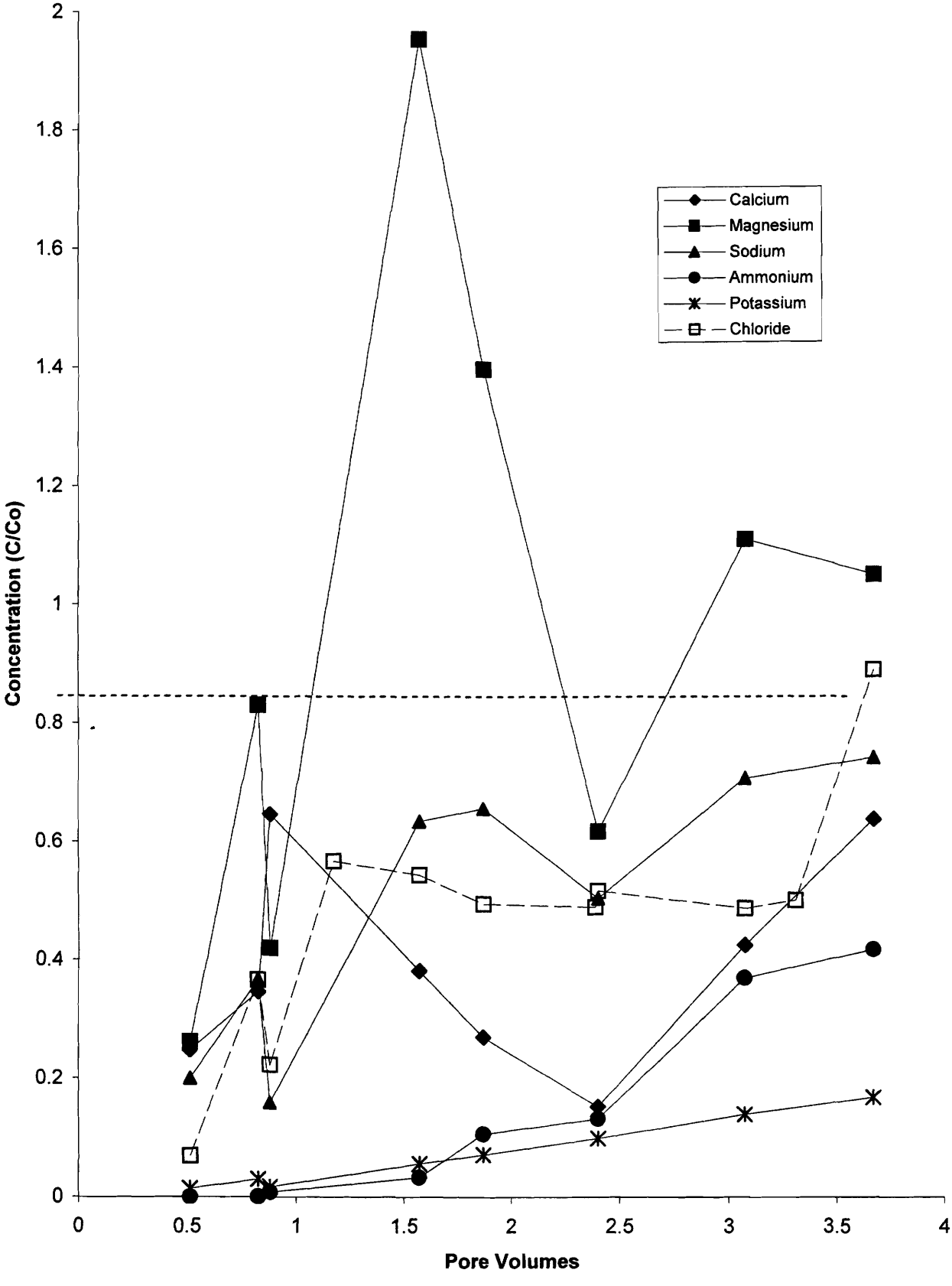

Figure 4.22 - Effluent chemistry changes for selected ions for Column No. 2

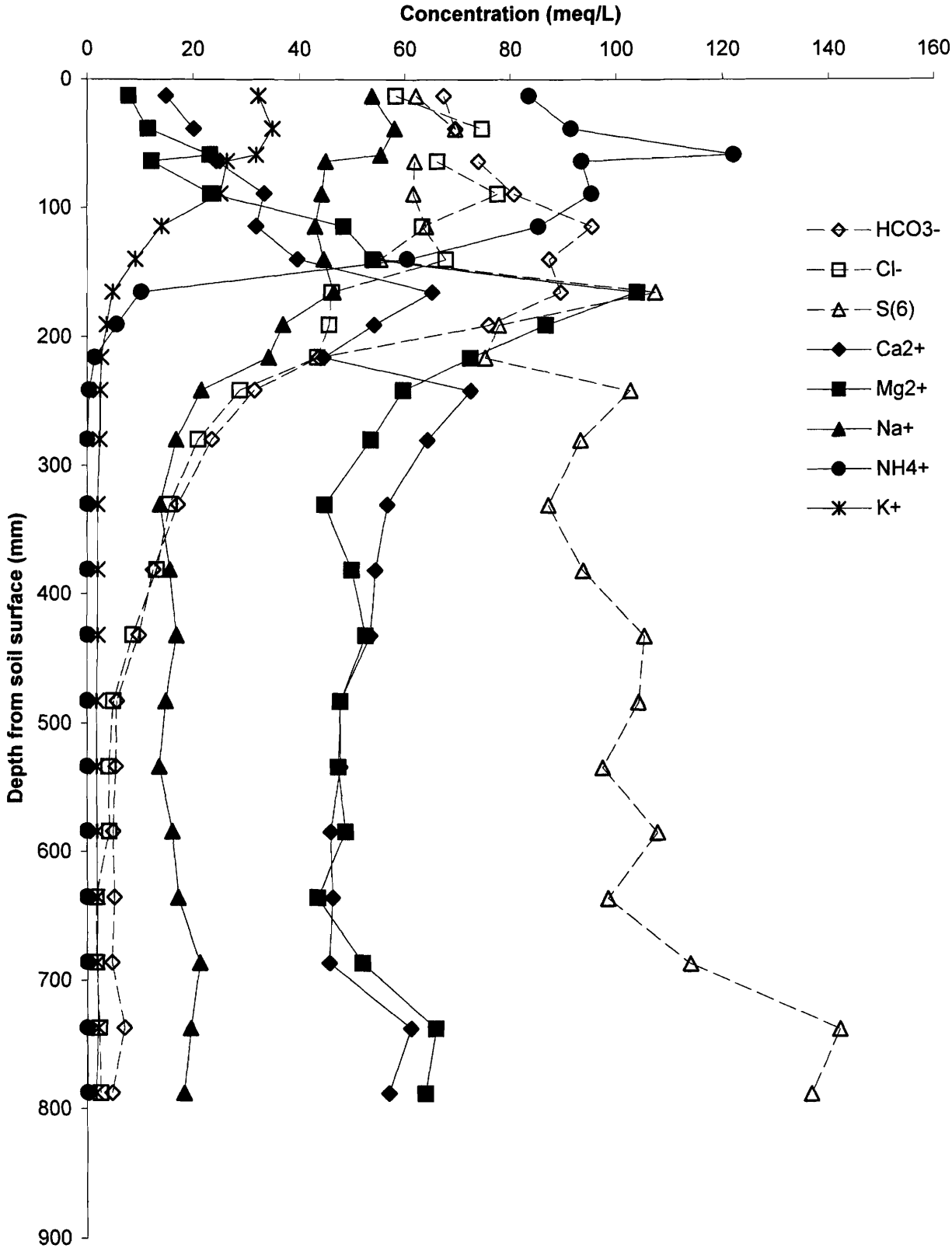

Figure 4.23 - Column No. 1 concentration of ions in solution with depth within the soil column

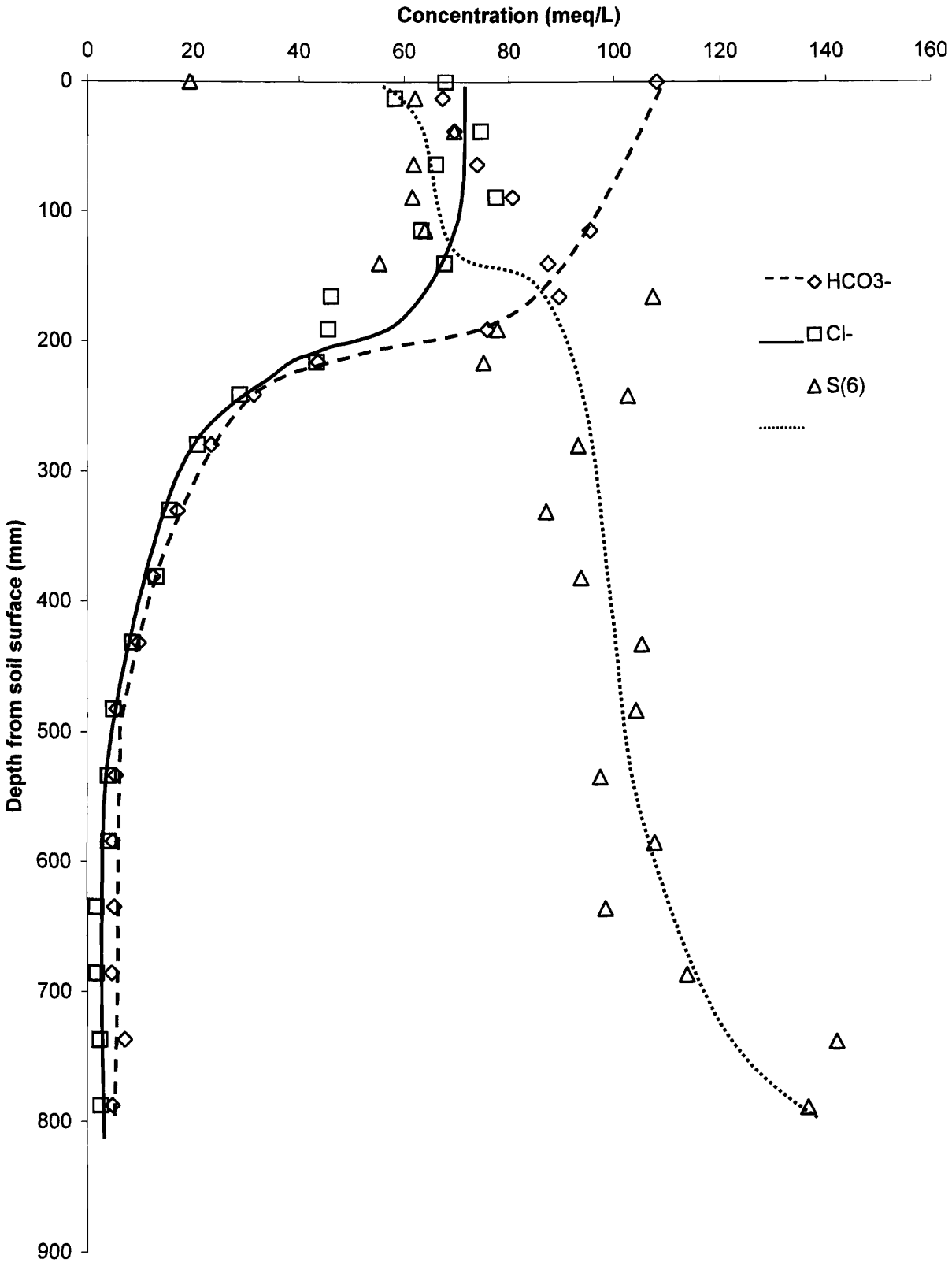

Figure 4.24 - Column No. 1 concentration of anions in solution with depth within the soil column

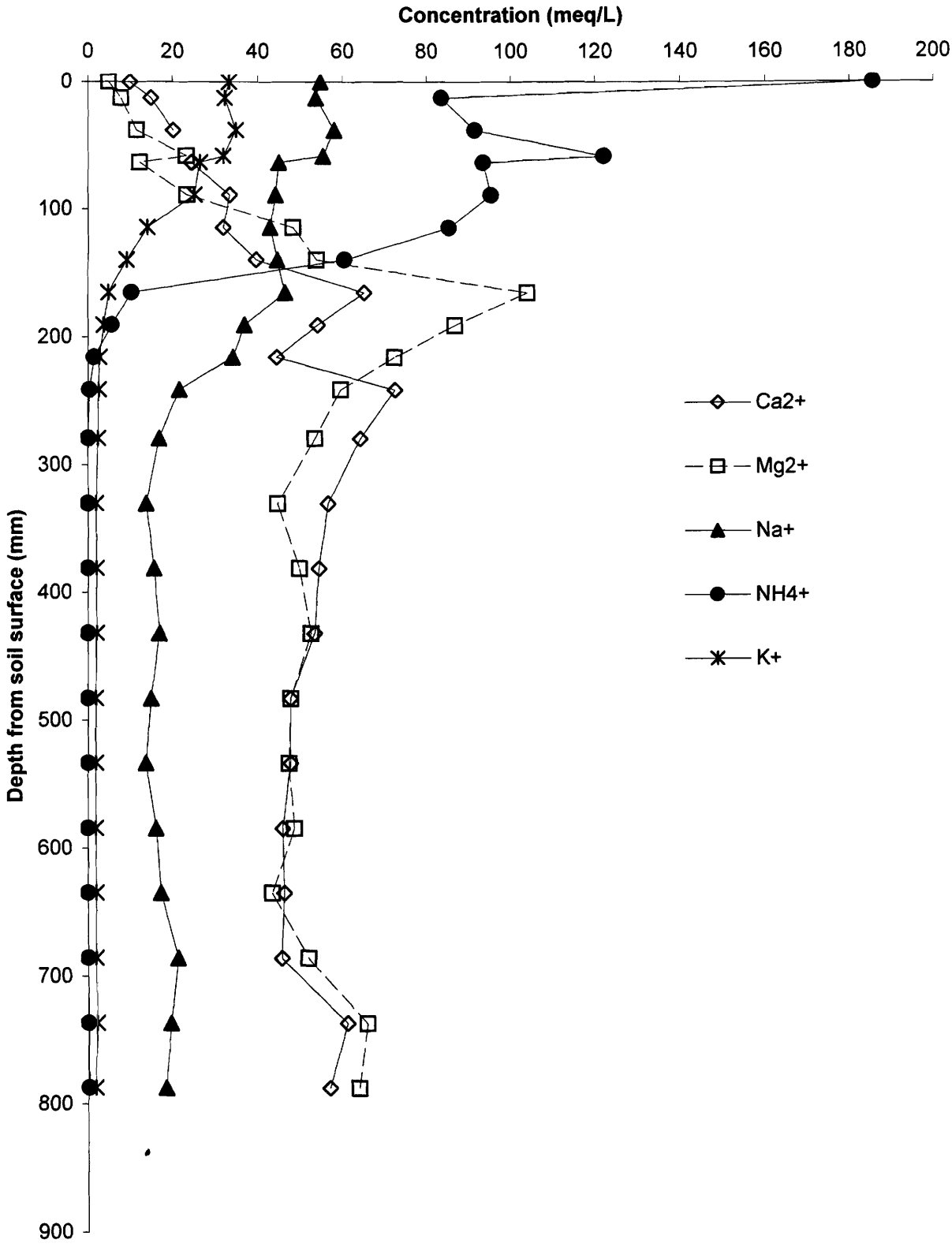

Figure 4.25 - Column No. 1 concentration of cations in solution with depth within the soil column

Table 4.7 - Column No. 1 (Clearfield Site Soils) saturated paste extraction results

Depth (mm)	HCO3- (meq/L)	Cl- (meq/L)	SO4-- (meq/L)	Ca++ (meq/L)	Mg++ (meq/L)	Na+ (meq/L)	K+ (meq/L)	Ba++ (meq/L)	N-NH4+ (meq/L)	EC (mS/cm)	Ionic Strength	Normality
13	67	58	62	15	8	54	35	1	95	9.2	0.24	0.40
38	70	75	70	20	12	58	32	4	94	10.3	0.27	0.43
64	74	66	62	24	12	45	26	4	91	8.2	0.25	0.41
89	81	78	62	33	23	44	25	6	85	10.4	0.28	0.44
114	95	63	64	32	48	43	14	7	84	8.9	0.30	0.45
140	87	68	55	40	54	45	9	7	60	7.8	0.29	0.42
165	90	46	107	65	104	46	5	14	10	7.0	0.39	0.49
191	76	46	78	54	87	37	4	11	6	6.9	0.31	0.40
216	44	43	75	44	72	34	3	10	1	6.7	0.26	0.33
241	32	29	103	72	60	22	3	11	0	6.1	0.29	0.33
279	23	21	93	64	53	17	2	5	0	4.8	0.25	0.28
330	17	16	87	57	45	14	2	3	0	4.5	0.22	0.24
381	13	13	94	54	50	16	2	3	0	4.4	0.22	0.24
432	10	9	105	53	52	17	2	1	0	4.3	0.23	0.25
483	6	5	104	48	48	15	2	1	0	4.1	0.21	0.23
533	5	4	97	48	47	14	2	1	0	4.0	0.21	0.22
584	5	4	108	46	49	16	2	1	0	4.0	0.22	0.23
635	5	2	99	46	43	17	2	1	0	4.0	0.20	0.21
686	5	2	114	46	52	21	2	1	0	4.2	0.23	0.24
737	7	2	142	61	66	20	2	7	0	4.2	0.29	0.31
787	5	3	137	57	64	18	2	0	0	4.0	0.27	0.29

Note: Results corrected to original moisture content

Exchangeable cation analysis of Column No 1 soil sections (Table 4.8) are similar to saturated paste extraction results with two notable exceptions. While quantities of exchangeable ammonium and potassium are high near the soil-manure interface (top of the column), exchangeable sodium levels are not significantly different throughout the column (Figure 4.26) indicating sodium is potentially held off exchange sites by competing cations. Exchangeable magnesium follows the same pattern as solution concentrations, while calcium quantities decrease only in locations with high magnesium and no other significant competing ions, and near the top of the column where monovalent cation concentrations become significant (Figure 4.26).

Column 1 pH remains relatively unchanged with depth; both TOC and CEC are highest near the top of the column (soil-manure interface) and decrease with depth (Figure 4.27) indicating TOC may be contributing to the CEC at the higher TOC concentrations.

Column No. 2 experienced approximately 3.9 pore volumes of flow during the column study (Figure 4.16) with breakthrough of calcium and magnesium after one pore volume (Figure 4.22) indicating some loss of calcium and magnesium from the system. Saturated paste extraction results for Column 2 are provided in Table 4.9 with the concentration of ions in solution with depth plotted in Figure 4.28 and 4.29. Although chloride reached a concentration of 90% of the source concentration after 3.9 pore volumes (Figure 4.22), Figure 4.29 indicates relatively constant chloride, bicarbonate and sulfate levels below 250 mm depth. Above this point chloride and sulfate increase significantly and then decrease to source concentrations near the column top indicating an accumulation zone for both anions. Bicarbonate concentrations remain relatively constant throughout the column well below the source concentration indicating a potential reaction with the soil ions or ions infiltrating from the manure. Nitrate levels for this Column were also negligible. Cation profiles (Figure 4.30) show ammonium and potassium concentrations increase from the base of the column to the top. Sodium levels remain unchanged from background concentrations with the exception of the top 100 mm where levels nearly double. Calcium and magnesium levels at the base of the

Table 4.8 - Column No 1 extractable cations

Depth (mm)	pH	TOC (g/kg)	CEC# (cmol/kg)	Ca++ (cmol/kg)	Mg++ (cmol/kg)	Na+ (cmol/kg)	K+ (cmol/kg)	N-NH4+ (cmol/kg)	Total Cations (cmol/kg)
				(cmol of 1+ ions per kg of soil = meq/100g)					
12.7	7.1	8.29	13.8	4.7	1.1	0.3	2.3	3.2	11.6
38.1	7.1	7.59	13.6	7.3	1	0.3	2.3	2.5	13.4
63.5	7.1	5.31	12.2	7.4	1	0.2	1.9	2.2	12.6
88.9	7.1	5.05	12.8	7.6	2.3	0.4	1.5	1.9	13.7
114.3	7.3	4.22	13	8	3	0.3	2.1	0.7	14.1
139.7	7.4	3.74	14	8.1	3.7	0.4	0.9	0.8	13.9
165.1	7.4	3.05	12.7	7.8	4	0.4	0.5	0	12.7
190.5	7.3	2.91	12.5	8.1	4	0.3	0.4	0	12.8
215.9	7.4	2.95	11.7	8.1	4.8	0.3	0.4	0	13.6
241.3	7.4	2.35	11.3	8.1	4.3	0.3	0.5	0	13.2
279.4	7.4	1.86	10.6	7.6	4.4	0.3	0.5	0	12.8
330.2	7.4	2.55	10.4	7.5	4.6	0.3	0.5	0	12.9
381	7.4	1.74	10.5	7.5	4.7	0.3	0.5	0	13
431.8	7.5	0.8	11.8	7	5	0.3	0.5	0	12.8
482.6	7.5	1.19	11.4	8.1	4.2	0.2	0.5	0	13
533.4	7.5	0.88	10.9	8.3	3.3	0.2	0.5	0	12.3
584.2	7.5	1.13	10.3	8.2	3.6	0.2	0.5	0	12.5
635	7.5	1.18	9.9	8.2	3.4	0.2	0.5	0	12.3
685.8	7.4	1.65	9.8	8	3.6	0.2	0.5	0	12.3
736.6	7.4	1.2	10.4	7.6	4.4	0.3	0.4	0	12.7
787.4	7.5	1.13	10.8	7.5	4.3	0.3	0.4	0	12.5

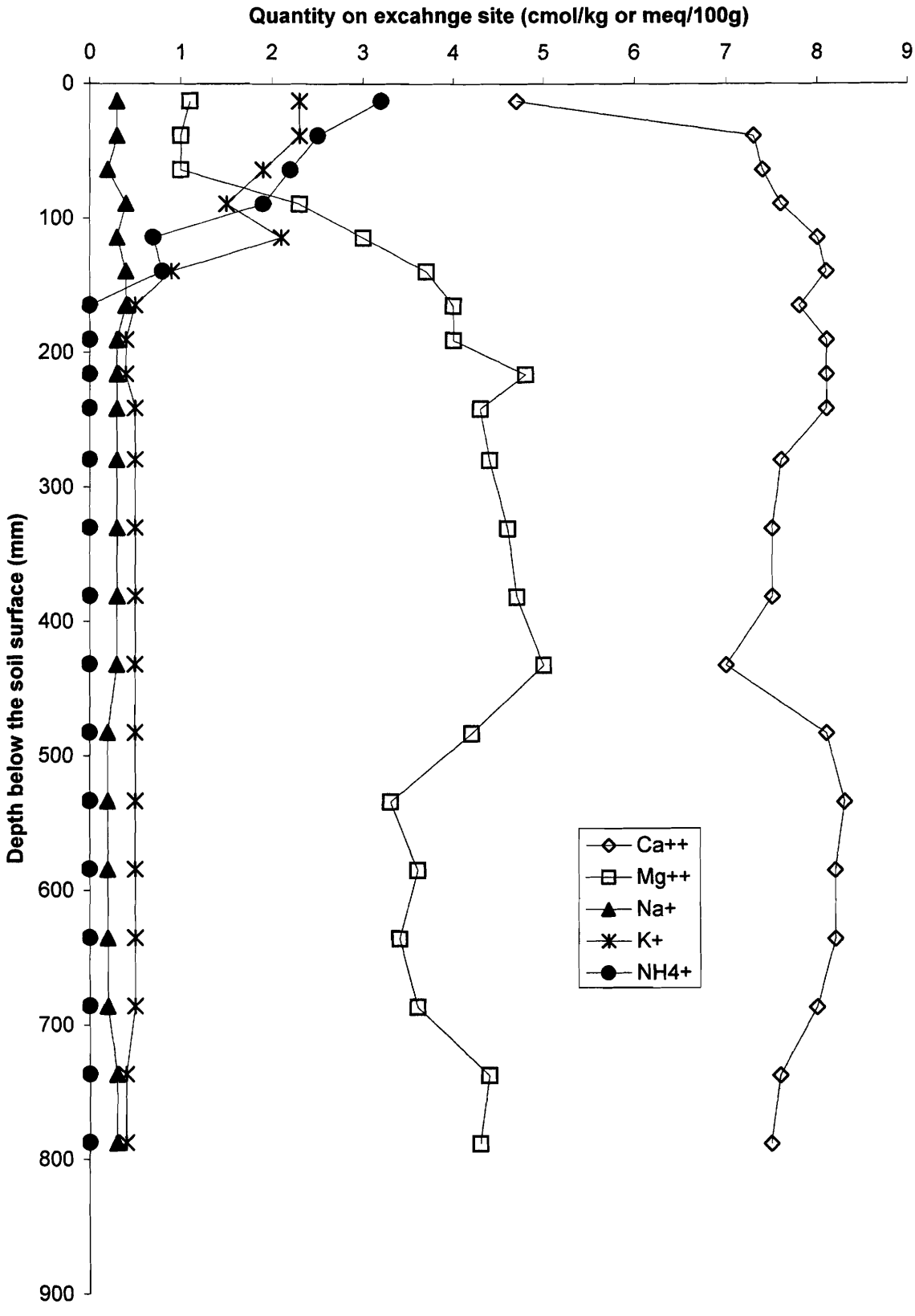

Figure 4.26 - Column No 1 distribution of ions on exchange sites as a function of depth below the surface of the soil column

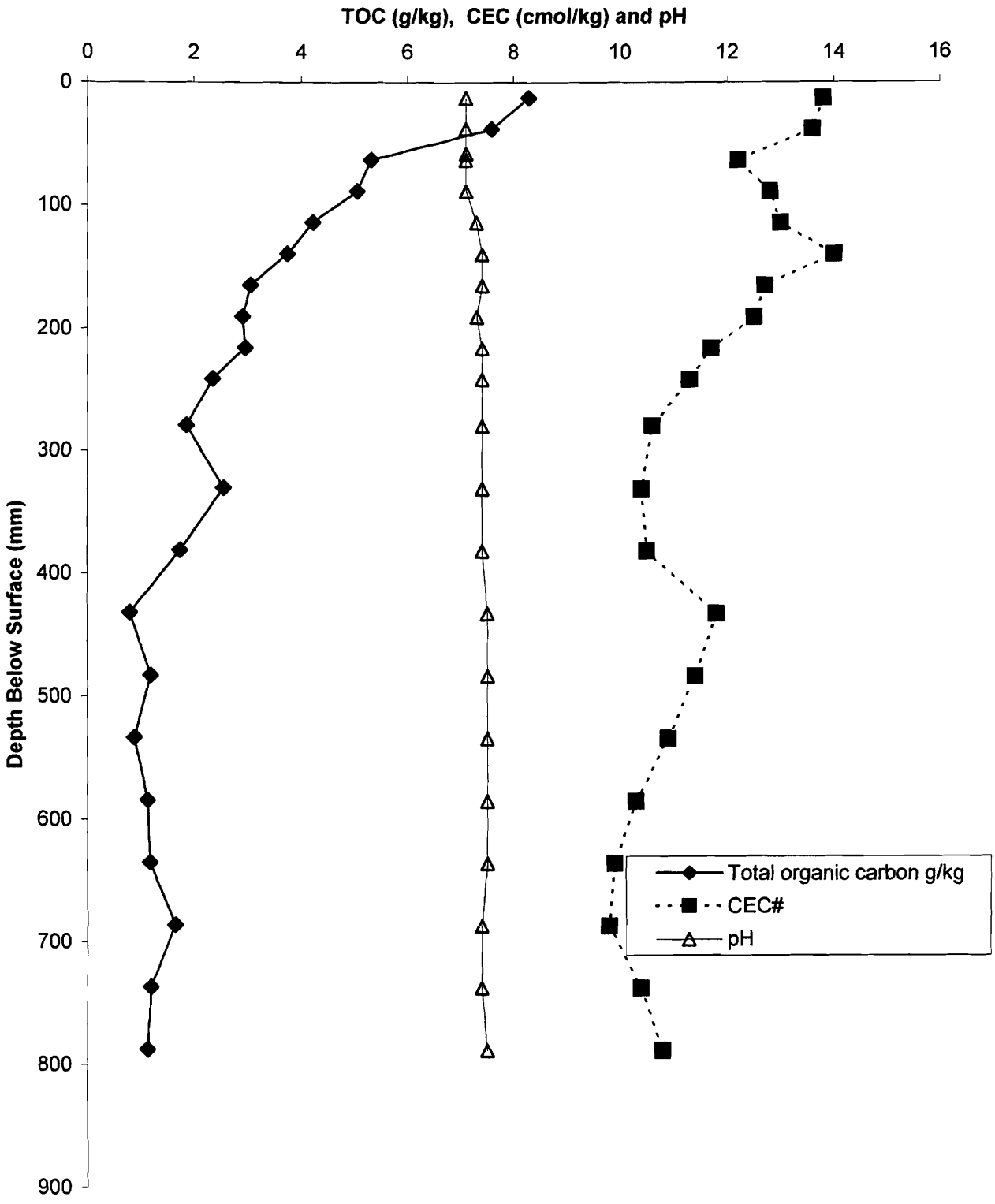

Figure 4.27: Column No. 1 TOC, CEC and pH vs depth within the column

Table 4.9 - Column No. 2 (Site No. 1 Soils) saturated paste extraction results corrected to original moisture content

Depth (mm)	HCO3- (meq/L)	Cl- (meq/L)	SO4-- (meq/L)	Ca++ (meq/L)	Mg++ (meq/L)	Na+ (meq/L)	K+ (meq/L)	Ba++ (meq/L)	N-NH4+ (meq/L)	EC (mS/cm)
13	15	84	34	10	11	11	26	1	71	6.3
38	16	102	57	13	17	18	30	1	92	7.8
64	15	66	48	7	9	13	26	1	73	6.8
83	17	49	43	4	4	12	23	0	61	4.3
95	9	31	23	3	2	10	14	0	31	2.3
114	6	31	17	2	1	9	12	0	27	2.3
140	15	10	18	1	0	7	9	0	23	2.0
178	12	11	11	1	0	7	6	0	18	2.2
229	20	16	14	2	2	9	10	0	25	2.3
279	17	15	9	2	2	11	9	0	22	2.8
330	18	15	8	1	1	10	8	0	20	2.9
381	16	12	7	1	1	7	7	0	17	2.8
432	14	11	4	1	0	6	5	0	16	2.3
483	14	11	7	2	1	7	5	0	17	2.1
533	13	11	6	2	1	7	5	0	16	2.2
584	11	9	6	1	1	6	3	0	15	2.0
635	13	10	7	1	1	7	3	0	17	2.1
686	12	9	6	1	1	6	3	0	15	2.1
737	12	10	6	1	2	7	2	0	15	1.9
787	19	8	3	2	2	11	3	0	12	1.9

Note: Results corrected for original water content

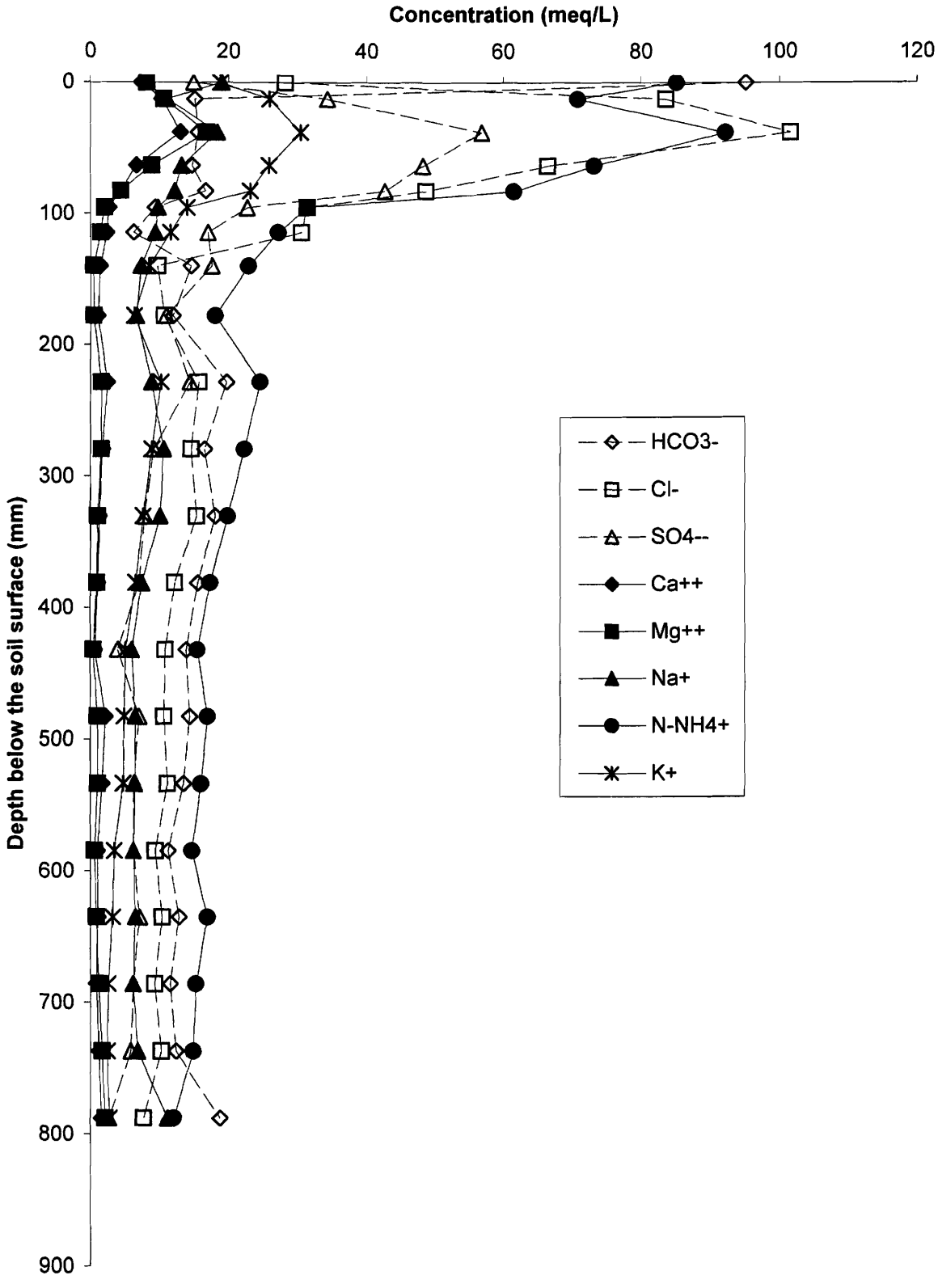

Figure 4.28 - Column No. 2 concentration of ions in solution at end of the column test

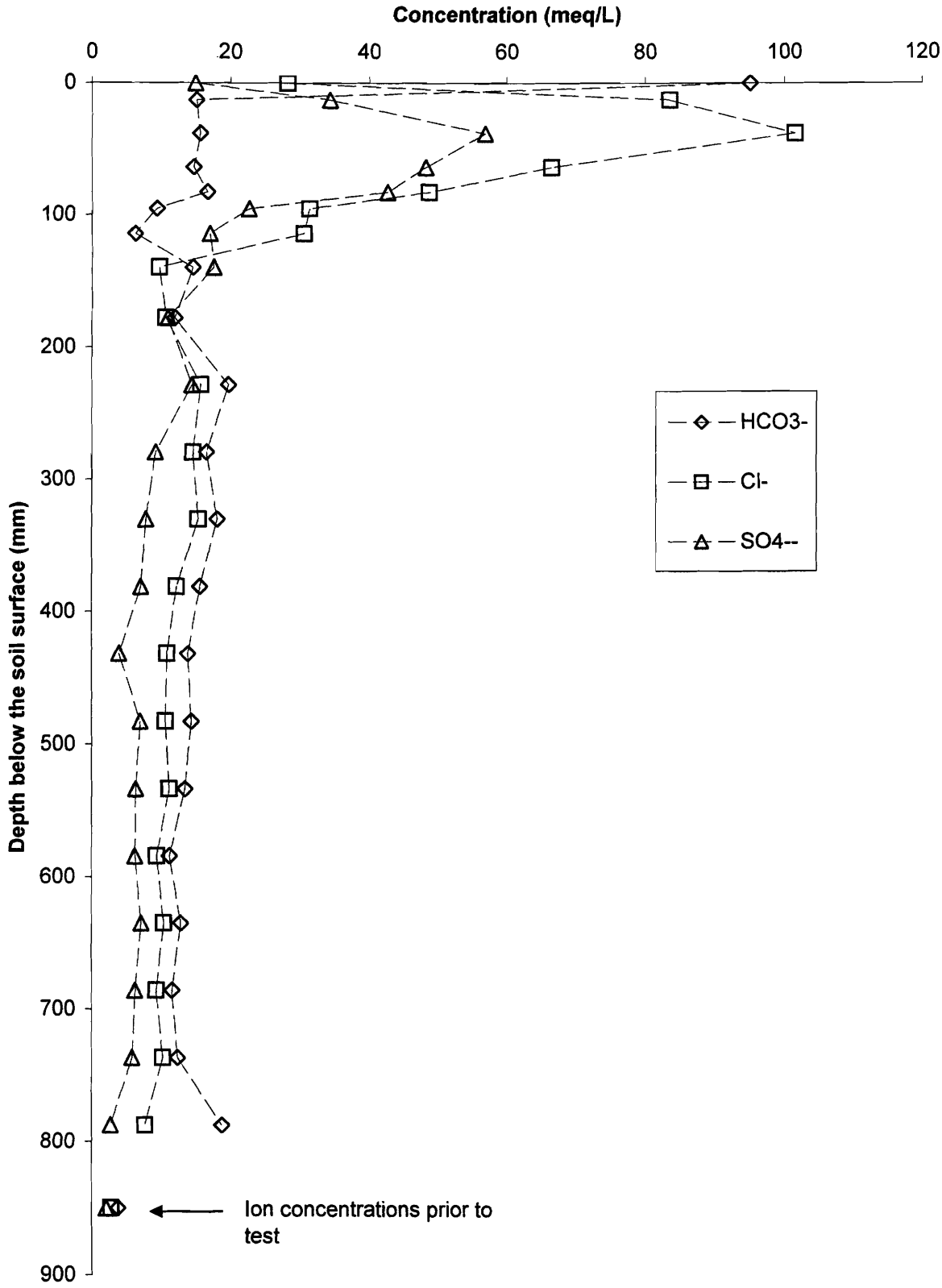

Figure 4.29 - Column No. 2 concentration of anions in solution at the end of the column test

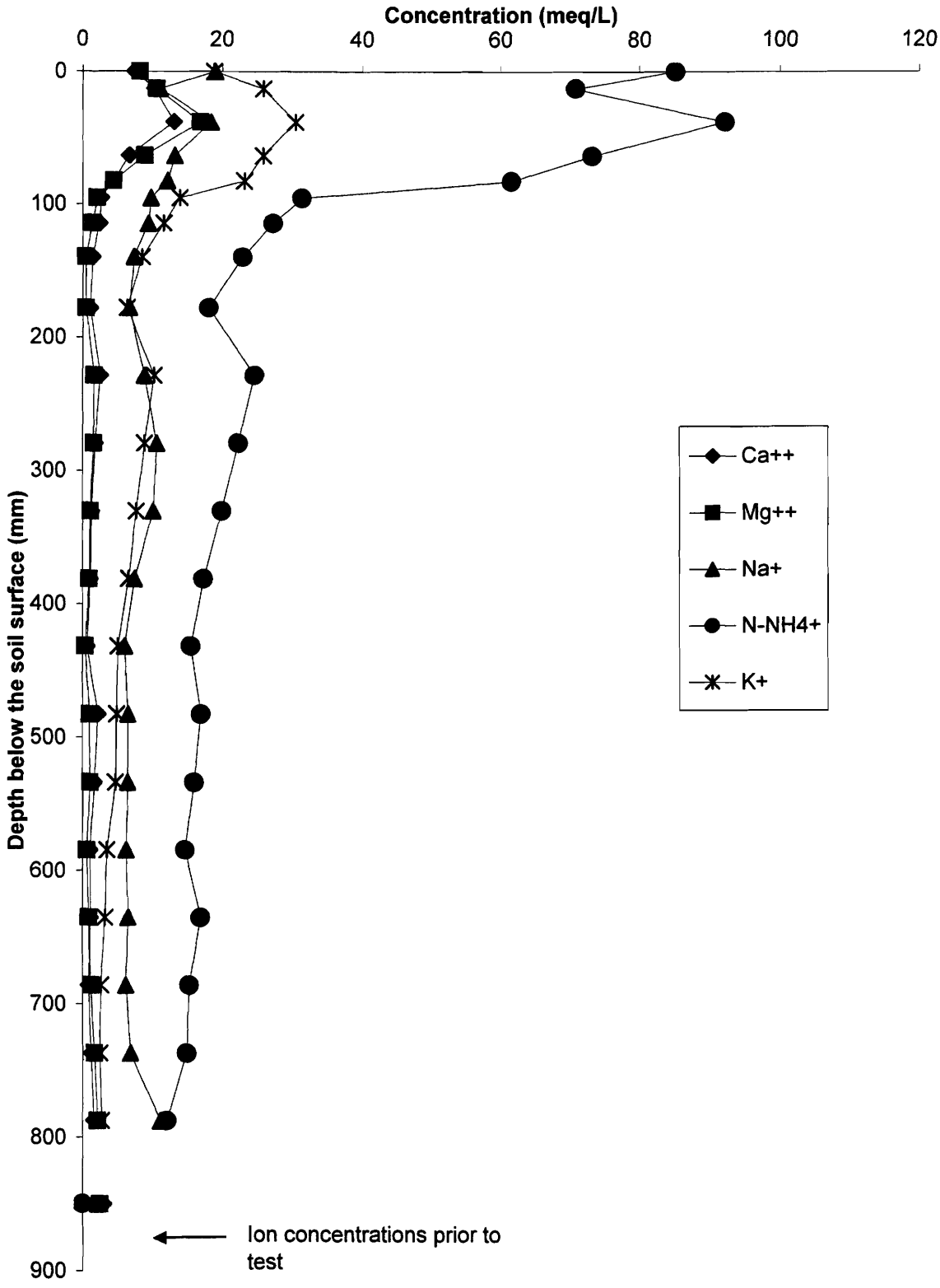

Figure 4.20 - Column No. 2 concentration of cations in solution at the end of the column test

column are substantially lower than background levels and remain at this concentration except in the upper 100 mm where they increase almost 10 fold to levels comparable to sodium.

Exchangeable cation analysis of Column No 2 soil sections (Figure 4.31, Table 4.10) indicate, with the exception of the top 100 mm, sodium concentrations remained relatively unchanged throughout the column even after over 3 pore volumes of flow. Potassium gradually increased from the base towards the top but decreased over the top 200 mm to near solution concentration. Ammonium on exchange sites generally increases from the column base to the top (similar to solution concentration increases). However, ammonium on exchange sites near the top of the column is variable and generally less, in sharp contrast to the substantial increase in solution ammonium in this same area. The increase in potassium and ammonium on exchange sites on the lower portion of the column is balanced by a loss of magnesium, and to some extent calcium, from exchange sites, but only from 100 to 250 mm below the soil manure interface. Between the soil manure interface (top of the column) and 100 mm depth, the slight increase in solution concentration of divalent cations appears to shift the preference on exchange sites toward the divalent cations and to calcium in particular (Figure 4.31).

pH remained relatively unchanged with depth, with the exception of slight decrease near the top of the column (Figure 4.32). Both TOC and CEC are highest near column top (soil-manure interface) and decrease with depth (Figure 4.32), indicating TOC may contribute to the CEC at higher TOC concentrations.

4.2.7 Ion exchange

Analyzing the change in cation concentration on the exchange sites revealed the impact of ion exchange on the transport of ammonium and potassium. In clay till material from the Clearfield Feeder Unit site in Column No 1, sodium is relatively uninvolved in any exchange reactions, but ammonium and potassium exchange for calcium and, to a

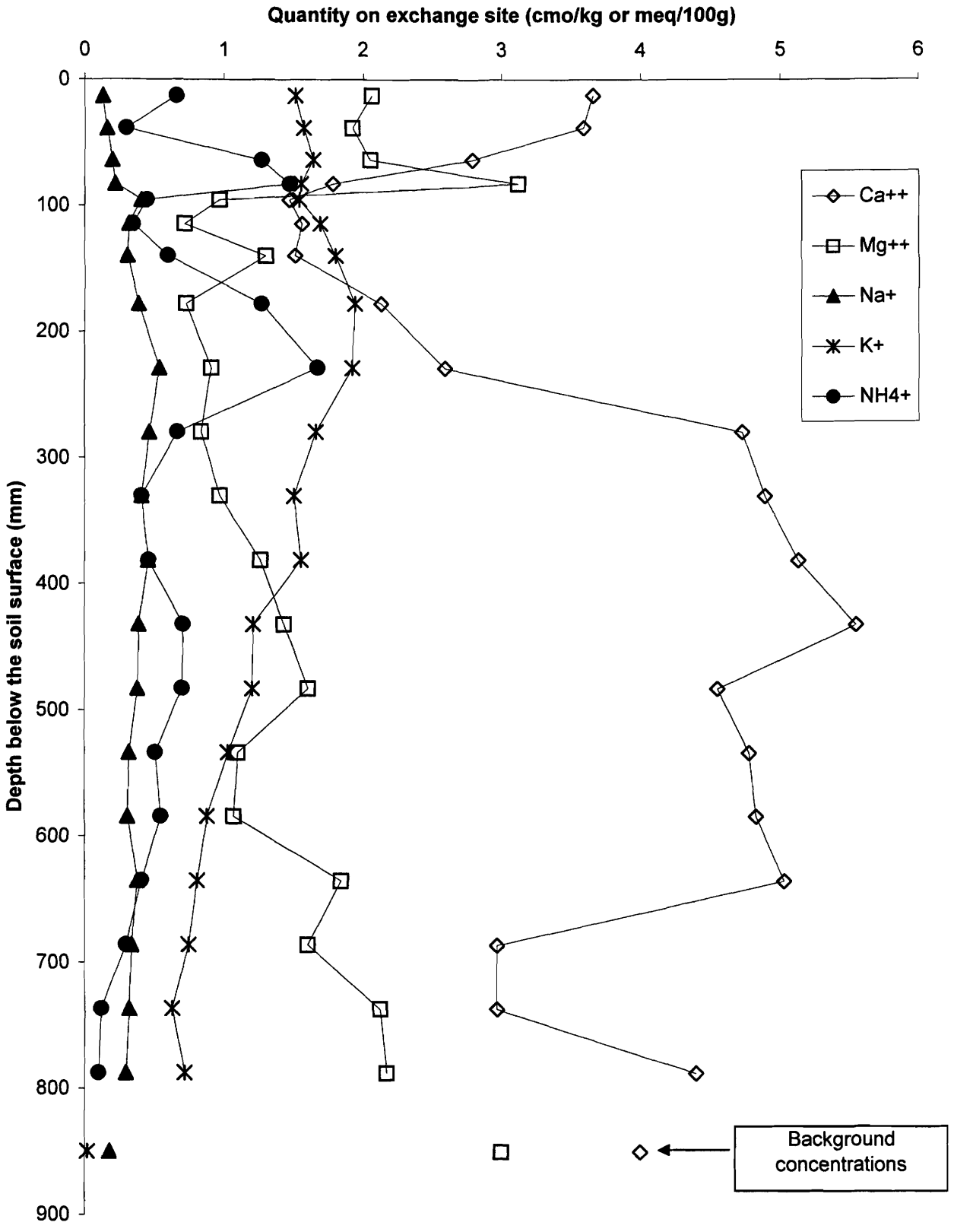

Figure 4.31 - Column No. 2 quantities of ions on the exchange sites as a function of depth below the soil surface

Table 4.10 - Column No 2 (Site No 1 soil) Extractable cations

Depth (mm)	pH	TOC (g/kg)	CEC# (cmol/kg)	Ca++ (cmol/kg)	Mg++ (cmol/kg)	Na+ (cmol/kg)	K+ (cmol/kg)	N-NH4+ (cmol/kg)	Total Cations (cmol/kg)
				(cmol of 1+ ions per kg of soil = meq/100g)					
13	7.7	1.69	7.94	3.66	2.06	0.13	1.51	0.66	8.02
38	7.6	1.49	7.45	3.59	1.92	0.16	1.57	0.30	7.54
64	8	1.18	7.86	2.79	2.05	0.20	1.64	1.27	7.95
83	7.8	2.46	8.28	1.78	3.12	0.22	1.55	1.47	8.14
95	7.9	0.58	6.97	1.47	0.97	0.41	1.54	0.45	4.84
114	8.2	0.22	5.61	1.56	0.72	0.32	1.69	0.35	4.64
140	8.3	1.04	5.95	1.51	1.30	0.31	1.80	0.60	5.52
178	8.3	1.02	6.54	2.13	0.73	0.39	1.94	1.27	6.46
229	8.3	0.89	7.94	2.59	0.91	0.54	1.92	1.67	7.63
279	8.2	0.66	8.38	4.73	0.84	0.47	1.66	0.67	8.37
330	8.1	1.30	7.86	4.89	0.97	0.41	1.50	0.41	7.77
381	8.3	0.59	8.15	5.13	1.26	0.46	1.55	0.46	8.86
432	8.3	1.40	8.01	5.55	1.43	0.39	1.21	0.71	9.29
483	8.3	1.60	7.22	4.55	1.60	0.38	1.20	0.70	8.43
533	8.1	1.20	6.91	4.78	1.10	0.32	1.03	0.51	7.74
584	8.2	0.47	6.81	4.83	1.07	0.31	0.88	0.55	7.64
635	8.1	1.18	7.56	5.03	1.84	0.38	0.81	0.41	8.47
686	8.2	1.09	5.35	2.97	1.60	0.34	0.75	0.30	5.96
737	8.4	0.91	5.72	2.97	2.12	0.32	0.63	0.12	6.16
787	8.4	0.67	6.72	4.40	2.17	0.30	0.72	0.10	7.69

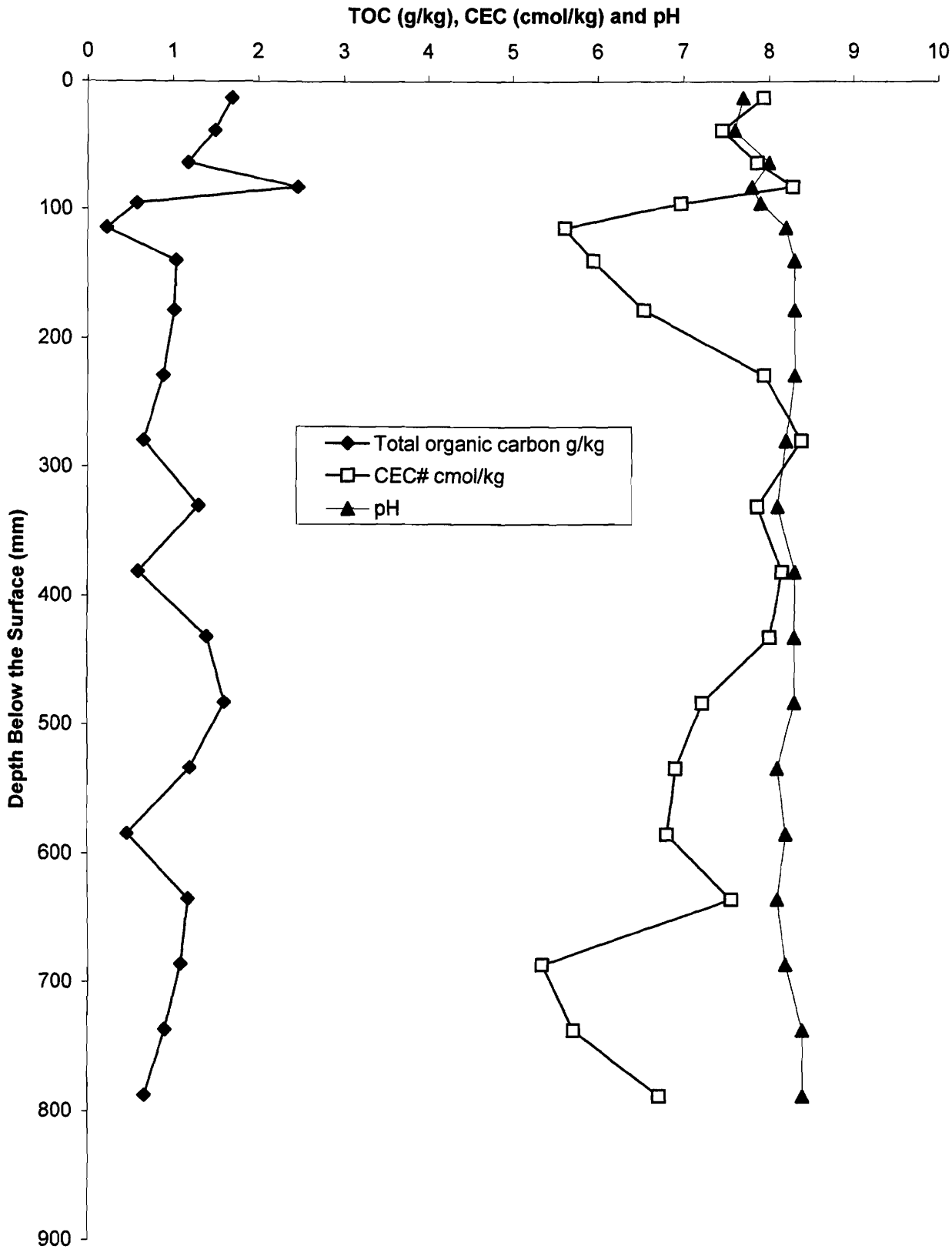

Figure 4.32 - Column No. 2: TOC, CEC and pH vs depth within the column

greater extent, magnesium (Figure 4.33). Some magnesium and calcium may precipitate, but there is evidence a large portion is displaced down the column.

Ion exchange in Column No. 1 may be affected by total organic carbon infiltration from ponded effluent. The CEC in Column No. 1 increased as total organic carbon increased (R^2=0.6; Figure 4.34) according to:

$$CEC = 1.453 \ln(TOC) + 10.439 \qquad [Eq\ 4.1]$$

In the sandy material in Column No 2, sodium again appears to play a minor role in the ion exchange process (Figure 4.35). Ammonium and potassium displaced large amounts of calcium and magnesium from the exchange sites. While calcium was displaced down the column, magnesium washed from the column. Effluent chemistry data (Figure 4.22) indicates magnesium concentration in the column exfiltrate reached a maximum C/Co concentration of 2 near mid–June, substantiating the conclusion magnesium originally on exchange sites was discharged from the column. These results are similar to others reported (Goodall and Quigley, 1977; Grove and Wood, 1979; Nicholson et al., 1983; Dance and Reardon, 1983; Ceazan et al., 1989; Beekman and Appelo, 1990; Bjerg and Christensen, 1993 Thornton et al., 2000).

The potential effect of organic carbon on ion exchange in Column No. 2 is not assessable; no significant increase in CEC could be attributed to TOC increase in the column.

4.2.8 Batch Tests

Solution concentrations of chloride, sodium and potassium were similar in batch tests conducted with soils from both Kelvington and Site No.1 (Tables 4.11 and 4.13). Ammonium and bicarbonate concentrations were lower for the Kelvington soil test possibly due to higher absorption of ammonium and carbonate reactions with calcium; calcium concentrations at higher dilutions were considerably greater in the Kelvington

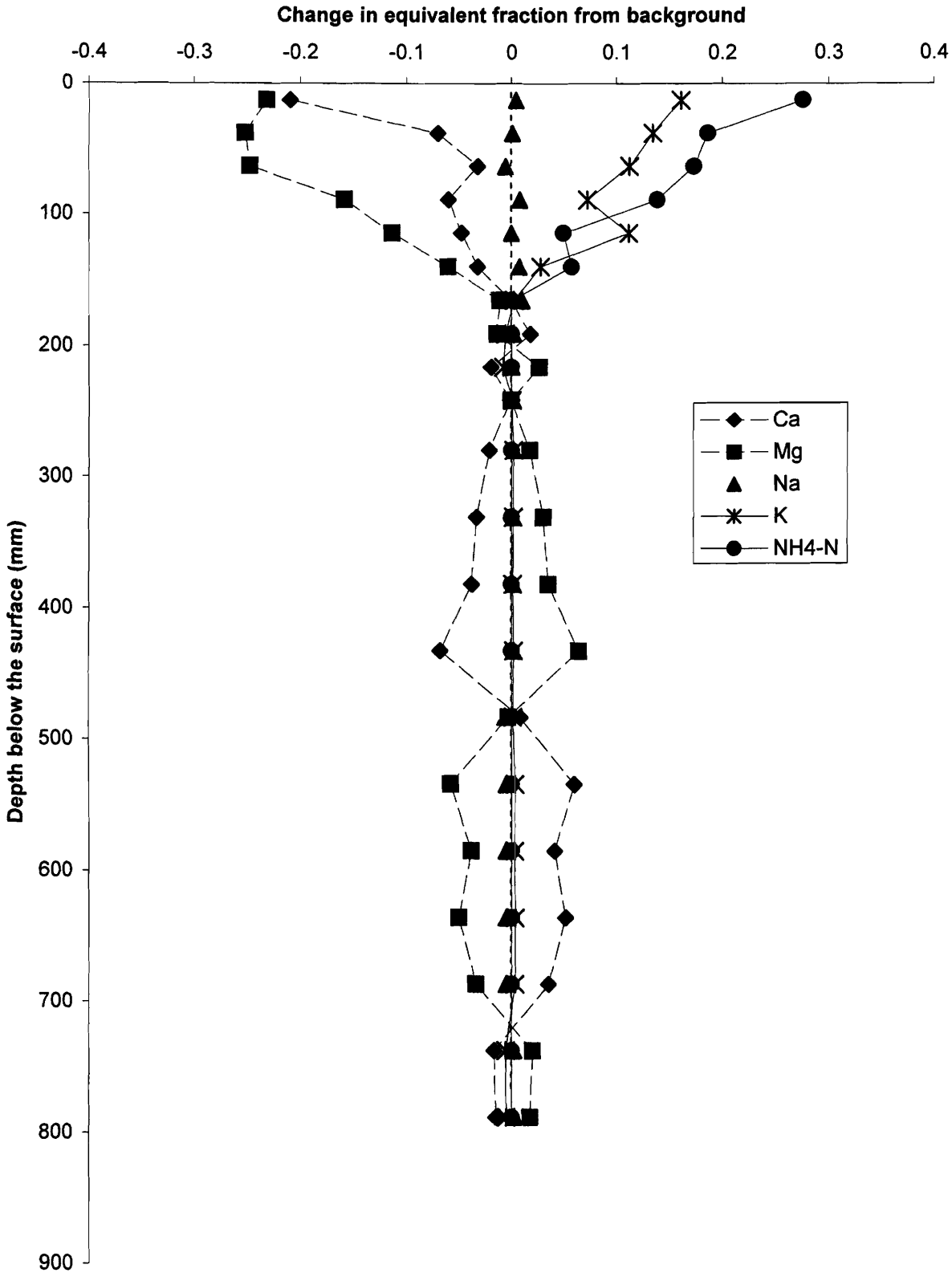

Figure 4.33: Column No. 1 change in equivalent fraction adsorbed as a function of depth in the column.

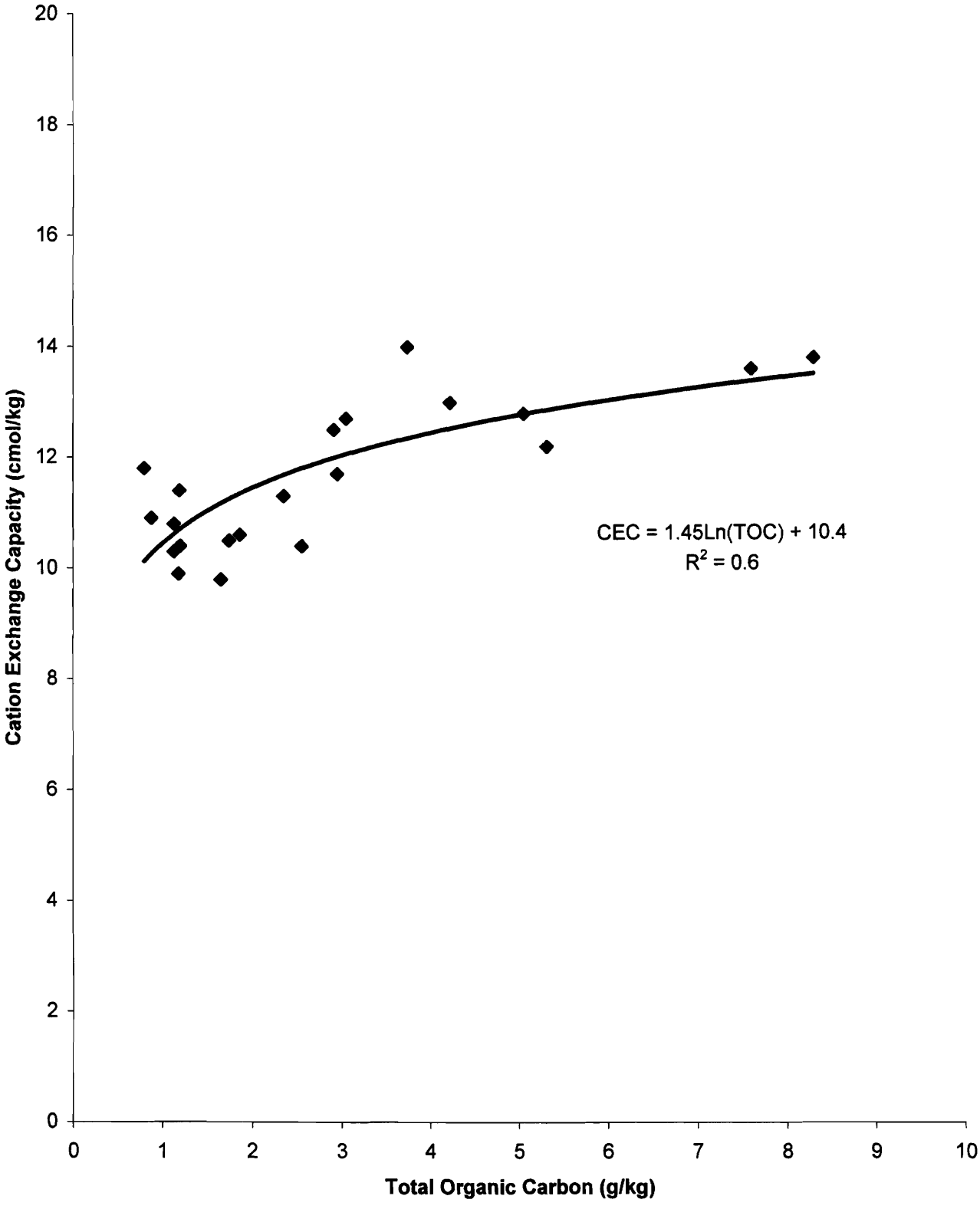

Figure 4.34: Column No. 1 cation excahnge capacity increase as a function of total organic carbon.

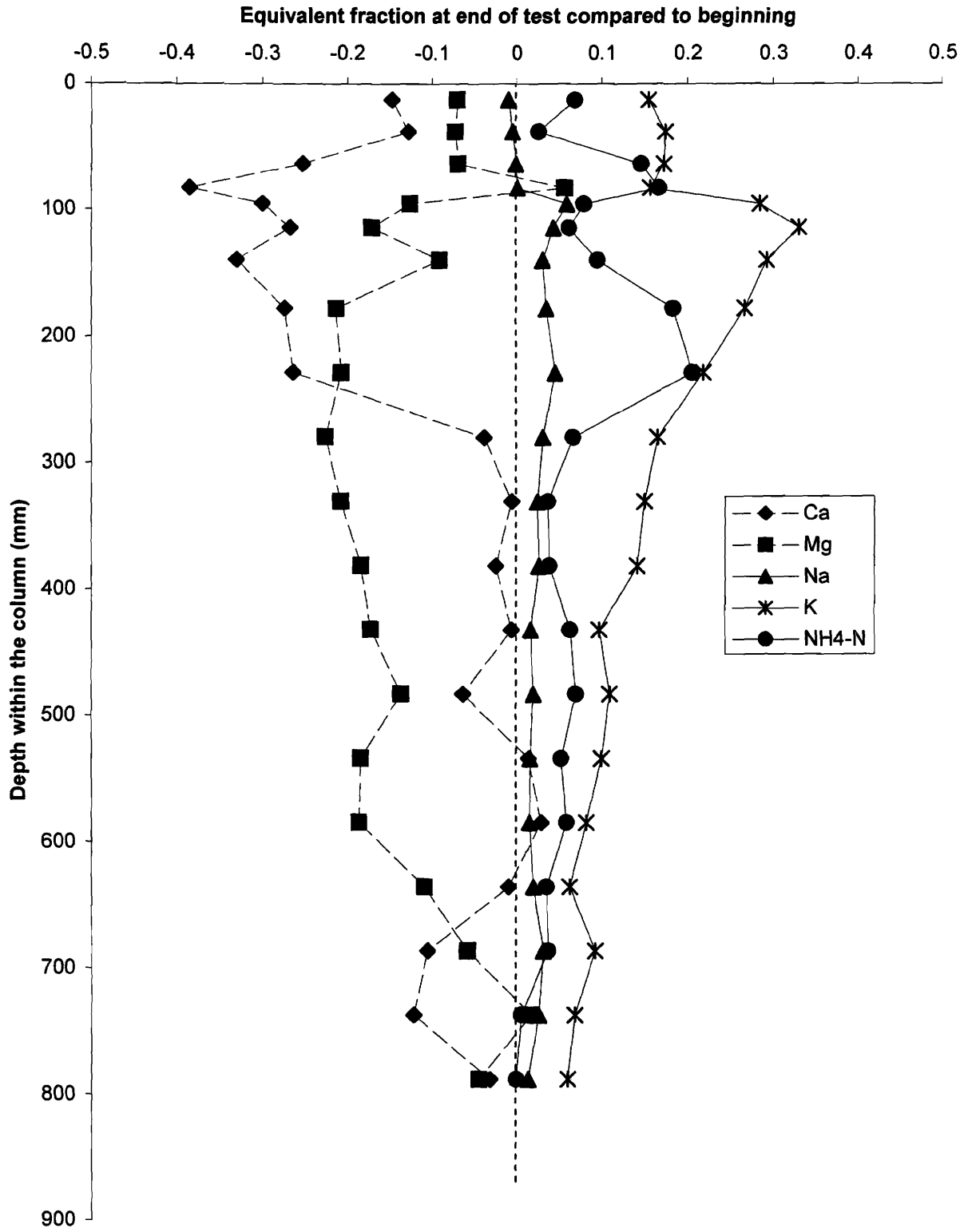

Figure 4.35: Column No. 2 change in equivalent fraction adsorbed at various depths within the soil column.

soil. Sulphate concentrations were also higher in the Kelvington soil test possibly from presence of calcium sulphate in the soil. Magnesium concentrations were similar for both samples at the higher dilutions but notably higher for Site No.1 soils at lower dilutions, possibly as a result of release of magnesium from soil exchange sites. Complete results of batch test chemistry are provided in Tables 4.11 to 4.14.

Table 4.11 - Concentration of ions in solution at the end of the batch test for the Kelvington soil.

Dilution (%)	HCO3- (meq/L)	Cl- (meq/L)	SO4-- (meq/L)	Ca++ (meq/L)	Mg++ (meq/L)	Na+ (meq/L)	K+ (meq/L)	N-NH4+ (meq/L)
90	12.4	4.3	27.1	13.0	4.4	3.9	3.8	16.4
80	21.0	9.1	29.2	5.0	4.7	7.4	7.4	27.1
70	32.1	13.8	29.2	1.7	4.7	10.0	10.7	40.7
60	45.2	17.5	31.3	1.5	4.9	13.5	14.3	55.0
50	63.3	21.7	31.3	1.3	5.2	17.4	18.4	70.7
40	81.6	26.4	35.4	0.9	5.4	21.3	23.0	85.7
30	103.6	30.5	31.3	0.9	5.3	24.4	26.6	99.9
20	118.4	33.9	31.3	0.9	5.4	27.4	29.7	114.2
10	136.1	38.4	33.3	1.2	5.5	30.4	33.5	128.5
0	157.2	43.4	33.3	1.1	5.7	34.4	37.9	142.8
Original	207	48	10	2	1	36	44	193

Table 4.12 - Concentration of exchangeable ions at the end of the batch test for the Kelvington soil.

Dilution (%)	Ca++ (meq/100g)	Mg++ (meq/100g)	Na+ (meq/100g)	K+ (meq/100g)	N-NH4+ (meq/100g)
90	9.5	1.8	0.3	1.0	1.8
80	4.0	0.7	0.2	0.7	1.7
70	6.8	1.6	0.6	1.6	3.4
60	6.2	1.7	0.8	2.0	4.4
50	5.9	1.6	0.8	2.1	4.8
40	5.4	1.4	1.5	2.4	4.3
30	4.4	1.1	0.9	2.0	4.0
20	4.7	1.2	1.0	2.2	4.4
10	5.5	1.5	1.3	2.7	5.3
0	5.6	1.4	0.8	2.2	4.6

Table 4.13 - Concentration of ions in solution at the end of the batch test for the Site No. 1 soil.

Dilution (%)	HCO3- (meq/L)	Cl- (meq/L)	SO4-- (meq/L)	Ca++ (meq/L)	Mg++ (meq/L)	Na+ (meq/L)	K+ (meq/L)	N-NH4+ (meq/L)
90	20.0	4.6	1.1	0.9	5.7	3.6	2.8	14.3
80	39.7	8.6	3.3	1.0	8.2	7.0	6.1	26.4
70	56.7	13.0	3.1	1.0	9.9	10.0	10.0	40.7
60	78.0	17.8	4.0	1.0	11.5	13.5	14.1	59.2
50	94.4	22.0	5.0	0.9	11.5	17.0	17.9	71.4
40	117.4	25.8	6.0	0.8	12.3	20.4	21.7	85.7
30	136.7	29.9	6.9	0.7	12.3	23.9	25.8	107.1
20	156.6	35.0	8.1	0.7	13.2	27.8	30.2	121.3
10	163.3	38.6	9.0	0.7	13.2	30.9	33.5	142.8
0	200.0	43.4	9.8	0.6	13.2	36.1	38.4	178.4
Original	207	48	10	2	1	36	44	193

Table 4.14 - Concentration of exchangeable ions at the end of the batch test for the Site No. 1 soil.

Dilution (%)	Ca++ (meq/100g)	Mg++ (meq/100g)	Na+ (meq/100g)	K+ (meq/100g)	N-NH4+ (meq/100g)
90	6.2	9.5	0.3	1.2	2.7
80	3.2	4.5	0.2	1.0	2.2
70	3.7	4.2	0.3	1.2	2.5
60	3.2	3.6	0.3	1.2	2.5
50	3.1	3.2	0.3	1.3	2.5
40	3.4	3.3	0.2	1.1	2.3
30	3.8	3.7	0.4	1.6	3.4
20	3.7	3.5	0.4	1.7	3.3
10	3.4	3.2	0.3	1.4	2.7
0	3.4	3.2	0.5	1.7	3.3

Results for the Kelvington soil show a rapid increase in potassium and ammonium absorbed and a rapid decrease in calcium and magnesium released at the highest dilutions (lowest solution strengths; Figure 4.36). Potassium and magnesium reach maximum concentrations near 2 and 1 meq/100g respectively, similar to results obtained from Column No. 1 (Figure 4.26). Sodium concentrations at the lower dilutions are higher than those which occurred during the column study. Ammonium absorption onto and calcium loss from the soil exchange complex are both higher than occurred during the column study. Calcium concentrations increase at the lower

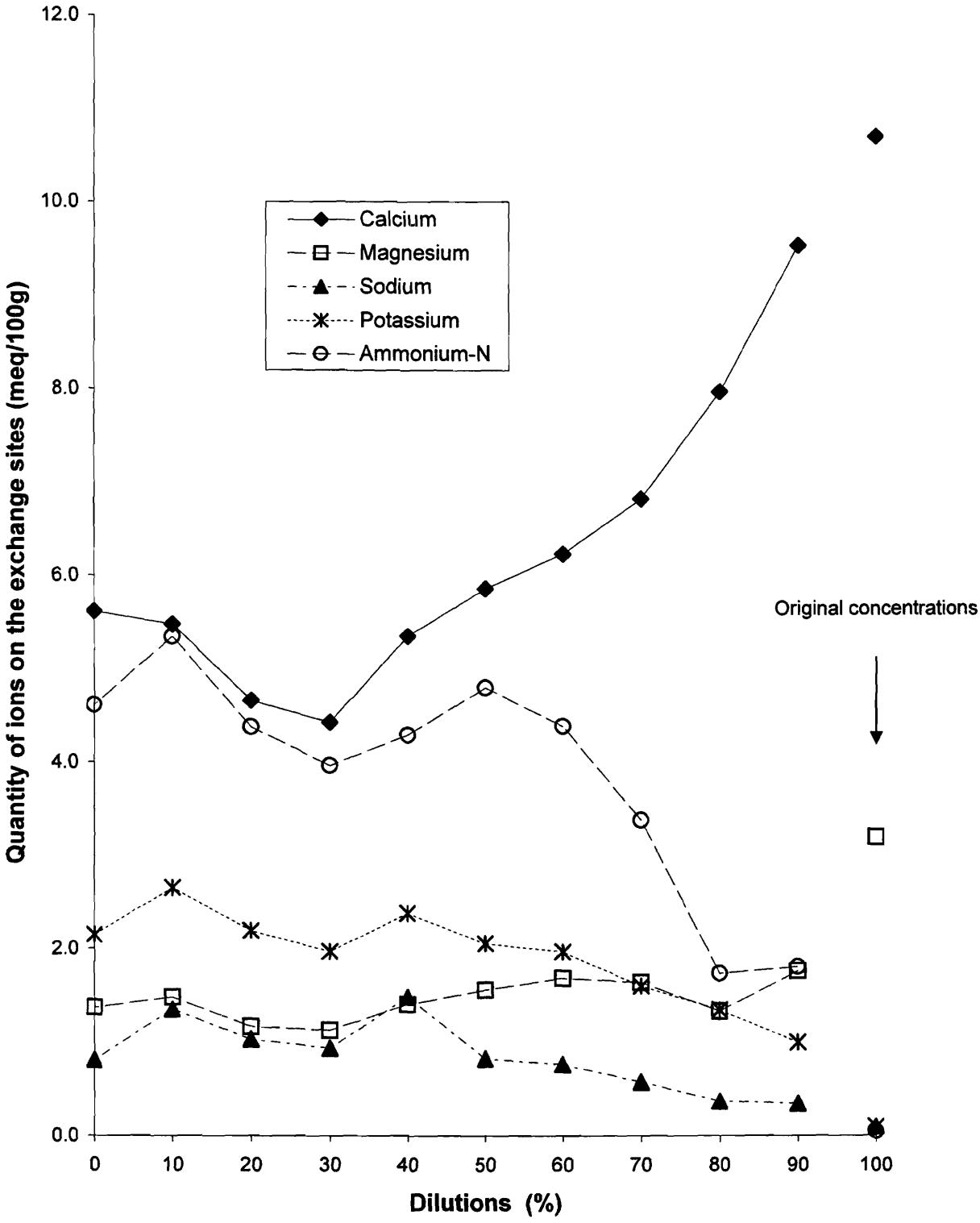

Figure 4.36: Quantities of ions on the exchange sites for the batch test results for the Kelvington soil.

dilutions indicating calcium absorption increases as ionic strength increases, as previously reported (Wiklander, 1964; McBride, 1994). Ammonium absorption decreases from 50 to 30% dilution even though this represents a substantial increase in ammonium added (Figure 4.36). Ammonium absorption increases from 30 to 10% dilution but then decreases again at 0% dilution. These observations may help explain solution chemistry patterns obtained in the column study; ammonium would absorb at lower concentrations (front of the plume), not absorb at moderate concentrations (middle of the plume), then absorb again at high concentrations.

Results for Site No. 1 soil (Figure 4.37) are similar to Kelvington soil. Initial absorption of potassium and ammonium at higher dilutions results in loss of calcium and magnesium from the exchange complex. Potassium reached a maximum concentration near 2 meq/100g, similar to results of Kelvington soil batch tests and both column tests. Sodium concentrations were less than Kelvington soil test results but similar to results from Column No. 2. Increased ammonium absorption with a reduction in dilution resulted in a continued reduction in magnesium on the exchange complex; absorbed calcium concentrations remained relatively constant. These results are similar to Column No.2, where magnesium was preferentially removed over calcium from the exchange complex.

4.2.9 Sorption Isotherm Analysis

Langmuir isotherm plots were produced for each cation found on soil exchange sites of the columns. Langmuir type analysis was chosen as most ions reached a maximum absorption at higher solution concentrations. Best-fit sorption isotherms were plotted against analytical data on a plot of quantity on exchange sites (S) versus concentration in solution (C) using the following relation (Fetter 1993):

$$\frac{C}{S} = \frac{1}{\alpha\beta} + \frac{C}{\beta} \qquad \text{[Eq 4.2]}$$

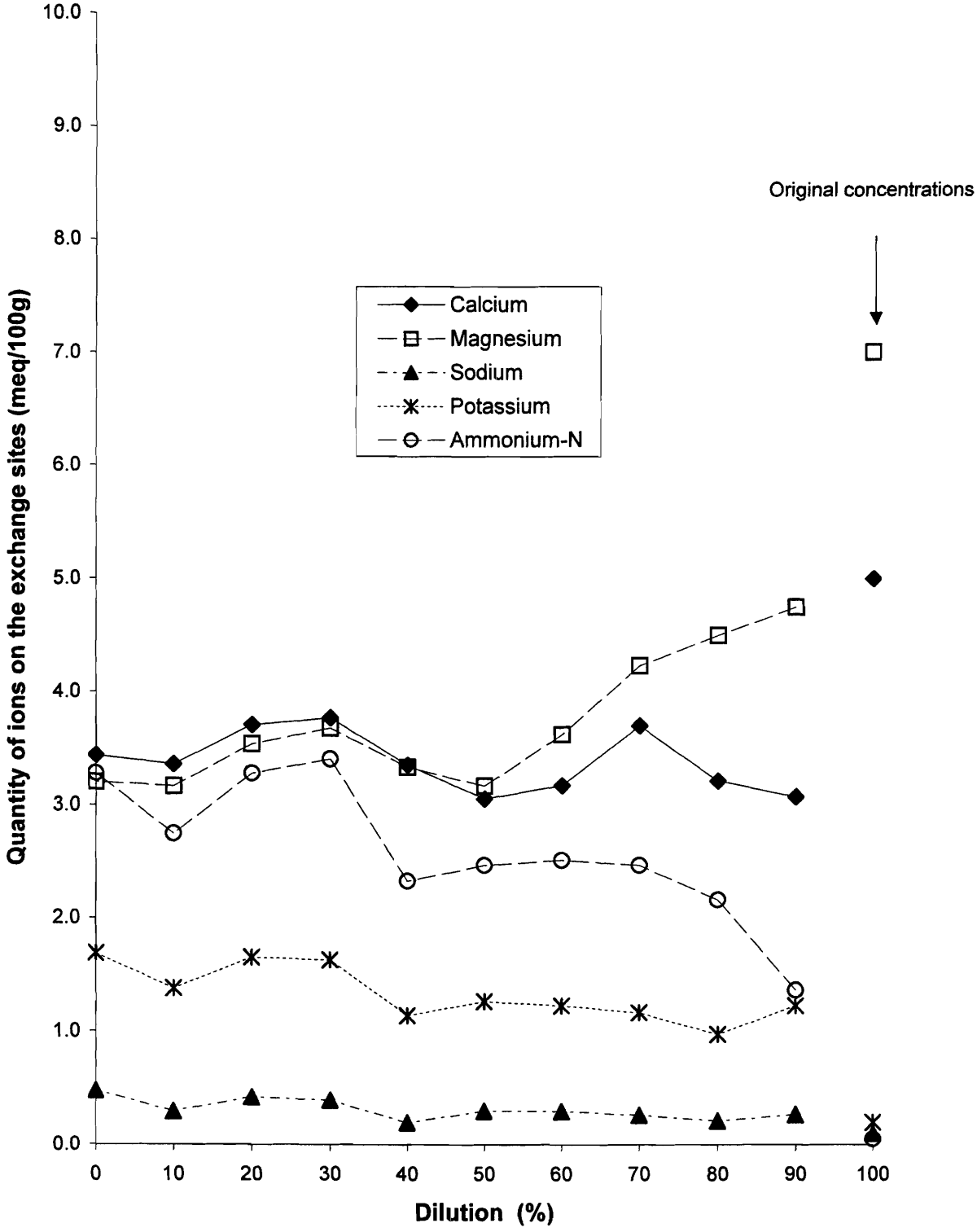

Figure 4.37: Quantities of ions on the exchange sites for the batch test results for Site No. 1 soil.

where:

β = maximum amount of solute which can be absorbed by the solid (Smax) and

α = an absorption constant related to binding energy.

Equation 5.2 can also be written as:

$$S = \frac{\alpha\beta C}{1+\alpha C} \qquad \text{[Eq 4.3]}$$

This form of the equation allows prediction of quantities of an ion on exchange sites for a given concentration in solution, and a relation for retardation by (Fetter 1993):

$$R = 1 + \frac{\rho}{\varepsilon}\left(\frac{\alpha\beta}{(1+\alpha C)^2}\right) \qquad \text{[Eq 4.4]}$$

where:

R = retardation factor for the Langmuir isotherm,

ρ = bulk density,

ε = porosity, and

$\frac{\alpha\beta}{(1+\alpha C)^2}$ can be considered as a distribution coefficient.

In this study, several factors changed simultaneously, each affecting the other. An example is an increase in sodium accompanied by a much larger increase in potassium and ammonium suppressing the effect of the sodium increase. As a result, isotherm plots were analyzed in relation to measured concentrations of ions in solution and quantity of ions on exchange sites.

4.2.9.1 Calcium

A Langmuir type plot of solution and exchange site calcium data for Column No. 1 and the Kelvington soil batch tests produced a linear trend (R^2=0.98) and values of β and α of 1667 mg/kg (8.3 meq/100g) and 0.083 L/mg respectively (Figures 4.38). Column

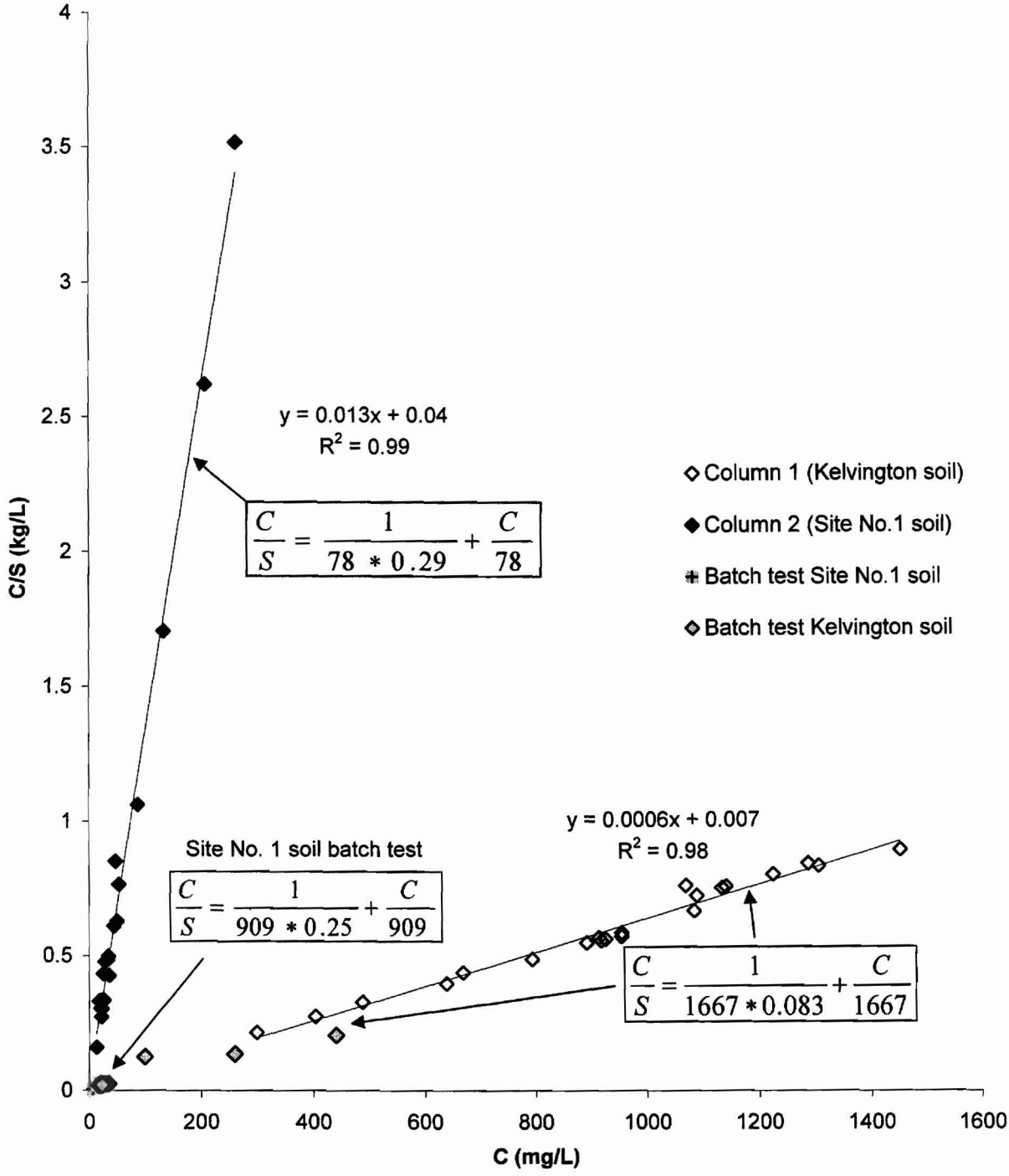

Figure 4.38: Langmuir isotherm plots for Calcium

No. 2 data also plotted as a linear relation (R^2=0.99) with values of β and α of 78 mg/kg (0.4 meq/100g) and 0.29 L/mg, respectively (Figure 4.38). Batch test results using the Site No. 1 soil produced values of β and α of 909 mg/kg (4.5 meq/100g) and 0.25 L/mg (Figure 4.38). While Column No. 2 and Site No. 1 results produced similar absorption constants, values of β suggest soils in Column No. 2 were depleted of calcium at the end of the test period.

Sorption of calcium in all cases appears to follow a typical Langmuir isotherm, increasing on the exchange sites to a maximum value. Values of β represent approximately 60% of the total exchange capacity measured for the soils in Column No. 1 and the Kelvington soil batch test, and 40% for the soils in the Site No. 1 soil batch test. This could result from an insufficient data set, finite sorption (Thornton et al., 2000) or the possibility that only a portion of the sites are available for exchange (Erskine, 2000).

4.2.9.2 Magnesium

Data for magnesium produces relatively linear plots on a Langmuir isotherm plot with R^2 values of 0.67, 0.94, 0.95 and 0.12 for Column No. 1, Column No.2, and Site No. 1 and Kelvington soil batch tests, respectively (Figure 4.39). Linear trendlines for Column No.2, and Site No. 1 and Kelvington soil batch tests indicate maximum sorption values (β) ranging from 142 to 333 mg/kg (1.2 to 2.7 meq/100g). Maximum sorption value (β) for Column No. 1 was 833 mg/kg (6.9 meq/100g). The bi-linear isotherms suggested by the data could result from differing sorption sites with differing energies (Fetter, 1977) or indicate a magnesium solution concentration necessary for magnesium to compete for soil exchange sites.

4.2.9.3 Sodium

Langmuir isotherm plots for sodium (Figure 4.40) produce relatively linear plots for both column and batch tests. Relatively small maximum absorption values (β) of 31 to 100 mg/kg (0.13 to 0.4 meq/100g) indicate no significant sorption for column tests and

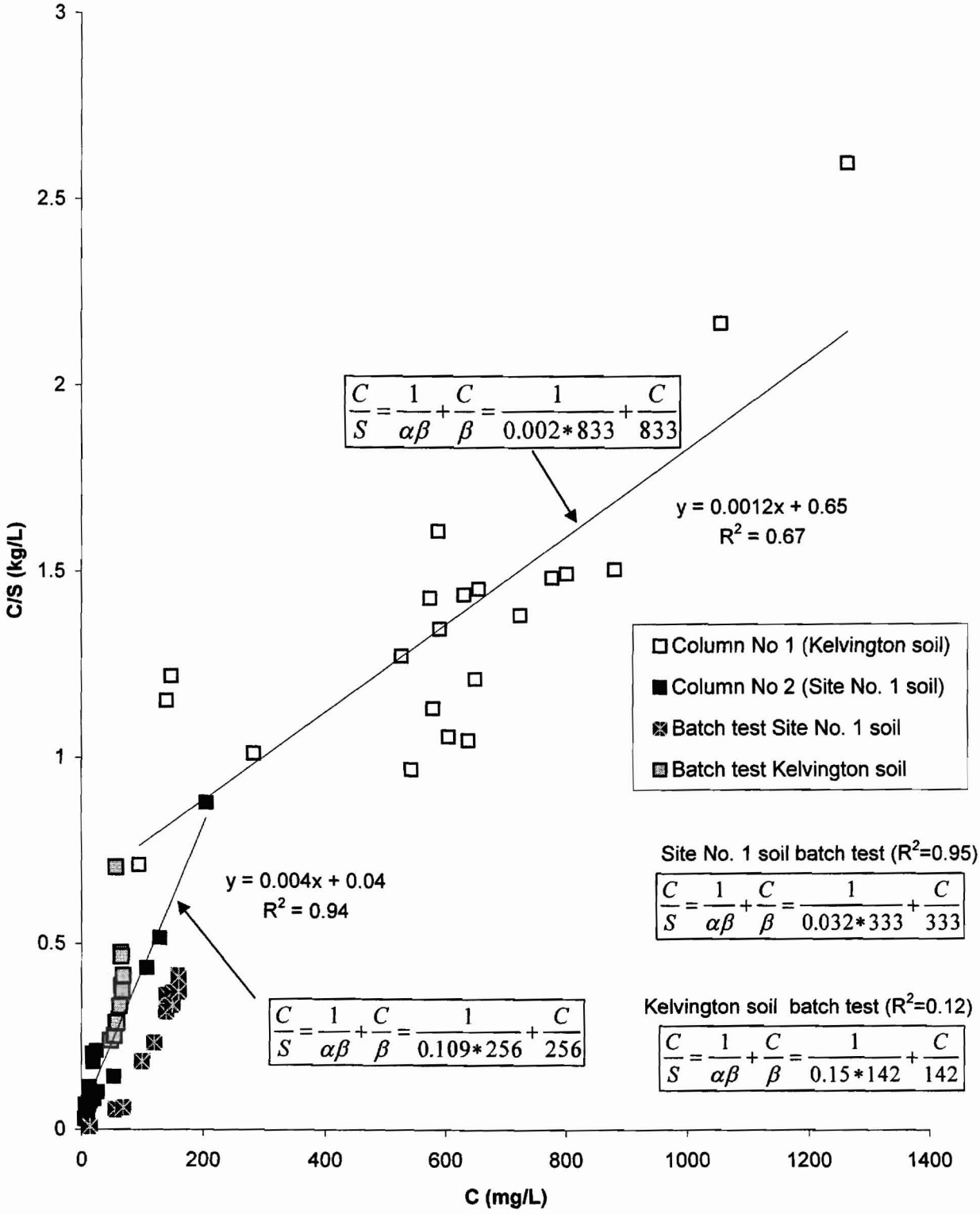

Figure 4.39 - Langmuir isotherm plots for Magnesium sorption.

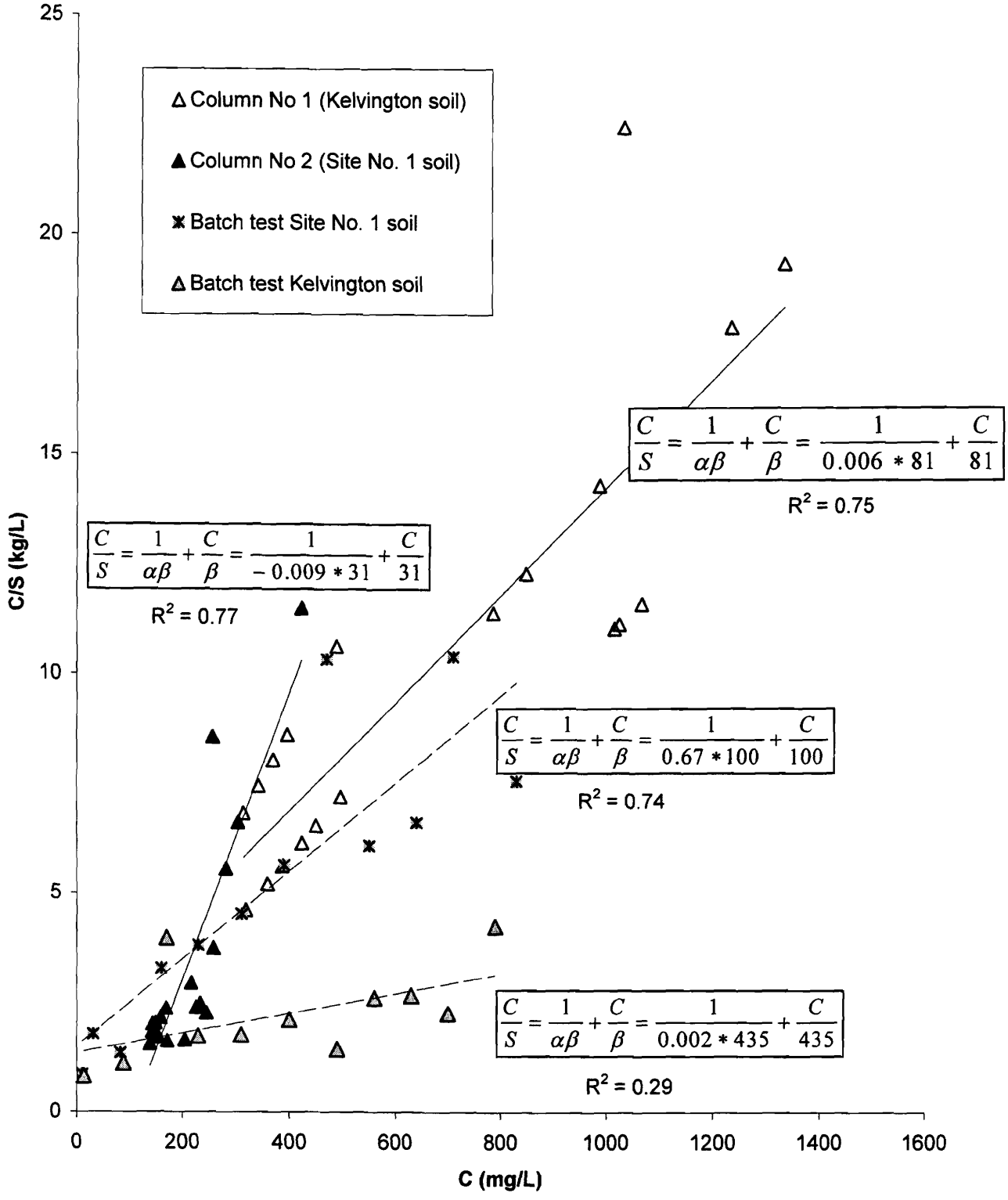

Figure 4.40: Langmuir isotherm plot for Sodium

the Site No. 1 batch test. β for the Kelvington soil batch tests was 435 mg/kg (2 meq/100g), similar to the maximum obtained from the lab test (Figure 4.36), and consistent with observations of sodium transport and generally accepted principles of the lyotropic series (Appelo and Postma, 1993). Sodium has the largest hydration shell of monovalent cations present; the combination of single charge and thick hydration layer would limit the ability of sodium to compete for exchange sites. Negative α (binding energy) values for soils in Column No 2 indicate desorption, or differences in ionic strength of solution in various samples resulting in an array of portions of several different isotherms.

4.2.9.4 Potassium

The Langmuir type sorption plot for potassium (Figure 4.41) produces a bilinear isotherm for soil from Column No 1 and a single linear relation for Column No. 2 and the batch tests. The first portion of the Column No.1 isotherm represents the area below the seepage plume with a calculated value of β of 175 mg/kg (0.45 meq/100g), similar to background concentrations of absorbed potassium. The upper portion of the isotherm represents the area near the front of the seepage front where potassium was initially absorbed. The isotherm line for the Kelvington soil batch test is parallel to this line, indicating similar maximum sorption for potassium of 1000 mg/kg (2.6 meq/100g). Results for Column No.2 and the Site No.1 soil batch test are similar, with a maximum sorption value (β) of 625 mg/kg (1.6 meq/100g) for both tests.

The two linear isotherm lines for the Column No 1 soil result from differing sorption sites with differing energies as suggested by Fetter (1977), or indicate potassium concentrations must reach levels above 150 mg/L before it can compete for exchange sites (see Figure 4.42). Potassium in the batch test was not subjected to external sources of cations and gradually increased to a maximum at the various concentrations added. Conversely, potassium in Column No. 1 was subjected to external sources of cations as a result of reactions in adjacent soils (Figure 4.25). The result is a pattern where potassium initially absorbs at the leading edge of the seepage front, then is held off

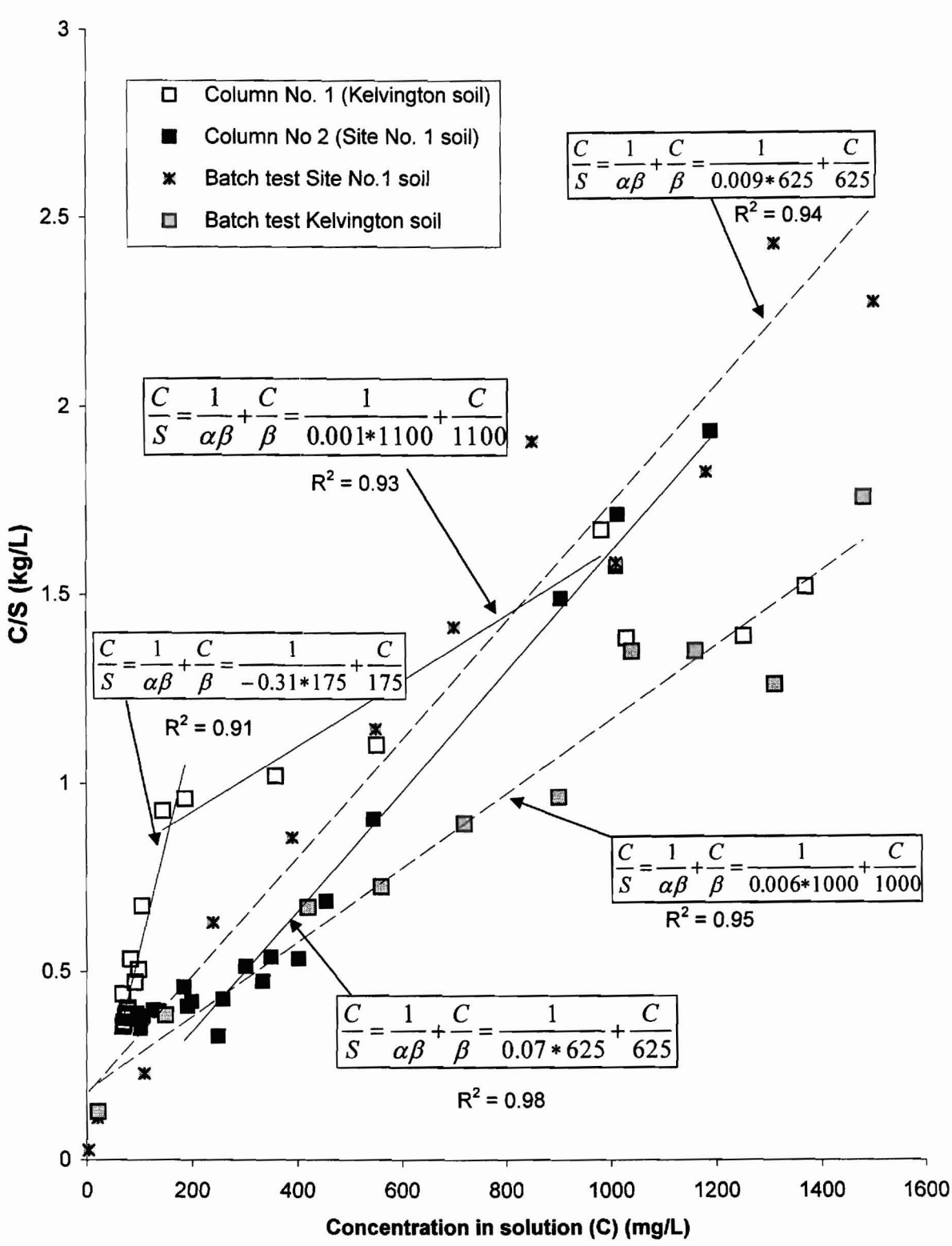

Figure 4.41: Potassium Langmuir isotherm plots.

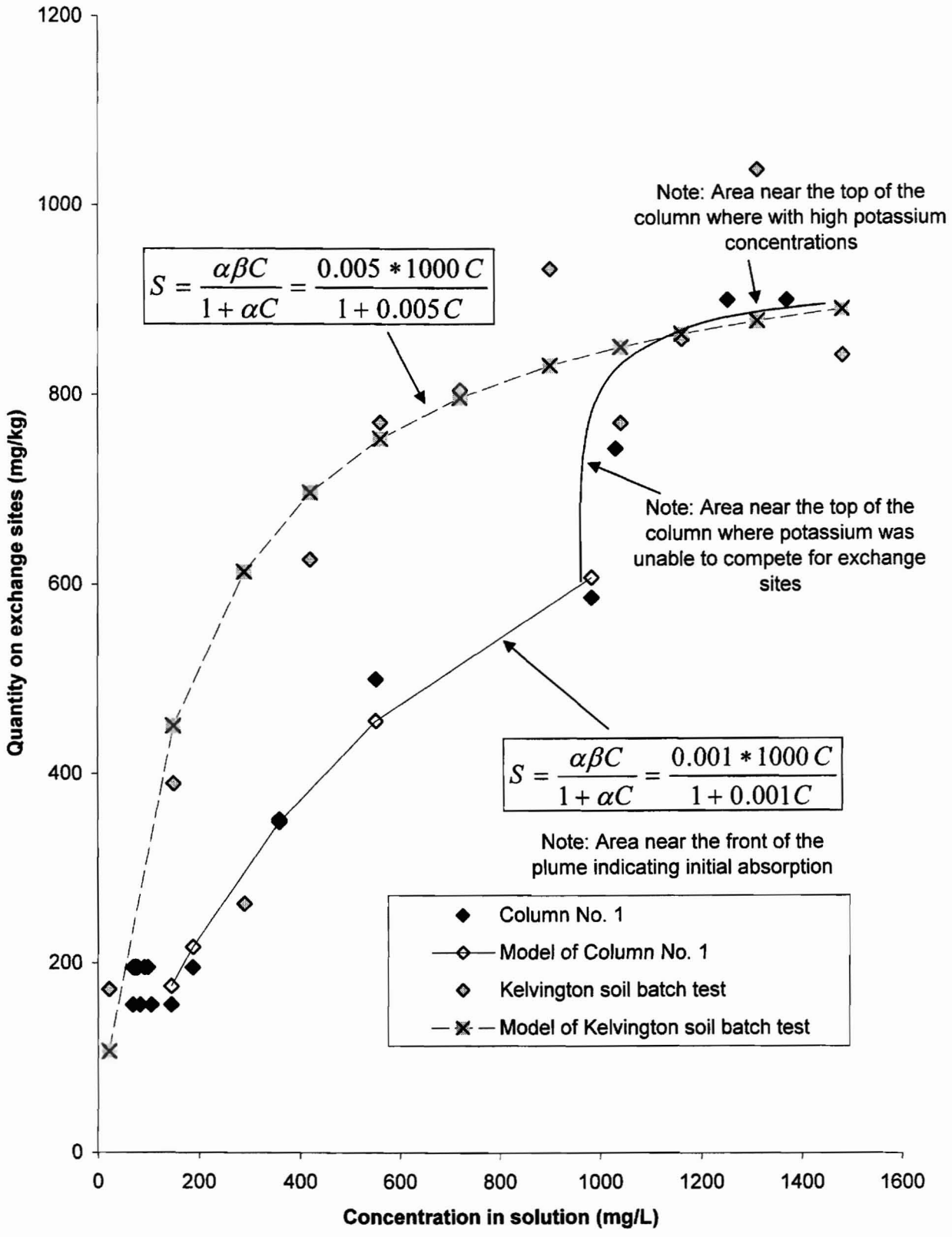

Figure 4.42: Potassium sorption isotherms for Column No.1 and the Kelvington soil batch test.

exchange sites (potentially by high ammonium concentration) at the plume midpoint, then absorbs again as potassium concentrations increase and competing ion concentrations decrease (Figure 4.42).

The Site No. 1 soil batch test again indicates a gradual increase in potassium on the exchange complex to a maximum concentration as potassium increases in concentration (Figure 4.43). Column No. 2 data indicates potassium may have desorbed or absorbed in certain locations within the column. Results also demonstrate a maximum absorption of 625 mg/kg (1.6meq/100g) at potassium concentration in solution above 600 mg/L, indicating potassium is able to remove other ions at concentrations above 600 mg/L, but has limited absorption for this soil at the concentrations used in these experiments. Both columns and batch tests indicate a maximum absorption (β) of potassium equal to approximately 23% of the total CEC.

4.2.9.5 Ammonium

Sorption isotherm plots for ammonium yielded linear plots for the Column No. 2 and batch test data, although the linear correlation to the Column No.2 data is low (R^2=0.32; Figure 4.44). The poor fit is likely the result of cation exchange competition as locations with ammonium concentrations above 500 mg/L also contained significant concentrations of calcium and magnesium. The isotherm plot for Column No. 2 and Site No. 1 soil batch test data (Figure 4.45) shows this effect; the isotherm for Column No. 2 follows the batch test data trend for ammonium concentrations less than 500 mg/L, but indicates ammonium was unable to compete for soil exchange sites where ammonium concentrations were above 500 mg/L. The maximum sorption (β) of 67 mg/kg (0.5 meq/100g; Figure 4.44) reflects the absorbed ammonium concentrations in the majority of sample locations within the column (Figure 4.31), and indicates distribution coefficients of 0.03 to 0.8 L/kg for the range of ammonium solution concentrations found in the column. Isotherm plots for the Site No. 1 soil batch test indicates a maximum sorption (β) value of 455 mg/kg (3.2 meq/100g) and an absorption coefficient (α) of 0.007 L/mg (Figure 4.45).

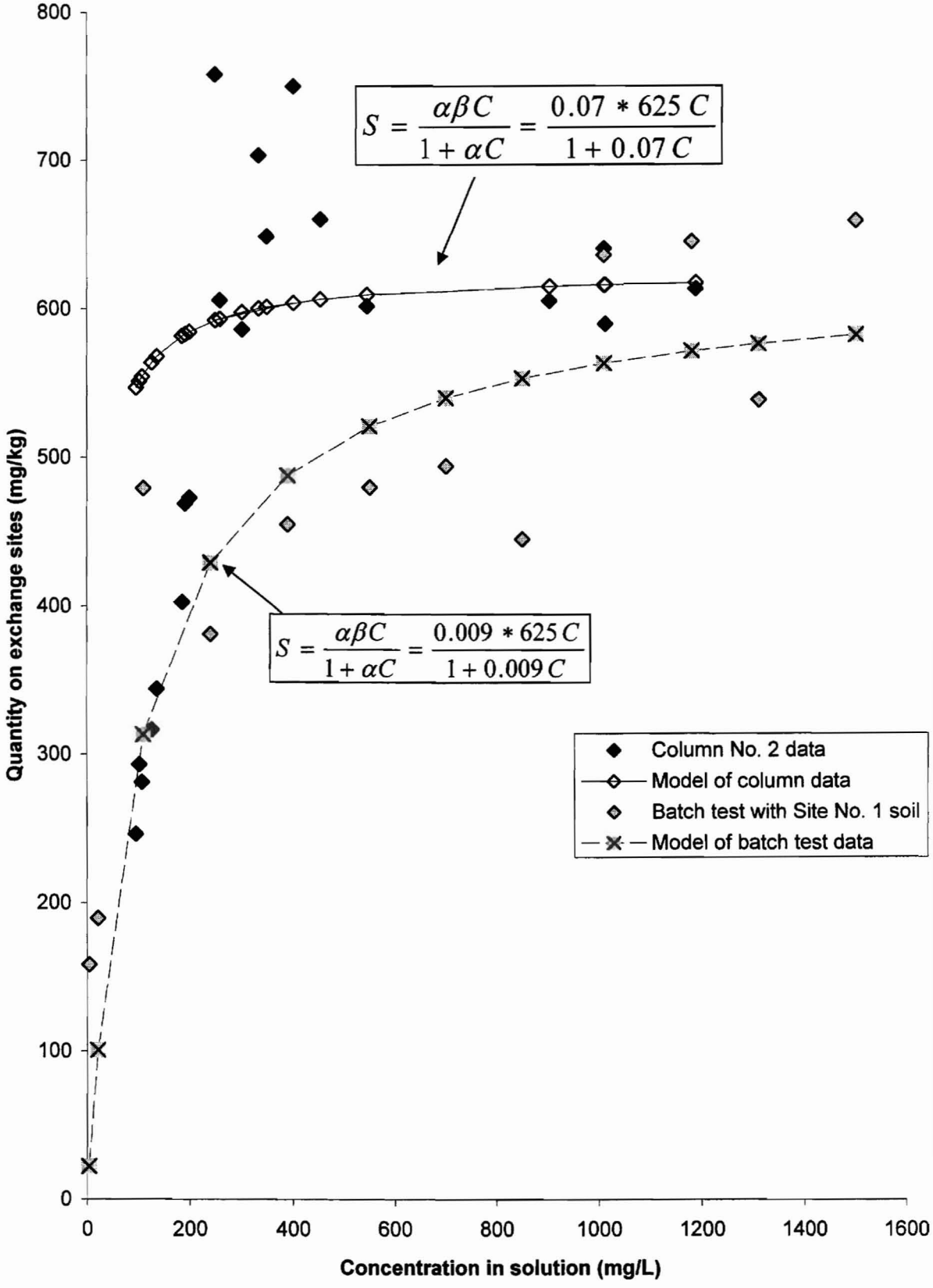

Figure 4.43: Potassium sorption isotherms for Column No. 2 and the Site No. 1 soil batch test.

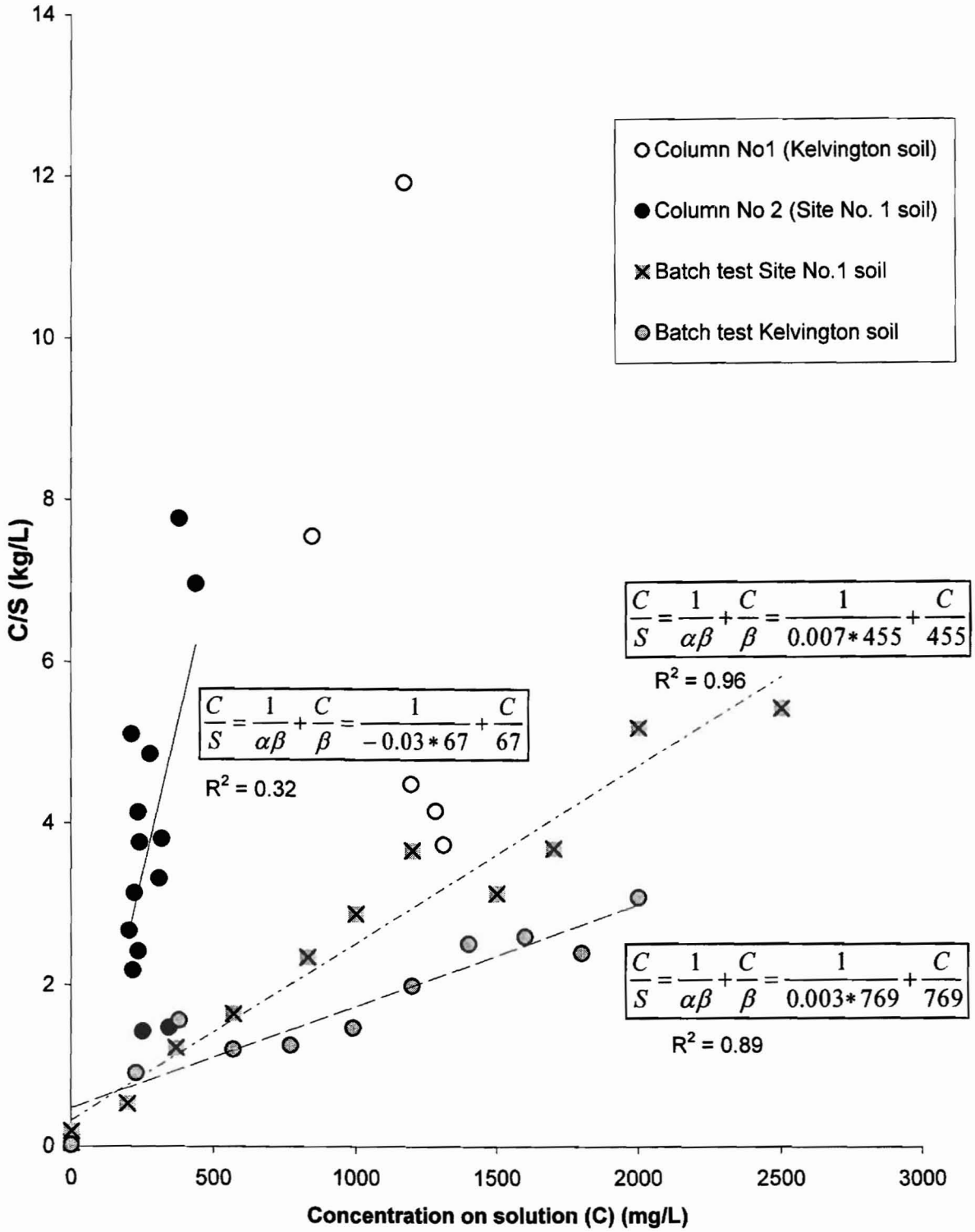

Figure 4.44: Langmuir isotherm plot for ammonium.

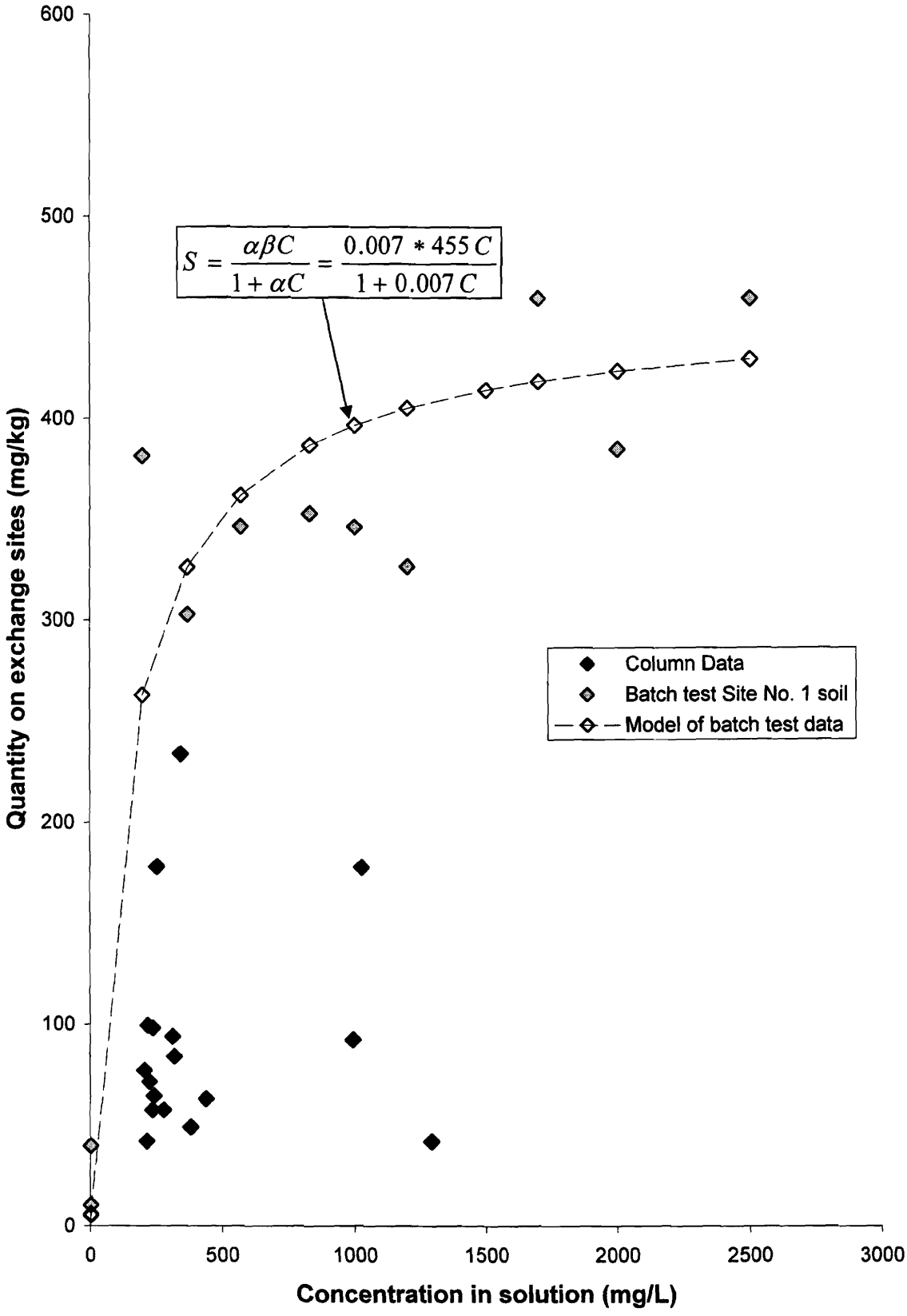

Figure 4.45: Ammonium sorption isotherms for Column No 2 and Site No.1 soil batch test data.

There is no discernable pattern for the Column No. 1 data on Figure 4.44, although the Kelvington batch test data indicates a maximum sorption (β) value of 769 mg/kg (5.5 meq/100g) and an absorption coefficient (a) of 0.003 L/mg (Figure 4.44), which agree with data from Figure 4.36. A possible explanation for the lack of a detectable isotherm on Figure 4.44 is ammonium's inability to compete for soil exchange sites within the column at solution concentrations less than 800 to 1000 mg/L (Figure 4.46). Ammonium solution concentrations above these values produced an isotherm with a similar slope to the Kelvington batch data at concentrations from 0 to 500 mg/L.

4.2.10 Langmuir Distribution Coefficient

Distribution coefficients can be calculated from the slope of the Langmuir isotherms using Equation 4.4 and the coefficients β and α as determined in the isotherm analysis. The coefficients β and α can also be used in several transport models, such as POLLUTE (Rowe et al., 1998), to define attenuation. Analysis of distribution coefficients as a function of concentrations of ions absorbed or in solution is useful when modeling the transport of multiple cations (Valocchi, 1981; Mansell et al. 1988). The variation of the distribution coefficient can be related to the exchange coefficient (Valocchi, 1981), or exchange equations can be incorporated in place of a distribution coefficient as in the case of some mixing cell models (Schulz and Reardon, 1983).

Figure 4.47 shows the calculated distribution coefficients for potassium using coefficient values shown on Figure 4.41. Batch test results indicate significantly higher distribution coefficients for potassium concentrations less than 200 mg/L, but similar to values produced by column tests for solution concentrations above 200 mg/L. Distribution coefficients for Column No. 1 range from a high of 1.2 L/kg at low potassium concentrations to a low of 0.18 L/kg at high potassium concentrations. Distribution coefficients for Column No. 2 are lower at 0.7 L/kg for the lowest potassium concentrations and decrease more rapidly to a low of 0.006 L/kg at high potassium concentrations. The lower distribution coefficients in column studies as opposed to batch tests likely result from high solution concentrations of calcium and

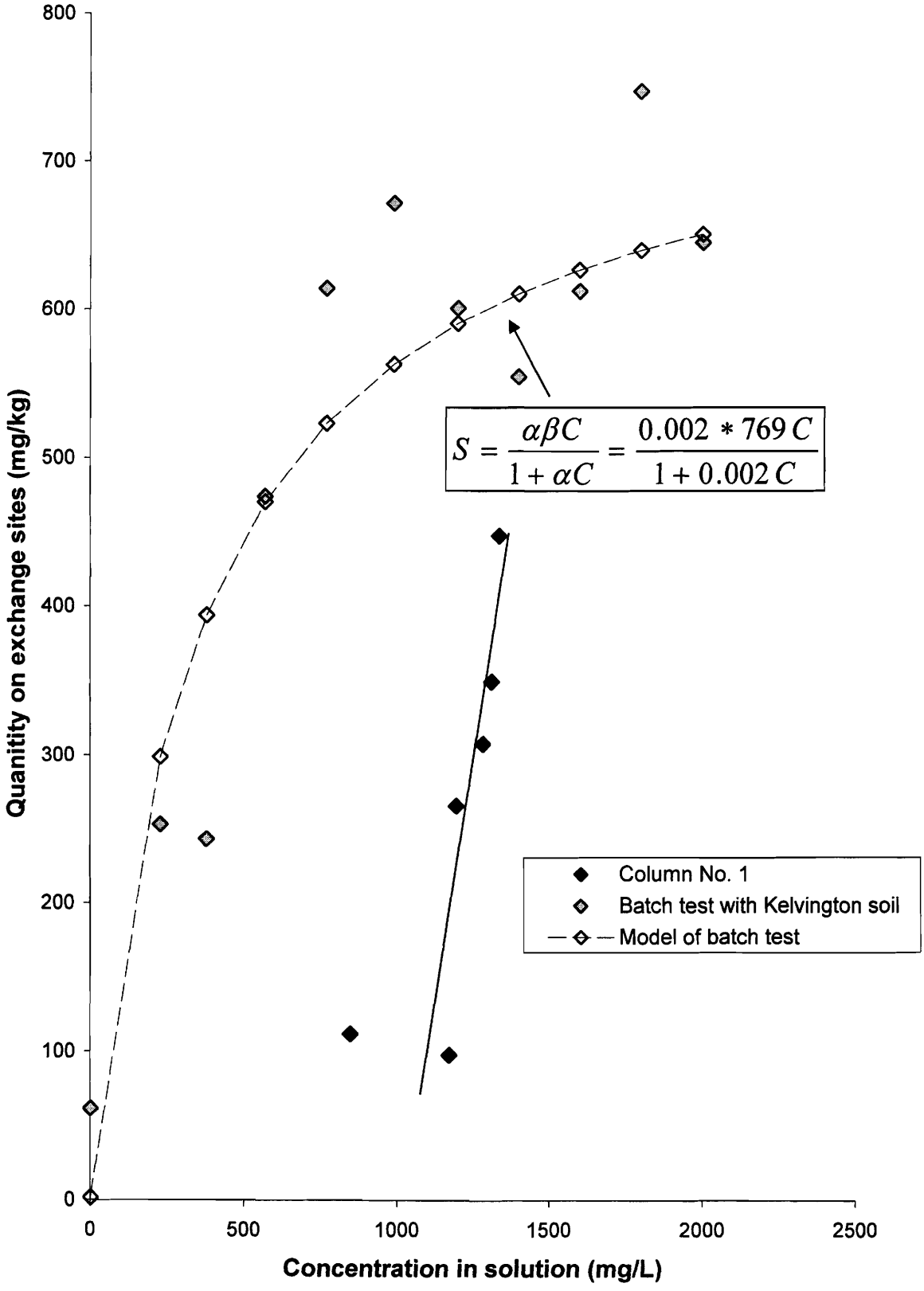

Figure 4.46: Ammonium isotherms for the Column No. 1 and Kelvington soil batch test data.

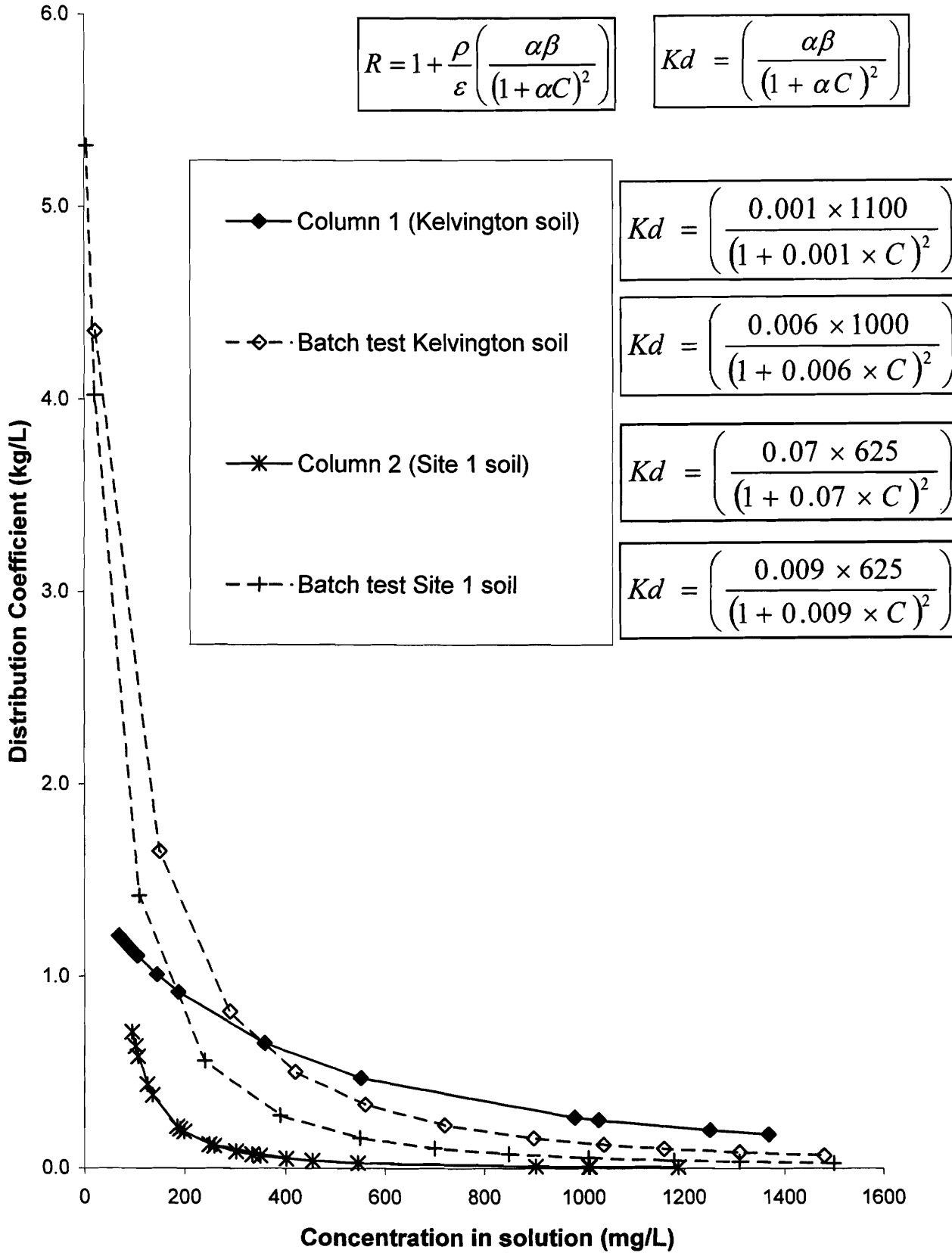

Figure 4.47: Potassium distribution coefficients calculated from the Langmuir iostherms for column and batch test data.

magnesium at the front of the plume where the lowest concentrations of potassium were detected; these high solution concentrations of divalent cations would limit the absorption of potassium.

Distribution coefficients for ammonium for the column tests could not be calculated as there was no way to determine meaningful α and β coefficients from the data. The distribution coefficients for ammonium would be expected to be influenced by the higher calcium and magnesium concentrations in the columns similar to the results obtained for the potassium. Distribution coefficients for ammonium for the two batch tests (Figure 4.48) ranged from a high of 3 L/kg at low ammonium concentrations to a low of 0.01 L/kg at high concentrations. Distribution coefficients were less than 0.8 L/kg for concentrations of ammonium greater than 200 mg/L.

Calculated distribution coefficients for ammonium agree with literature values of 0.08 to 0.4 L/kg (Ceazan et al. 1989; unconfined aquifer used for sewage disposal, Cape Cod, MA) and 0.34 to 0.87 L/kg (Erskine 2000; landfill leachate, UK). Distribution coefficients for ammonium 10 to 15 times higher have been reported when working with unsaturated organic soils (top soil; Clothier et al. 1988). The distribution coefficients convert to retardation factors of 1 to 7 for potassium and 1 to 5 for ammonium using measured values of bulk density and porosity for these soils. These values compare with published values from studies of landfill leachate and sewage infiltration (Table 4.15).

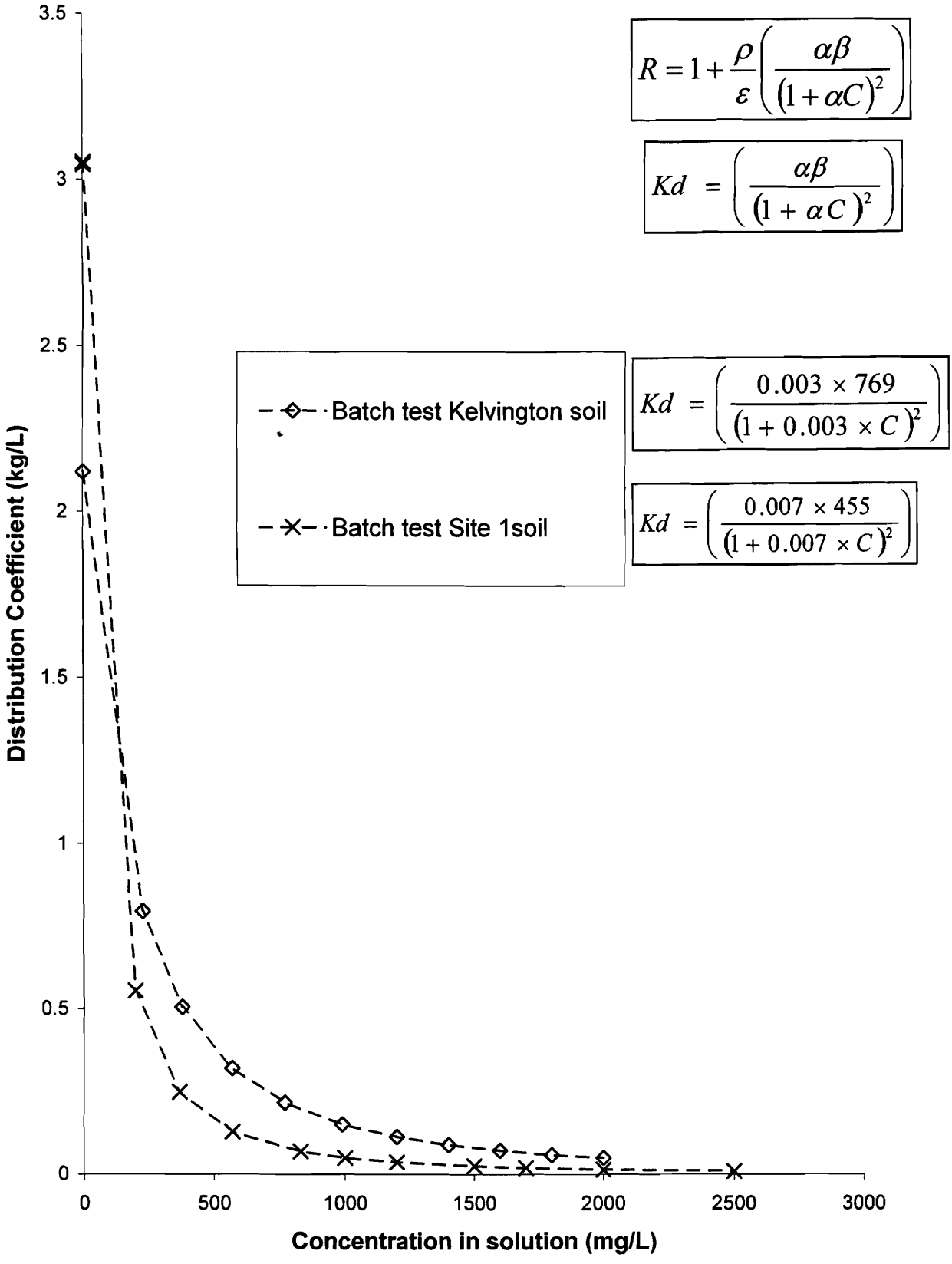

Figure 4.48: Ammonium distribution coefficients calculated from the Langmuir isotherms for the batch test data.

Table 4.15 – Retardation factors for ammonium and potassium

Reference	Erskine (2000)	Ceazan et al. (1989)	Bjerg and Christensen (1993)	Dance and Reardon (1983)	Thorton et al. (2000)	Thorton et al. (2001)	This study
Solution Type	landfill leachate	landfill leachate	landfill leachate	landfill leachate	landfill leachate	landfill leachate	hog manure
CEC of soil used (meq/100g)	2.5	0.5	1	0.5	1.6 – 3.2	0.2 – 3	7 – 12
NH4-N	<3	2.5-3.5			1.3-2.5	1.1-2.1	1-5
K		3.5	10	2-2.2	1.3-2.6	1.1-2	1-7

4.2.11 Transport modeling of Column No. 1

Concentration profiles for various ion species from Column No. 1 were compared to results of transport modeling using POLLUTEv6 (Rowe et al., 1998). The model assumed a constant source concentration and a free draining 1 m thick soil layer. A value of 0.01 m^2/yr ($3x10^{-6}$ cm^2/s) was used for the diffusion coefficient for chloride as per Shackelford and Daniel (1991) and GEONET Consulting Ltd. (2000). Average pore water velocity was reduced from an initial value of $9.7x10^{-6}$ m/s to $1.5x10^{-8}$ m/s 13 days after manure placement. For an average grain size of 0.02 mm, the Peclet number would initially be 0.6 and reduce to approximately 0.001 indicating transport after day 13 should be diffusion controlled (Fetter 1993). A coefficient of hydrodynamic dispersion of 0.03 m^2/yr provided a reasonable fit to the chloride analytical data (Figure 4.49).

Predicted potassium breakthrough was similar to the analytical data when a coefficient of hydrodynamic dispersion of 0.03 m^2/yr and distribution coefficient of 0.15 were used (Figure 4.50). Slightly better results were obtained when attenuation was defined as a Langmuir type absorption and α and β were set at 0.001 L/mg and 1100 mg/kg respectively (Figure 4.41).

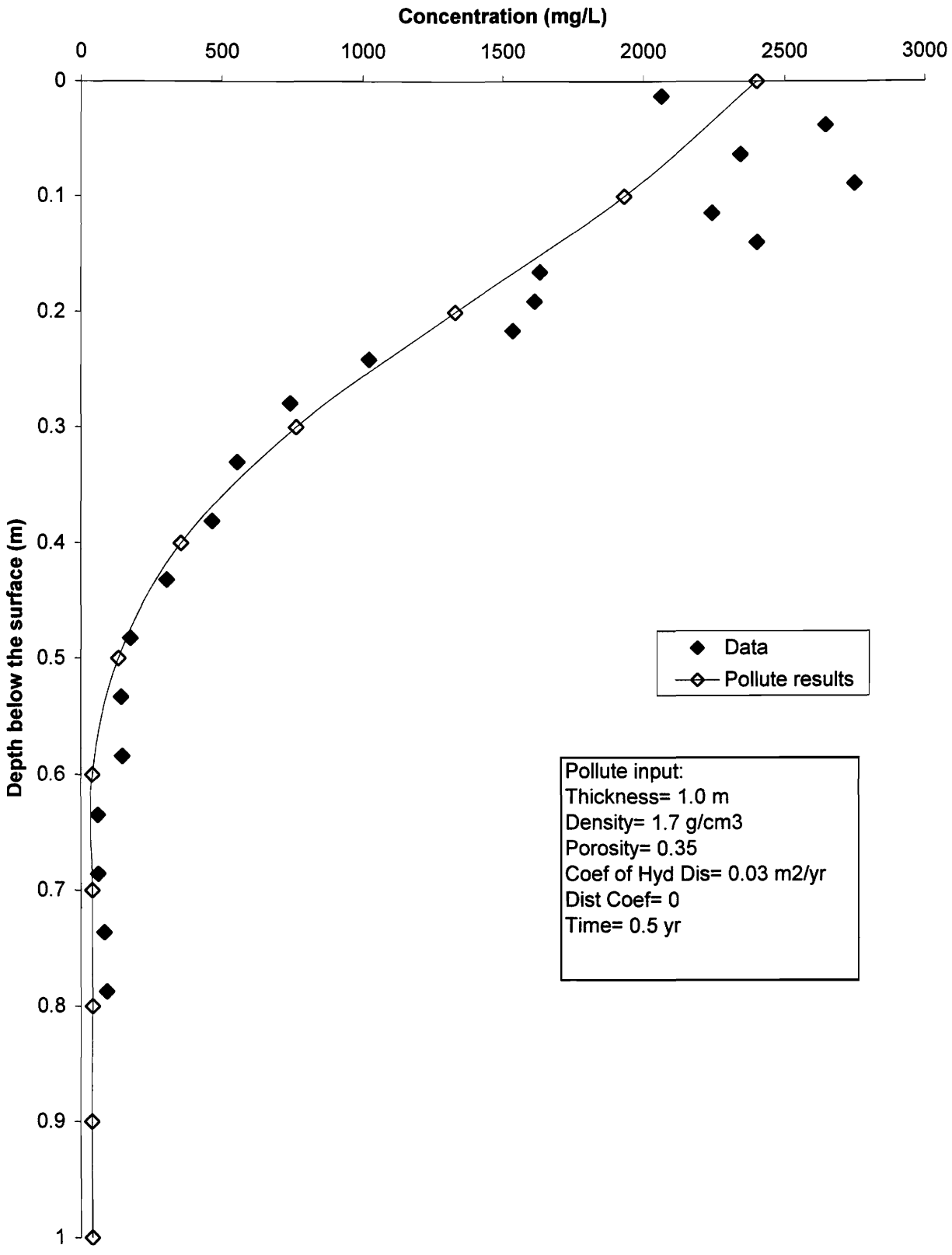

Figure 4.49 - Column No 1 POLLUTE model of chloride transport.

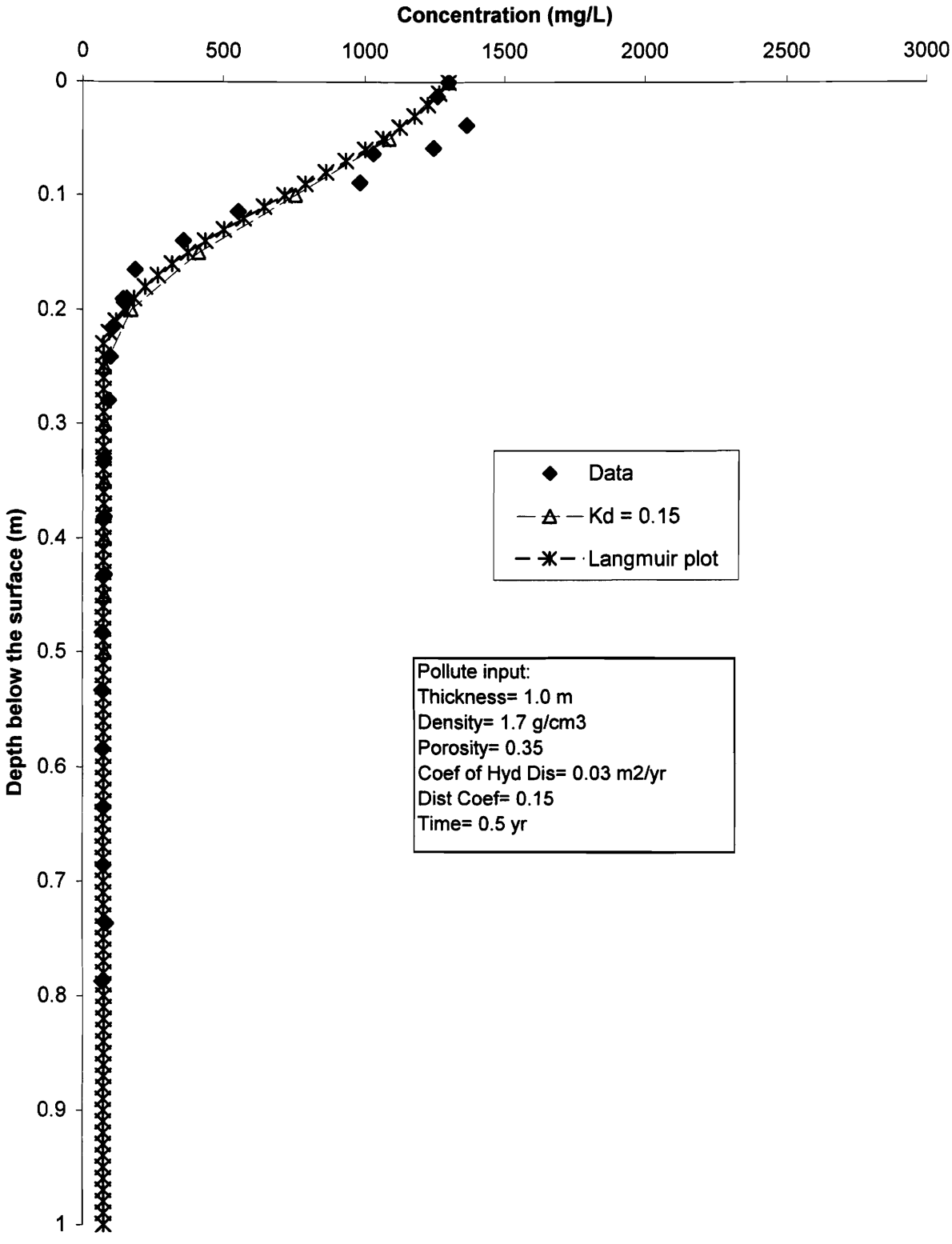

Figure 4.50: Column No. 1 POLLUTE model of potassium transport.

Modeled ammonium results (Figure 4.51) using a coefficient of hydrodynamic dispersion of 0.03 m^2/yr and distribution coefficient of 0.7 were similar to experimental data at the leading edge of the plume but more attenuated at the mid point of the plume. Modeled results more closely matched experimental results at the mid point of the plume when attenuation was defined as a Langmuir type absorption and α and β were set at 0.003 L/mg and 769 mg/kg respectively (Figure 4.44). Langmuir coefficients as determined from the batch tests appear to underestimate ammonium absorption near the front of the plume. This deviation from the model could result from several factors including:

1. Column freezing may have a caused freeze separation, forcing ions down with the freezing front from the top of the column, and then potentially drawing ions up as frost lenses formed.
2. Average pore water velocity for the first 0.05 pore volumes of the column (0.5 pore volumes in the top 100 mm) were several orders of magnitude higher than used in the model.
3. The distribution coefficient used for ammonium may be too low.
4. The distribution coefficient may decrease at higher concentrations.
5. Low ammonium concentrations at the front of the plume are attenuated, ammonium concentrations in the middle of the plume are unattenuated as other ion concentrations are higher, and then ammonium concentrations near the soil surface are sufficiently high enough to initiate ammonium absorption.

4.2.12 Exchange Coefficients

The use of a distribution coefficient implies all chemical processes are accounted for within the coefficient, including ion exchange, dissolution and precipitation. Calculating each process separately is an alternate methodology commonly employed in mixing cell models (Schulz and Reardon, 1983; Parkhurst and Appelo, 1999). In this study, ion exchange appears to be the dominating factor affecting transport of the various cations of concern. Precipitation and dissolution will affect ion concentrations in solution but the resulting solution concentration will dictate ion exchange behavior.

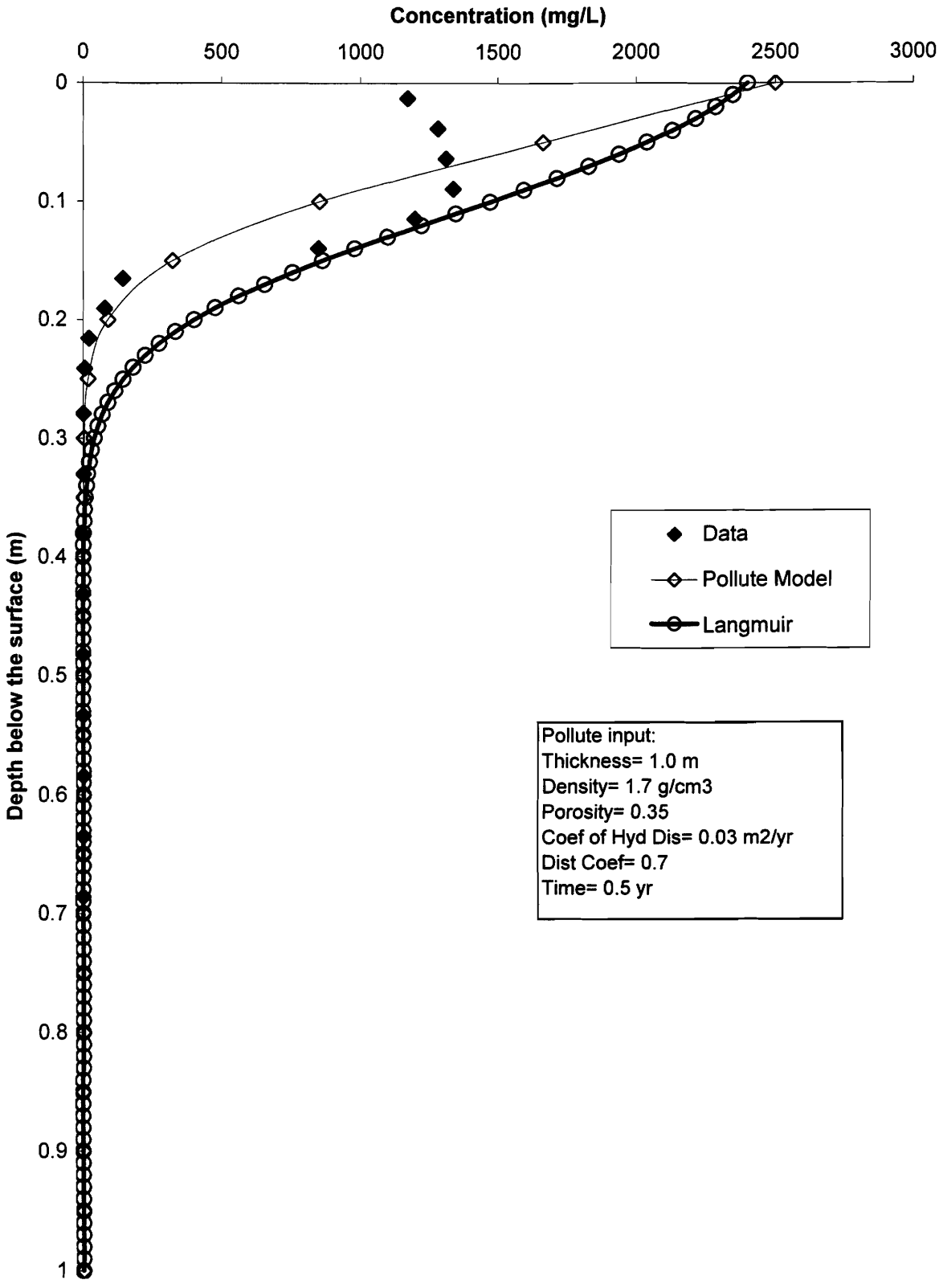

Figure 4.51: Column No. 1 POLLUTE modelling of ammonium transport.

Modeling with the experimental data was conducted to define mathematical functions to determine ion exchange. Work beyond the scope of this thesis would be incorporation of these functions into a mixing cell model.

Ion chromatograph theory has been incorporated into groundwater models by several researchers (Valocchi et al., 1981; Charbeneau, 1988), and involves use of ion exchange coefficients to determine distribution of ions between absorbed and solution phases. Exchange coefficients have been included in analytical and mixing cell reactive transport models for some time. While the simplest solution is the case where a constant exchange coefficient is assumed (Appelo and Postma, 1993), variable exchange coefficients to model reactive transport involving ion exchange have been suggested and/or attempted by several researchers (Rubin and James, 1973; Valocchi et al., 1981; Schulz and Reardon, 1983; Mansell et al., 1988; Bjerg et al., 1993; Appelo and Postma, 1993).

Determination of exchange coefficients, and their dependence on either absorbed or solution concentrations or both, have generally been accomplished in the laboratory using field materials subjected to varying concentrations of various ions in solution; these values provide reasonable results when used to model field situations (Valocchi et al., 1981; Dance and Reardon, 1983; Schulz and Reardon, 1983; Bjerg et al., 1993). We sectioned columns after approximately 6 months of effluent ponding and transport through soil columns. Individual samples were assumed to represent individual tests of solutions of various concentrations in contact with a common soil taken from a field site of interest. These "individual samples" were analyzed to determine selectivity coefficients. Batch tests were conducted using the same soils. While batch tests provide better experimental control, column testing evaluated a wider range of ion concentration as a result of ion accumulations. The analysis which follows focuses on modeling the column study data.

Cited studies above used Gaines-Thomas type equations for determination of exchange coefficients similar to the method described by Equations 2.29 to 2.32 in Section

2.4.2.3. The difference between these equations and those used in other studies is the number of moles used in the stoichiometric reaction. This study uses the equations as described by Appelo and Postma (1993) and Parkhurst and Appelo (1999) where the monovalent divalent exchange reaction is balanced using 1 mole of monovalent cation; other studies used 1 mole of divalent cation. In the case of sodium for calcium exchange, we find:

$$Na + 0.5Ca - X_2 \leftrightarrow Na - X + 0.5Ca^{2+} \qquad \text{[Eq. 4.5]}$$

and an exchange coefficient of:

$$K_{Na/Ca} = \frac{\beta_{Na}}{\beta_{Ca}^{0.5}} \frac{\left[Ca^{2+}\right]^{0.5}}{\left[Na^{+}\right]} \qquad \text{[Eq. 4.6]}$$

If Equation 4.5 is balanced using 1 mole of sodium as per Valocchi et al. (1981), Dance and Reardon (1983), and others, then Equation 4.6 becomes:

$$K'_{Na/Ca} = \frac{\beta_{Na}^{2}}{\beta_{Ca}} \frac{\left[Ca^{2+}\right]}{\left[Na^{+}\right]^{2}} \qquad \text{[Eq. 4.7]}$$

For comparison to the published literature, this means $(K_{Na/Ca})^2 = K'_{Na/Ca}$. Similarly, appropriate conversions must be made when converting exchange coefficients between reference ions such as:

$$K_{Ca/Mg} = \frac{K_{Na/Mg}}{K_{Na/Ca}} \qquad \text{[Eq. 4.8]}$$

Equations similar to Equation 4.8 can determine any exchange coefficient between two ions given their exchange coefficient referenced to a common ion. Care must be taken to ensure selectivity coefficients have been determined from the same set of equations or appropriate conversions have been made prior to comparison of results between studies.

Appelo and Postma (1993) provide a summary of selectivity coefficients referenced to sodium ($K_{Na/I}$) determined from the compilation of Bruggenwert and Kamphorst (1982; Table 4.16). In addition, $K_{Na/I}$ values from Valocchi et al. (1981) can be calculated from the data reported and converted to the convention used by Appelo and Postma (1993; Table 4.16) keeping in mind Valocchi et al. (1981) assumed ion activity coefficients to be equal for both ions involved and thus used ion concentration in their calculations.

These values are the default values used in the geochemical model PHREEQC (Parkhurst and Appelo, 1999). A majority of studies reference selectivity coefficients to calcium ($K_{Ca/I}$) as it is usually the base-saturating ion (Table 4.17). Further discussion will focus on selectivity coefficients referenced to sodium and calcium; coefficients referenced to other ions can be calculated using Equation 4.8.

Table 4.16 Selectivity coefficients for $K_{Na/I}$

Ion "I"	Selectivity Coefficient	
	Appelo and Postma (1993)	[1]Valocchi et al. (1981)
Ca^{2+}	0.40 (0.3-0.6)	0.11
Mg^{2+}	0.50 (0.4-0.6)	0.36
K+	0.20 (0.15-0.25)	0.07
NH4+	0.25 (0.2-0.3)	0.33

[1]Assume activity coefficients equal and therefore used ion concentration in calculation

Table 4.17 Selectivity coefficients for $K_{Ca/I}$

Ion "I"	Selectivity	Coefficient		
	Appelo and Postma (1993)	[1]Valocchi et al. (1981)	Berg et al. (1993)	Reardon et al. (1983)
Mg^{2+}	1.3	3.3	0.4 to 9.0	0.38 to 8.7
Na+	2.5	9.1	0.001 to 900	0.15 to 6E6
K+	0.5	0.64	Variable	4E-7 to 1E-4
NH4+	0.63	3		

[1]Assume activity coefficients equal and therefore used ion concentration in calculation

Activities were determined using the geochemical model PHREEQC (Parkhurst and Appelo, 1999). Equivalent fractions were determined for each ion from analytical data using:

$$\beta_i = \frac{\frac{meq_i}{100g}}{CEC\left(\frac{meq}{100g}\right)} \qquad \text{[Eq. 4.9]}$$

Modeling of ion exchange coefficients was accomplished using Equations 2.29 through 2.33. Experimental values for exchange coefficients for each individual sample can be calculated from the equivalent fraction of each ion and the activities calculated using PHREEQC. The five equations include the five equivalent fractions representing the fraction of the exchange site occupied by each cation and the four ion exchange coefficients. To obtain a best fit model to the data as a whole, the four ion exchange coefficients were assumed unknown. Substitution of Equations 2.29 through 2.32 into Equation 2.33 provides a second order quadratic equation (Equation 4.10) which can be solved for β_{Na} by inputting the four ion exchange coefficients. Substituting the same values of ion exchange coefficients and the calculated value of β_{Na} in Equations 2.29 through 2.32 results in modeled values of the remaining equivalent fractions.

$$\beta_{Na}^2\left(\frac{[Ca^{2+}]}{K_{Na/Ca}^2[Na^+]^2}+\frac{[Mg^{2+}]}{K_{Na/Mg}^2[Na^+]^2}\right)+\beta_{Na}\left(1+\frac{[K^+]}{K_{Na/K}[Na^+]}+\frac{[NH_4^+]}{K_{Na/NH_4}[Na^+]}\right)-1=0 \quad \text{[Eq.4.10]}$$

Each sample data was modeled using measured activities in solution and defining the four ion exchange coefficients ($K_{Na/I}$) as unknowns. Microsoft Excel Solver (developed by Leon Lasdon, University of Texas at Austin, and Allan Waren, Cleveland State University) solved for the ion exchange coefficients so modeled equivalent fractions for each ion were as close as possible to experimental values. The Microsoft Excel Solver tool uses the Generalized Reduced Gradient (GRG2) nonlinear optimization code; this method was used to solve the values of the four ion exchange coefficients so the square of the difference between the experimental equivalent fraction and the modeled equivalent fraction was minimized. Modeled results were identical to experimental values for an individual sample. To model trends in the change of the ion exchange coefficients, the same optimization tool can solve the ion exchange coefficients for all samples simultaneously (entire sum of the sum of the square of the differences between the experimental equivalent fractions and the modeled equivalent fractions is minimized). A result of the modeling is a table of selectivity coefficients which will reproduce experimental equivalent fractions given activities of each ion in solution for each individual sample or location within the column. These selectivity coefficients can

vary due to natural variability within the soil and as a result of experimental analytical uncertainties.

Changes in the value of the selectivity coefficients as a function of the ionic strength of the solution, the concentration of the ion in solution, the quantity of the ion on the exchange complex or a combination of these or other factors were then determined by trial and error and visual analysis of the data with some thought to the ion of most concern. This methodology is similar to Mansell et al. (1988). Preference was given to factors such ions in solution which could be estimated using advection-diffusion transport modeling, with the hope results could be applied to reactive transport models in the future.

Results for Column No 1 soil (CI-till) indicate selectivity coefficients with respect to sodium ($K_{Na/I}$) are best correlated to the fraction of monovalent cations in solution (M^*_{cat}; Figure 4.52) giving the following relationships:

$$K_{Na/Ca} = 0.05(M^*_{cat})^{-1.35} \qquad R^2 = 0.82 \qquad \text{[Eq. 4.11]}$$

$$K_{Na/Mg} = 0.097(M^*_{cat})^{-1} \qquad R^2 = 0.86 \qquad \text{[Eq. 4.12]}$$

$$K_{Na/NH4-N} = 1.82 - 1.92(M^*_{cat})^{4.3} \qquad R^2 = 0.81 \qquad \text{[Eq. 4.13]}$$

$$K_{Na/K} = 0.07 \qquad \text{[Eq. 4.14]}$$

These modeled selectivity coefficient functions (Figure 4.53) yield selectivity coefficients for $K_{Na/Ca}$ and $K_{Na/Mg}$ of 0.15 to 0.22 and 0.22 to 0.28 respectively in samples representing background conditions (500 to 800 mm depth), 0.2 to 0.23 and 0.25 to 0.28 respectively for samples from the "hard water front" area (250 to 450 mm depth), with values decreasing towards the top of the column from 0.2 to 0.05 and 0.25 to 0.1, respectively. These ranges are slightly lower than Appelo and Postma (1993) but similar to Valocchi et al. (1981).

The modeled selectivity coefficient for $K_{Na/K}$ is 0.07; for $K_{Na/NH4}$ the range is from 0.1 at the top of the column (highest ammonium concentration) to 1 at very low ammonium concentrations (Figure 4.54). The $K_{Na/K}$ value is higher than Appelo and Postma (1993)

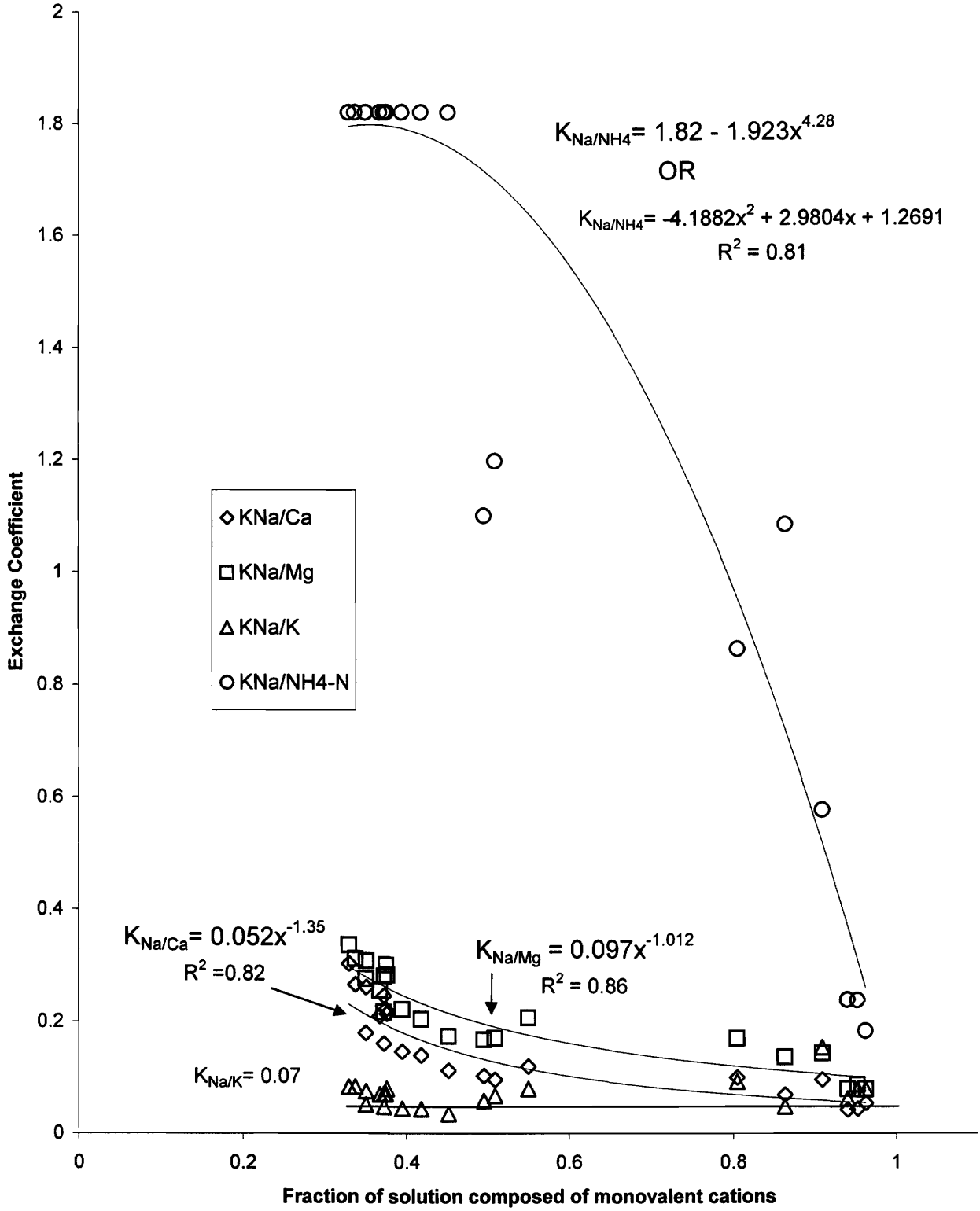

Figure 4.52: Column No. 1 modeled exchange coefficients vs. experimental values as a function of the fraction of monovalent cations in solution.

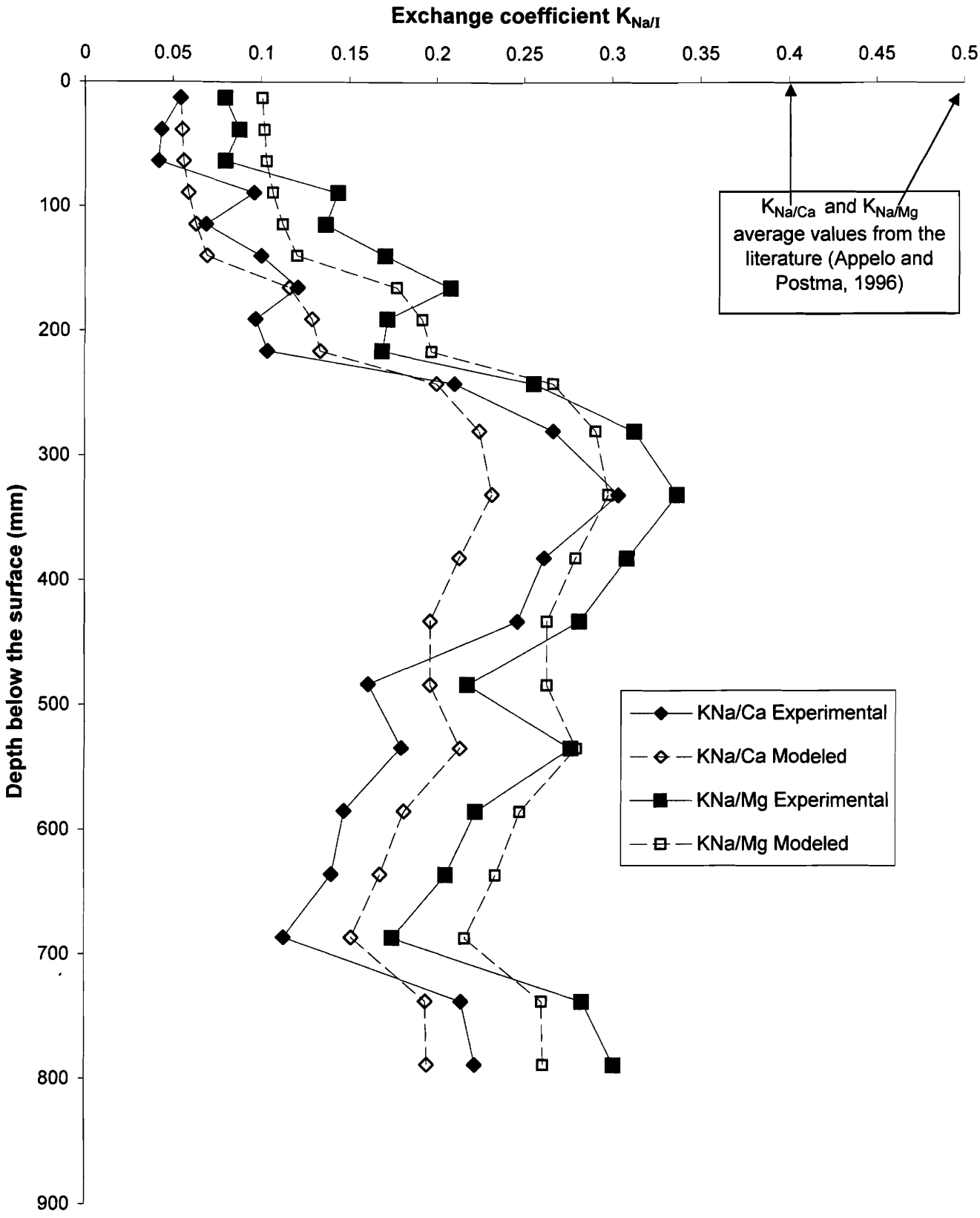

Figure 4.53: Column No. 1 cacluated and modeled selectivity coefficients.

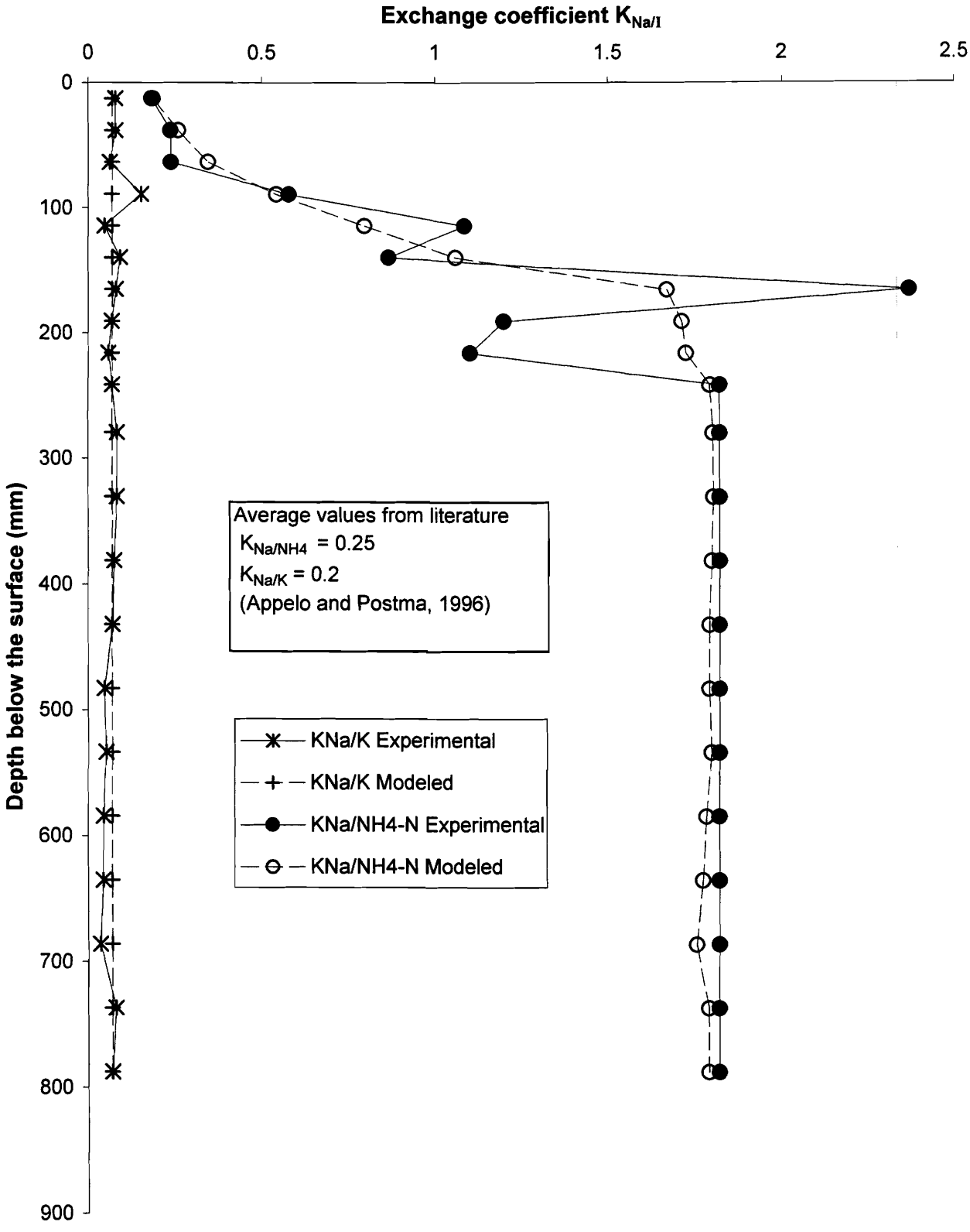

Figure 4.54: Column No.1 experimental and modeled selectivity coefficients for potassium and ammonium.

but the same as Valocchi et al. (1981); selectivity coefficients for $K_{Na/NH4}$ agree with both references at moderately high ammonium concentrations (near the top of the column).

Comparison of actual or experimental selectivity coefficients and modeled coefficients values (Figures 4.53 and 4.54) show reasonable agreement for $K_{Na/Ca}$, $K_{Na/Mg}$, and $K_{Na/K}$; values for $K_{Na/NH4}$ appear to be less critical above values of 1. Determination of selectivity coefficients indicated changes in equivalent fractions determined using modeled coefficient values was most sensitive to calcium and magnesium values and least sensitive to ammonium values (especially at low ammonium values). As ammonium (and monovalent cation) concentrations increased, selectivity coefficients for calcium and magnesium decreased.

Recalculation of equivalent fractions as determined using ion solution activities and modeled selectivity coefficients show reasonable agreement for all ions (Figure 4.55) with correlation coefficients for calcium, magnesium, sodium, potassium and ammonium of 0.68, 0.91, 0.41, 0.95 and 0.97 respectively. Calculated equivalent fractions of calcium and magnesium show mirror image deviations from experimental values.

Modeled values for selectivity coefficients $K_{Na/I}$ also correlated well with the ratio of monovalent (M_{cat}) to divalent cations (D_{cat}) in solution ($R_{M/D}$) (Figure 4.56) yielding the following equations:

$$K_{Na/Ca} = 0.15(R_{M/D})^{-0.4} \qquad R^2=0.72 \qquad \text{[Eq. 4.15]}$$

$$K_{Na/Mg} = 0.22(R_{M/D})^{-0.33} \qquad R^2=0.81 \qquad \text{[Eq. 4.16]}$$

$$K_{Na/NH4-N} = -0.39Ln(R_{M/D}) + 1.4 \qquad R^2=0.83 \qquad \text{[Eq. 4.17]}$$

$$K_{Na/K} = 0.07 \qquad \text{[Eq. 4.18]}$$

Similar results are obtained by plotting $K_{Ca/I}$ as a function of the ratio of monovalent (M_{cat}) to divalent (D_{cat}) cations in solution ($R_{M/D}$) (Figure 4.57).

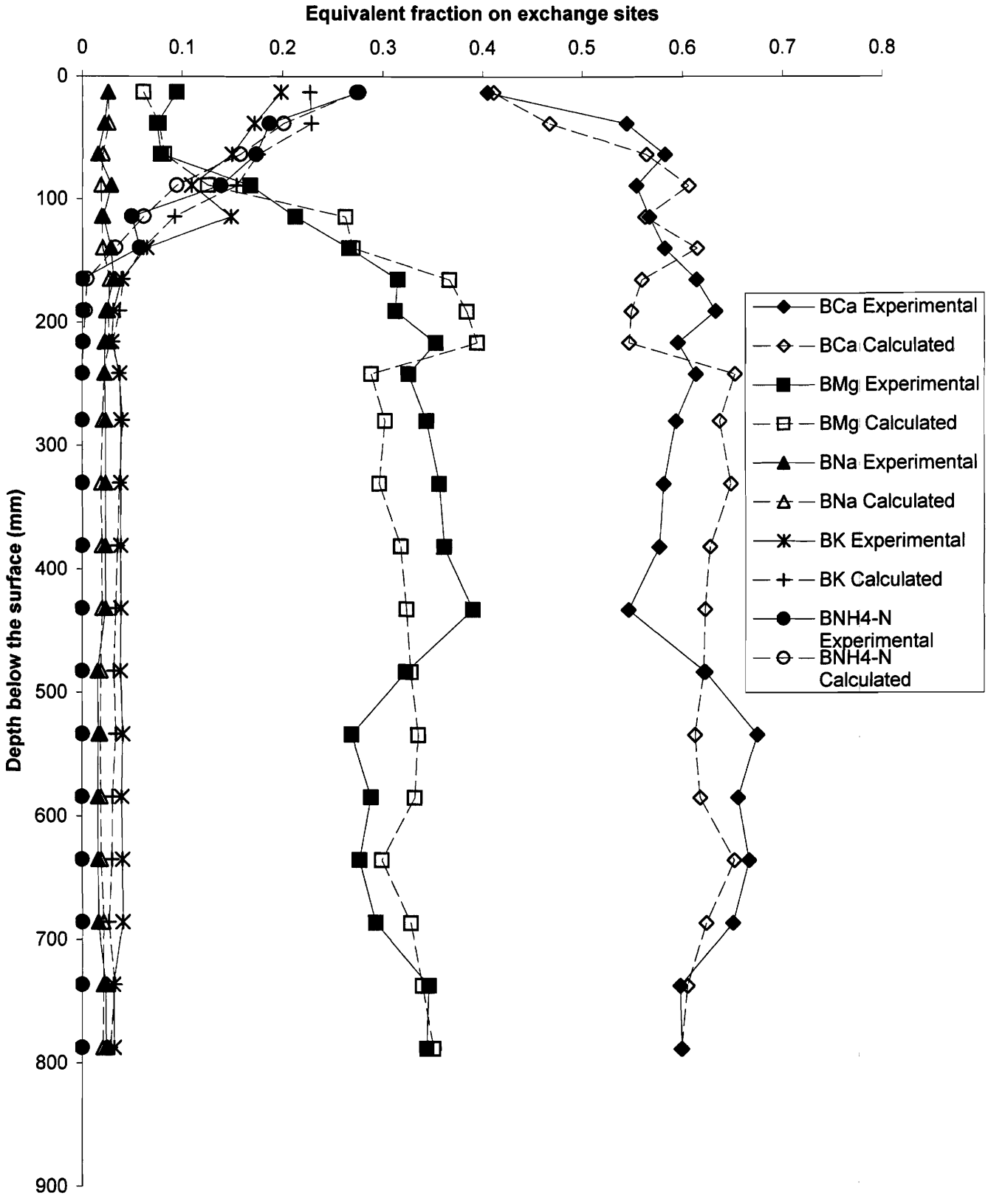

Figure 4.55: Column No. 1 comparison of experimental and calculated equivalent fractions on soil exchange sites.

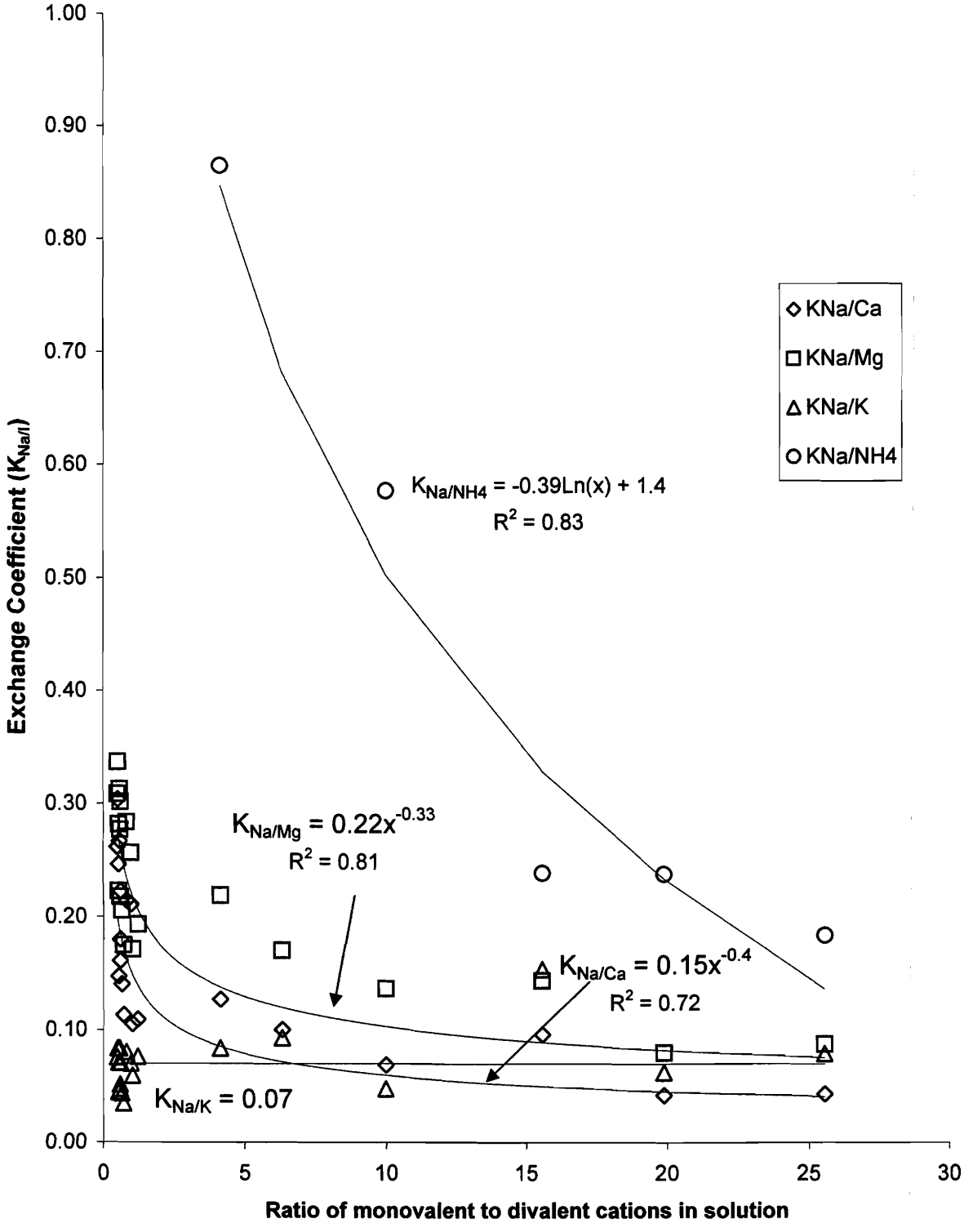

Figure 4.56: Column No. 1 selectivity coefficients with respect to sodium and as a function of the ratio of monovalent to divalent cations in solution.

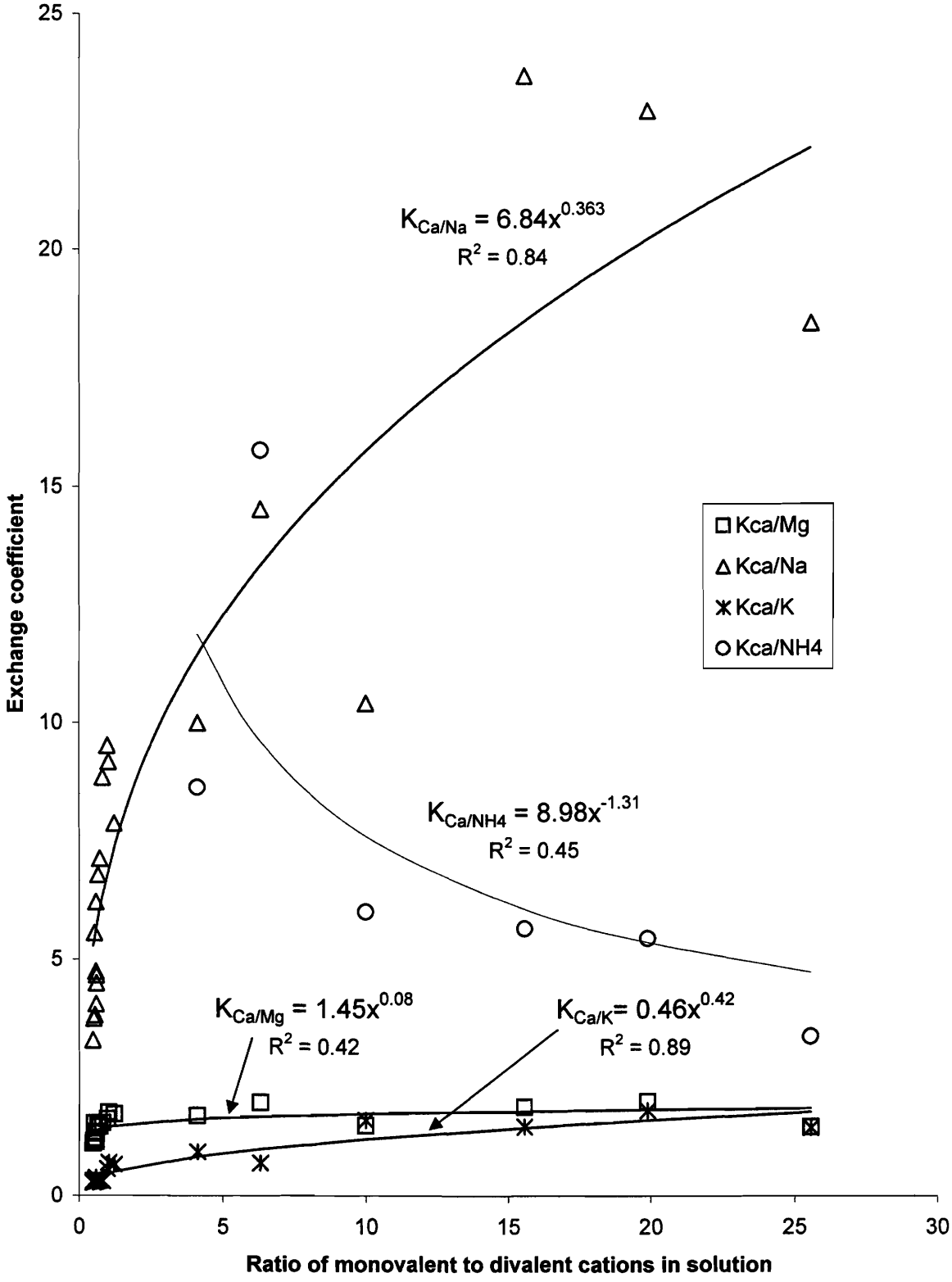

Figure 4.57: Column No. 1 selectivity coefficients with respect to calcium as a function of the ratio of monovalent to divalent cations in solution.

Soils from Column No.2 (SPSM-sand) did not show a selectivity coefficient correlation to the fraction of monovalent cations in solutions, as this value was essentially constant (0.97 to 0.99) throughout the column. A correlation to the ratio of monovalent to divalent cations in solution was also not evident though this value varied significantly throughout the column. Trial and error and data interpretation indicated the best correlation was obtained when the selectivity coefficient changed as a function of the quantity of calcium on the exchange sites (Ca_{abs}; Figure 4.58). Analysis indicated both $K_{Na/K}$ and $K_{Na/NH4}$ could be considered constant for all samples at values of 0.28 and 2.06 respectively; $K_{Na/Ca}$ and $K_{Na/Mg}$ varied as a function of the quantity of calcium on exchange sites. The spreadsheet modeling resulted in the following relationships:

$$K_{Na/Ca} = 0.48(Ca_{abs})^{-0.68} \qquad R^2=0.48 \qquad \text{[Eq. 4.19]}$$

$$K_{Na/Mg} = 0.36(Ca_{abs})^{-0.16} \qquad R^2=0.04 \qquad \text{[Eq. 4.20]}$$

Although correlation between modeled and experimental data is low for magnesium coefficients, the model does predict equivalent fractions (discussed in a subsequent section). These equations yield values of $K_{Na/Ca}$ and $K_{Na/Mg}$ ranging from 0.15 to 0.37 and 0.8 to 0.34 respectively for the range of values obtained for the quantity of calcium on the exchange sites. While the value of $K_{Na/Ca}$ and $K_{Na/Mg}$ are slightly lower than other studies (Table 4.16), values at lower quantities of absorbed calcium are within the reported range. The calculated value of $K_{Na/K}$ is within the range of values from Appelo and Postma (1993) but higher than determined for soil samples from Column No 1. $K_{Na/NH4}$ is an order of magnitude higher than values given in Table 4.16 independent of the amount of calcium on the exchange sites.

Again, Equation 4.8 can be used to determine selectivity coefficients with respect to calcium (Figure 4.59) yielding $K_{Ca/I}$ values as a function of the quantity of calcium on exchange sites. Values of $K_{Ca/Mg}$, $K_{Ca/Na}$, $K_{Ca/K}$, and $K_{Ca/NH4-N}$ range from 0.9 to 1.8, 2.4 to 7.0, 0.70 to 1.60, and 6.0 to 13.0 respectively. Values of $K_{Ca/Mg}$, $K_{Ca/Na}$, and $K_{Ca/K}$ are similar to literature values (Table 4.17); values for $K_{Ca/NH4-N}$ are an order of magnitude higher than Appelo and Postma (1993).

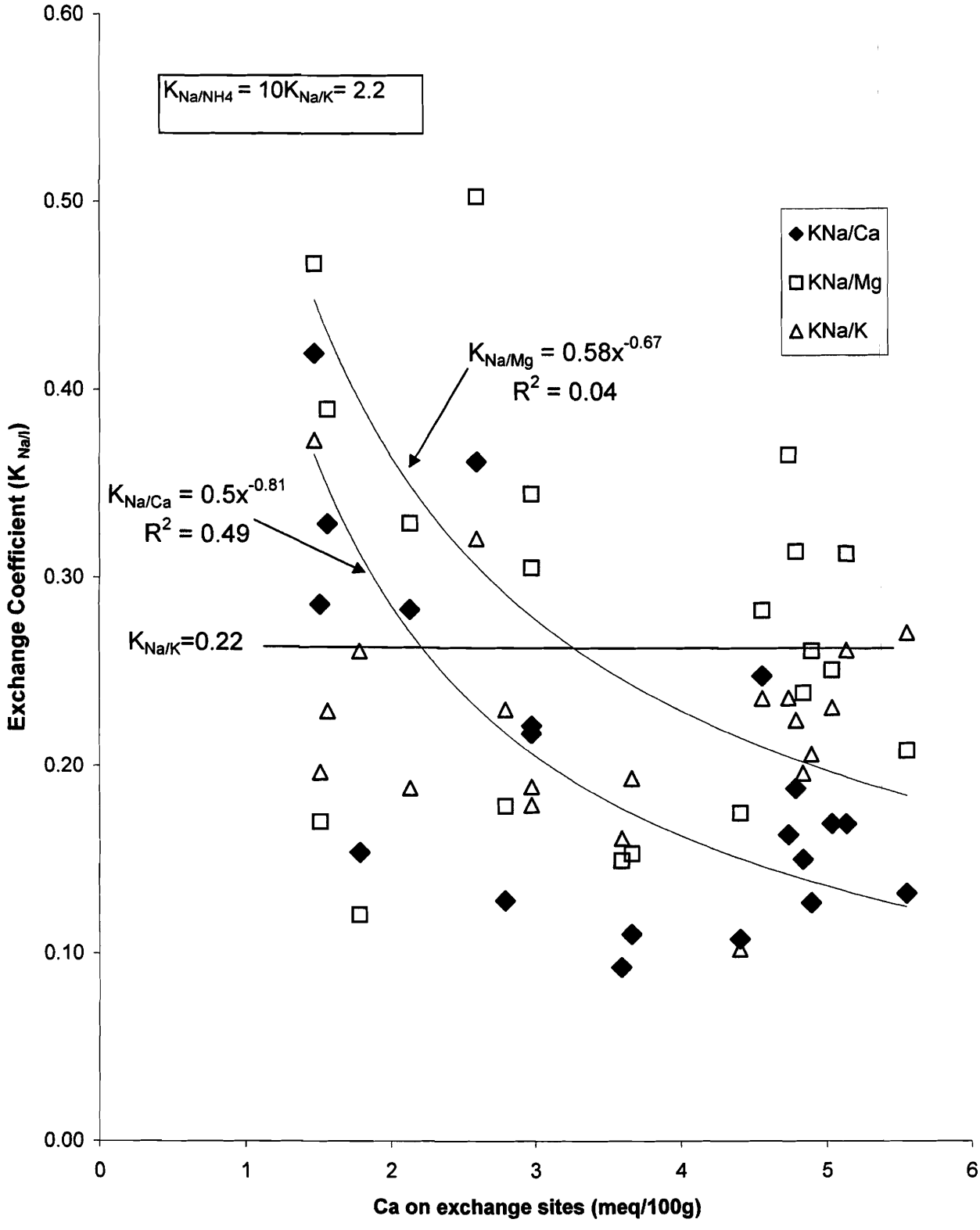

Figure 4.58: Column No. 2 exchange coefficients with respect to sodium as a function of Ca absorbed on exchange sites.

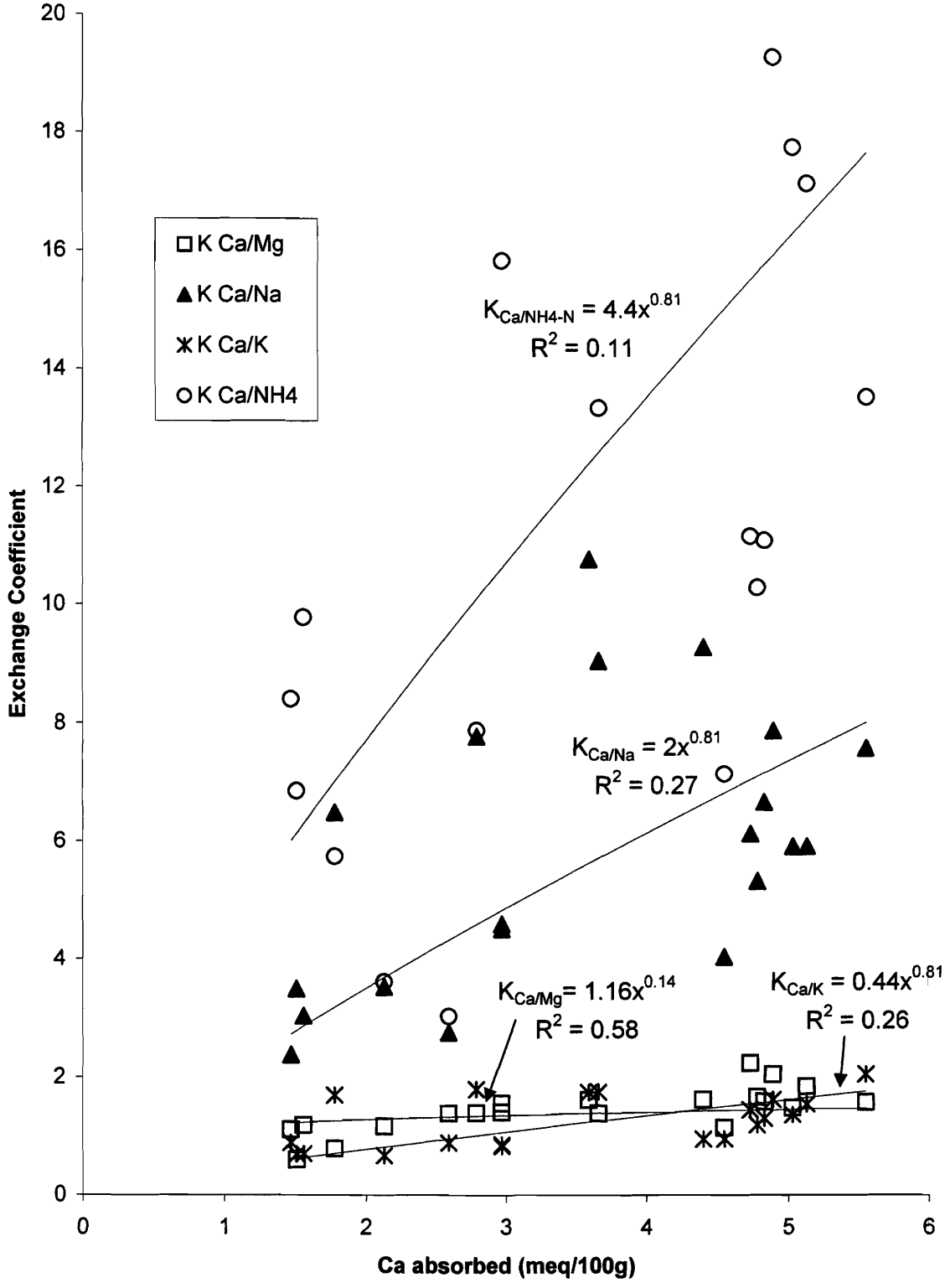

Figure 4.59: Column No. 2 modeled exchange coefficients with respect to calcium as a function of absorbed calcium.

Comparison of experimental and modeled selectivity coefficients referenced to sodium ($K_{Na/I}$) for Column No. 2 soil (Figures 4.60 and 4.61) show the relationship for calcium ($K_{Na/Ca}$) is a very good approximation of experimental data with some deviation for samples taken near the top of the column. Magnesium ($K_{Na/Mg}$) coefficients determined using modeled functions are an average of experimental values for samples taken below 200 mm within the column, and higher than experimental for samples taken above. The constant value for the potassium selectivity coefficient ($K_{Na/K}$) is a reasonable average of experimental values which show little deviation between all samples. As with Column No 1 soils, experimental ammonium selectivity coefficients ($K_{Na/NH4-N}$) are quite variable due in part to variability of the equivalent fraction of ammonium on the soil phase. The constant value proposed is an average of experimental values.

Comparing experimental equivalent fractions of ions occupying exchange sites with fractions calculated using the modeled functions for $K_{Na/I}$ given above (Figures 4.62 and 4.63) shows the fraction of exchange sites occupied by calcium and sodium can be obtained with reasonable accuracy using modeled functions and values for selectivity coefficients. Magnesium, potassium and ammonium, however, deviate from experimental values in the upper 250 mm of the column, suggesting potential interaction and or dependency between these three ions. Regardless of the deviations noted, the proposed functions and constants for selectivity coefficients provide reasonable predictions of the fraction of the exchange complex covered by each ion for the 20 samples taken from Column No. 2. Correlation coefficients are 0.66, 0.89, 0.67, 0.81 and 0.51 for calcium, magnesium, sodium, potassium and ammonium respectively. A comparison of experimental results and equivalent fractions calculated using default ion selectivity values from Appelo and Postma (1993) and Parkhurst and Appelo (1999) indicate the use of default values would overestimate ammonium absorption while underestimating magnesium and to a greater extent calcium absorption (Figures 4.64 and 4.65).

Ion exchange coefficients determined from batch test data (Figures 4.66 and 4.67) show significantly different functions for the value for calcium and magnesium as opposed to

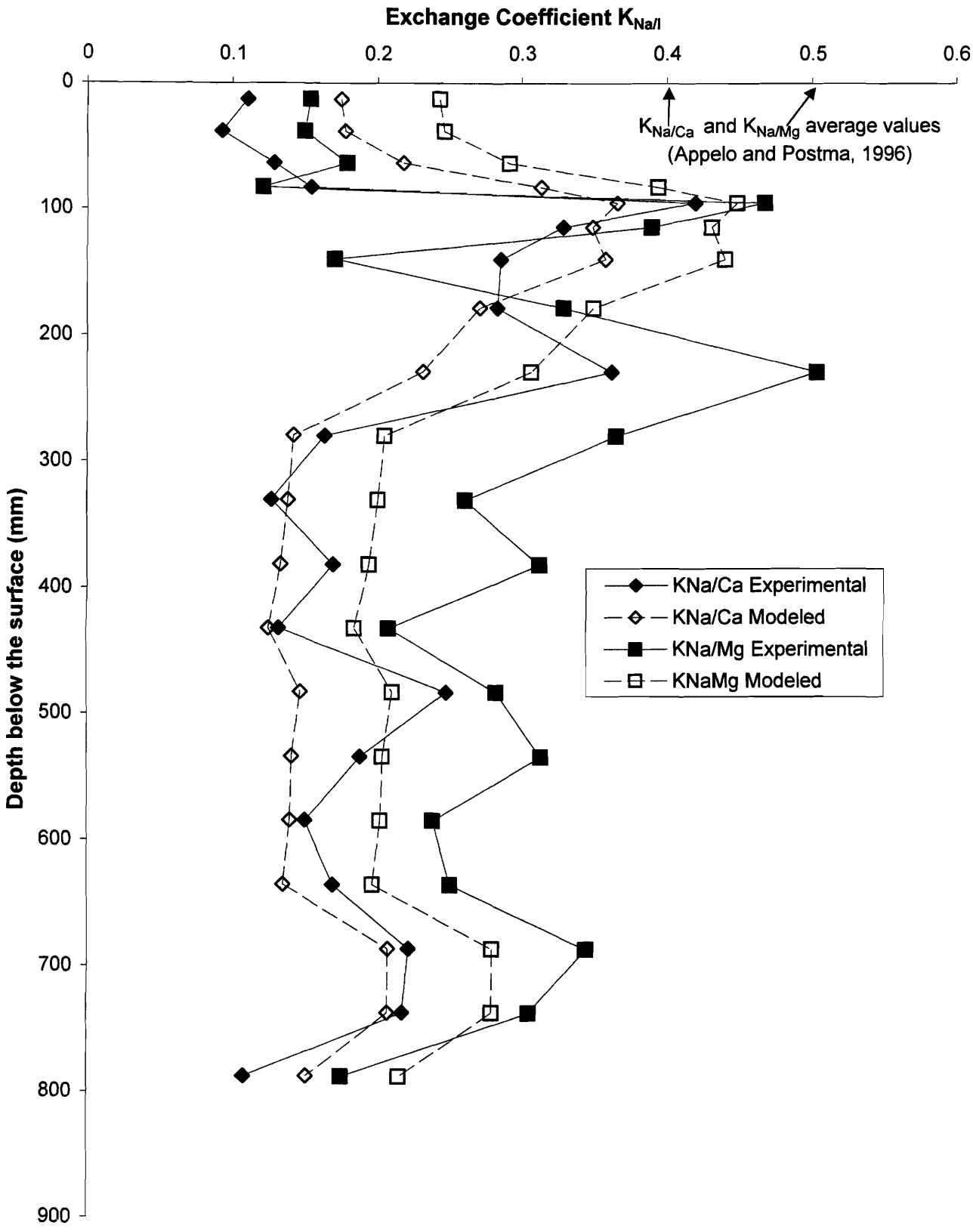

Figure 4.60: Column No. 2 experimental and modeled selectivity coefficients for calcium and magnesium.

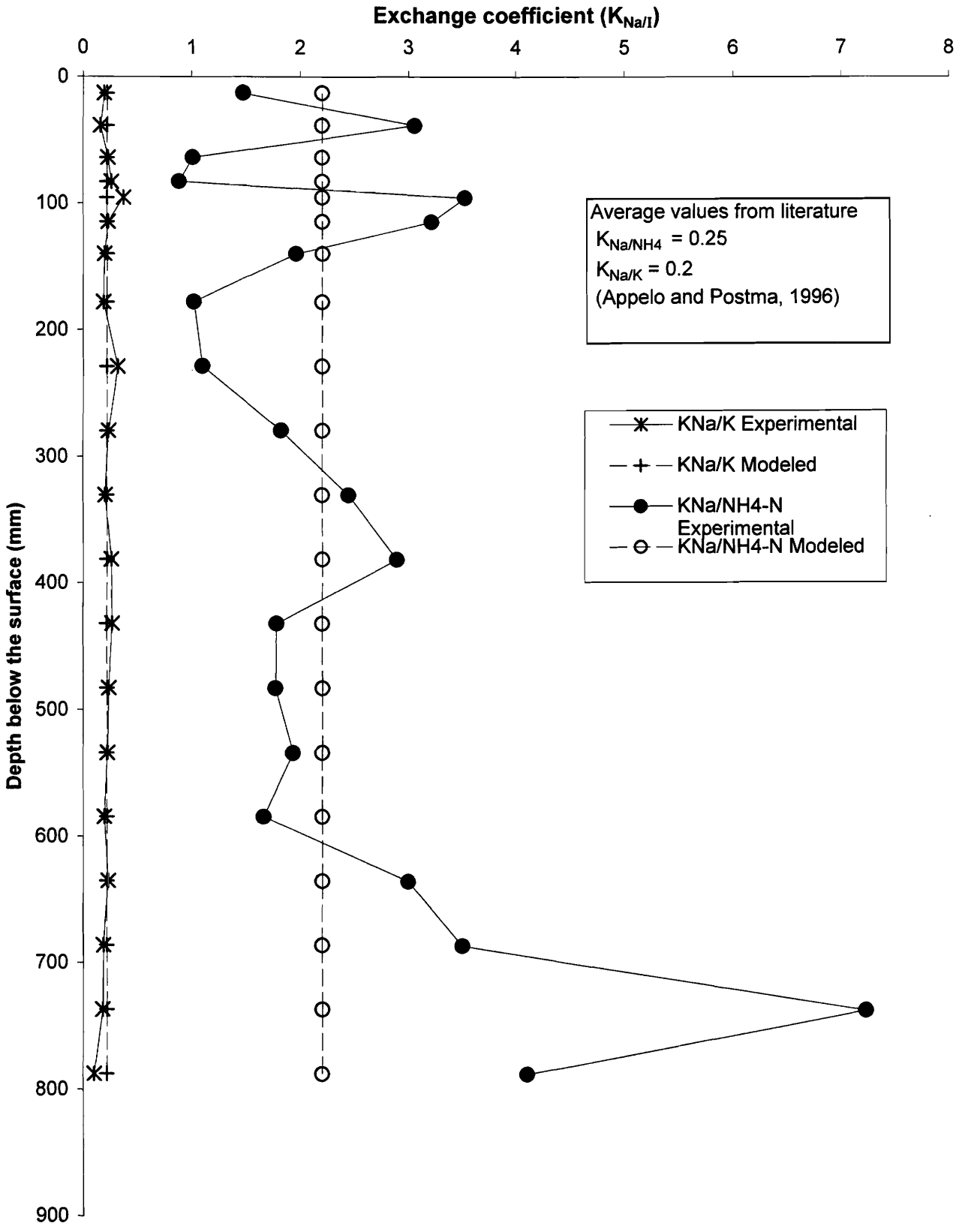

Figure 4.61: Column No. 2 experimental and modeled selectivity coefficients for potassium and ammonuim.

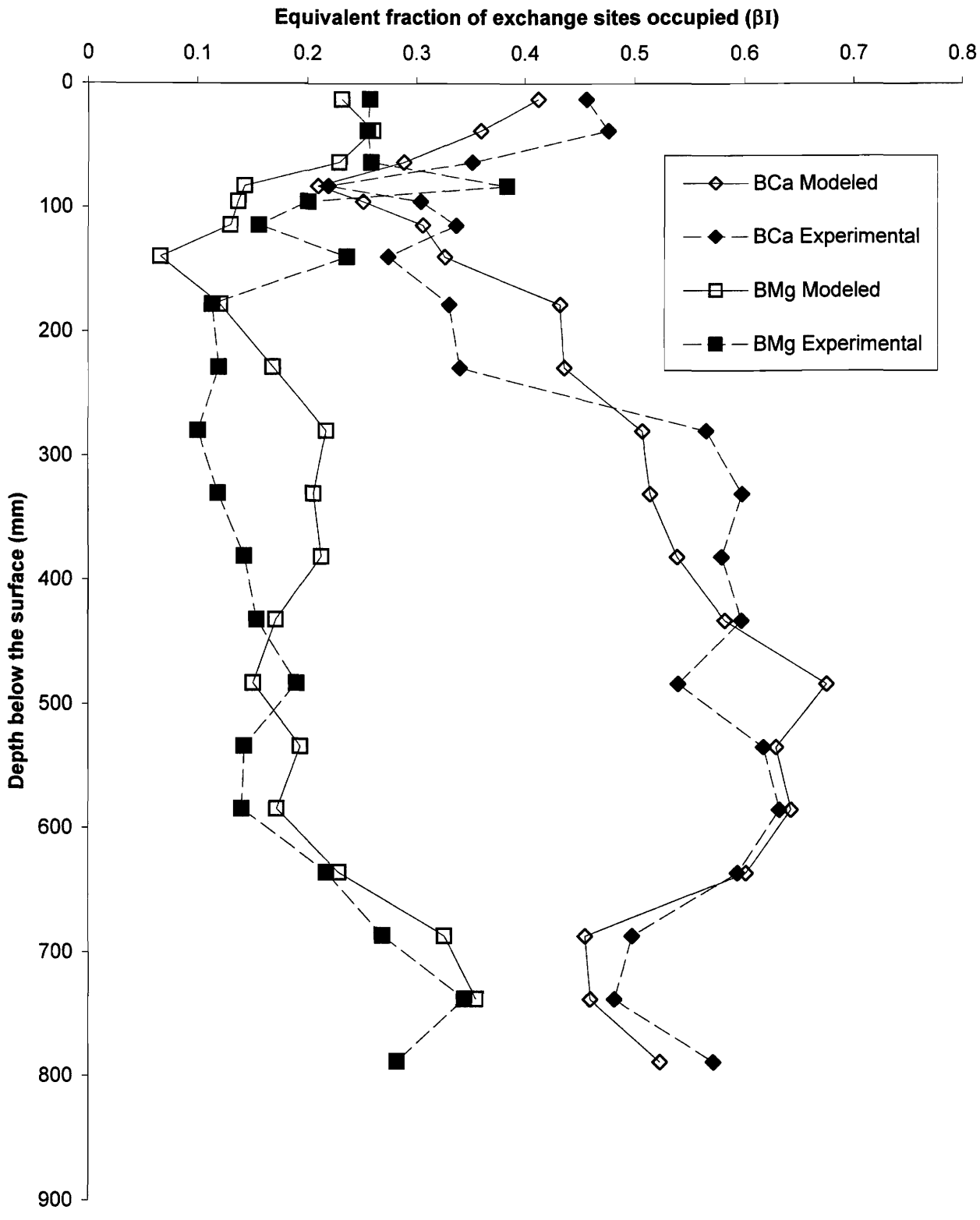

Figure 4.62: Column No. 2 equivalent fractions of aborbed divalent ions: experimental values versus calculated values.

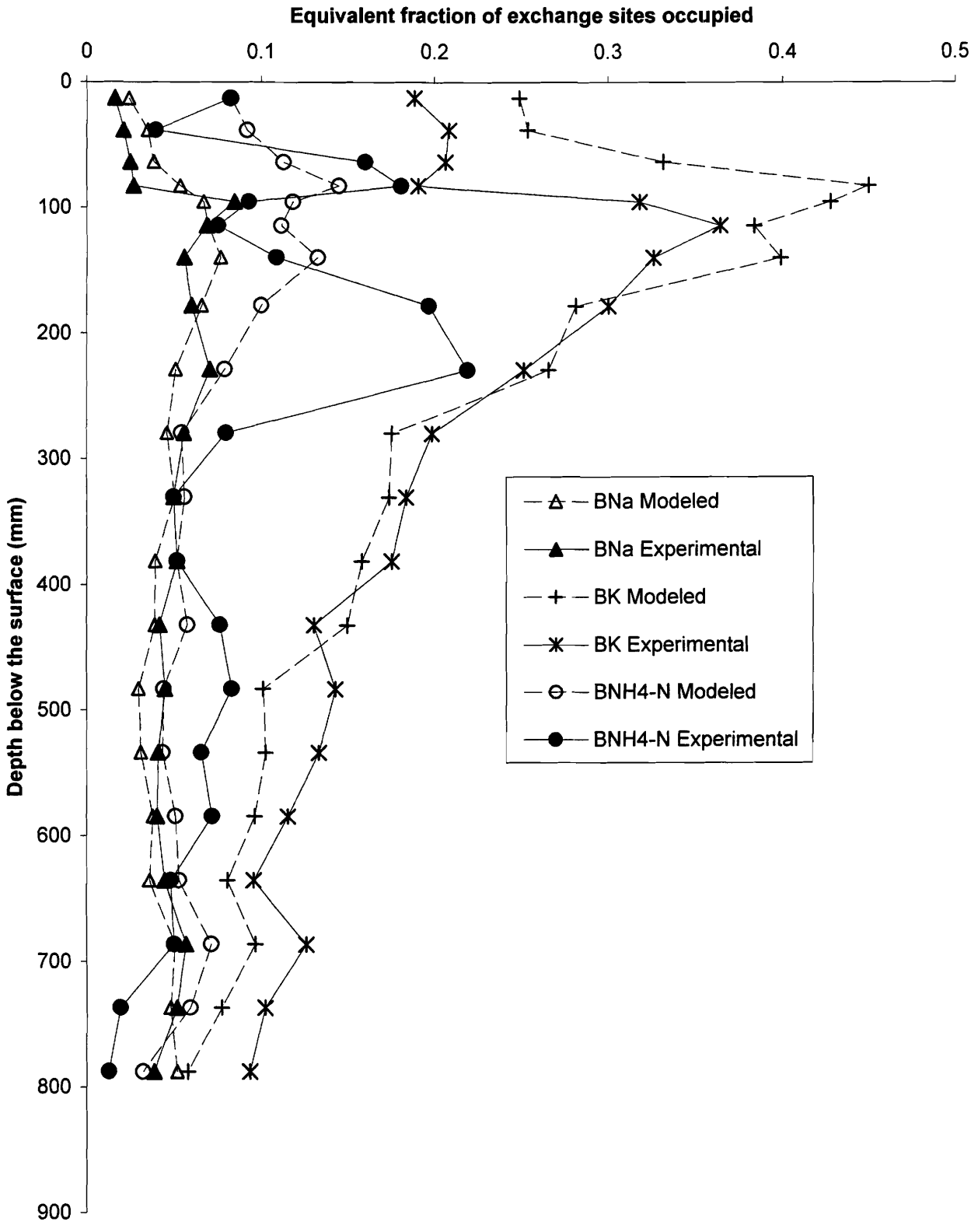

Figure 4.63: Column No. 2 equivalent fraction of absorbed monovalent ions: experimental versus calculated values.

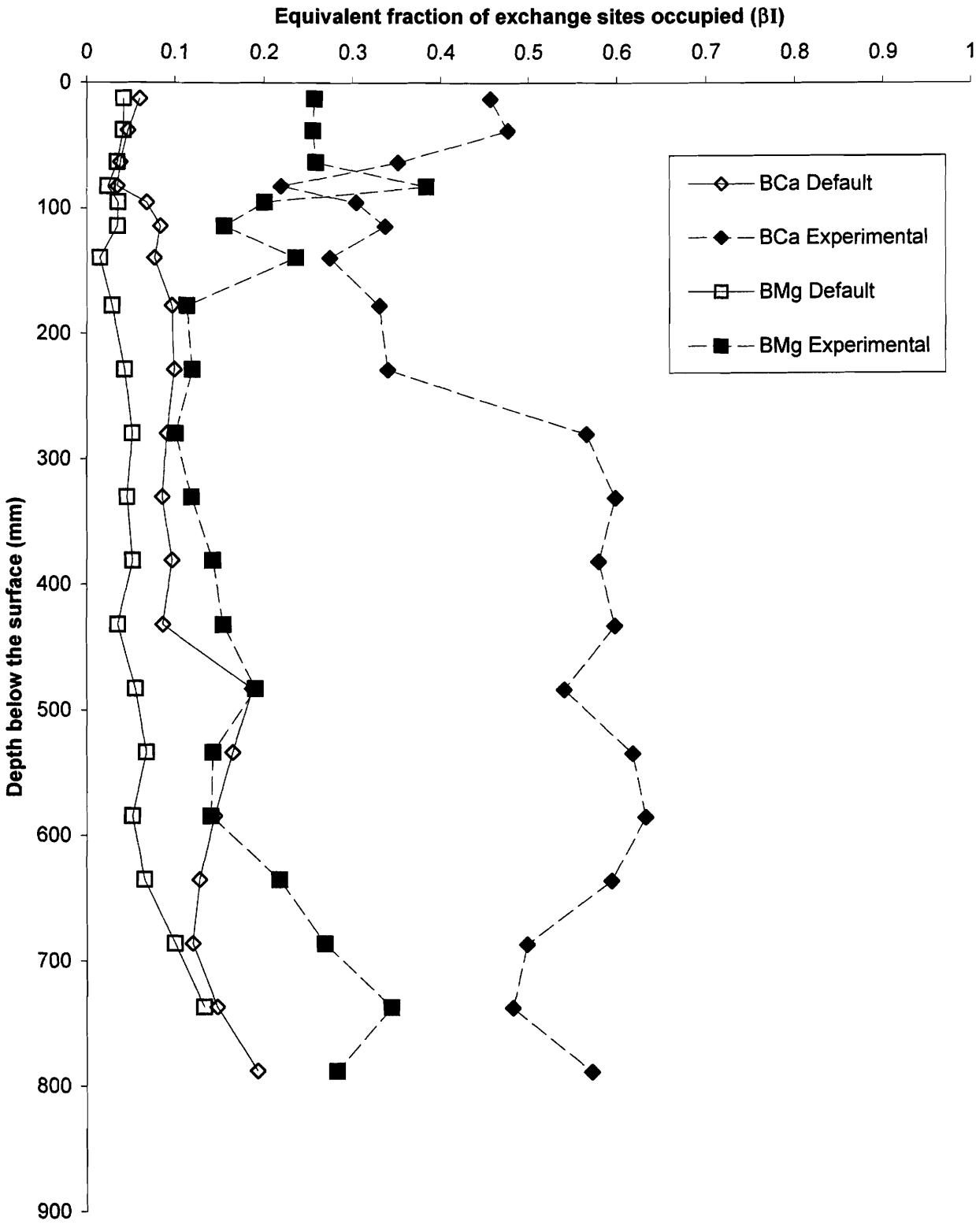

Figure 4.64: Column No. 2 equivalent fractions of absorbed divalent ions: experimental selectivity coefficients versus default selectivity coefficients .

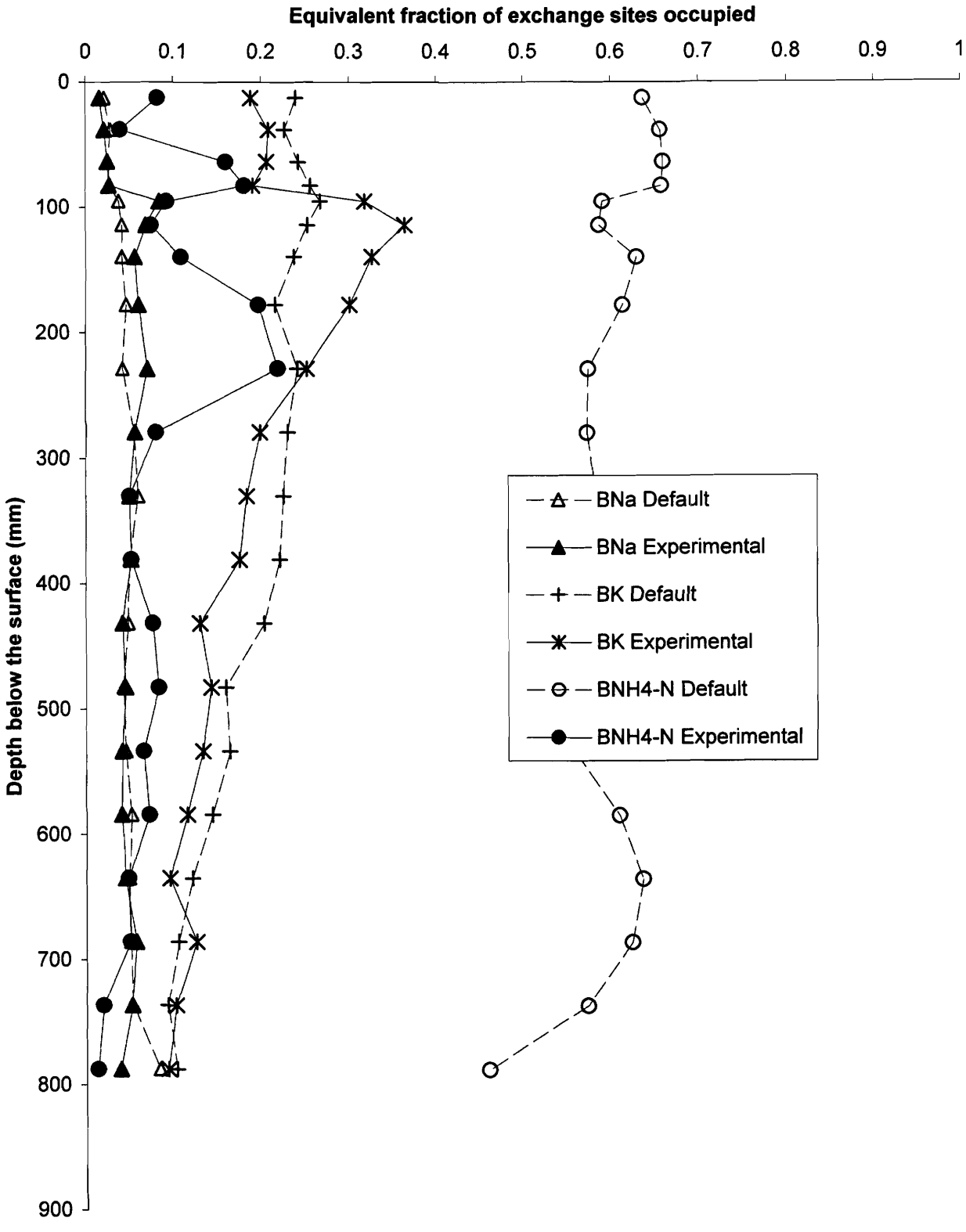

Figure 4.65: Column No. 2 equivalent fraction of absorbed monovalent ions: experimental selectivity coefficients versus default selectivity coefficients.

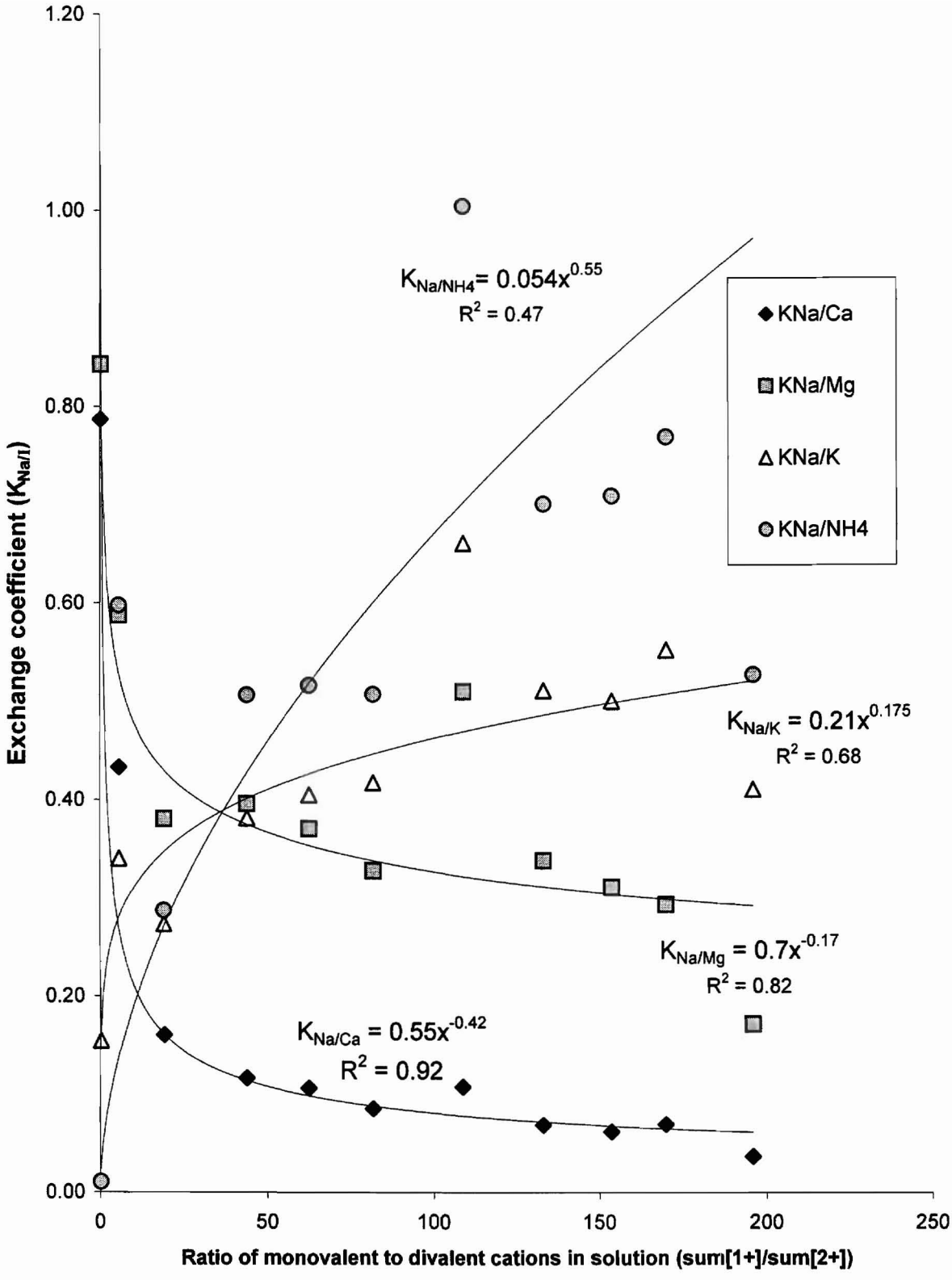

Figure 4.66 - Kelvington soil batch test selectivity coefficients referenced to sodium versus the ratio of monovalent to divalent cations in solution

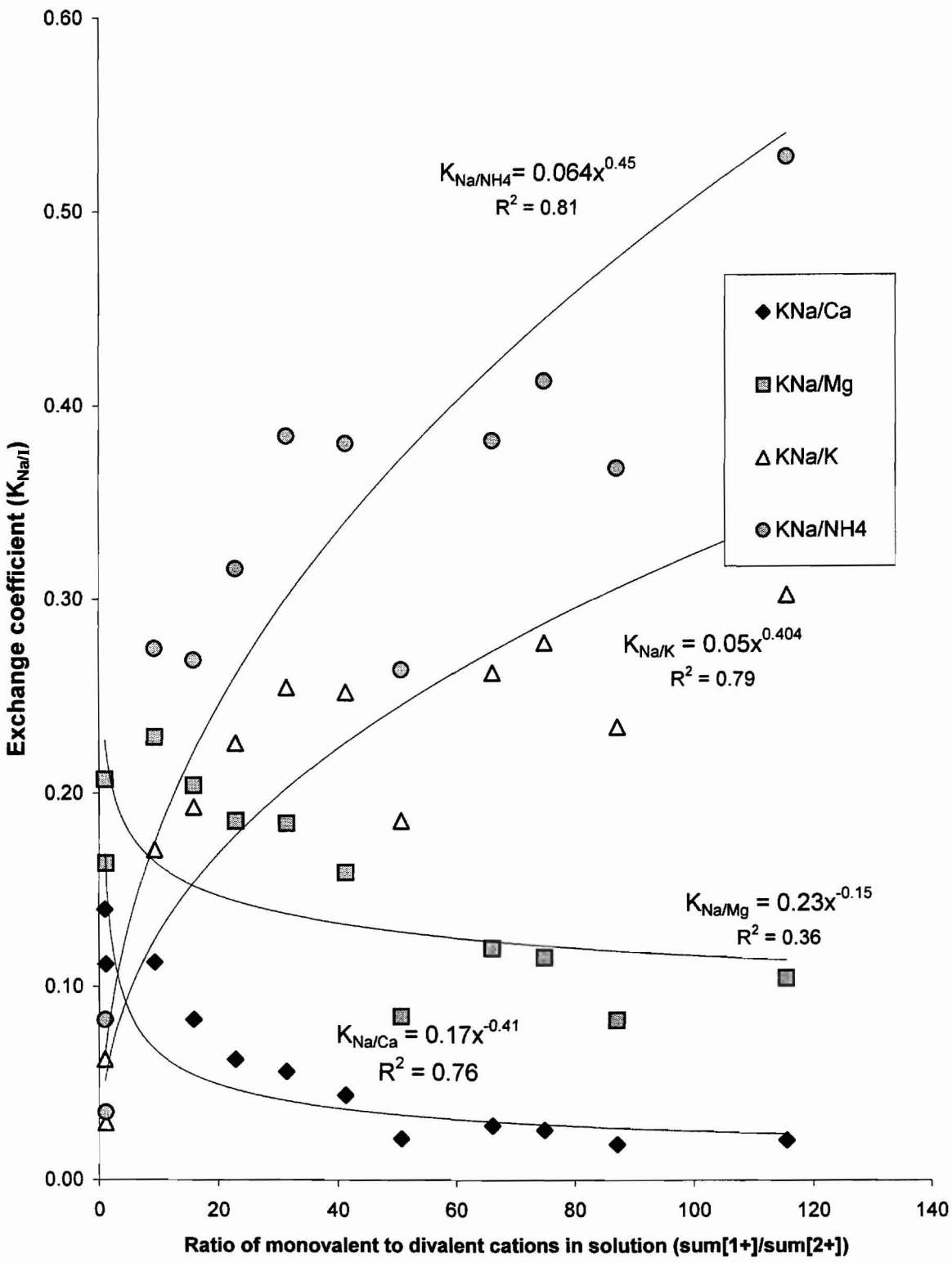

Figure 4.67 - Site No 1 soil batch test selectivity coefficients referenced to sodium versus the ratio of monovalent to divalent cations in solution

potassium and ammonium. This indicates experimental methodology must replicate field conditions as closely as possible.

The selectivity sequence of ions, or lypotropic series, has several variations with the most similar one derived by Erskine (2000) from Appelo and Postma (1993): Li<Na<Mg<Ca<Ba<NH4<K<Cs. Using data from Column 1 and the same methodology as discussed above gives Na<NH4<Mg<Ca<K for low fractions of monovalent cations in solution and Na<NH4<Mg<K<Ca for fractions of monovalent cations in solution above 0.8; extrapolation of the functions presented indicates at fractions above 0.97 the series would be Na<Mg<K<Ca<NH4 (Figure 4.52). Thus, when ammonium dominates the solution, it would be able to remove significant quantities of other ions from the exchange sites. Similar results can be derived from Column No. 2 soil data giving NH4<Na<K<Mg<Ca for conditions when higher quantities of calcium occupy exchange sites and NH4<Na<Mg<Ca<K when calcium occupies less than 3 meq/100g on the exchange sites (Figure 4.58).

Figure 4.68 illustrates the change in equivalent fraction on the exchange sites for each ion with depth in Column No. 1 similar to the analysis of Grove and Wood (1979). Increases in potassium and ammonium are balanced with decreases in magnesium and to lesser extent calcium. This represents increases of up to 2 and 3 meq/100g for potassium and ammonium respectively and decreases of up to 3.4 and 2.4 meq/100g for magnesium and calcium respectively (Figure 4.68). These values translate to an increase of 430% in the quantity of potassium and undeterminable increases of ammonium on the exchange sites, balanced by decreases of 77% and 34% for magnesium and calcium respectively (Figure 4.69). More than 70% of the original magnesium was removed by exchange with monovalent ions before a significant amount of calcium was removed even though, in the absence of the effect of the monovalent ions, magnesium and calcium appear to exchange for one another at lower locations within the column (Figure 4.68). The lower exchange between calcium and magnesium is likely the result of the "hard water front" noted earlier at this location. The pattern indicates effluent would experience an increase in magnesium followed by

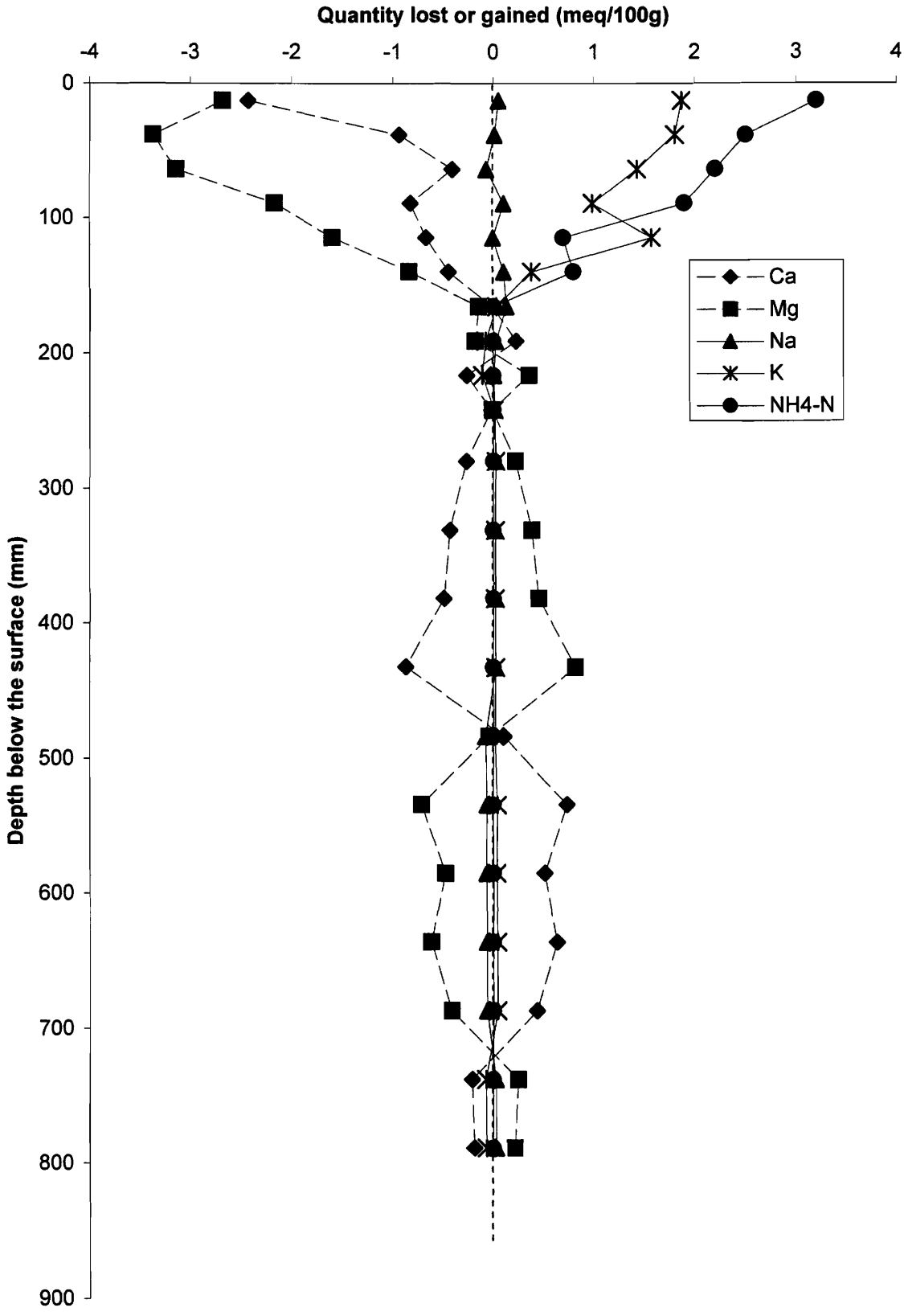

Figure 4.68: Column No. 1 quantity of ions released or adsorbed as a function of depth in the column.

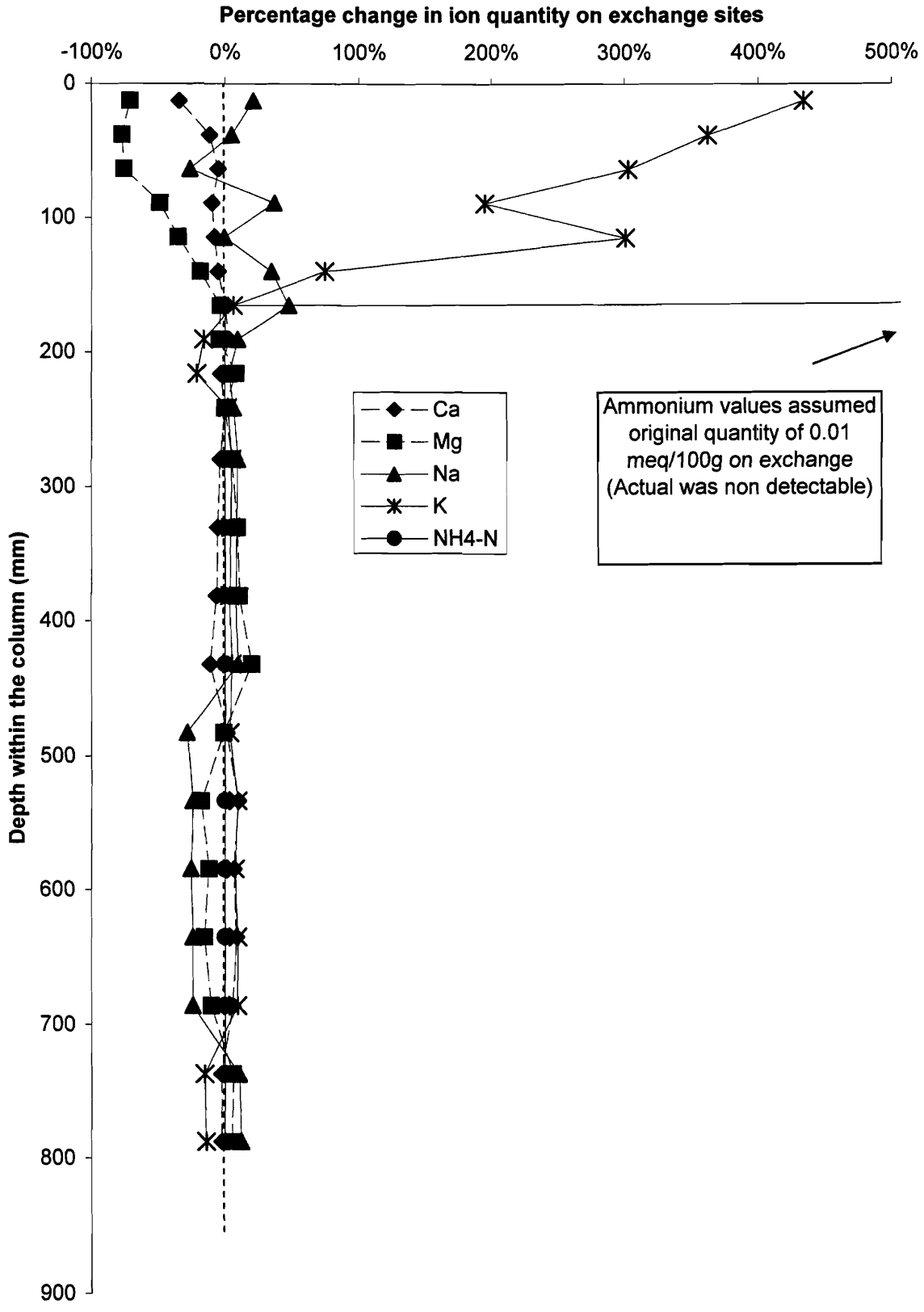

Figure 4.69: Column No. 1 percentage change in the amount of each ion adsorbed.

one of calcium and then another of magnesium. This pattern of peaks and plateaus caused by ion exchange phenomenon has been noted by several researchers (Valocchi et al. 1981; Dance and Reardon, 1983; Bjerg et al., 1993; Thorton et al., 2000).

Figure 4.70 shows the change in equivalent fraction on the exchange site for each ion with depth in Column No. 2. Increases in potassium, and to a lesser extent ammonium and sodium, are initially balanced with a loss of magnesium. As more monovalent cations take up positions on the exchange complex, calcium begins to be removed while the loss of magnesium remains constant. This indicates only a certain percentage of the available magnesium is easily removable, potentially supporting the theory of two different types of sites proposed by Fetter (1977) and others. A balance of equivalents lost or gained (Figure 4.70) shows 1.7 to 2 meq/100g of magnesium is removable before calcium begins to be removed. This is balanced by a gain of 0.5 to 1 meq/100g of potassium, 0 to 0.6meq/100g of ammonium and 0.1 to 0.25 meq/100g of sodium. Calcium removal appears to mirror ammonium gain suggesting a potential interaction between these two ions. Mass or equivalents lost or gained does not give a clear indication of the change in the status of each ion on the exchange complex. Figure 4.71 shows the percent change of each ion compared to the quantity of each ion originally on the exchange sites. Up to 70 and 65% of magnesium and calcium are removed from the exchange sites corresponding to increases of up to 1500, 1000 and 200% for ammonium, potassium and sodium. Only 4% of calcium was removed until 70% of magnesium had been removed from the exchange sites similar to the results of Column No. 1.

Calculation of saturation indices for Columns No.1 and 2 indicate column No.1 soils are supersaturated with both calcite and gypsum in the background soil. Calcite saturation increases near the top of the column with permeating bicarbonate and release of calcium from exchange sites, while the soil becomes undersaturated with respect to gypsum near the top of the column with the loss of sulphate from solution (Figure 4.72). Column No. 2 soils are undersaturated with respect to all minerals plotted with

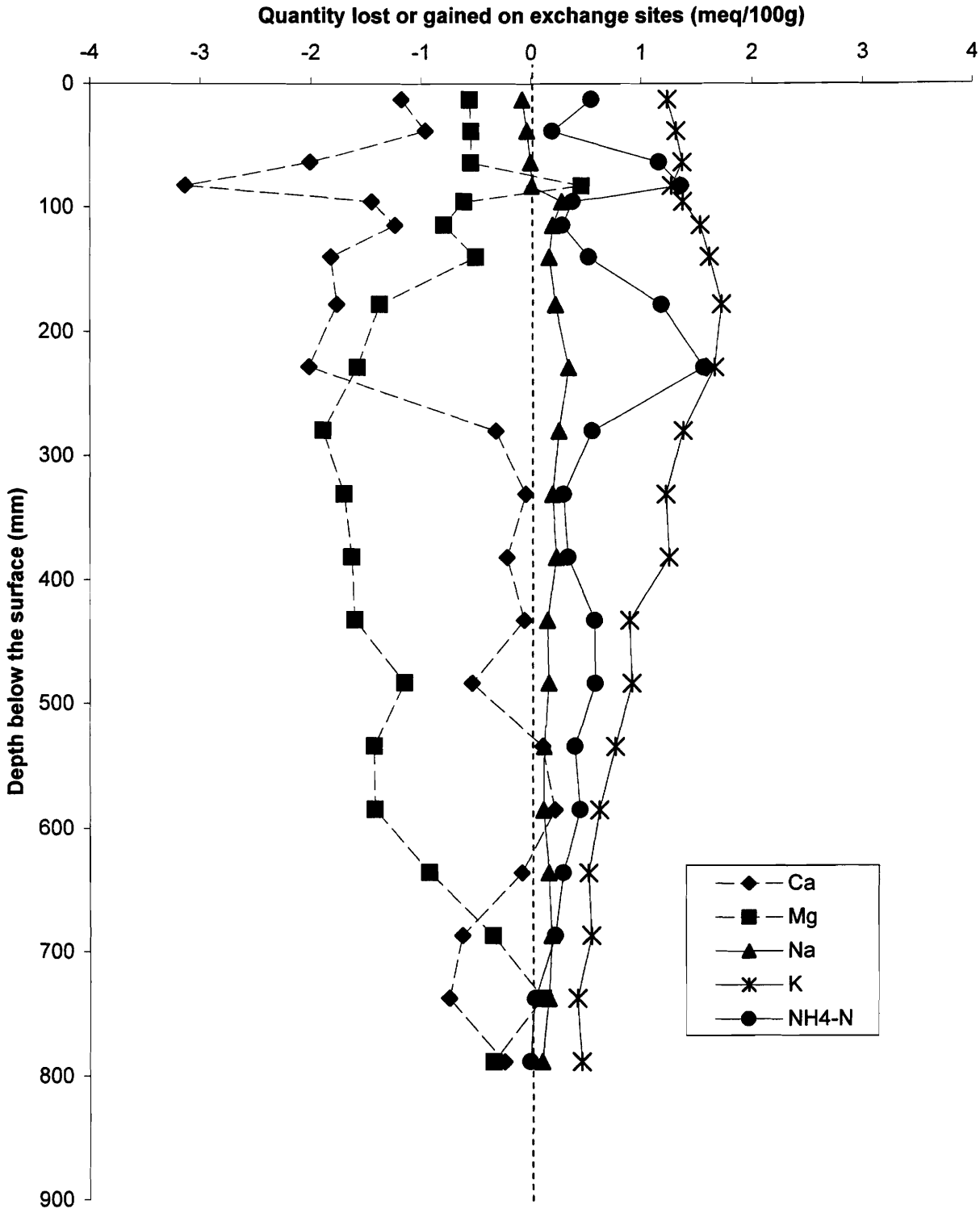

Figure 4.70: Column No. 2 quantity of ions released or adsorbed at various depths within the column.

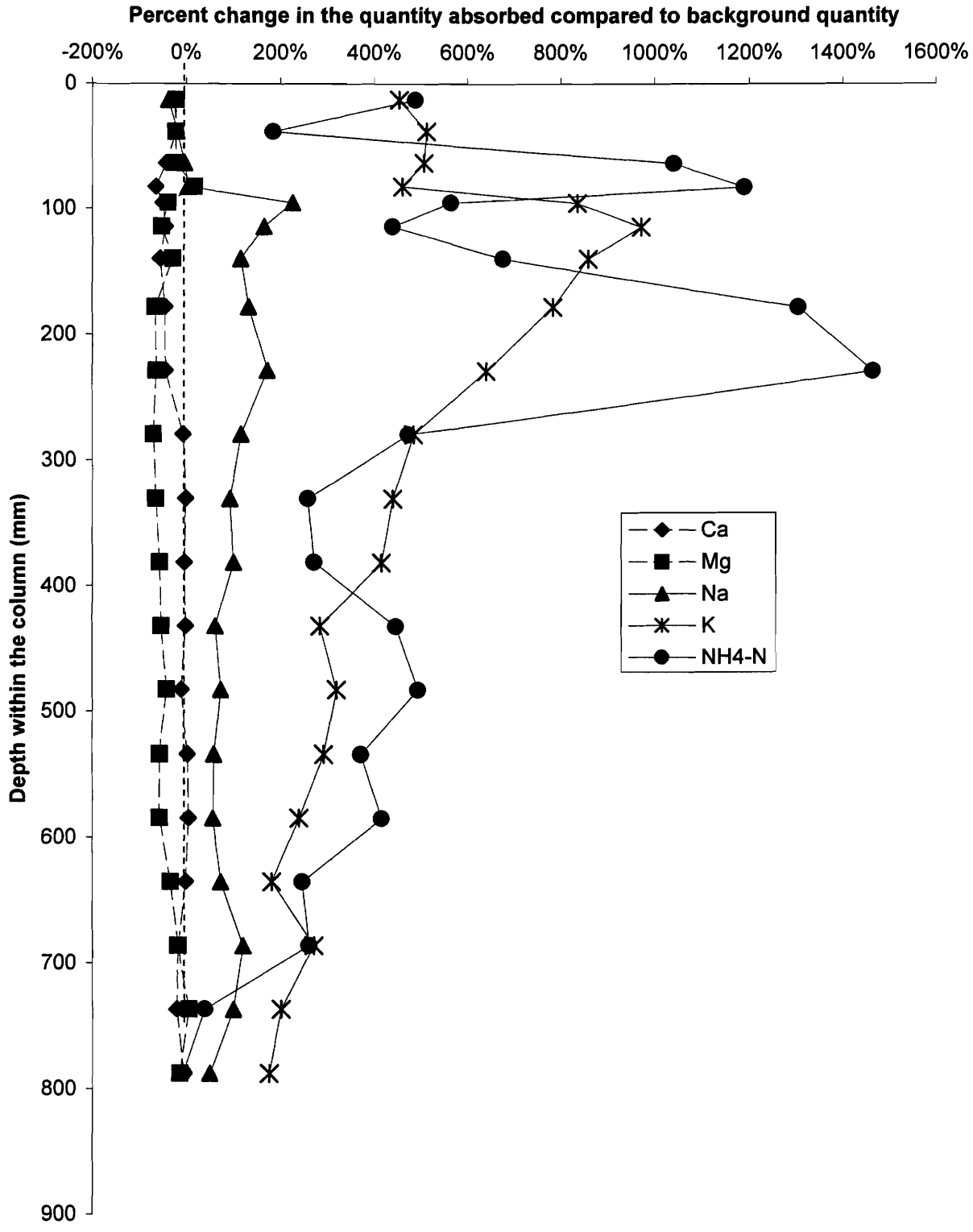

Figure 4.71: Column No. 2 percentage change in the quantity of each ion adsorbed at various depths within the column.

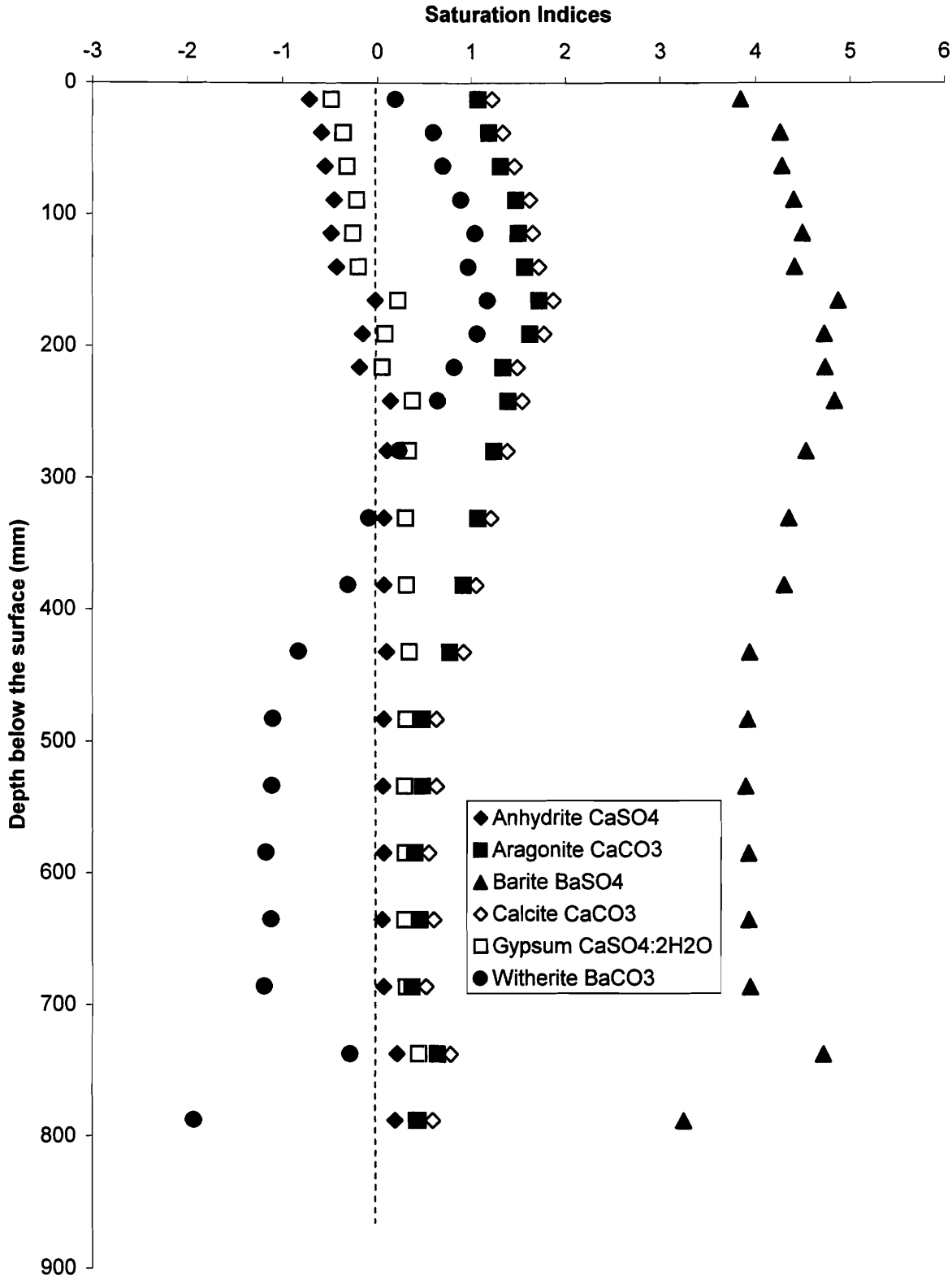

Figure 4.72: Column No. 1 Saturation Indices as a function of depth within the column.

the exception of Whitherite until within 50 mm of the top of the column where they also become supersaturated with respect to calcite (Figure 4.73).

Modeling of Column No. 1 using PHREEQC (Parkhurst and Appelo, 1999) for a 200 mm length of column and using the default selectivity coefficients as those given by Appelo and Postma (1993; Figure 4.74) shows the model underestimates magnesium release or overestimates calcium release from exchange sites, indicates sulfate loss from solution with increases of calcium and magnesium (SI gypsum>1), and overestimates sodium, ammonium and potassium retardation by a factor of ~2. Refinements of selectivity coefficients for the soil and solution to be modeled would likely bring model results quantitatively closer to experimental data.

4.2.13 Estimation of distribution coefficients from selectivity coefficients

Distribution coefficient changes are not obvious from inspection of changes in selectivity coefficients. To analyze these changes, distribution coefficients were determined using Equation 2.47. The modeled selectivity coefficients determined to give the best fit to experimental equivalent fractions and activity of the ion were used in the calculation. Recalculation of the distribution coefficients gives a slightly clearer picture of the effects changing environment during transport has on retardation of intruding cations, namely potassium and ammonium. The distribution coefficient of both ions decreases as ionic strength of the solution increases (Figure 4.75). The effect on potassium is much more pronounced than on ammonium (and sodium). The distribution coefficient for potassium decreases from a maximum of approximately 2.5 to 3 for both soils by the following functions:

Column No 1: $Kd' = -11.5\,I + 3.7$ $R^2=0.5$ [Eq. 4.21]

Column No 2: $Kd' = -12.5\,I + 2.8$ $R^2=0.7$ [Eq. 4.22]

While the distribution coefficient for ammonium for Column No 1 shows a reducing trend, the data is quite variable. Column No 2 shows a more obvious trend given by:

Column No 2: $Kd' = -1.25\,I + 0.28$ $R^2=0.7$ [Eq. 4.23]

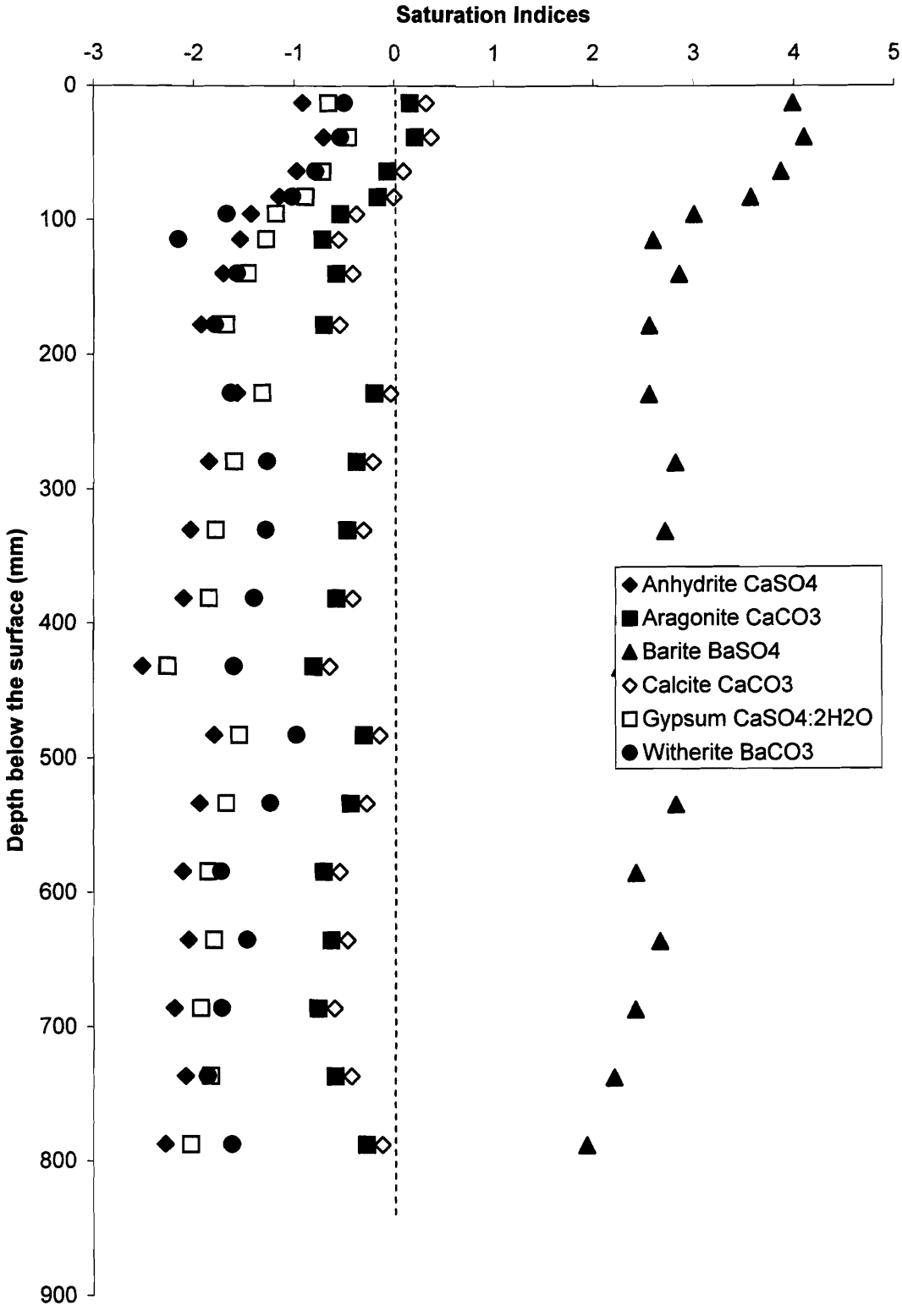

Figure 4.73: Column No. 2 Saturation Indices as a function of depth within the column.

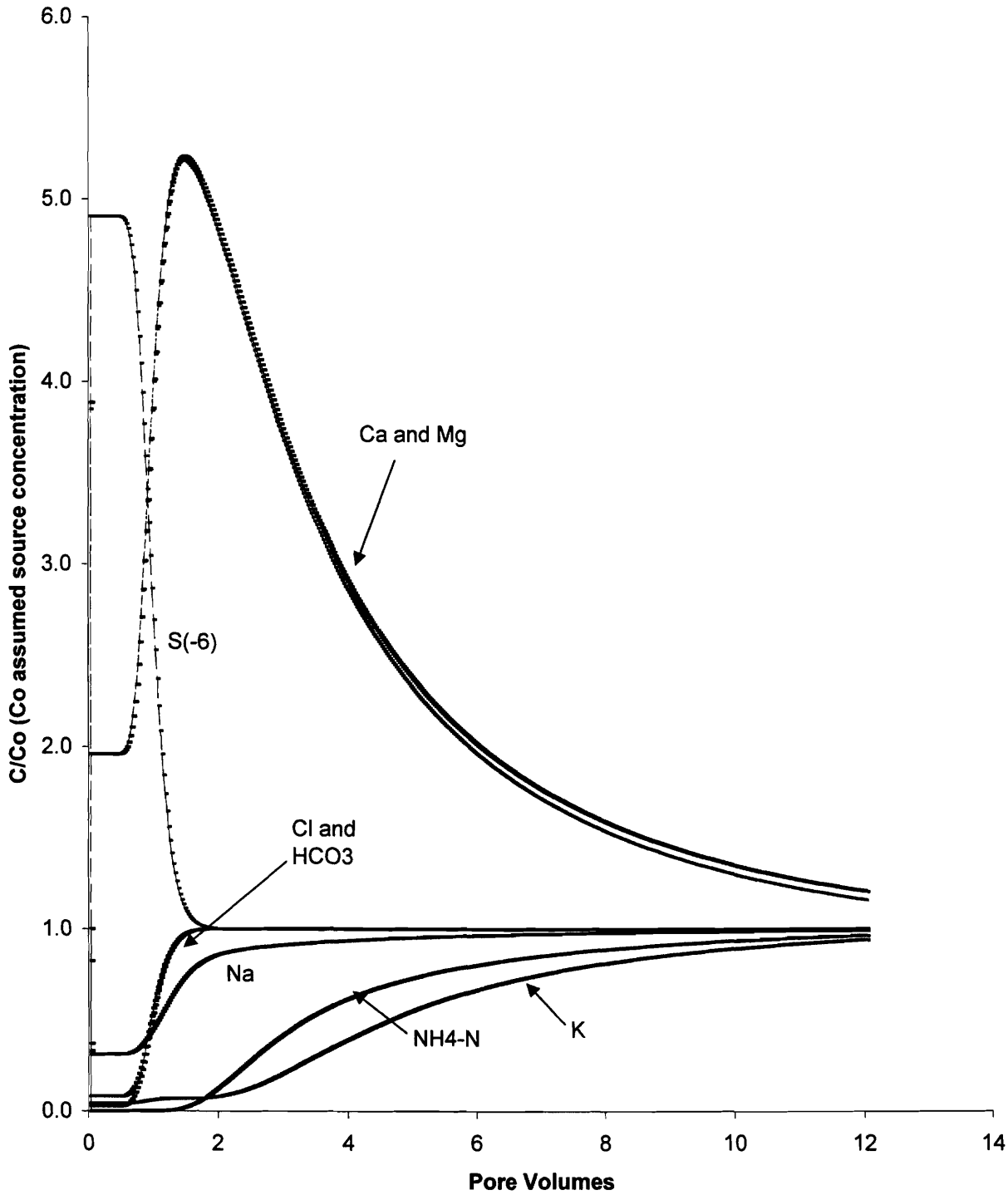

Figure 4.74 - Column No. 1 (Kelvington soil) PHREEQC modeled breakthrough curve results. Column modeled over 200 mm using default constant selectivity coefficients after Appelo and Postma (1993)

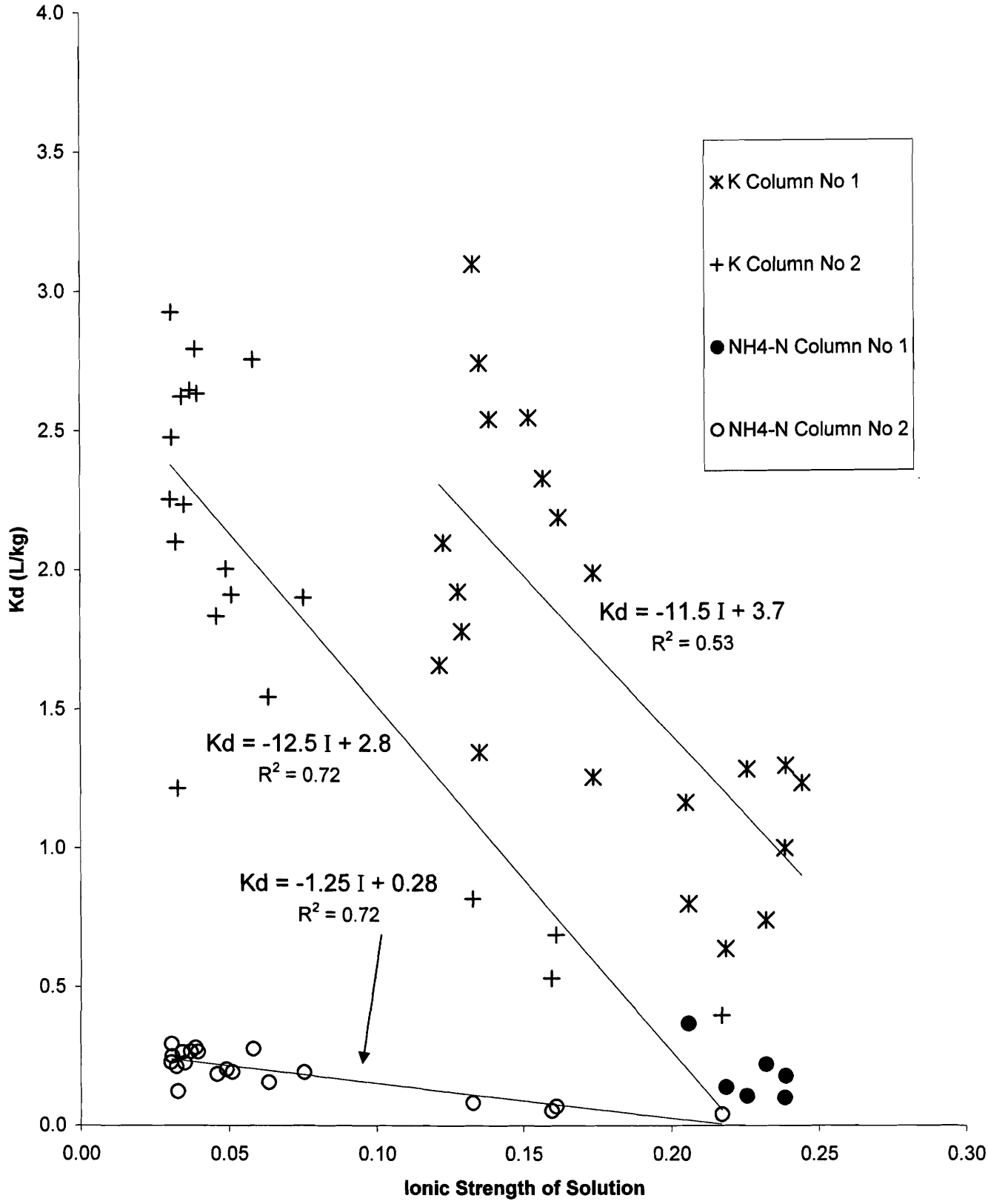

Figure 4.75: Distribution coefficients calculated from modeled selectivity coefficients.

Equation 4.23 being 1/10 that of Equation 4.22 is simply the result of the selectivity coefficient for ammonium ($K_{Na/NH4}$) being 10 times that for potassium ($K_{Na/K}$).

Since the selectivity coefficients show dependence on the fraction of monovalent cations in solution and the quantity of calcium absorbed, the distribution coefficients might also show dependence on these two parameters. A complicating factor, however, is the fraction of monovalent cations in solution is relatively constant for data from Column No 2. The ratio of monovalent to divalent cations in solution ($R_{1+/2+}$) has greater variance and was therefore chosen as the potential parameter to analyze. Plotting the distribution coefficient for ammonium as a function of the ratio of monovalent to divalent cations in solution (Figure 4.76) shows a reasonable dependence upon ammonium distribution coefficients, increasing as the ratio of monovalent to divalent cations in solution increases following the function:

Column No 1: $Kd' = 0.05\ R_{1+/2+}$ $R^2=0.89$ [Eq. 4.24]

Column No 2: $Kd' = 0.12 \ln(R_{1+/2+}) - 0.07$ $R^2=0.8$ [Eq. 4.25]

For comparison purposes, distribution coefficients for potassium were also analyzed as a function of the ratio of monovalent to divalent cations in solution ($R_{1+/2+}$) (Figure 4.77). This analysis indicates distribution coefficient for the soil from Column No 1 decreases as the ratio of monovalent to divalent cations in solution increases; the distribution coefficient for soil from Column No. 2 increases as the ratio of monovalent to divalent cations in solution increases. Equations relating these two parameters are given by:

Column No 1: $Kd' = 1.3\ (R_{1+/2+})^{-0.29}$ $R^2=0.86$ [Eq. 4.26]

Column No 2: $Kd' = 1.2 \ln(R_{1+/2+}) - 0.7$ $R^2=0.84$ [Eq. 4.27]

Again, the distribution coefficients for potassium for soils from Column No 2 are 10 times those for soils from Column No 1 reflecting the difference in selectivity coefficients.

Distribution coefficients calculated from modeled selectivity coefficients are in the same range of values as determined using isotherms: 0.5 to 3.5 L/kg for potassium and 0.05 to 0.4 L/kg for ammonium. The isotherm determined distribution coefficients

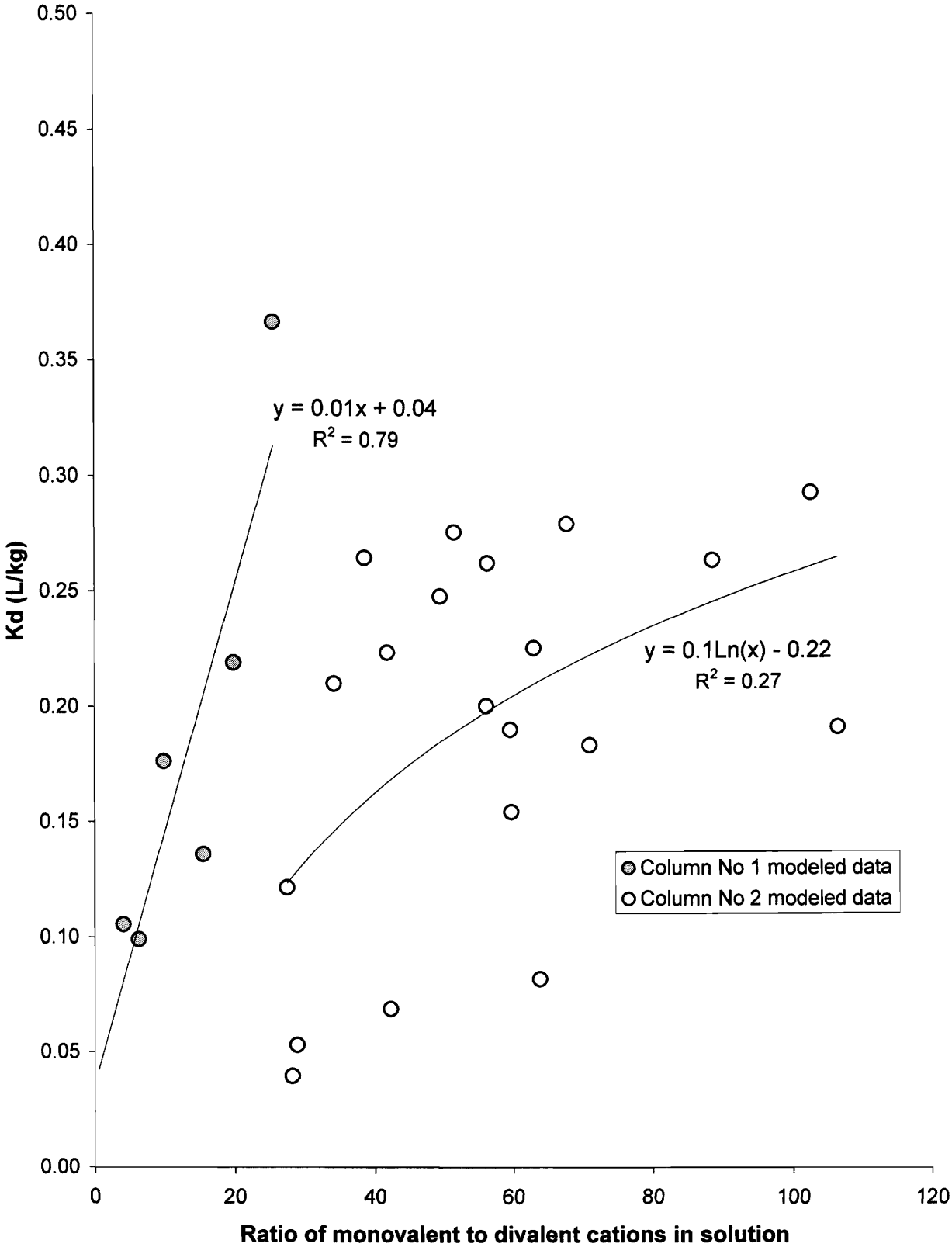

Figure 4.76: Distribution coefficients for ammonium calculated using modeled selectivity coefficients as a function of the ratio of monovalent to divalent cations in solution.

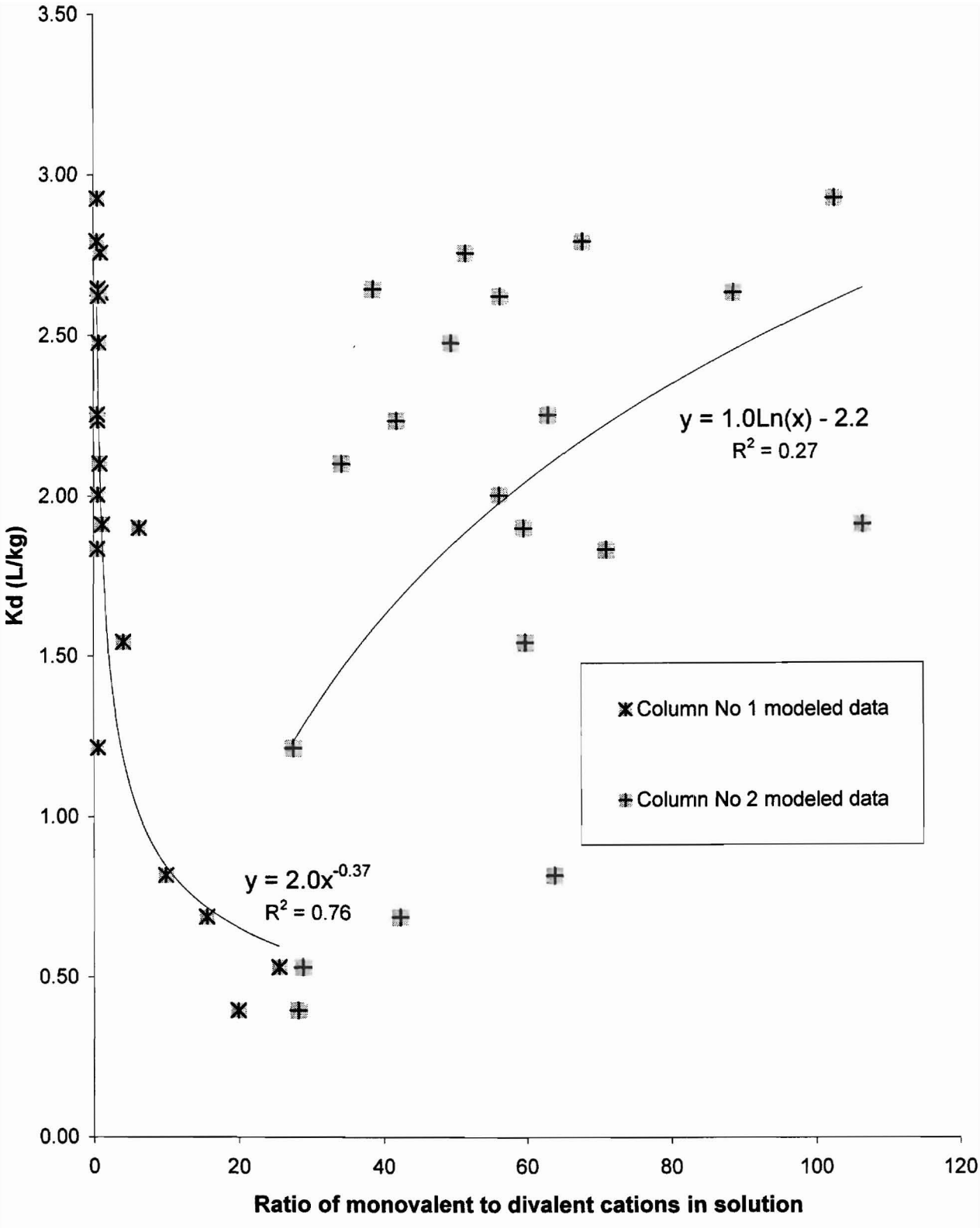

Figure 4.77: Distribution coefficient for potassium calculated using modeled selectivity coefficients as a function of the ratio of monovalent to divalent cations in solution.

decreased to a low near zero for relatively high concentrations of potassium or ammonium. This reflects that the equations used to determine the distribution coefficients do not necessarily take into account the interactions of ammonium and potassium with the other ions in solution at the ratios of monovalent to divalent cations in solution shown in Figures 4.76 and 4.77. The distribution coefficients calculated from the modeled selectivity coefficients for potassium and ammonium convert to retardation factors of 3 to 13 for potassium and 1.2 to 3 for ammonium. These values are similar to those reported by others (Table 4.15; Dance and Reardon, 1983; Ceazan et al., 1989; Bjerg and Christensen, 1993; Erskine, 2000; Thorton et al., 2000; Thorton et al., 2001).

4.2.14 Laboratory study conclusions

The attenuation of ammonium and potassium can be explained by ion exchange. The replacability of ions on the exchange sites followed the general form of the lyotropic series Na<Mg<Ca<NH4<K with the exception of ammonium. The ability of ammonium to replace other ions was reduced when the percentage of monovalent cations in solution was less than 80% and/or when conditions dictated larger quantities of calcium on the exchange sites as per McBride (1994). The quantity of calcium on the exchange sites also reduced the ability of potassium to replace other ions but to a lesser extent than ammonium.

Absorption isotherm analysis indicates each ion may have a maximum absorption level for a particular soil that is less than the total CEC of the soil. An example is potassium only able to occupy 23% of the soil exchange sites in both soils test. This may have resulted from solutions used in this study containing relatively high concentrations of several ions. Each ion may be able to occupy more exchange sites if the soil were flushed with a solution containing high concentration of a single cation. Removal of ions from exchange sites showed a similar behaviour. In both column studies, 70% of magnesium was removed from soil exchange sites by ion exchange before any significant quantity of calcium was removed. At the same time, once 70% of the

magnesium was removed, calcium was removed preferentially over magnesium suggesting the remaining 30% may be difficult to displace.

Ion exchange selectivity coefficients with respect to sodium for calcium, magnesium and potassium for Column No. 2 were similar to values of Appelo and Postma (1993) and used by Parkhurst and Appelo (1999), and approximately 50% less for Column No. 1 which matched values of Valocchi et al. (1981). Selectivity coefficients for ammonium with respect to sodium reported by both Valocchi et al. (1981) and Appelo and Postma (1993) are in the range determined for Column No.1 at higher ammonium concentrations while the selectivity coefficient for Column No. 2 is an order of magnitude higher suggesting relatively low selectivity for ammonium.

Use of the default selectivity coefficients to model equivalent fractions of ions occupying soil exchange sites was shown to overestimate ammonium absorption and underestimate calcium and magnesium absorption. Distribution coefficients calculated from selectivity coefficients ranged between 0.05 and 0.4 for ammonium and 0.5 and 3.0 for potassium. These values are consistent with those determined from studies involving landfill leachate but much lower than those reported to be currently used in practice (Erskine 2000), suggesting ammonium is much less attenuated than may have been expected when some waste containment facilities were constructed.

4.3 Field Investigation

4.3.1 Site Geology and Hydrogeology

The top 100 m at this site consists of stratified silty clay drift, underlain by ~60 m of noncalcareous silt and clay of the Bearpaw Formation. The ensuing 200 to 300 m are of the Lea Park Formation - Upper Colorado Group (SRC 1967). Surface geology of the area is classified as eolian plains with some dunes over glaciolacustrine plains (SRC 1987). Test drilling indicates 100 to 300 mm of topsoil followed by silts and sands to a depth of 5 to 7 m. This is followed by layered soft sands, silts and clays overlaying stiff clay at depths of 5

to 10 m below grade. Watertable elevations range from 1.5 to 3 m below ground surface. Groundwater in the upper unconfined aquifer generally flows in a south south-easterly direction as determined from water levels of two piezometers and an abandoned unconfined aquifer water well, all 200 to 300 m from the EMS.

4.3.2 Site Layout

Test hole locations were selected based on information available from previous studies and soil sampling as described in Section 3.3.3. Piezometer locations are indicated on Figure 3.3.

4.3.3 Soils Analysis Results

Testhole logs and laboratory testing results are available in the Saskatchewan Agriculture Food and Rural Revitalization report No. 97000061entitled "Long Term Performance and Safety of Earthen Hog Manure Storages" (Fonstad 2000).

4.3.4 Results of N(5) and N(-3) 2MKCl Extraction from Soil Cores

Test hole C29 (Figure 4.78) indicate background levels of nitrogen are minimal with some naturally occurring ammonium. C14 (Figure 4.79) and C17 (Figure 4.80) indicate significant nitrogen contamination to at least 22 m south of the EMS and to depths of 6 to 8 m below grade. Nitrogen below the water table occurs in the ammonium state (N(-3)) indicating reducing conditions. Some elevated nitrate (N(-5)) levels occurs above the water table indicating this zone may be aerobic and/or the water table at the site fluctuates in this zone. Additionally, nitrogen (ammonium) contamination appears contained by a clay layer at 6 to 8 m below grade. Nitrogen contamination does not extend to C22 (Figure 4.81) located 33 m from the EMS. Figure 4.82 compiles this information along with a geologic cross section compiled from the testhole logs (Fonstad 2000).

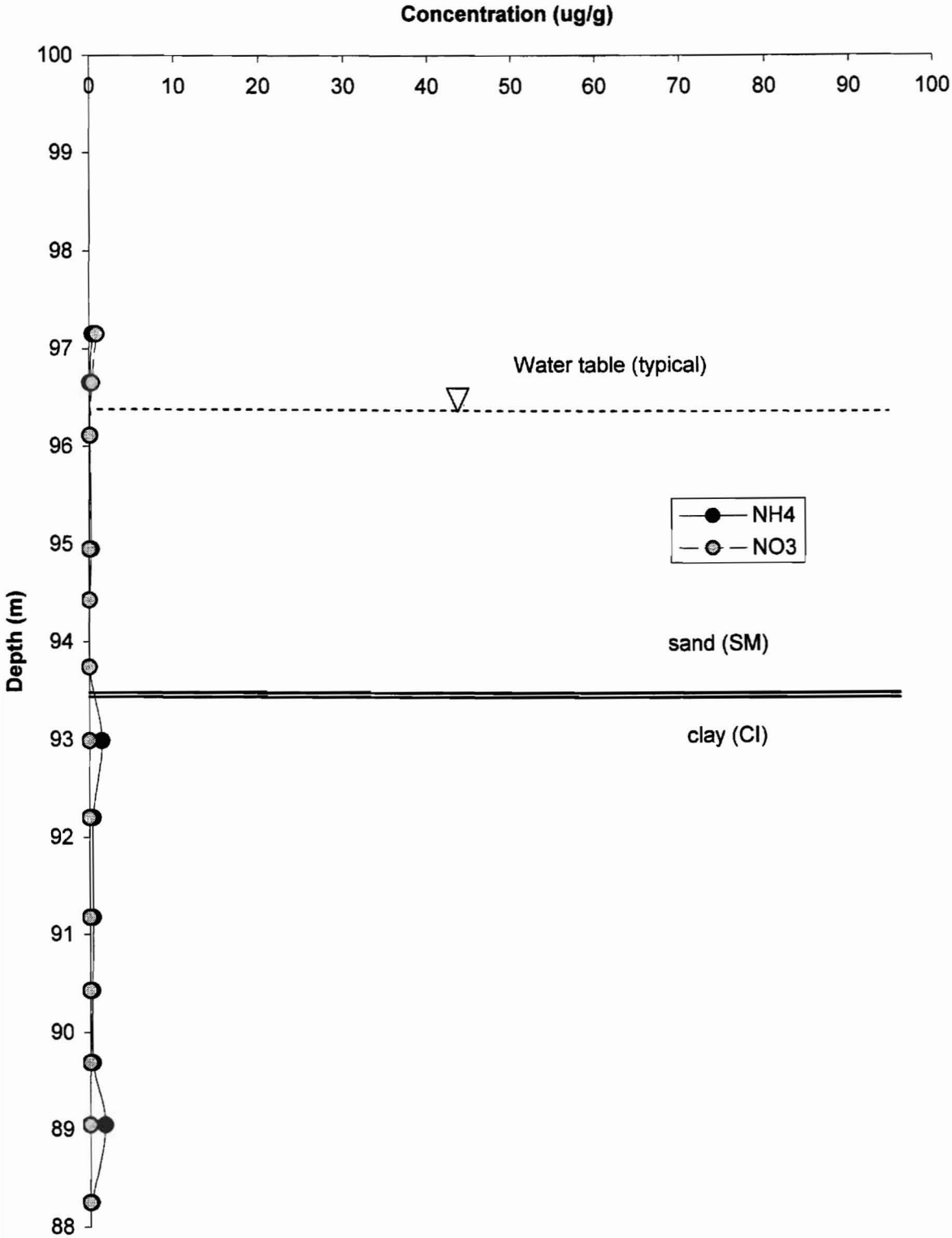

Figure 4.78: Site No. 1, 2MKCl extraction results for test hole C29 on the north side of EMS

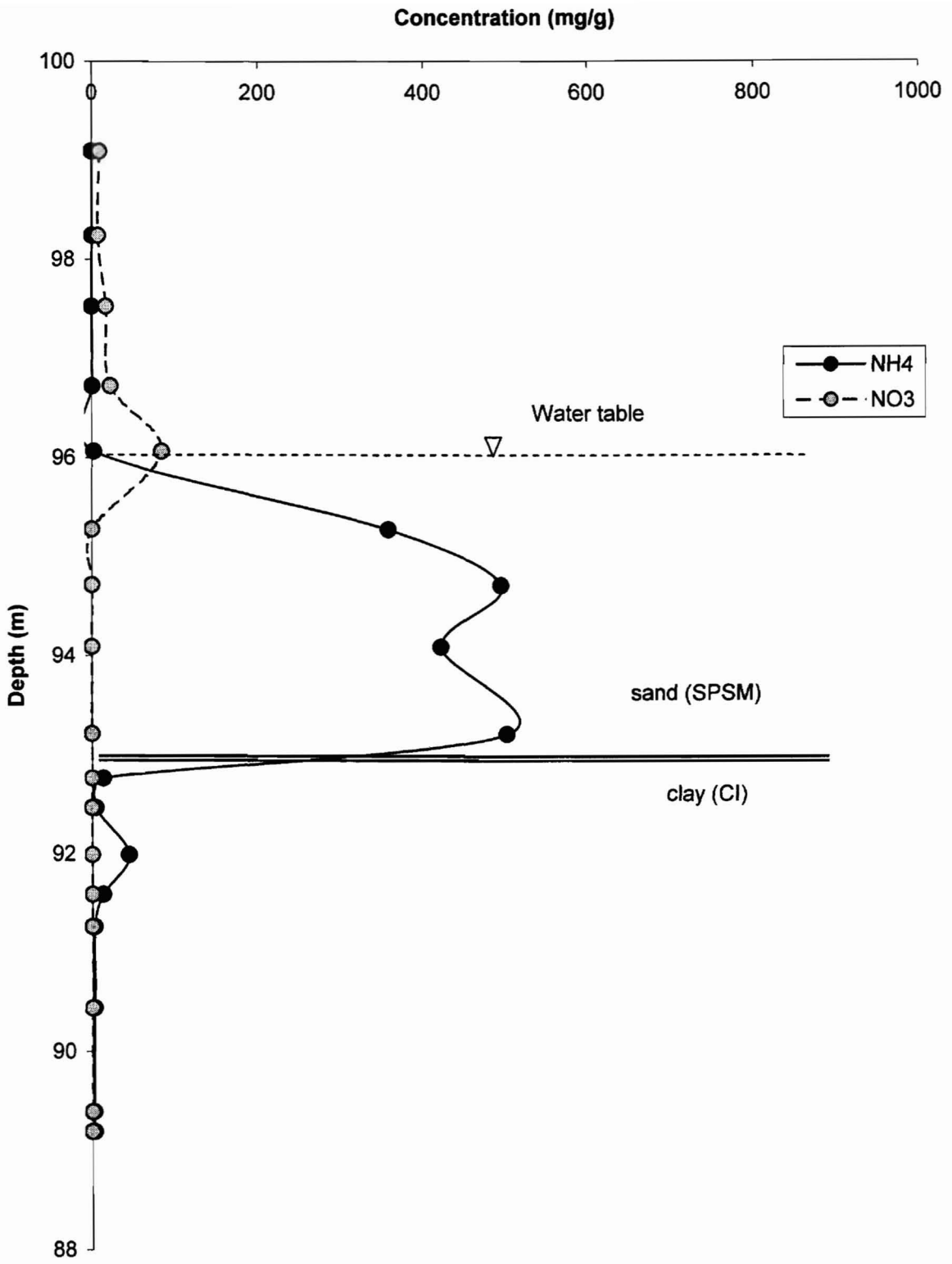

Figure 4.79: Site No. 1, Test hole C14 12 meters south of EMS.
2MKCl extraction results for ammonium and nitrate

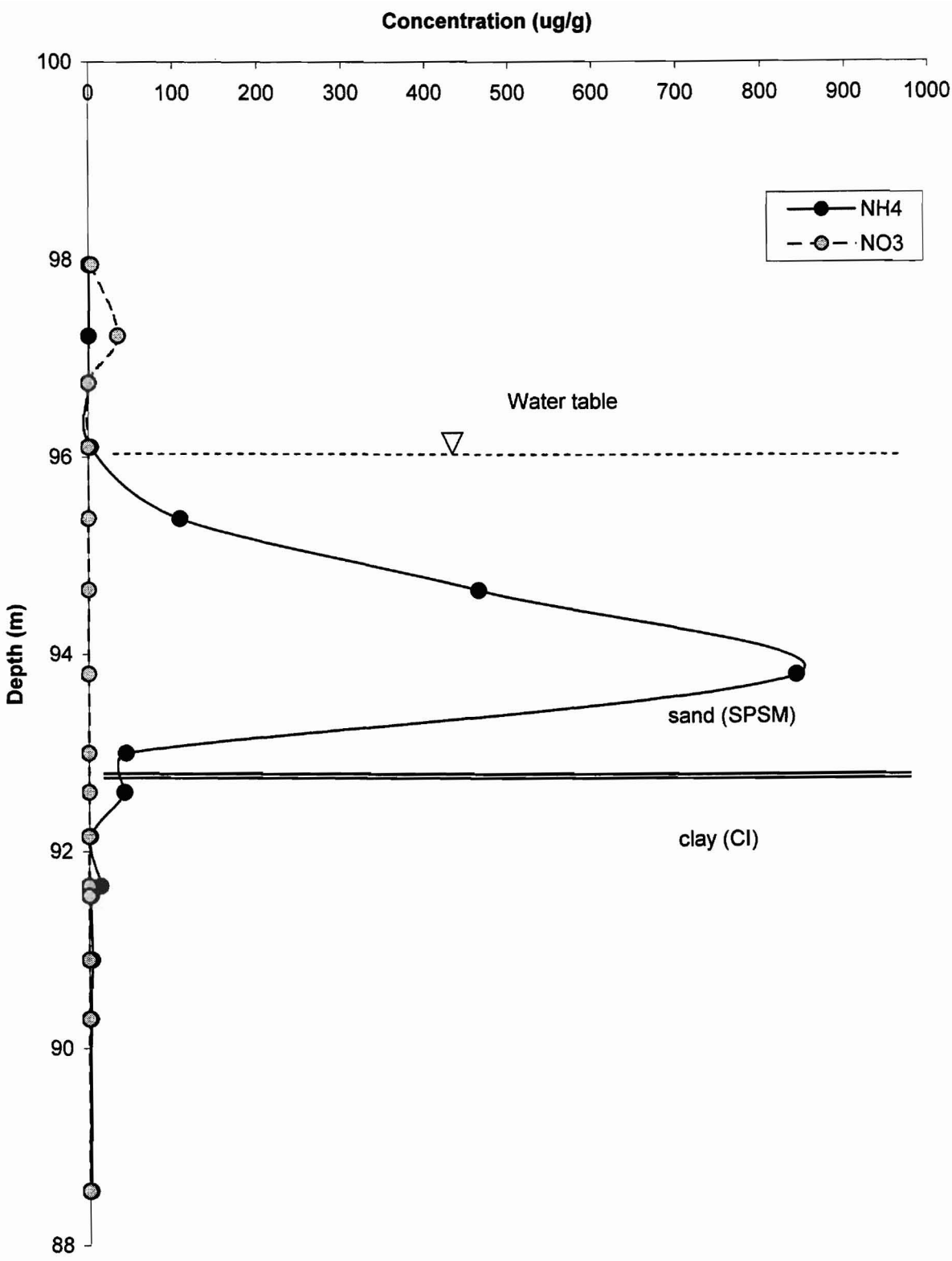

Figure 4.80 -Site No. 1, Test hole C17 22 meters south of EMS.
2MKCl extraction results for ammonium and nitrate

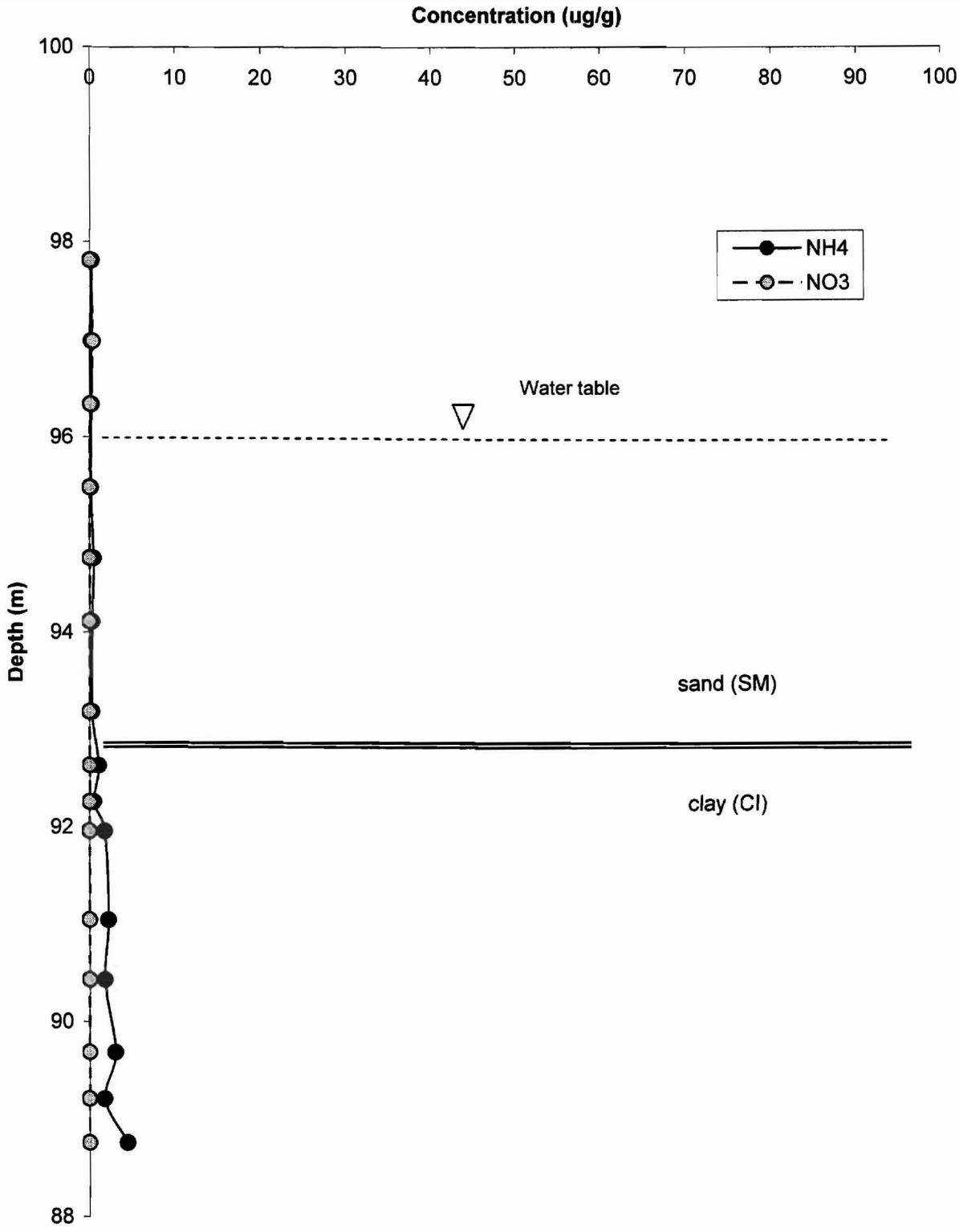

Figure 4.81 - Site No. 1, Test hole C22 33 meters south of the EMS. 2MKCl extraction resutls for ammonium and nitrate.

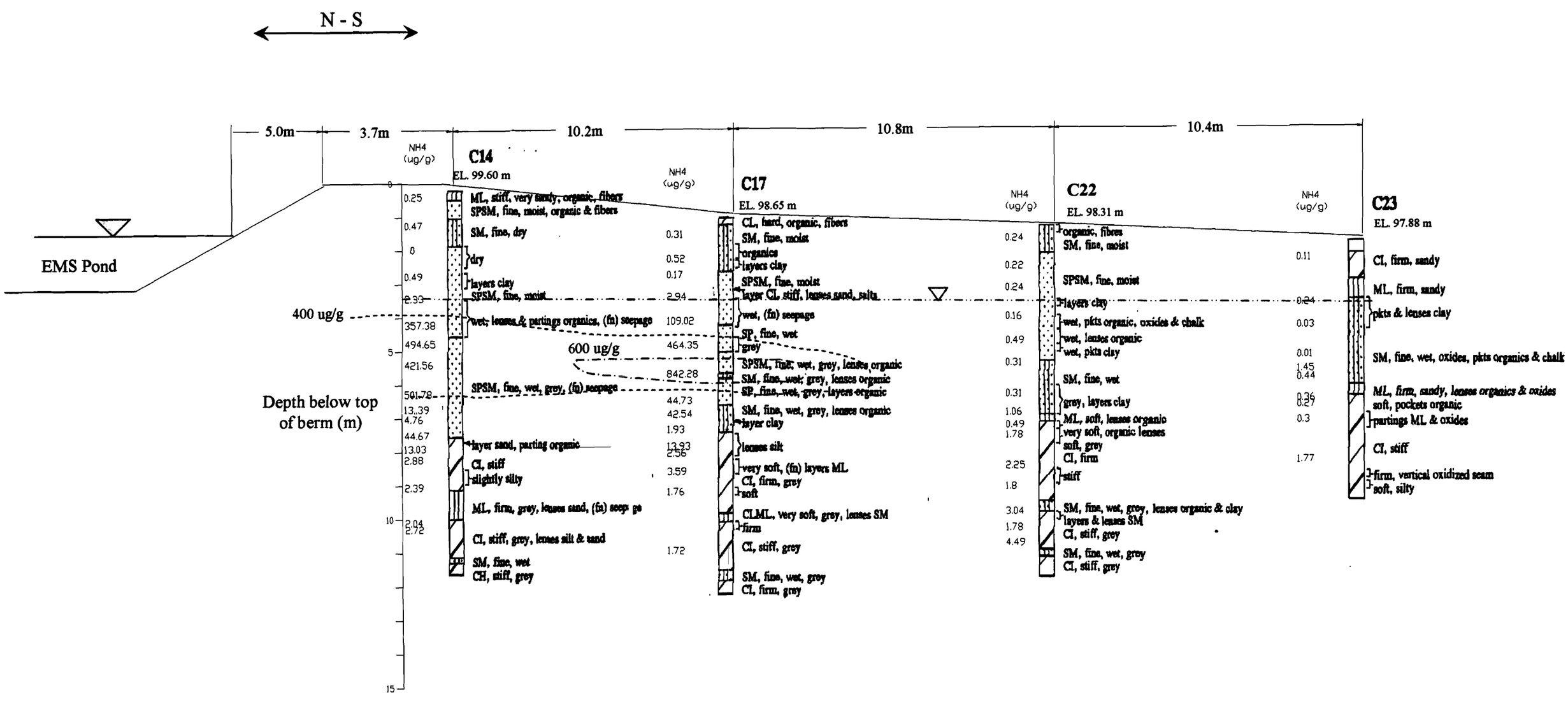

Figure 4.82 - ADF Research Site No.1 north-south cross section of the south side of the EMS showing test hole logs with ammonium concentrations determined from soil samples using 2M KCl extraction.

4.3.5 Water Table, ORP, and Soil Gas Field Readings

Water level readings taken at various times during the year and for times when the EMS liquid level was at various elevations indicate the water table is relatively insensitive to the EMS liquid level (Figure 4.83), although seepage from the EMS may cause a slight change in gradient on its south side. Water table elevation contours from water level readings in October 2000 (Figure 4.84) and May 2004 (Figure 4.85) confirm a groundwater flow direction in the south to south-east direction. Vertical downward gradients near the EMS ranged from 5 to 9%; vertical gradients at the remaining locations fluctuated between slightly upward or downward depending on time of year and soil moisture conditions.

ORP readings taken January 2002, September 2003 and May 2004 (Figures 4.86 to 4.88) indicate slightly reducing conditions (-100 to 100 mV) below the water table, consistent with other groundwater investigations conducted in soils of the area (Richards, 1997). ORP readings in January 2002 ranged between -200 and -100 mV in the unconfined aquifer, and could be the result of reduced oxygen availability due to frozen surface soils and the relatively high levels of microbial substrate in the aquifer at these locations. ORP readings in the vadose zone indicate Eh values of +200 to +300 mV. Soil gas sampling in September 2003 indicated 20% oxygen near the soil surface and 18% oxygen near the water table which corresponds with ORP readings. Temperatures below the water table remained relatively constant between 4–6 °C for all three sampling dates.

4.3.6 Water Sampling Results

Electrical conductivity (EC) at piezometer nests on the north and south sides of the EMS were plotted as a function of depth to indicate the extent of the plume (Figure 4.89 to 4.92). EC measurements indicated high total dissolved solids (TDS) in the groundwater directly below the EMS (Figure 4.90) compared to readings taken from piezometers C29 and C30 located on the north side (Figure 4.89). Although the EC of

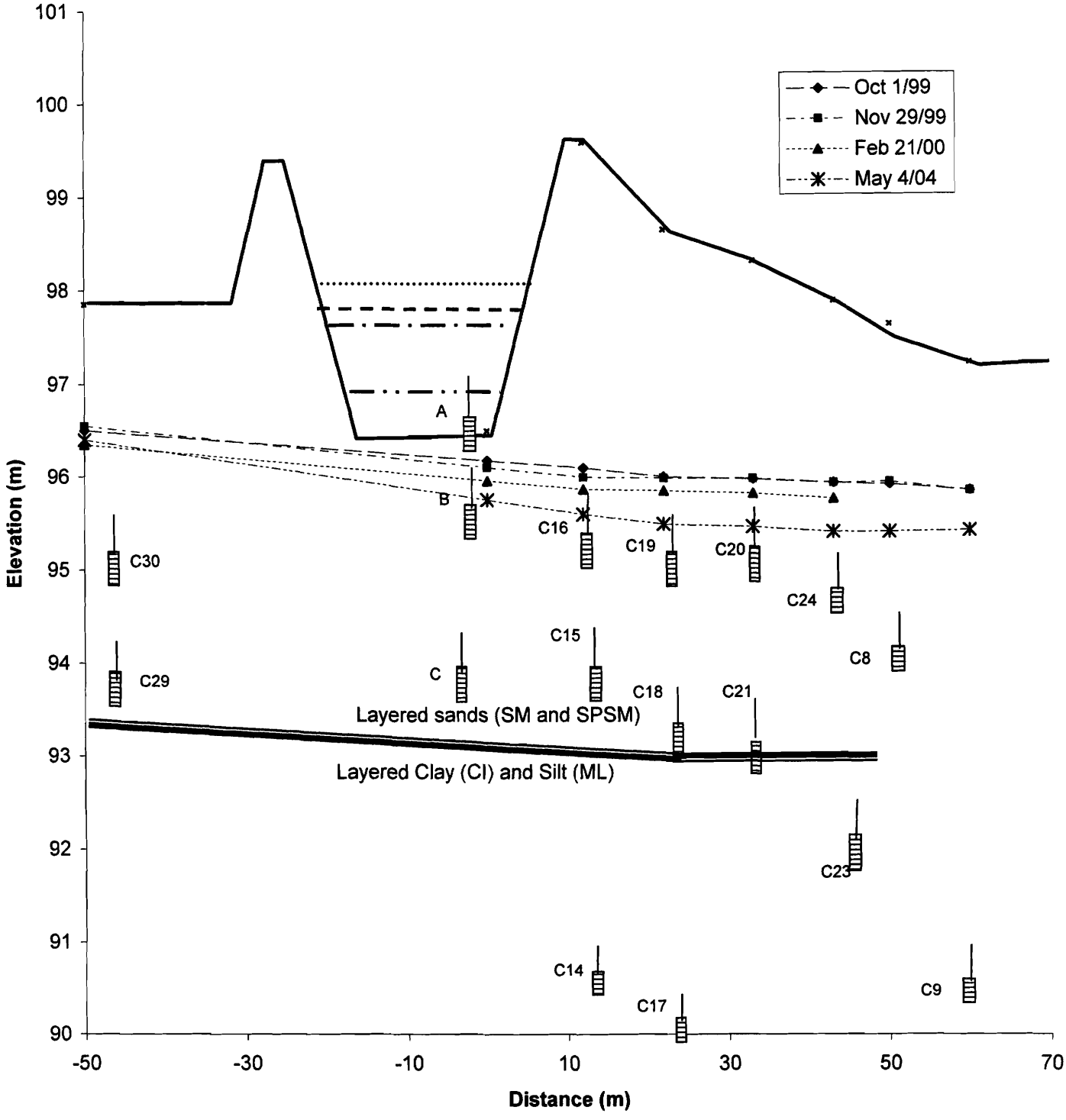

Figure 4.83 : Site No. 1 groundwater elevations and locations of piezometer tips

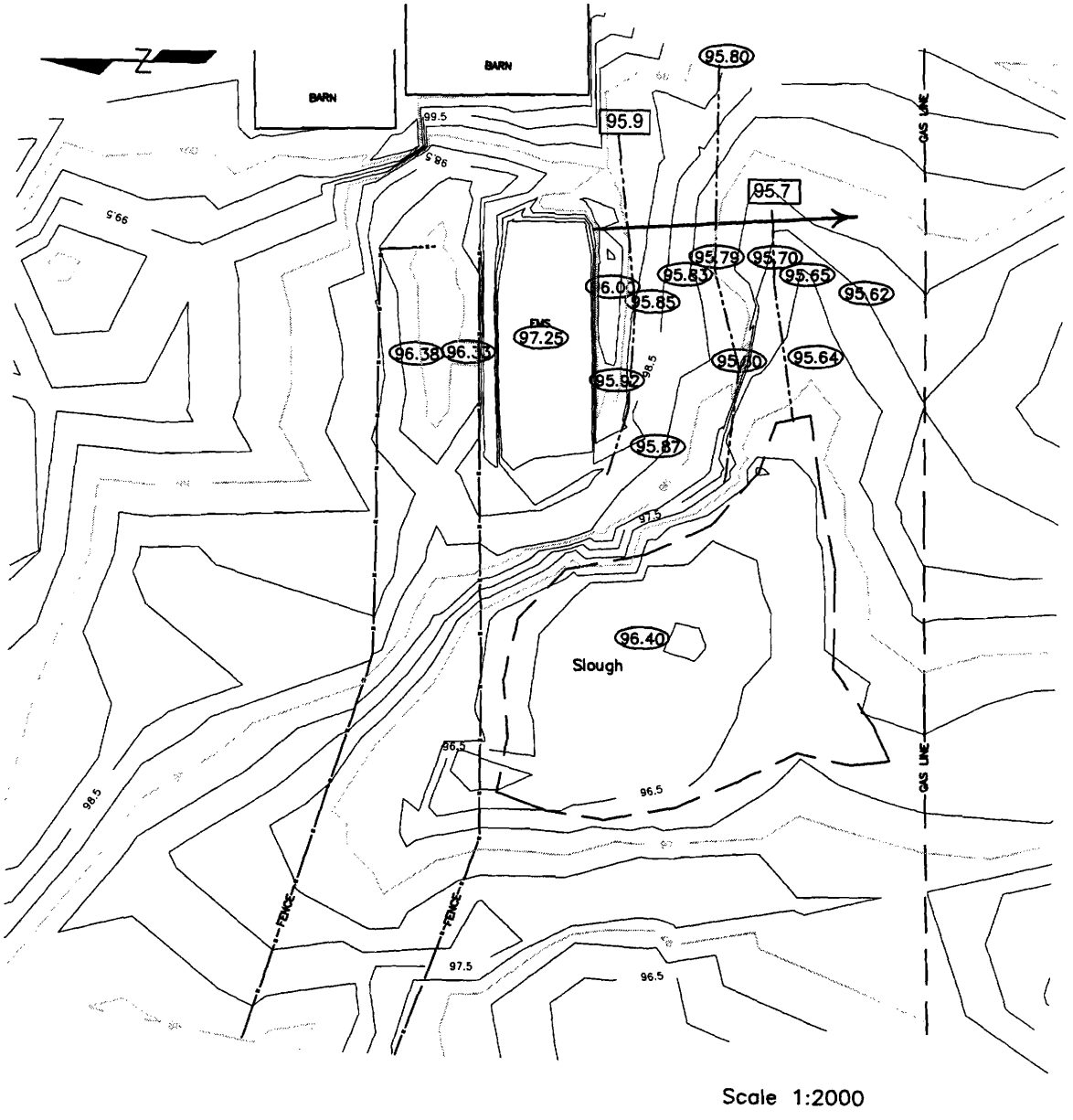

Figure 4.84 - Water level elevation contours at Site No. 1, October 2000

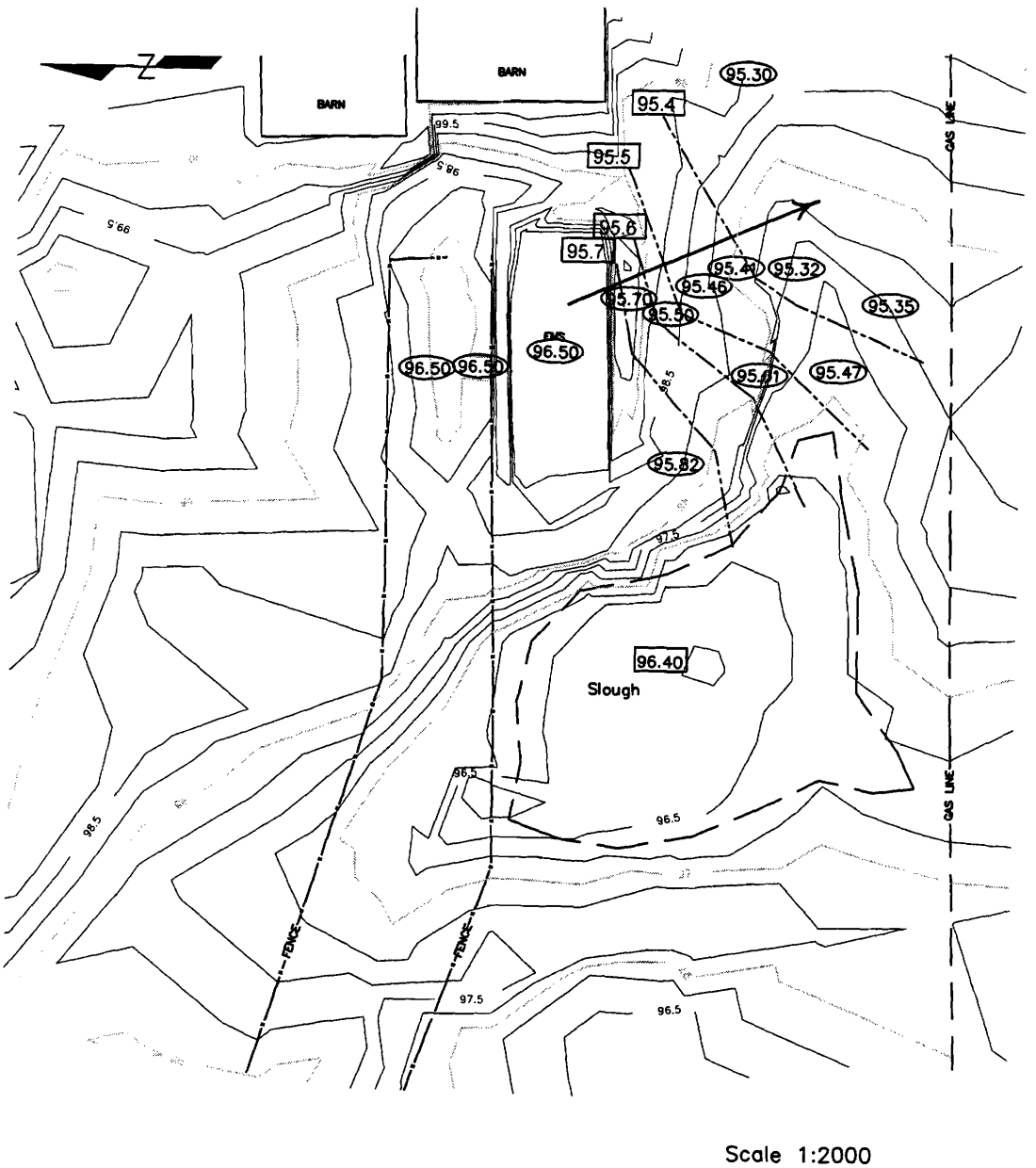

Figure 4.85 - Water level elevation contours at Site No. 1, May 2004

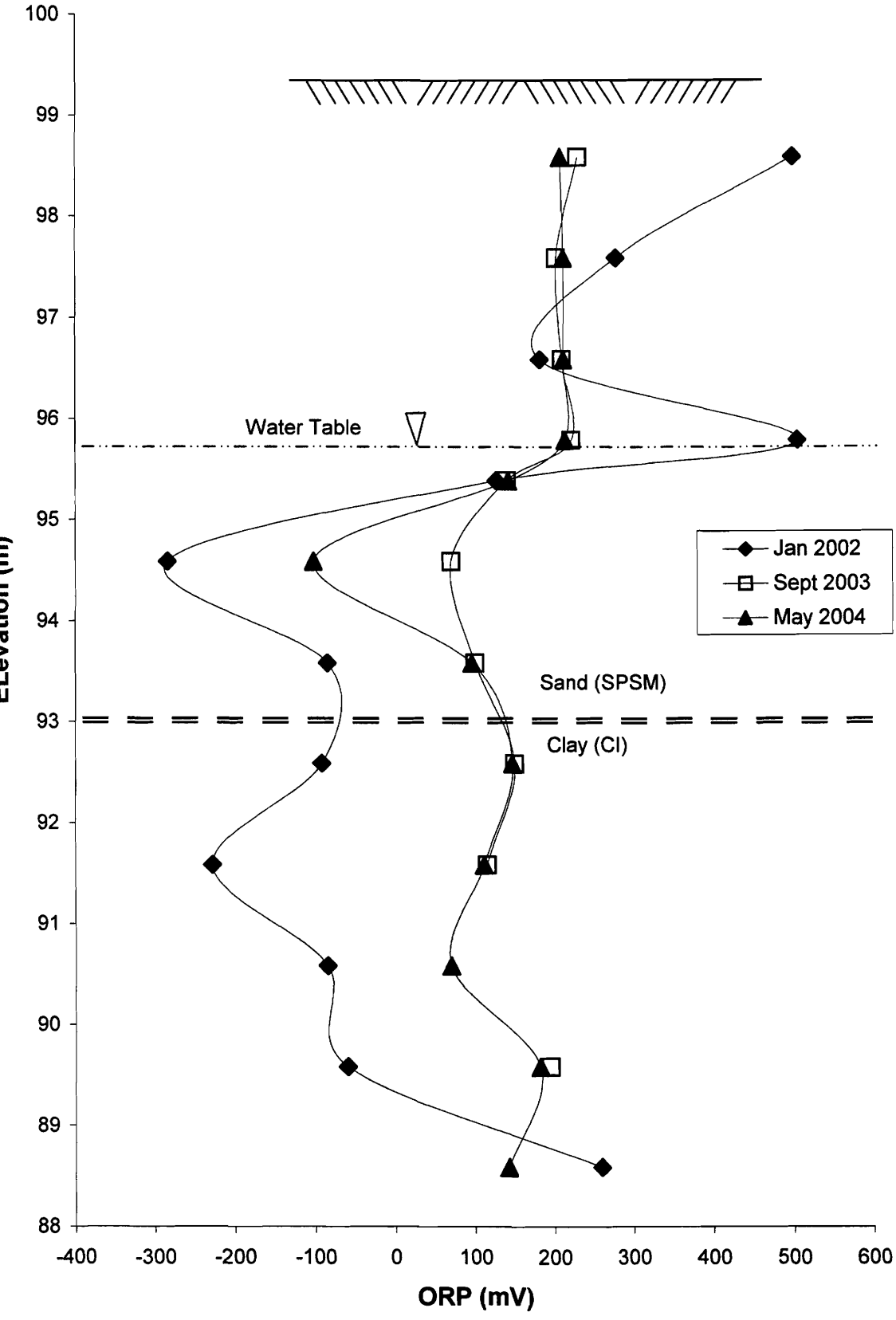

Figure 4.86 - Site No. 1 ORP (Eh) readings 12 meters south of the EMS

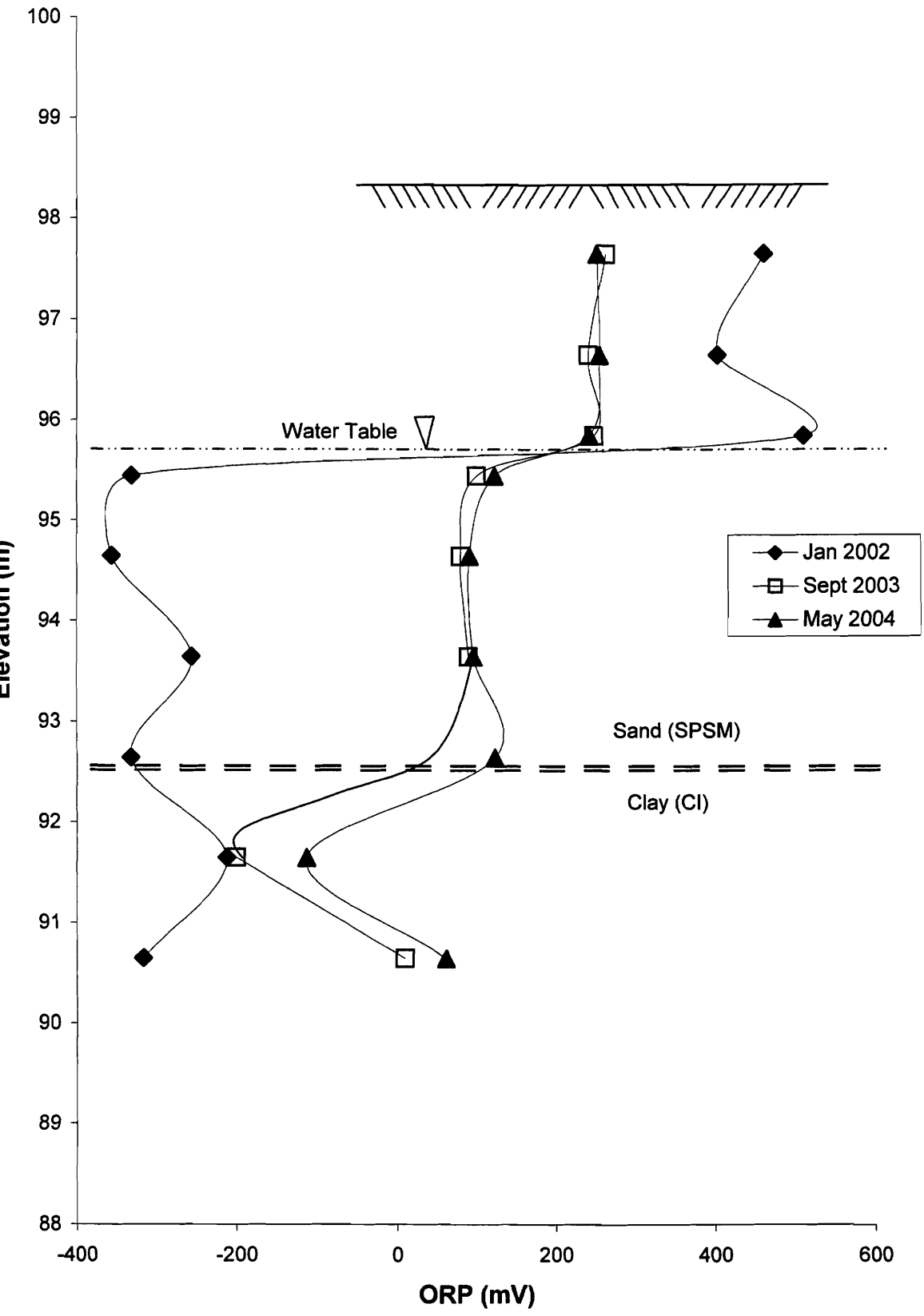

Figure 4.87 - Site No. 1 ORP (Eh) readings 22 meters south of the EMS

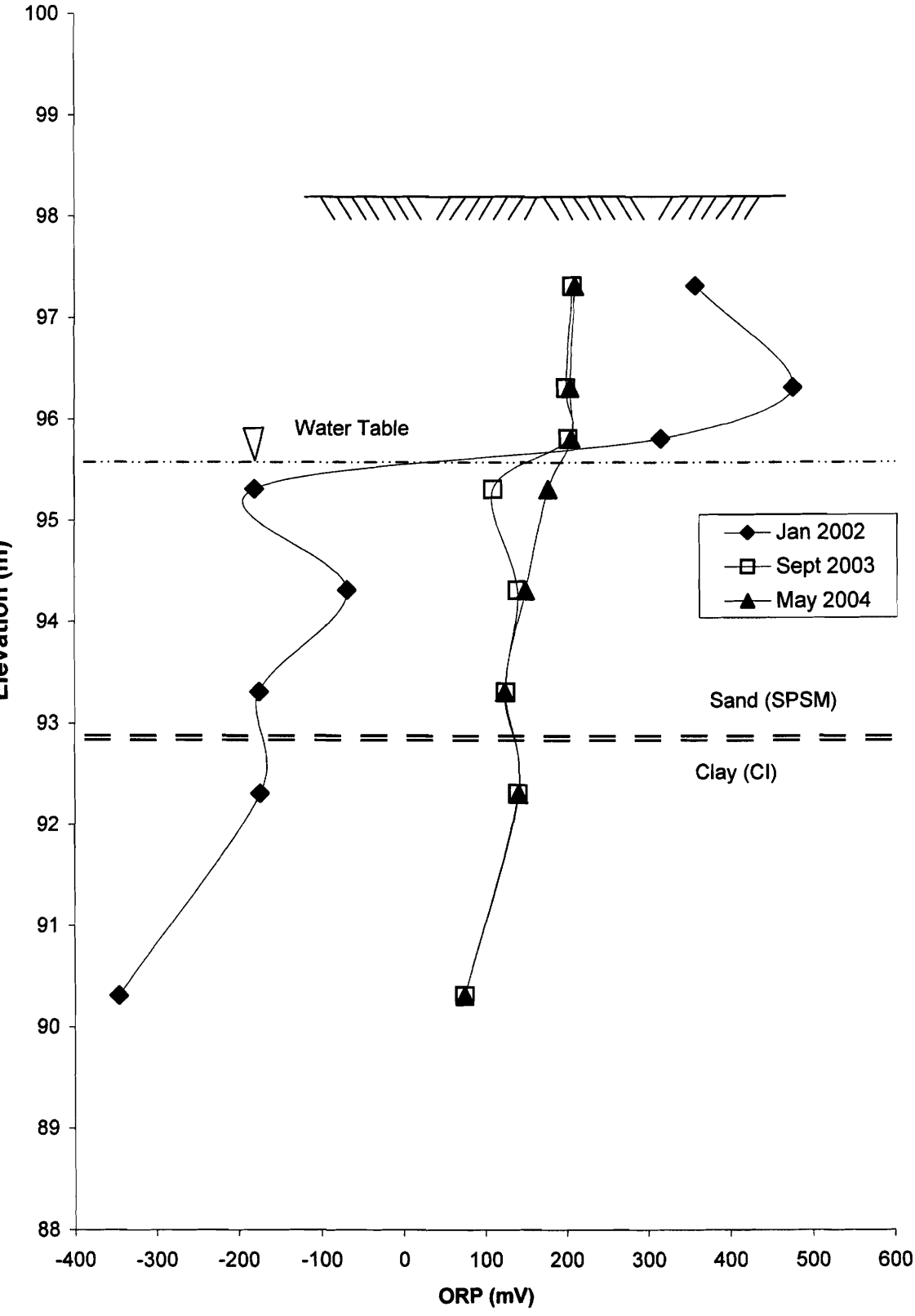

Figure 4.88 - Site No. 1 ORP (Eh) readings 33 meters south of the EMS

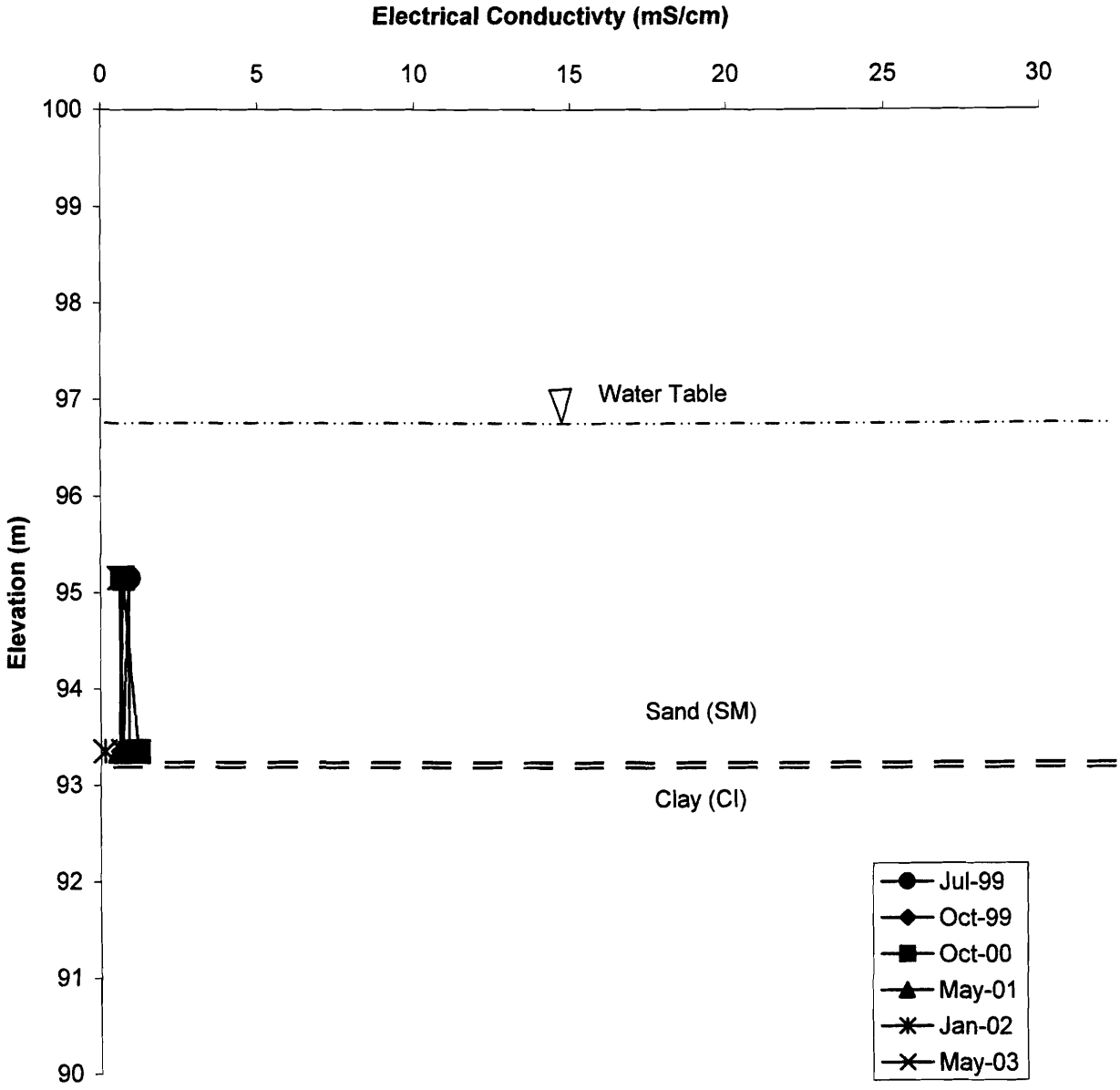

Figure 4.89 - Site No. 1 electrical conductivity of the groundwater at the piezometer nest 20 meters north of the EMS (C29 and C30)

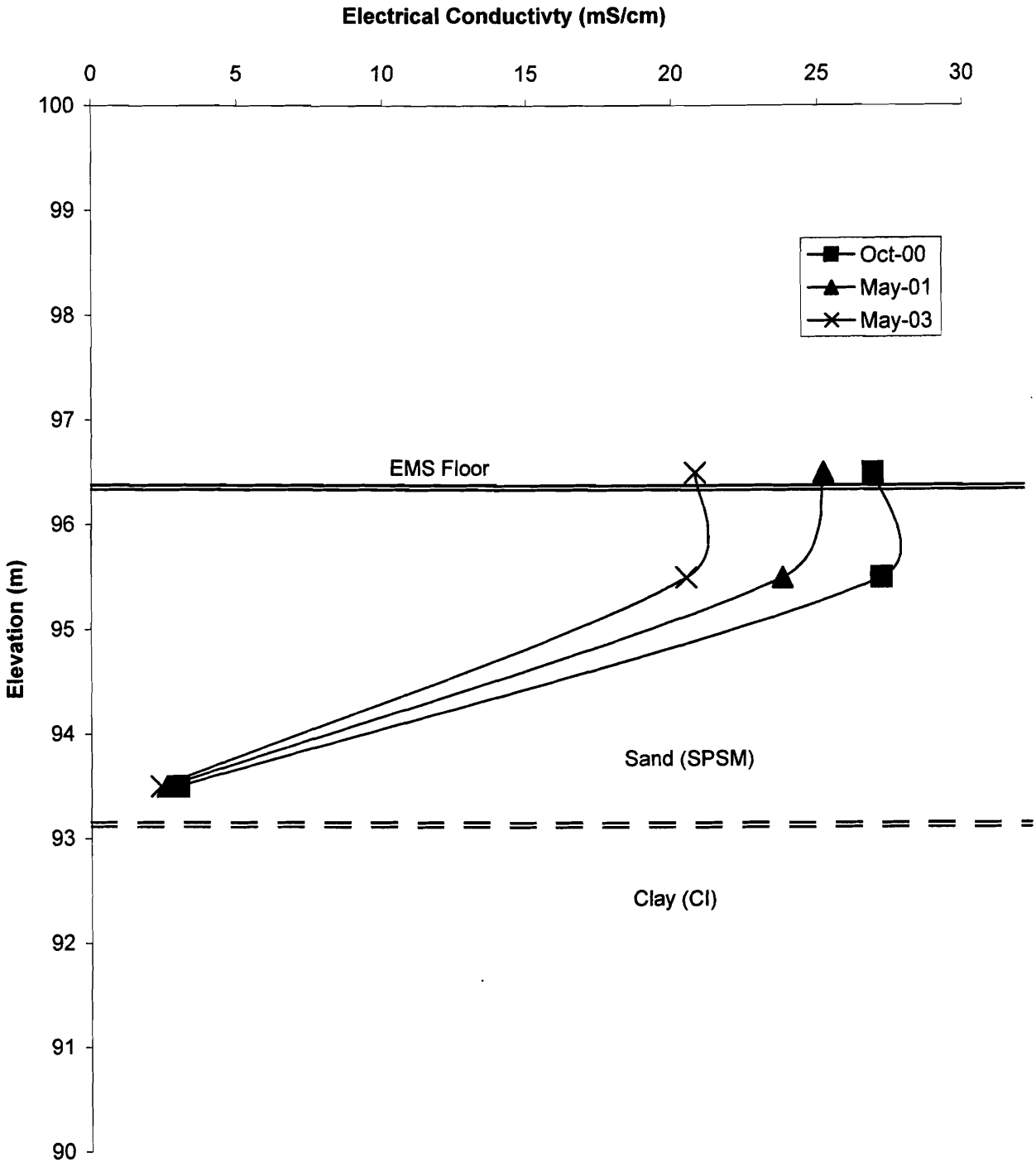

Figure 4.90: Site No. 1 electrical conductivity of the groundwater directly below the EMS

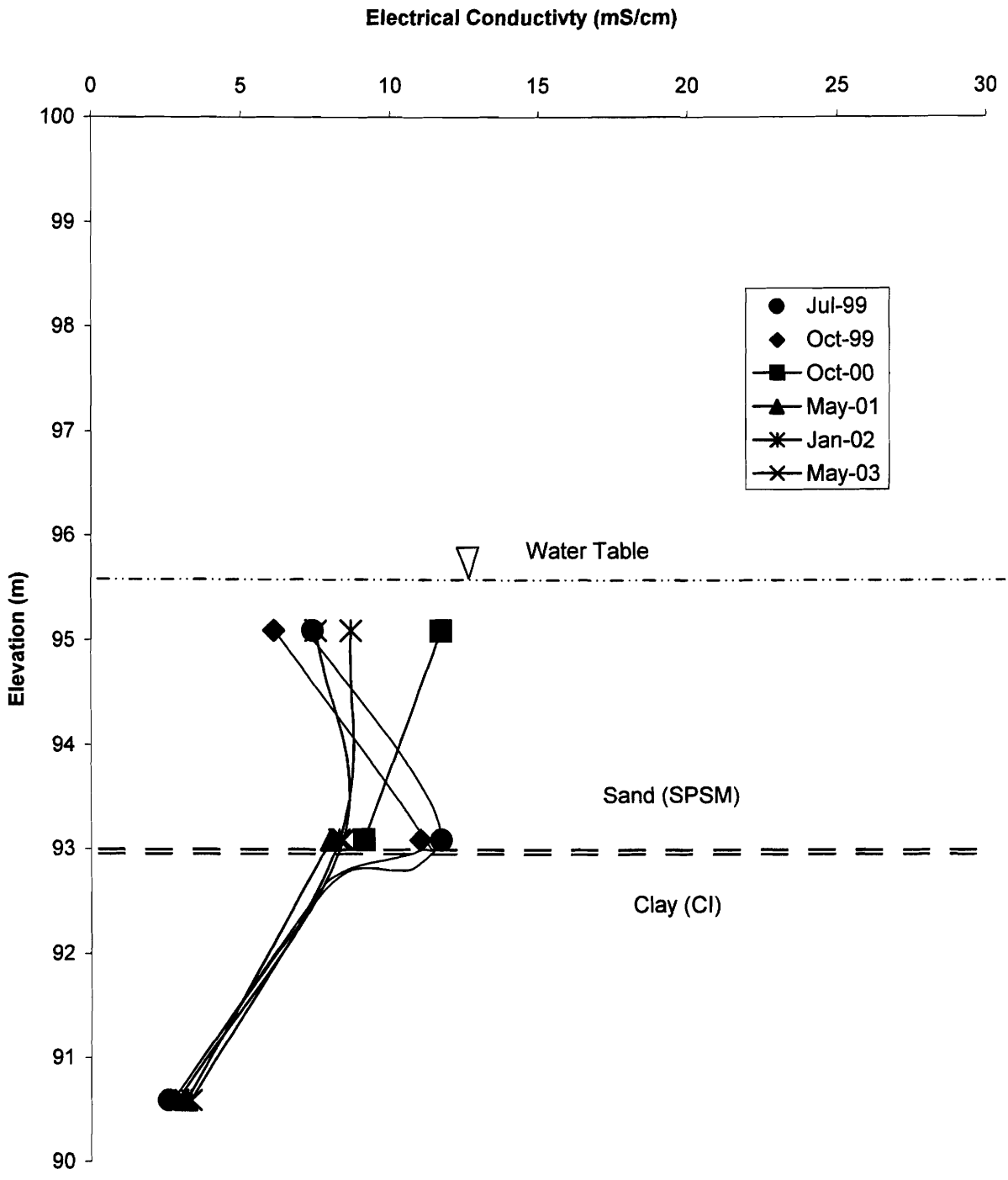

Figure 4.91: Site No. 1 electrical conductivity of the groundwater at the piezometer location 12 meters south of the EMS (C14 through C16)

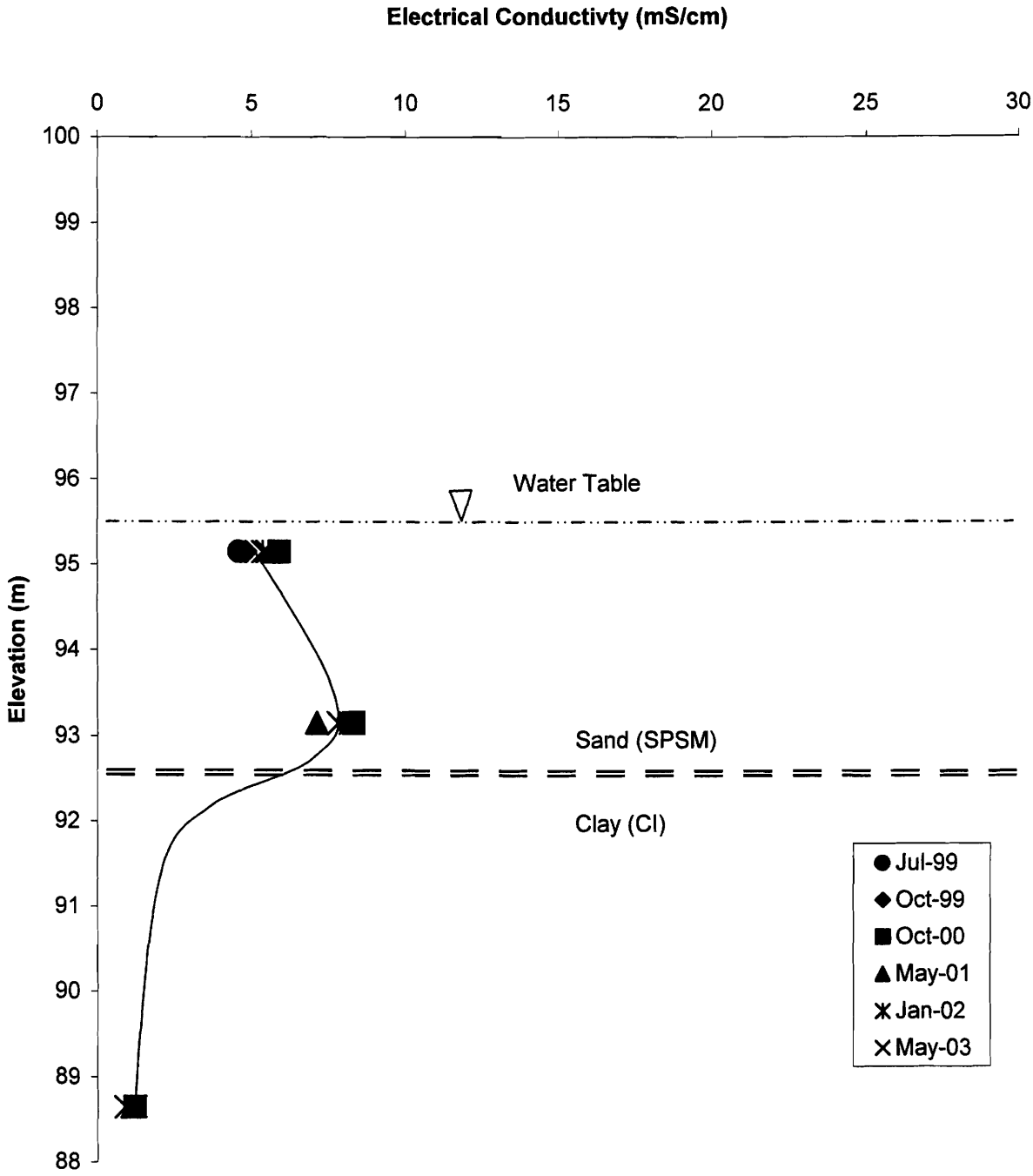

Figure 4.92: Site No. 1 electrical conductivity of the groundwater at the piezometer location 23 meters south of the EMS (C17 through C19)

the waters 2 m below the EMS floor are an order of magnitude less than the EC 1 m below the EMS floor, the 2 m EC levels are still three times those measured at C29. Figures 4.91 and 4.92 show elevated EC readings 5 to 12 times levels indicated in piezometer C29. Both these locations (12 and 23 m south of the EMS) indicate an area of high EC (or TDS) near the base of the upper sand (SPSM) layer; this would be consistent with groundwater encountering seepage from the EMS as it moves from north to south. The plume which develops will have a higher TDS than surrounding groundwater; this difference causes the mixed water to move downward as it transports south. This downward movement continues until the lower hydraulic conductivity clay layer is encountered. These results are similar to investigations of contaminant plumes at landfill sites (Nicholson et al., 1983; Bjerg et al. 1995).

More detailed water sampling was conducted at piezometers located in the most concentrated areas of the plume (as indicated by EC measurements). Locations chosen represent a transect through the center of the plume based on the groundwater gradient indicated by water table elevations. Complete laboratory results are given in Tables 4.18 (mg/L) and 4.19 (meq/L) for February 2000 sampling and in Tables 4.20 (mg/L) and 4.21 (meq/L) for May 2004 sampling. Ion concentrations indicate the plume is advancing and redox conditions within the plume may fluctuate enough to allow nitrification and denitrification to occur. Alkalinity and potassium concentrations along the transect remained relatively constant while chloride and sodium concentrations at C24 (43 m from the EMS) double within the four year period; organic carbon concentrations also increased from 14 to 570 mg/L. Other evidence of plume advancement and changing redox conditions at C24 are doubling in concentration of magnesium, reduction in sulphate and manganese concentrations, and the ten fold increase in barium and iron concentrations in solution. Although no significant nitrite or nitrate concentrations were found, ammonium nitrogen concentrations decreased by half by C15 (12 m from the EMS) and from 180 to <1 mg/L by C21 (33 m from the EMS) indicating nitrification and denitrification are likely occurring at these locations.

Table 4.18 - Water analysis results for piezometers located within the plume at Site No. 1 - Feb, 2000

Monitor well No.		C29	Source	C15	C18	C21	C24
Distance from Source (m)		-20	0	12	22	33	43
	units						
pH		7.4	8.27	7.17	7.96	6.9	6.66
Ca	mg/L	52	90	56	56	272	364
Mg	mg/L	25	2.7	273	711	140	123
Na	mg/L	29	529	362	258.5	202	46
K	mg/L	66	2400	496	81	5.4	8.9
N(-3)	mg/L	0.6	3722	1494	780	180	1.6
Alkalinity	mg/L	253	12200	4940	4600	1206	807
Cl	mg/L	29	1590	900	875	786	293
S(6)	mg/L	82	357	141	46	16	263
P	mg/L	0.37	350	2.9	2	0.06	0.48
S(-2)	mg/L		0.02	0.1	0.02	0.07	
Ba	mg/L	0.11	0.087	5.5	5.4	2.5	0.5
Fe	mg/L	0.55	0.016	13	21	94	0.069
Mn	mg/L	0.36	0.054	0.05	0.045	0.54	5.5
Si	mg/L	6	81.3	25.7	34	28	21
Sr	mg/L	0.48	0.34	2.7	6.9	2.8	2.1
Inorganic Carbon	mg/L	61	9230	1190	1100	145	194
Organic Carbon	mg/L	5.6	6300	1200	530	250	14

Table 4.19 - Water analysis results for piezometers located within the plume at Site No. 1 - Feb, 2000

Monitor well No.		C29	Source	C15	C18	C21	C24
Distance from Source (m)		-20	0	12	22	33	43
	units						
pH		7.4	8.27	7.17	7.96	6.9	6.66
Ca	meq/L	2.6	4.5	2.8	2.8	13.6	18.2
Mg	meq/L	2.1	0.2	22.5	58.5	11.5	10.1
Na	meq/L	1.3	23.0	15.7	11.2	8.8	2.0
K	meq/L	1.7	61.4	12.7	2.1	0.1	0.2
N(-3)	meq/L	0.0	206.3	82.8	43.2	10.0	0.1
Alkalinity	meq/L	5.1	244.0	98.8	92.0	24.1	16.1
Cl	meq/L	0.8	44.9	25.4	24.7	22.2	8.3
S(6)	meq/L	1.7	7.4	2.9	1.0	0.3	5.5
P	meq/L	0.01	11.30	0.09	0.06	0.002	0.02
S(-2)	meq/L		0.001	0.003	0.001	0.002	
Ba	meq/L	0.002	0.001	0.080	0.079	0.036	0.007
Fe	meq/L	0.020	0.001	0.466	0.752	3.366	0.002
Mn	meq/L	0.013	0.002	0.002	0.002	0.020	0.200
Si	meq/L	0.2	2.9	0.9	1.2	1.0	0.7
Sr	meq/L	0.005	0.004	0.031	0.079	0.032	0.024

Table 4.20 - Water analysis results for piezometers located within the plume at Site No. 1 - May 2004

Monitor well No.		C29	Source	"B"	C16	C15	C14	C19	C18	C17
Depth			96.5	95.8	95.8	93.8	91.3	95.9	93.9	89.4
Distance from Source (m)		-20	0	0	12	12	12	22	22	22
pH		7.94	8.27	7.03	6.66	6.68	6.97	6.97	7.32	7.06
Ca	mg/L	64	90	28	106	44	359	84	39	157
Mg	mg/L	28	2.7	39	126	439	216	148	442	52
Na	mg/L	26	529	476	223	349	83	252	338	51
K	mg/L	37	2400	1510	478	272	8	81	106	7.8
N(-3)	mg/L	0.28	3722	2300	600	620	0.67	420	710	0.56
Alkalinity	mg/L	245	12200	9000	3095	4180	1245	1650	4515	315
Cl	mg/L	28	1590	1100	499	830	578	670	785	28
S(6)	mg/L	74	357	160	120	110	7.9	71	34	340
N(5)	mg/L	0.01		2.3	110	0.74	0.01	1.5	0.79	0.03
P	mg/L	0.11	350	14.5	0.61	3.8	0.18	0.61	2.1	0.05
S(-2)	mg/L		0.02	5.6	0.01	0.11		0.02	0.04	
Ba	mg/L	0.16	0.087	0.35	0.52	1.67	4.17	1.71	4	0.29
Fe	mg/L	0.79	0.016	5.27	2.02	5.02	34.7	16.5	9.13	2.2
Mn	mg/L	0.38	0.054	0.092	0.15	0.1	0.26	0.52	0.039	0.72
Si	mg/L	3.5	81.3	9.6	5.6	12.9	7	13.4	11.8	9.4
Sr	mg/L	0.55	0.34	1.31	3.47	2.88	4.19	1.26	4.36	0.9
Inorganic Carbon	mg/L		9230							
Organic Carbon	mg/L	4.7	6300	750	58	380	270	84	410	8

Monitor well No.		C20	C21	C22	C24	C23	C8	C27	C28	C9	C10
Depth		95.9	93.9	89.6	95.1	92.4	93.8	94.8	91.3	89	93.7
Distance from Source (m)		33	33	33	44	44	51	60	60	68	86
pH		6.78	6.89	7.16	6.89	6.54	7.36	6.7	6.76	7.13	6.62
Ca	mg/L	276	274	140	362	116	228	126	253	121	120
Mg	mg/L	133	144	52	254	43	86	75	83	42	39
Na	mg/L	302	265	53	85	31	39	33	33	26	23
K	mg/L	7.7	6.1	7.6	5.5	5.5	6.5	3.8	5.2	5.1	4.8
N(-3)	mg/L	0.6	0.49	0.4	0.27	0.13	0.08	0.14	0.12	0.79	0.23
Alkalinity	mg/L	1055	1005	335	1055	330	405	365	315	330	330
Cl	mg/L	755	750	16	645	97	212	75	255	61	55
S(6)	mg/L	16	16	330	10	170	330	100	310	180	170
N(5)	mg/L	0.14	0.06			0.85	0.01	0.15		0.07	0.01
P	mg/L	0.29	0.37	0.04	0.17		0.05	0.02	0.05	0.1	
S(-2)	mg/L				0.02				0.01		
Ba	mg/L	2.38	3.44	0.3	6.31		0.34	0.35	0.28	0.56	
Fe	mg/L	81.9	67.4	2.3	86.2		0.01	4.78	3.5	4.36	
Mn	mg/L	1.67	0.23	0.8	0.62		0.63	1.6	0.59	0.71	
Si	mg/L	14.9	13.6	9.4	8.8		5	10.2	7.5	8.4	
Sr	mg/L	2.78	3.13	0.89	4.05		1.41	0.73	1.45	0.78	
Inorganic Carbon	mg/L										
Organic Carbon	mg/L	100	300	7	570		10	6.4	9.8	7.9	

Table 4.21 - Water analysis results for piezometers located within the plume at Site No. 1 - May 2004

Monitor well No.		C29	Source	"B"	C16	C15	C14	C19	C18	C17
Ground Elevation		98.6	96.8	96.8	100.34	100.34	100.34	99.4	99.4	99.4
Depth		94.3	96.5	95.8	95.8	93.8	91.3	95.9	93.9	89.4
Distance from Source (m)		-20	0	0	12	12	12	22	22	22
pH		7.4	8.27			7.17			7.96	
Ca	meq/L	3.2	4.5	1.4	5.3	2.2	17.9	4.2	1.9	7.8
Mg	meq/L	2.3	0.2	3.2	10.4	36.1	17.8	12.2	36.4	4.3
Na	meq/L	1.1	23.0	20.7	9.7	15.2	3.6	11.0	14.7	2.2
K	meq/L	0.9	61.4	38.6	12.2	7.0	0.2	2.1	2.7	0.2
N(-3)	meq/L	0.02	265.7	164.2	42.8	44.3	0.05	30.0	50.7	0.04
Alkalinity	meq/L	4.9	244.0	180.0	61.9	83.6	24.9	33.0	90.3	6.3
Cl	meq/L	0.8	44.9	31.0	14.1	23.4	16.3	18.9	22.1	0.8
S(6)	meq/L	1.5	7.4	3.3	2.5	2.3	0.2	1.5	0.7	7.1
N(5)	meq/L	0.00		0.16	7.85	0.05	0.00	0.11	0.06	0.00
P	meq/L	0.00	11.30	0.47	0.02	0.12	0.01	0.02	0.07	0.00
S(-2)	meq/L		0.001	0.169	0.000	0.003		0.001	0.001	
Ba	meq/L	0.002	0.001	0.005	0.008	0.024	0.061	0.025	0.058	0.004
Fe	meq/L	0.028	0.001	0.189	0.072	0.180	1.243	0.591	0.327	0.079
Mn	meq/L	0.014	0.002	0.003	0.005	0.004	0.009	0.019	0.001	0.026
Si	meq/L	0.1	2.9	0.3	0.2	0.5	0.2	0.5	0.4	0.3
Sr	meq/L	0.006	0.004	0.015	0.040	0.033	0.048	0.014	0.050	0.010

Monitor well No.		C20	C21	C22	C24	C23	C8	C28	C27	C9	C10
Ground Elevation		99.06	99.06	99.06	98.63	98.63	98.31	98.06	98.06	98	98.23
Depth		95.9	93.9	89.6	95.1	92.4	93.8	94.8	91.3	89	93.7
Distance from Source (m)		33	33	33	44	44	51	60	60	68	86
pH			6.9		6.66						
Ca	meq/L	13.8	13.7	7.0	18.1	5.8	11.4	6.3	12.6	6.0	6.0
Mg	meq/L	10.9	11.8	4.3	20.9	3.5	7.1	6.2	6.8	3.5	3.2
Na	meq/L	13.1	11.5	2.3	3.7	1.3	1.7	1.4	1.4	1.1	1.0
K	meq/L	0.2	0.2	0.2	0.1	0.1	0.2	0.1	0.1	0.1	0.1
N(-3)	meq/L	0.04	0.03	0.03	0.02	0.01	0.01	0.01	0.01	0.06	0.02
Alkalinity	meq/L	21.1	20.1	6.7	21.1	6.6	8.1	7.3	6.3	6.6	6.6
Cl	meq/L	21.3	21.2	0.5	18.2	2.7	6.0	2.1	7.2	1.7	1.6
S(6)	meq/L	0.3	0.3	6.9	0.2	3.5	6.9	2.1	6.5	3.8	3.5
N(5)	meq/L	0.01	0.00			0.06	0.00	0.01		0.005	
P	meq/L	0.01	0.01	0.00	0.01		0.00	0.00	0.00	0.00	
S(-2)	meq/L				0.001				0.000		
Ba	meq/L	0.035	0.050	0.004	0.092		0.005	0.005	0.004	0.008	
Fe	meq/L	2.933	2.414	0.082	3.087		0.000	0.171	0.125	0.156	
Mn	meq/L	0.061	0.008	0.029	0.023		0.023	0.058	0.021	0.026	
Si	meq/L	0.5	0.5	0.3	0.3		0.2	0.4	0.3	0.3	
Sr	meq/L	0.032	0.036	0.010	0.046		0.016	0.008	0.017	0.009	

A chloride, bicarbonate (Figure 4.93) and sodium (Figure 4.94) front is evident at ~43 m from the EMS, while ammonium and potassium are attenuated to a distance of <33 m (Figure 4.93). Magnesium concentrations peak at ~20 m and again at 43 m from the EMS; concentrations at these locations are 150 and 100 times EMS effluent concentrations and 15 and 10 times background groundwater concentrations, respectively. These magnesium concentrations are likely the result of ion exchange absorbing potassium and ammonium and releasing magnesium. Calcium concentrations peak at ~43 m from the EMS, at 4 times the EMS effluent concentration and 6 times the background groundwater concentration. These calcium concentrations are likely a result of ion exchange where calcium is released and magnesium absorbed, due to the high magnesium levels discussed earlier.

Figures 4.95 to 4.100 show geologic sections of the site with concentration profiles for chloride and alkalinity (Figure 4.95), potassium and ammonium (Figure 4.96), sodium and sulphate (Figure 4.97) magnesium and calcium (Figure 4.98), pH and nitrate Figrue 4.99) and organic carbon and electrical conductivity (Figure 4.100). These profiles indicate a plume extending ~60 m south of the EMS and potentially extending vertically down to ~6 m below the EMS. The vertical transport is indicated by elevated concentrations of chloride, alkalinity, organic carbon, magnesium and calcium in the partially confined sand layer at approximately 6–7 m below grade. Potassium and ammonium appear confined to the upper unconfined sand layer and are attenuated compare to the chloride plume. Potassium experiences a relative constant attenuation; ammonium attenuation appears limited to near the leading edge of the ammonium plume, possibly the result of high magnesium and calcium concentrations at this location limiting absorption of ammonium to soil exchange sites. A magnesium front is evident at ~20 m from the EMS. Magnesium and calcium produce a hard water front ~30 to 50 m from the EMS, and on the north side of the partially confined sand layer at 6 to 7 m below grade (Figure 4.96).

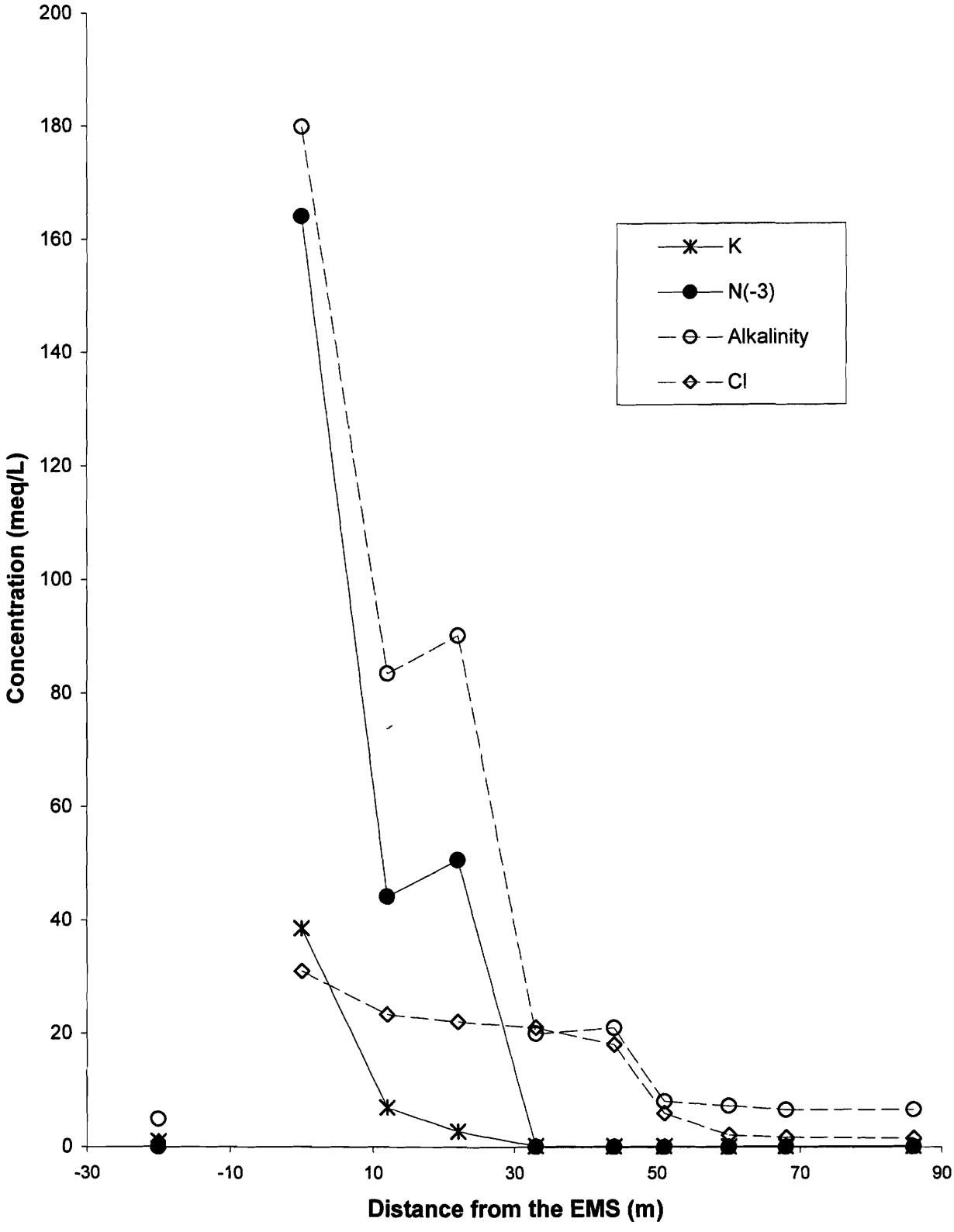

Figure 4.93: Concentrations of selected ions (May 2004) at various distances from the EMS through an assumed transect of the seepage plume.

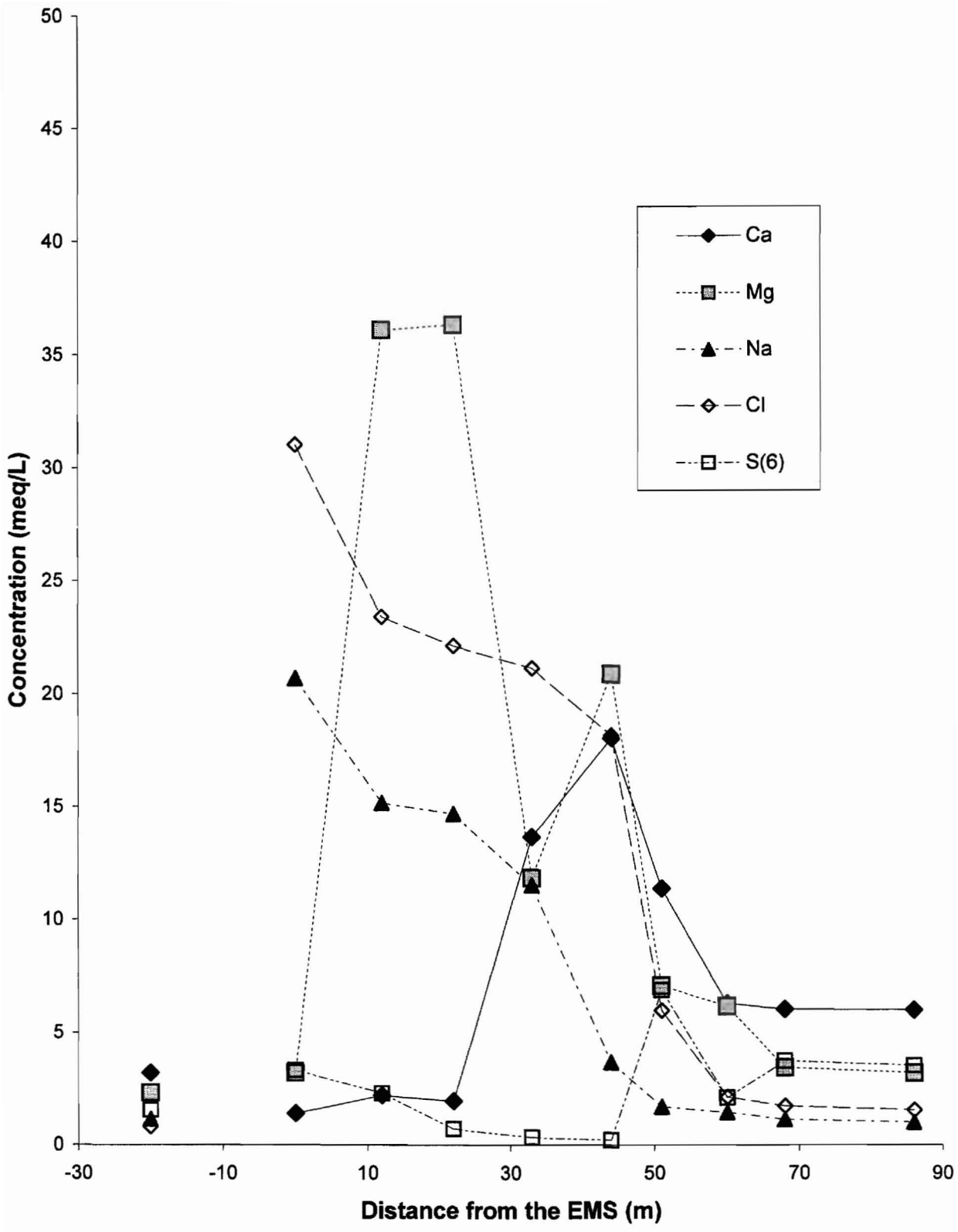

Figure 4.94: Concentrations of selected ions (May 2004) at various distance from the EMS through an assumed transect of the seepage plume.

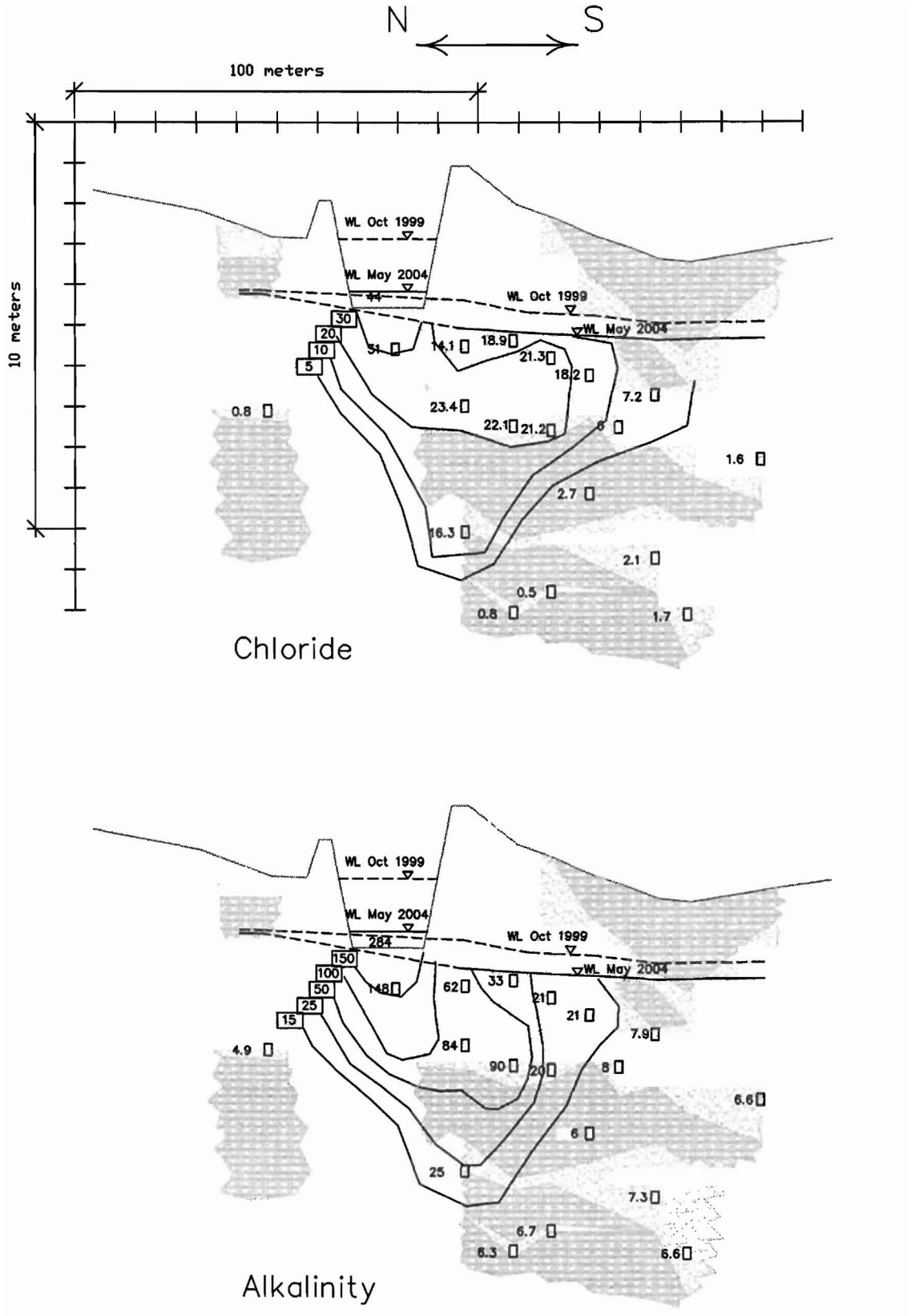

Figure 4.95: Site No. 1 chloride and alkalinity concentrations in the plume May 2004 (units are meq/L)

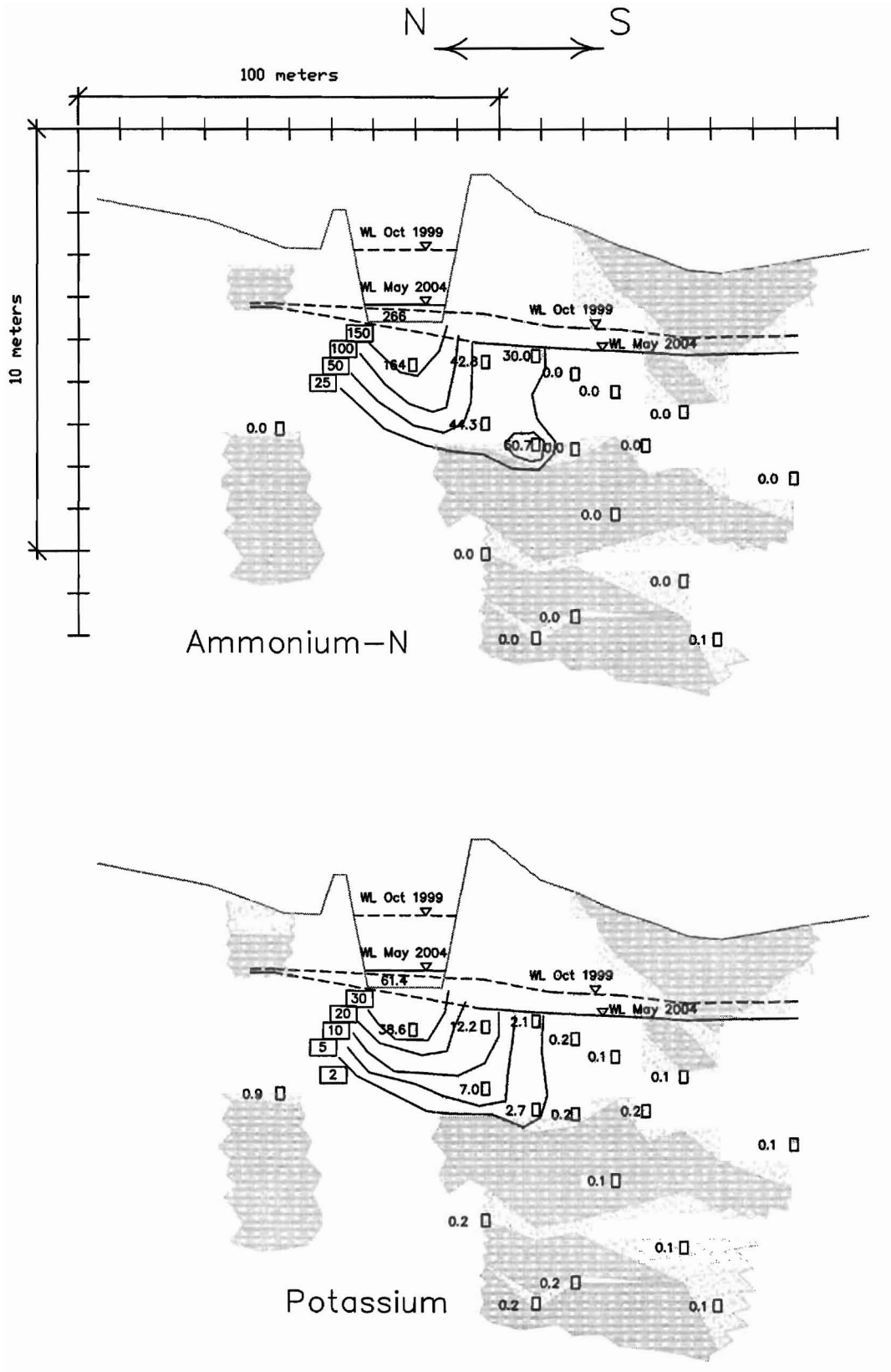

Figure 4.96: Site No. 1 ammonium and potassium concentrations in the plume May 2004 (units are meq/L)

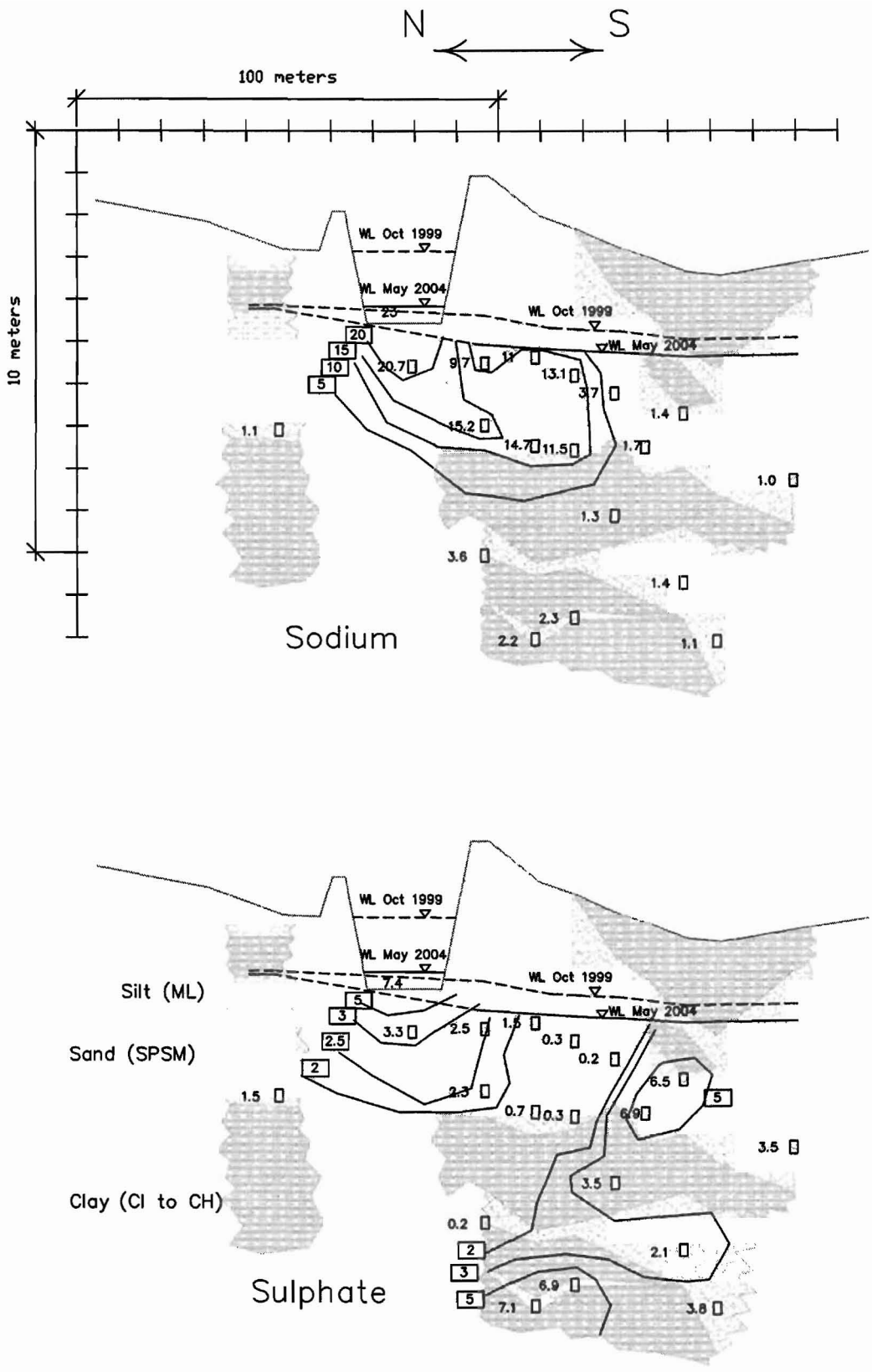

Figure 4.97: Site No. 1 sodium and sulphate concentrations in the plume May 2004 (units are meq/L)

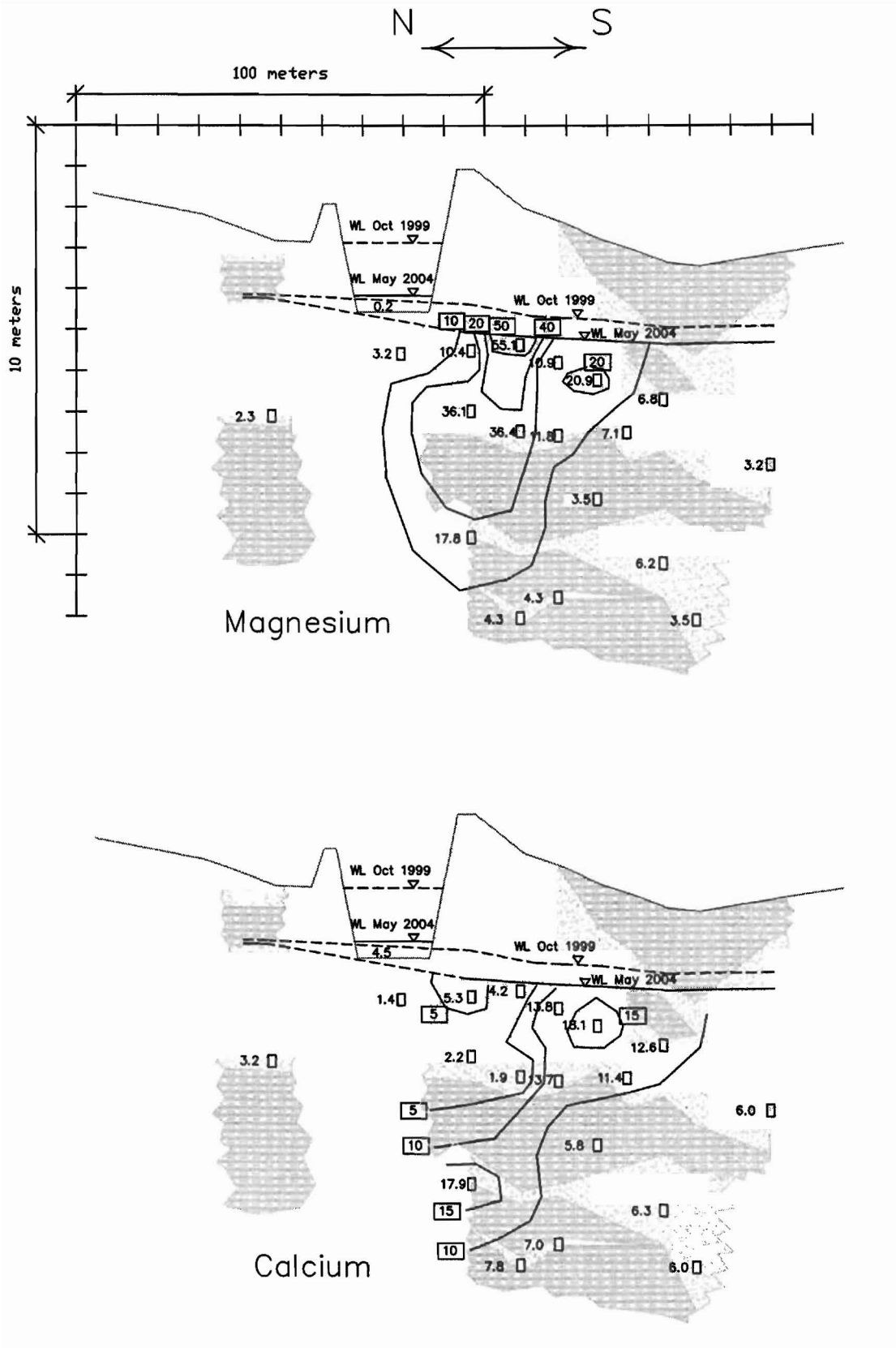

Figure 4.98: Site No. 1 magnesium and calcium concentrations in the plume May 2004 (units are meq/L)

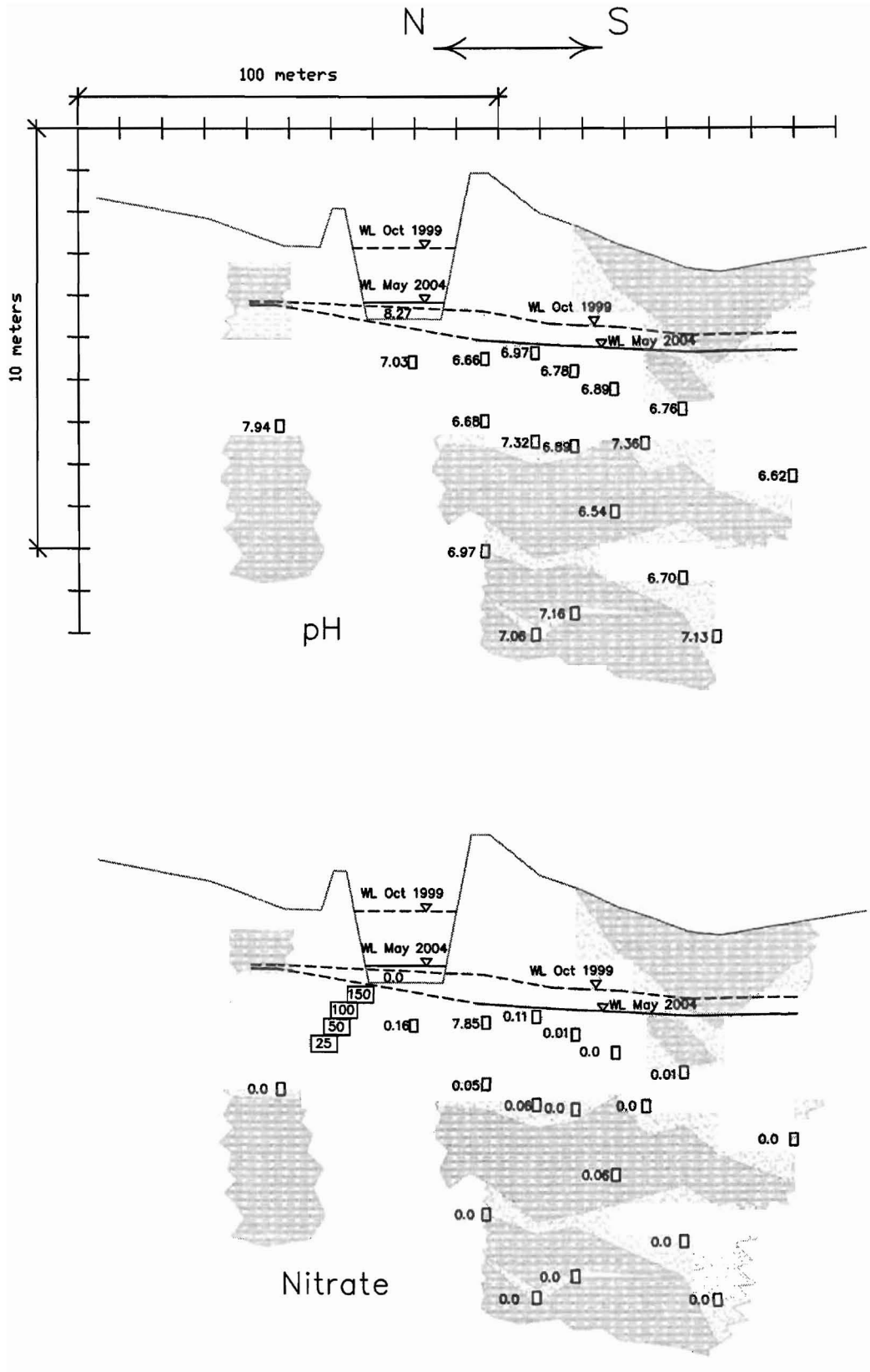

Figure 4.99: Site No. 1 pH and nitrate (units are meq/L) concentrations in the plume May 2004

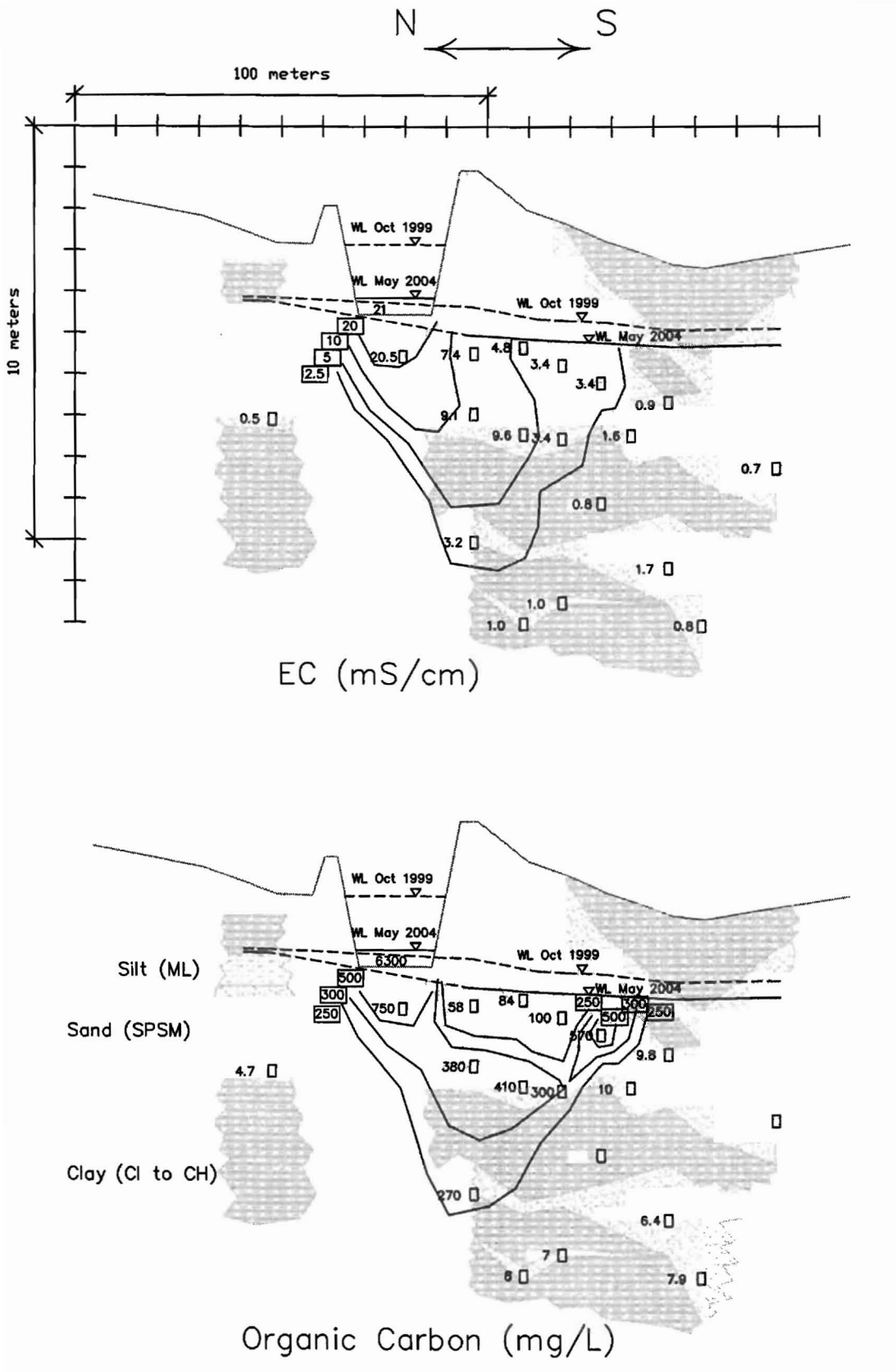

Figure 4.100: Site No. 1 EC and organic carbon concentrations in the plume May 2004

4.3.7 Microbial Sampling Results

Microbial sampling was conducted to confirm chemical and ORP probe data which suggest aerobic conditions at the groundwater surface and anaerobic conditions below 1 m below the groundwater surface. Microbial counts indicate the presence of significant numbers of anaerobic bacteria, including methanogenic bacteria, within 1 m of the EMS floor (Figure 4.101). These populations reduced to near zero in the lower portion of the sand layer, indicating aerobic conditions or a lack of a microbial food source. Since ORP readings indicate anaerobic conditions, we assume low population numbers are due to fresh water movement from north to south forcing the microbial food source (seepage) away from this location. Fecal and total coliforms were only detected at the base of the storage and 1 m below the storage (Figure 4.101).

Bacterial counts at the piezometer nest located ~12 m south of the EMS (C13 to C16; Figure 4.102) indicate reducing conditions with depth. Higher numbers of sulphate reducers were detected in the mid zone of the upper sands and low numbers at the base of the sands where methanogen counts (and corresponding anaerobic counts) were higher. Water sampling data also indicated reducing conditions with depth, due to high nitrate concentrations near the water table which reduced with depth, and increasing ammonium concentrations with depth.

Water sampling at the piezometer nest 23 m south of the EMS (C7 and C20 to C22) indicated presence of an effluent plume but no significant nitrogen concentrations (Figures 4.96 and 4.99). Microbial analysis (Figure 4.103) also indicates a contaminant plume still exists as anaerobic and methanogenic bacterial counts ranged from 100 and 170 CFU/mL respectively near the water table to ~500 CFU/mL for both near the base of the upper sands. These counts confirm anaerobic conditions below the water table and the presence of a nutrient source.

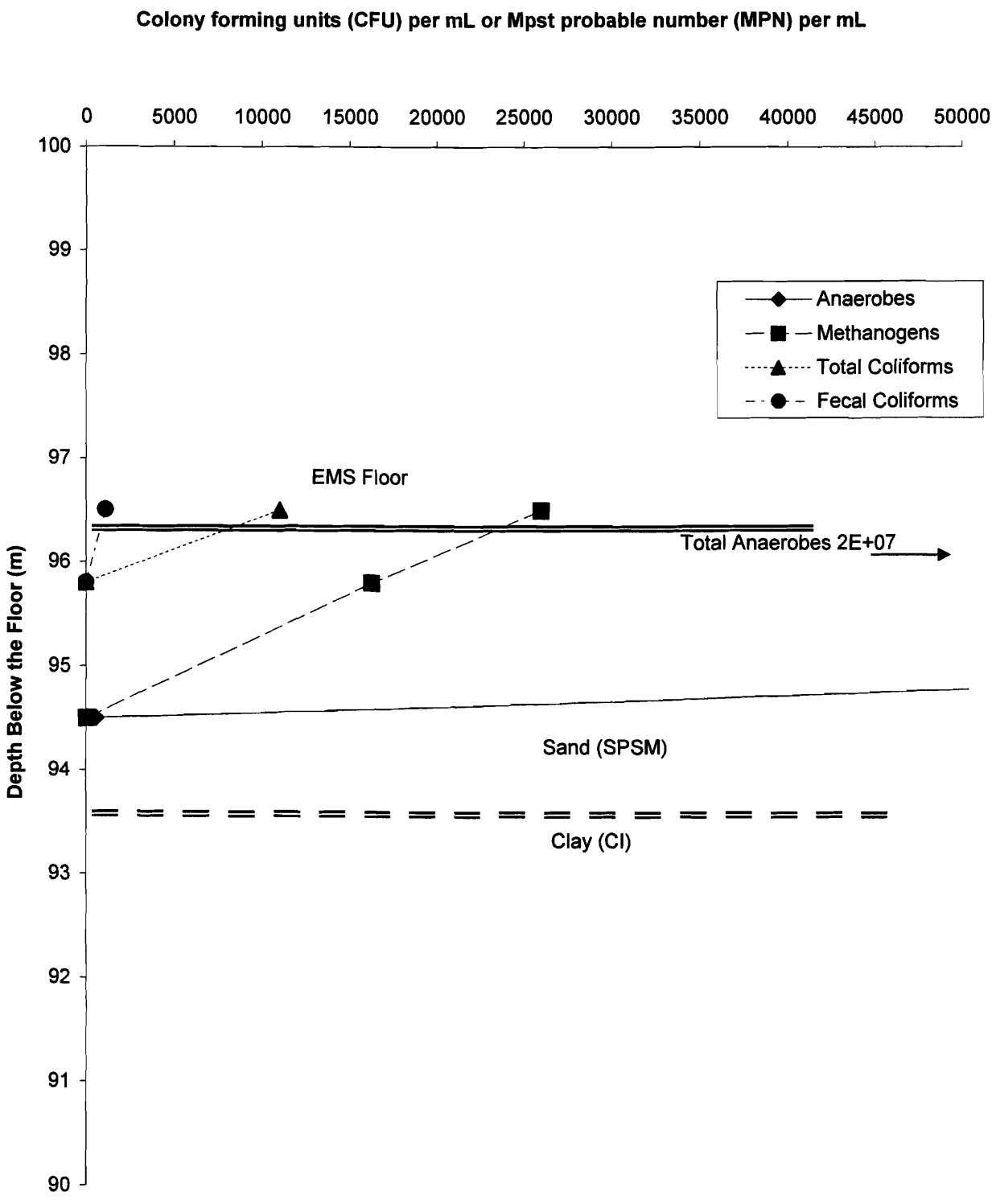

Figure 4.101: Site No.1 microbial sampling results for spring 2001.
Locations directly below the EMS.

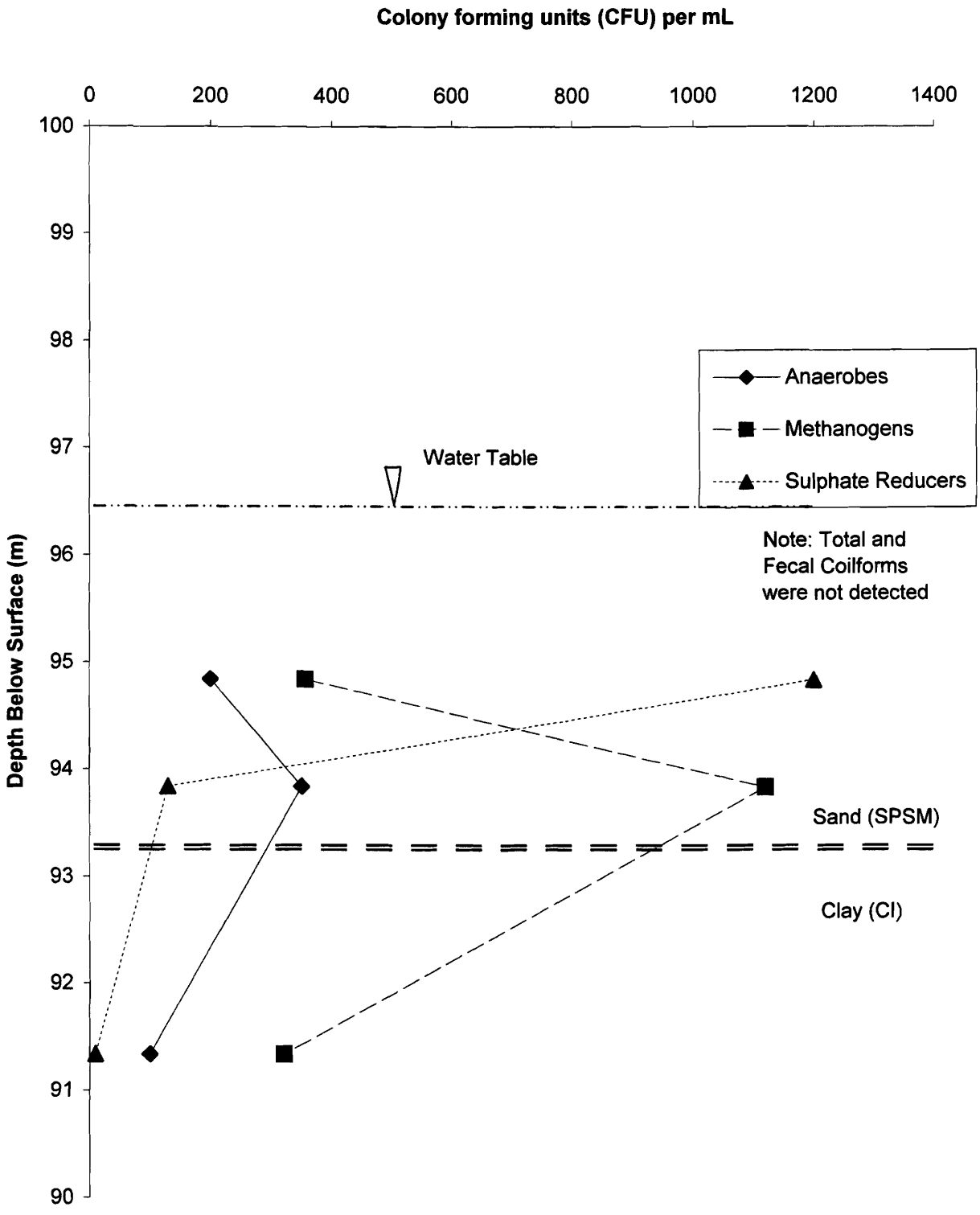

Figure 4.102: Site No.1 microbial sampling results for spring 2001. Piezometers C13 through C16 (12 meters south of the EMS).

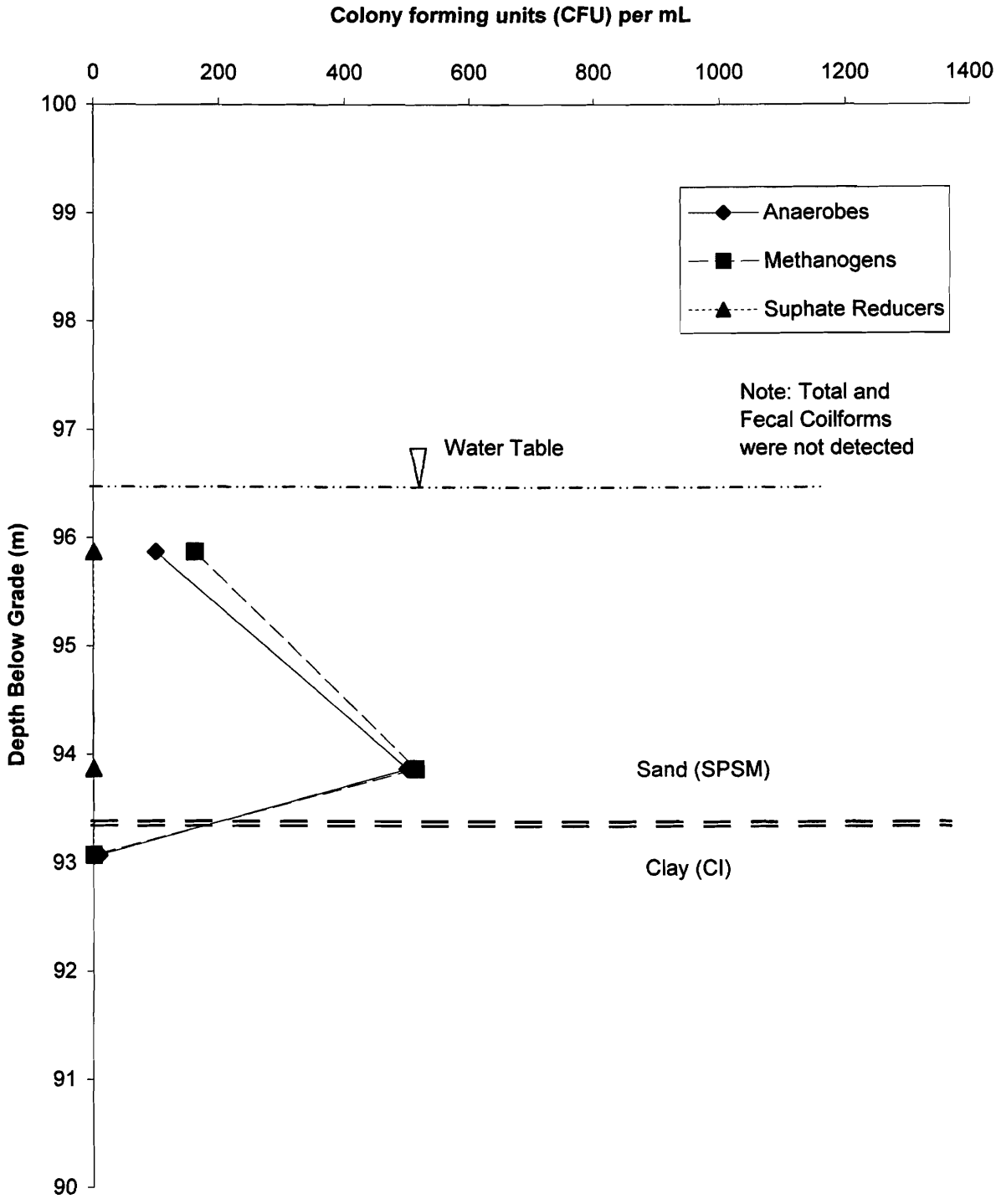

Figure 4.103: Site No.1 microbial sampling results for spring 2001. Piezometers C20 through C22 (33 meters south of the EMS).

4.3.8 Analysis of Field Data for ADF Research Site No 1

Results of test drilling, soil extractions, routine water samples and microbial sampling indicate the plume extends south from the EMS within the unconfined aquifer above a confining clay layer ~6 m below grade, and vertically down directly adjacent to the EMS. ORP readings and microbial populations indicate reducing conditions occur within the plume, although nitrification does occur in the upper regions of the plume near the water table and potentially at the leading edge of the plume.

If the EMS is considered a line source perpendicular to the groundwater flow direction, it may then be possible to analyze a transect near the center of the plume using the solution for the advection-dispersion equation for second-type boundary conditions as describe by Fetter (1993). The cross-section chosen for this analysis includes water analysis results from February 2000 from piezometers C29 (background, 20 m north), the EMS solution (source), C15 (12 m south), C18 (23 m south), C21 (33 m south) and C24 (43 m south) at a depth of ~6 m below grade and 2–3 m below the water table. This zone marks the top of the fine-grained soil which provides a lower confining layer. Concentrations in this area were the highest at each piezometer nest location.

Concentrations along this transect are plotted as a function of distance away from the EMS in Figure 4.104. The chloride concentration profile is assumed to be formed by a non attenuated ion and will be used for comparison. Sodium follows this same profile indicating it also is likely moving unattenuated, as indicated by the column study. Magnesium and calcium show marked increases at 12 m and 33 m from the storage, respectively, demonstrating ion exchange coinciding with decreases in both alkalinity and pH, and potentially indicating carbonate mineral precipitation. Figure 4.105 shows the same data plotted without ammonium and alkalinity in order to provide a clearer indication of trends for the remaining ions. Sulphate (S(-6)) decreases at 22 m and 33 m locations away from the EMS potentially indicating gypsum precipitation. Ammonium and potassium both appear to be attenuated, with potassium to a greater extent.

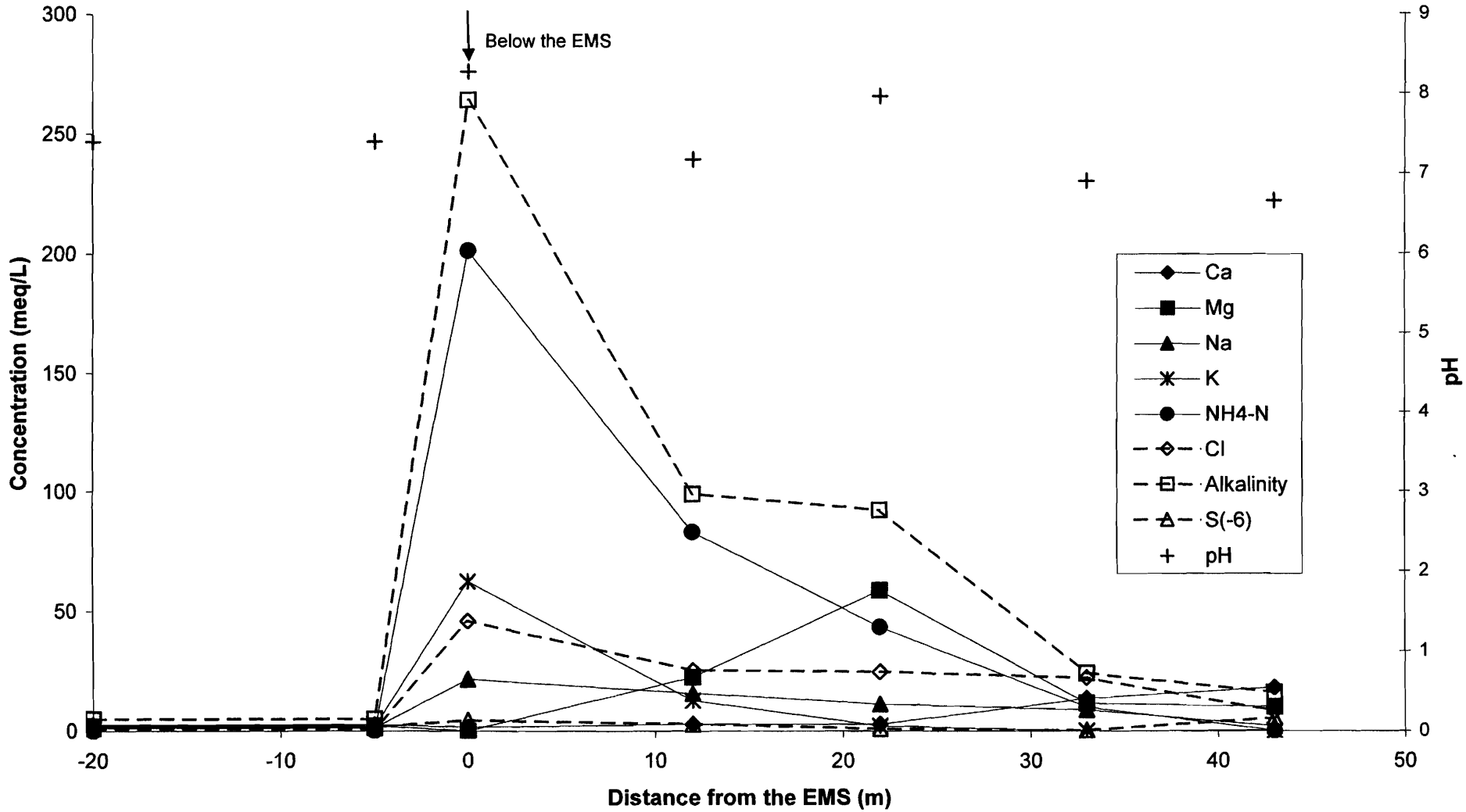

Figure 4.104: Groundwater chemistry of a transect through the plume at Site No. 1

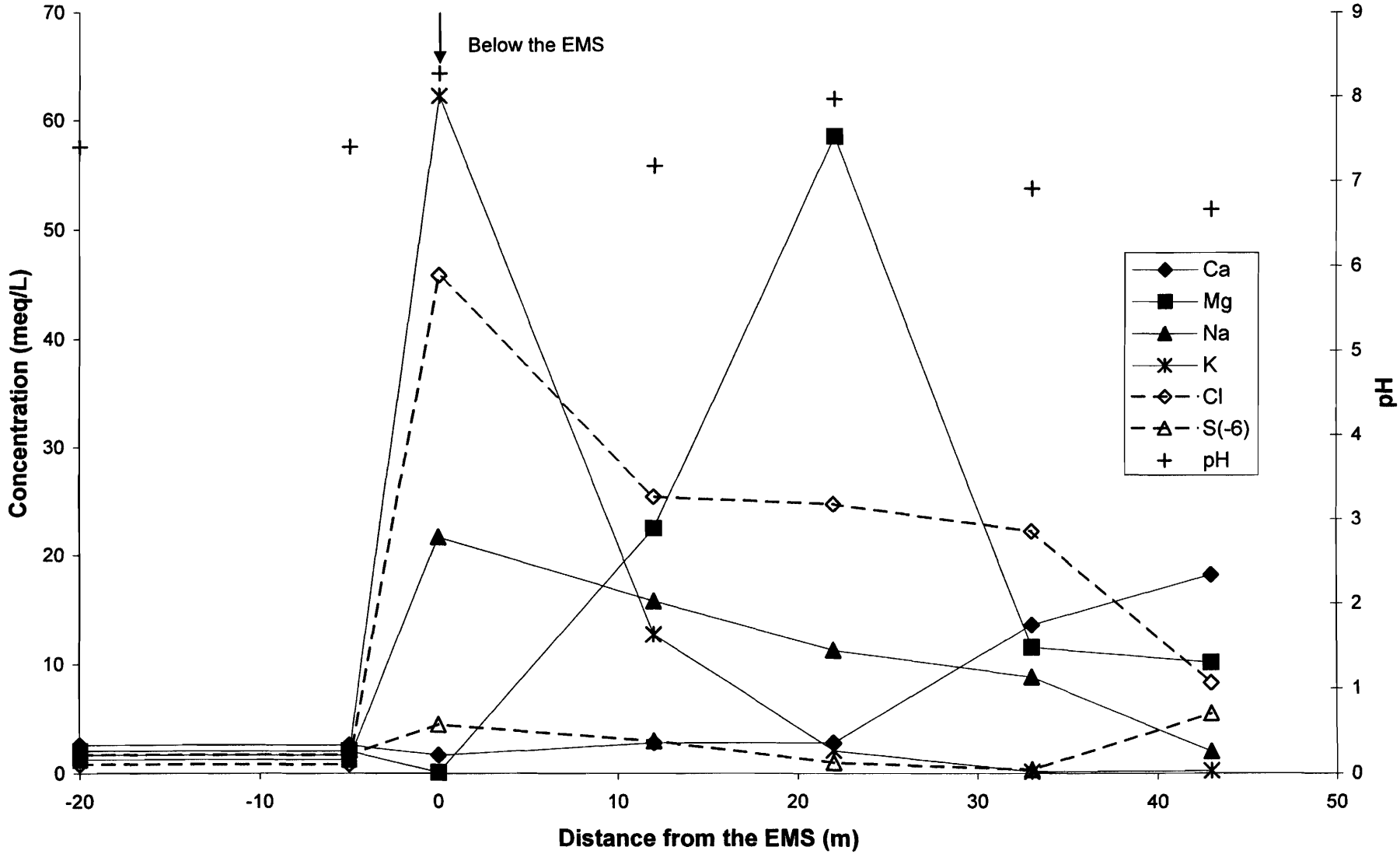

Figure 4.105: Groundwater chemistry of a transect through the plume at Site No.1 (without alkalinity and ammonium)

NETPATH (Plummer et al. 1994) can be used to model mixing of waters with known concentrations. We know background water concentrations, leachate concentrations and resulting concentrations at the first monitoring piezometer location. The model requires some educated guessing of potential mineral phases and exchange reactions to be defined in an input file along with the relevant concentration for each sample (background, leachate, and piezometer). A typical input file for the mineral phases would be:

Mineral Phases	Exchange Reactions
Calcite CaCO3	CH2O CH2O
Chalcedony SiO2	NaX NaX
Dolomite CaMg(CO3)2	NH4X NH4X
FeS(ppt) FeS	MgX2 MgX2
Goethite FeOOH	CaX2 CaX2
(Note: Gypsum could also have been added)	KX KX

The exchange reaction "CH2O" was entered to represent organic matter since dissolved organic carbon showed similar transport to chloride and was present in relatively high concentrations. In addition, these soils typically contain some organic matter. The organic matter was entered primarily as an electron donor.

Execution of the model results in several potential solutions which satisfy background water mixing with EMS seepage to result in the sample found at C15. However, only a few models were plausible and some evaluation was required. The model generated two plausible solutions (Table 4.22).

Table 4.22: Results of NETPATH (Plummer et al. 1994) modeling of mixing of raw effluent and background water.

	Model No. 1	Model No. 2	
Solution fractions:			
Solution 2	0.56	0.56	(moles of effluent)
Solution 6	0.44	0.44	(moles of background water)
Solution 3	1.00	1.00	(moles of resulting water matching that found in C15)
Phase mole transfer:			
Calcite	-0.51E-02	-4.12E-02	CaCO3
Chalcedony	0.01E-02	0.01E-02	SiO2
Dolomite	0.55E-02	2.35E-02	CaMg(CO3)2
FeS(ppt)	-0.07E-02	-0.07E-02	FeS
Goethite	0.10E-02	0.10E-02	FeOOH
CH2O	0.17E-02	0.17E-02	CH2O
NaX	1.30E-02	1.32E-02	NaX
NH4X	-4.40E-02	-4.35E-02	NH4X
CaX2		1.81E-02	CaX2
MgX2	1.80E-02		MgX2
KX	-0.57E-02	-0.58E-02	KX

Positive values indicate release into solution while negative values indicate a loss from solution. Both models indicate a mixing ratio of 56% effluent with 44% background water, precipitation of calcite and FeS, dissolution of the remaining minerals, release of sodium and divalent cations to solution and loss of potassium and ammonium to the exchange complex. These results are compatible with trends in the field data.

A standard method of analysis is to plot the data as a function of the concentration in the effluent entering the system. The mixing ratios supplied by the NETPATH results provide a method of determining mixed concentration of the water below the EMS. Using these concentrations as the source concentration (Co) results in the relative concentrations profiles shown in Figures 4.106, 4.107 and 4.108. Background data has been plotted at an arbitrary distance of 60 m from the storage for comparison purposes. The distance of 60 meters from the EMS is justified as concentrations of ions past this point are relatively constant (May 2004 sampling results; Table 4.20). Figure 4.106 indicates magnesium and calcium reach maximum concentrations of 57 and 5 times

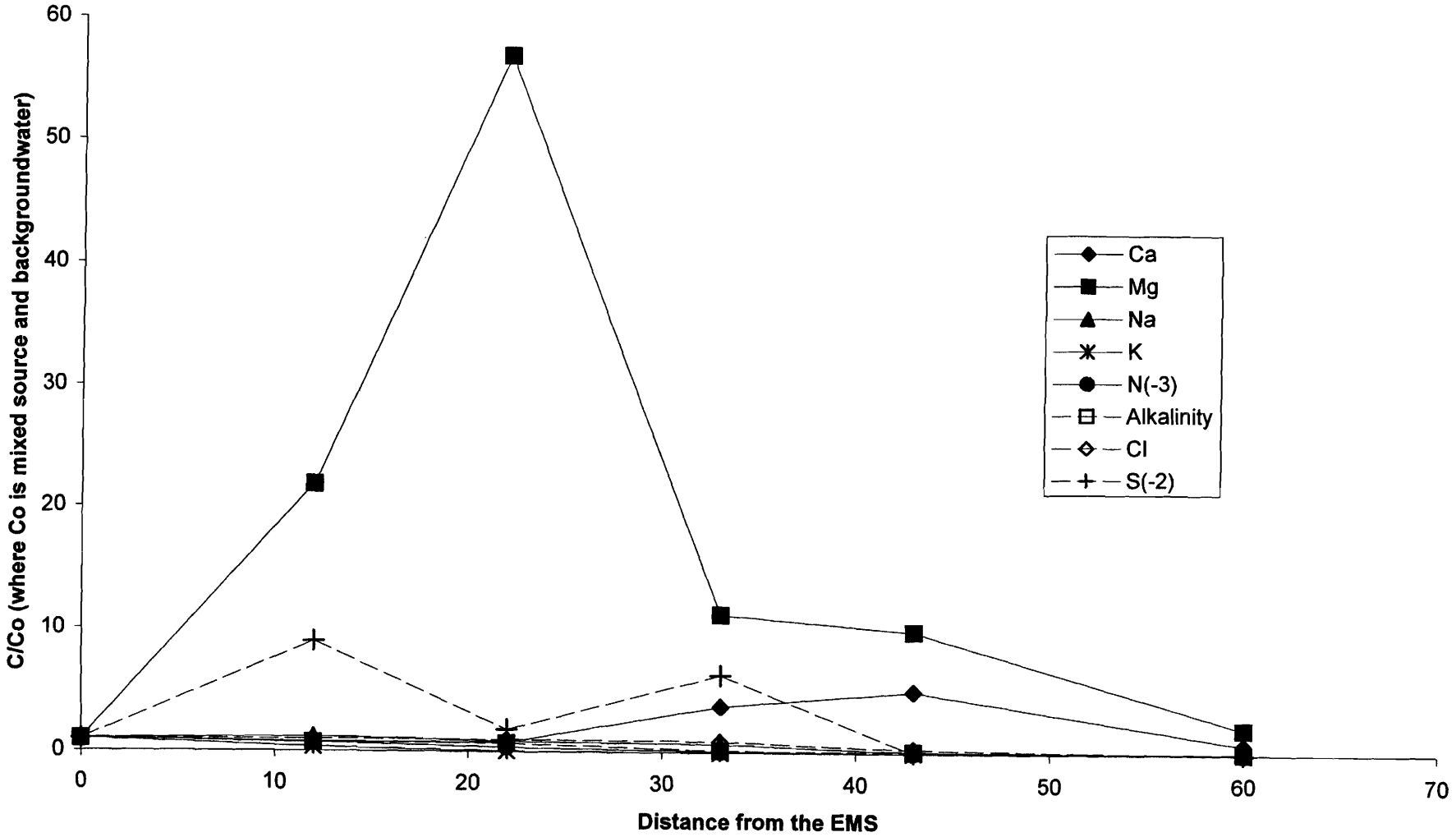

Figure 4.106: Relative ion concentrations as a function of distance from the EMS determined using a source concentration of 56% effluent and 44% groundwater as determined by NETPATH

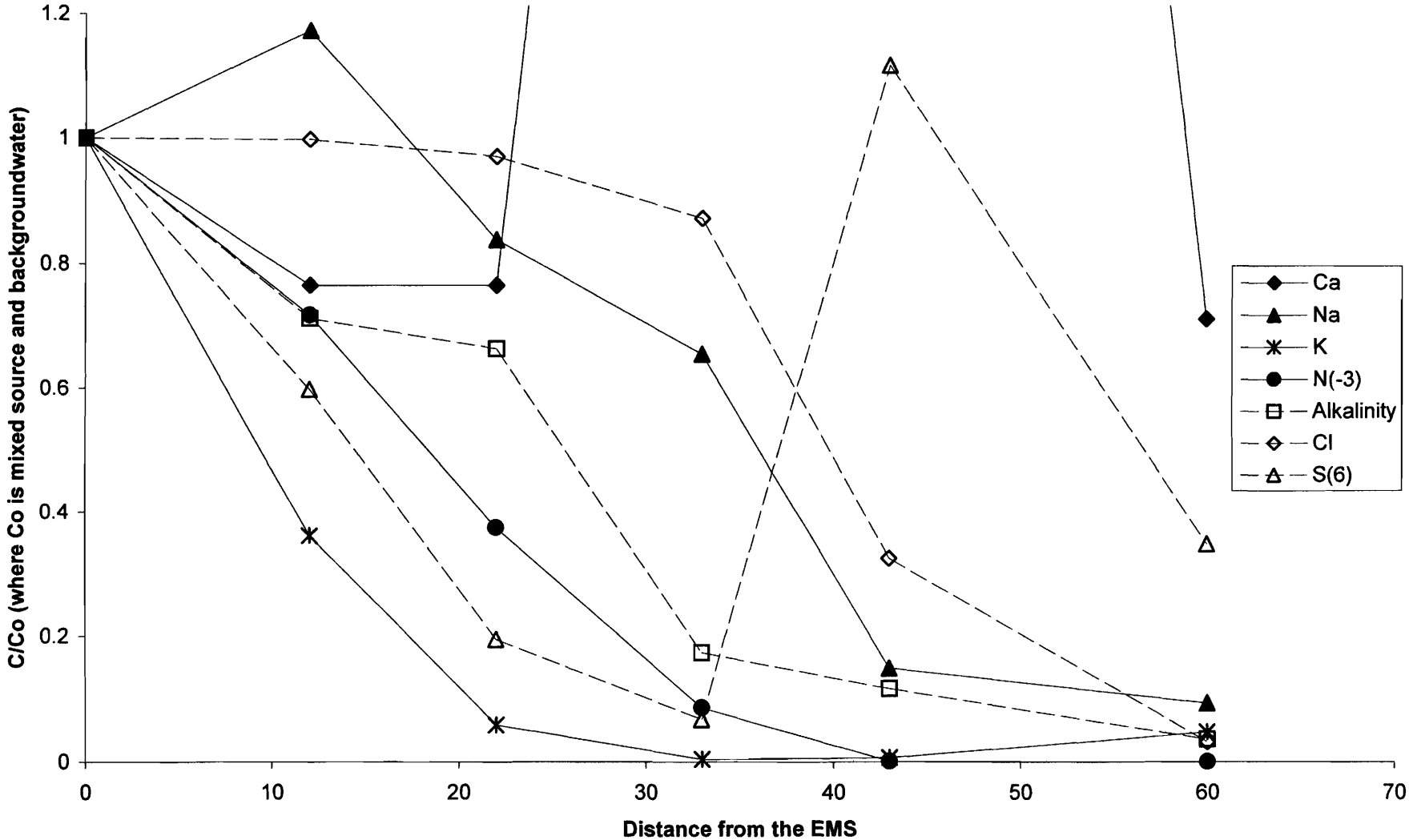

Figure 4.107: Relative ion concentration as determined using a source concentration of 56% effluent and 44% groundwater (NETPATH results) as a function of distance from the EMS.

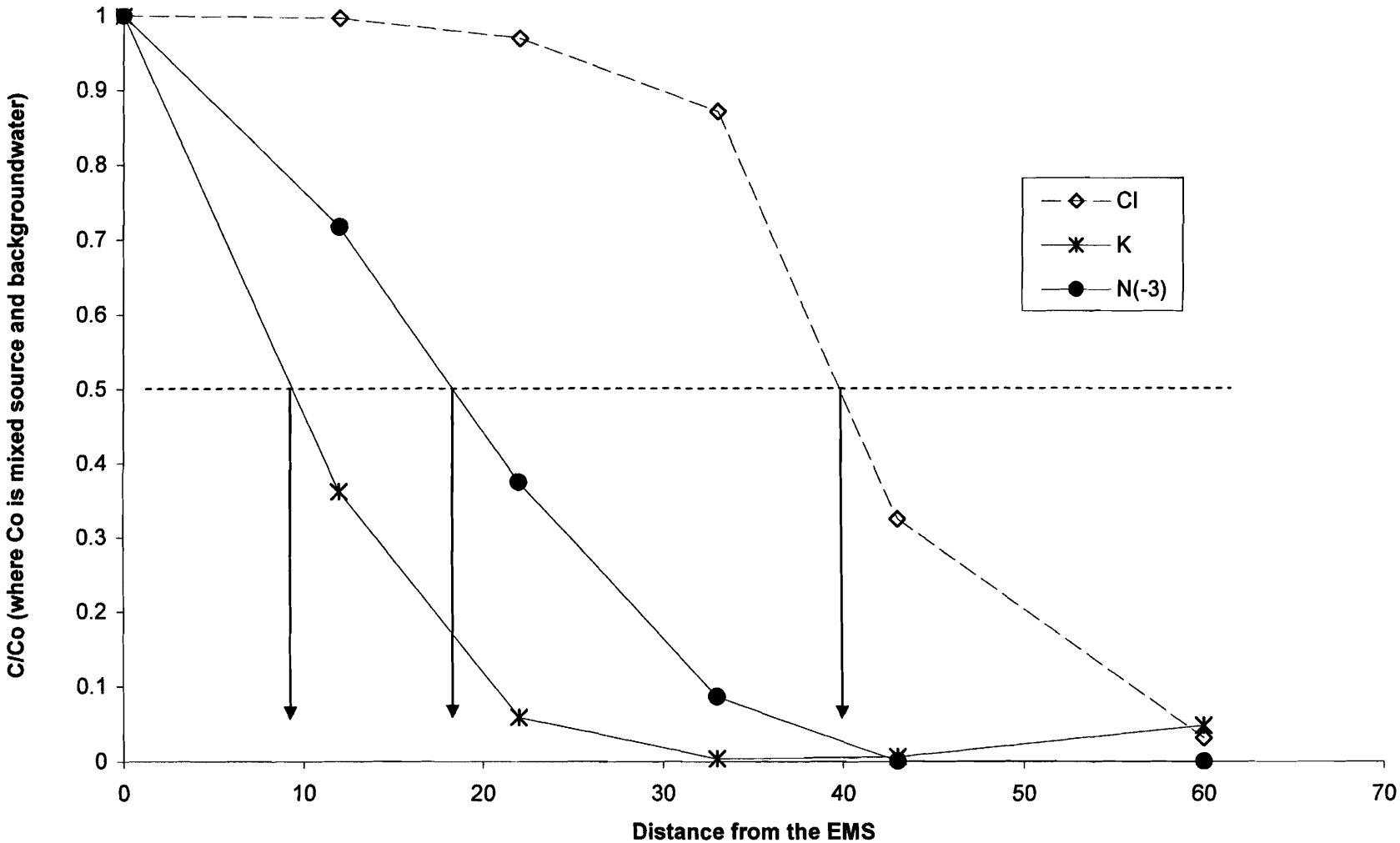

Figure 4.108: Relative ion concentrations for chloride, ammonium and potassium as determined using a source concentration of 56% effluent and 44% groundwater (NETPATH result) versus distance from the EMS.

their concentration in the mixed groundwater and EMS effluent at distances of 23 and 43 m, respectively. These peak concentrations are 263 and 4 times the effluent concentration for magnesium and calcium and ~28 and 7 times background concentrations, respectively. These concentrations are well above either background or effluent concentrations indicating either ion exchange or mineral dissolution has released magnesium and calcium into solution. This halo of divalent cations in solution near the front of the plume is termed the "hardness halo" or "hard water front" and is common in situations were the intruding liquid contains high concentrations of monovalent cations. This halo of divalent cations, which were the base saturating cations on the exchange complex prior to intrusion of the effluent, is generally caused by their release from the exchange complex due to exchange with intruding monovalent cations. Examples of this phenomenon occur in seawater intrusion studies (Beekman and Appelo, 1990), municipal sewage disposal/treatment (Ceazan et al., 1989) and landfill leaching studies (Goodall and Quigley, 1977; Bjerg and Christensen, 1993; Thorton et al., 2000).

Plotting the concentration in solution divided by the concentration in the background water as a function of distance from the EMS (Figure 4.109) shows alkalinity and sulphate levels at a distance of 13 m from the EMS are 41 and 1.7 times background concentrations, respectively. Calculation of saturation indices obtained using the same software used for speciation (PHREEQC, Parkhurst and Appelo, 1999), indicates the system is initially undersaturated with respect to most minerals with the exception of Barite and some iron minerals (Figure 4.110 and Table 4.23). When effluent enters, the system becomes supersaturated with respect to calcium carbonate minerals but remains undersaturated with respect to sulphate minerals. As a result, calcite precipitation may occur especially in areas with high bicarbonate concentrations. Gypsum dissolution may contribute magnesium and calcium to solution although the relatively high concentrations of these cations would suggest that ion exchange is their main source in the plume. The disappearance of sulphate from the system may result from sulphate reduction and/or FeS precipitation; iron reaches levels of 3 meq/L in areas of low sulphate and saturation indices for pyrite exceed 10.

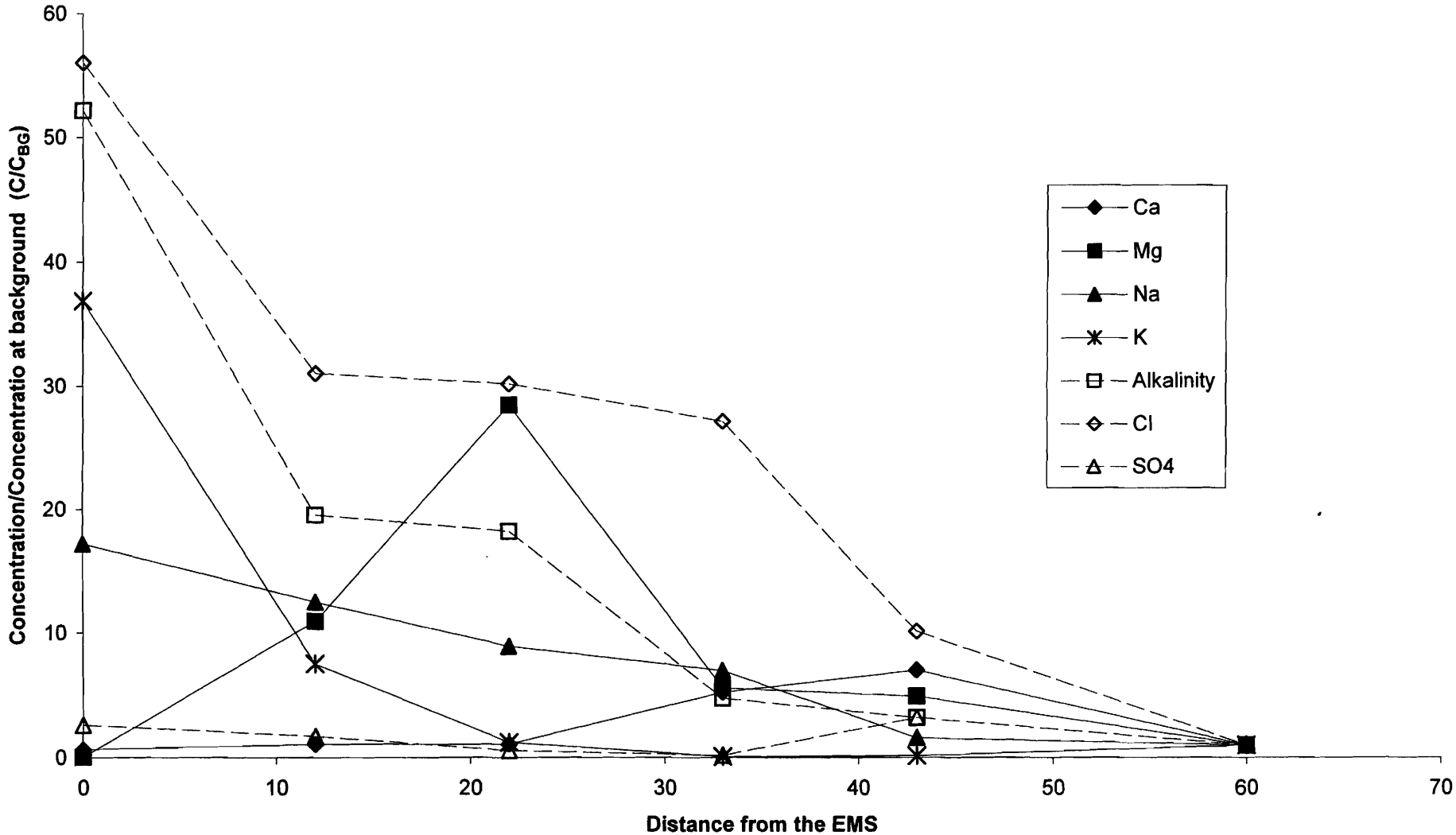

Figure 4.109: Ion concentrations relative to background water concentrations versus distance from the EMS.

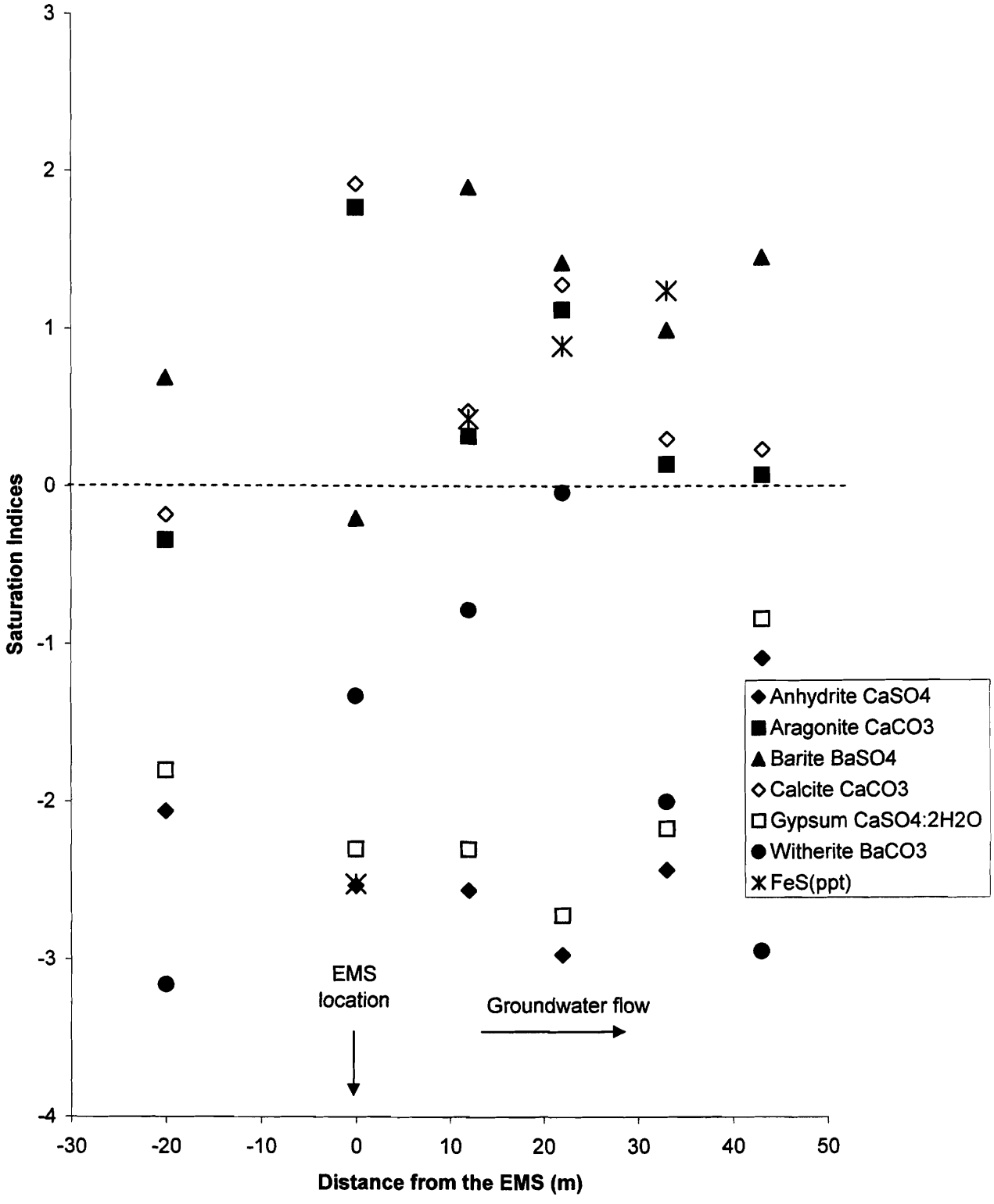

Figure 4.110: Saturation Indices of select mineral phases as a function of distance from the EMS.

Table 4.23: Site No. 1 Saturation Indices

	Piezometer	C29	Source	C15	C18	C21	C24
Phase	Distance (m)	-20	0	12	22	33	43
Amm(g)	Amm	-9.18	-3.9	-6.1	-5.6	-9.72	-9.53
Anhydrite	CaSO4	-2.06	-2.53	-2.56	-2.97	-2.43	-1.09
Aragonite	CaCO3	-0.34	1.77	0.32	1.12	0.14	0.07
Barite	BaSO4	0.69	-0.2	1.9	1.42	0.99	1.45
Calcite	CaCO3	-0.18	1.92	0.48	1.28	0.3	0.23
Celestite	SrSO4	-2.12	-2.87	-1.9	-1.96	-2.45	-1.36
Chalcedony	SiO2	-0.21	0.78	0.44	0.56	0.46	0.34
Chrysotile	Mg3Si2O5(OH)4	-7.89	-3.6	-5.96	0.32	-7.69	-9.59
CO2(g)	CO2	-2.03	-1.28	-0.59	-1.45	-1.14	-0.84
Dolomite	CaMg(CO3)2	-0.64	2.63	1.68	3.63	0.36	0.03
Fe(OH)3(a)	Fe(OH)3	-2.03	-6.16	-4.82	-3.18	-3.94	-5.88
FeS(ppt)	FeS		-2.52	0.43	0.89	1.24	0.01
Goethite	FeOOH	3.86	-0.27	1.08	2.71	1.95	-0.84
Gypsum	CaSO4:2H2O	-1.8	-2.3	-2.3	-2.72	-2.17	-11.39
H2(g)	H2	-13.87	-7.34	-8.05	-7.84	-8	-28.43
H2S(g)	H2S		-6.65	-5.06	-6.32	-5.13	0.48
Hematite	Fe2O3	8.2	1.09	2.62	5.9	4.37	-1.15
Hydroxyapatite	Ca5(PO4)3OH	-0.45	10.05	-1.31	1.43	-3.5	-25.12
Jarosite-K	KFe3(SO4)2(OH)6	-15.39	-27.67	-22.63	-21.86	-22.68	-10.91
Mackinawite	FeS		-1.78	1.16	1.63	1.98	-7.04
Melanterite	FeSO4:7H2O	-6.17	-9.33	-5.78	-6.11	-5.11	-67.3
O2(g)	O2	-62.34	-70.2	-73.98	-74.39	-74.07	-6.43
Pyrite	FeS2		4.85	10.45	9.45	11.15	-24.54
Quartz	SiO2	0.27	1.2	0.93	1.04	0.95	0.82
Sepiolite	Mg2Si3O7.5OH:3H2O	-5.08	-1.14	-2.71	1.67	-3.82	0.73
Sepiolite(d)	Mg2Si3O7.5OH:3H2O	-7.44	-3.91	-5.07	-0.7	-6.19	-5.3
Siderite	FeCO3	-0.06	-0.37	1.51	2.4	1.86	-7.67
SiO2(a)	SiO2	-1.12	-0.08	-0.47	-0.35	-0.45	-1.48
Strontianite	SrCO3	-1.65	0.11	-0.26	0.89	-1.12	-0.57
Sulfur	S		-5.27	-3.2	-4.67	-3.32	-1.44
Talc	Mg3Si4O10(OH)2	-4.89	1.59	-1.65	4.85	-3.34	-5.49
Vivianite	Fe3(PO4)2:8H2O	-1.05	-2.5	1.34	2.87	1.35	-6.76
Witherite	BaCO3	-3.16	-1.33	-0.78	-0.04	-2	-2.95

Reduction in alkalinity along the flow path as calcium increases is accompanied by a decrease in pH, suggesting calcite precipitation by:

$$Ca + HCO_3^- \rightarrow CaCO_3 + H^+ \qquad \text{Eq. 4.28}$$

similar to the results of Thornton et al. (2000) working with field and column data studying landfill leachate. Alkalinity concentrations within the first 22 m from the EMS are slightly less than expected (Figure 4.107), supporting the assumption of calcite precipitation. Relative sulphate concentrations decrease over the first 33 m from the EMS (Figure 4.107). Sulphate reduction may be responsible for at least some of the reduction. Relative sulphide concentrations in this same area are ~6 to 9 times the concentration of the effluent-groundwater mix (Figure 4.106). This is a zone of low ORP (indicated by Eh readings and microbiological sampling) and also the area where the system is supersaturated with Barite (BaSO4) and Pyrite (FeS), suggesting the FeS(ppt) and Barite may contribute to the reduction in sulphate concentrations.

Figure 4.109 suggests ammonium and potassium are retarded with respect to chloride by factors of ~2.1 and 4.4, respectively. Although ammonium may be affected by microbial degradation in addition to adsorption, these retardation factors agree with laboratory results of this and other studies (Table 4.15). Retardation factors were calculated using the solution to the advection-dispersion equation for second-type boundary conditions as describe by Fetter (1993) and the following parameters:

- Hydraulic conductivity of the soil = 3.6×10^{-6} m/s (from laboratory columns)
- porosity = 0.47 (determined from PFRA test results)
- groundwater gradient = 0.01 m/m (determined from groundwater elevations at the site)
- dispersivity of 1/100 of the travel distance (GEONET Consulting Ltd., 2000)
- effective diffusion coefficient for potassium of 0.5×10^{-10} cm^2/s (also assumed for ammonium) (Goodall and Quigley, 1977)

This gives a groundwater flux of 3.6×10^{-8} $m^3/s/m^2$, a velocity of 1.8×10^{-8} m/s and retardation factors for ammonium and potassium of 2.1 and 4.3, respectively, which agree with values determined in Figure 4.109. For a bulk density of 1.45 mg/m3 and a porosity of 0.47, the distribution factors for ammonium and potassium would be 0.35

and 1.1, respectively. These are within the range of values determined by the laboratory study and the literature cited.

4.3.9 Summary of field findings

Multispecies transport through the sandy material at this site has resulted in plume consisting of a hardness halo in advance of the plume and attenuation of ammonium and potassium. Ion exchange as a result of ammonium and potassium in the EMS effluent has caused release of magnesium and calcium into solution. Magnesium release is much greater than calcium suggesting magnesium release occurs first as was indicated in the lab study. Precipitation of minerals appears to attenuate the transport of bicarbonate while precipitation and microbial reduction appear to reduce sulphate levels in the plume. Ammonium and potassium transport are retarded by factors of approximately 2 and 4 respectively. This relatively low attenuation of ammonium should be of concern when evaluating EMS sites.

4.4 Simulation of Column No. 1

To test or demonstrate the effect of variable selectivity coefficients on the attenuation of nitrogen (ammonium), a simulation was conducted using the modeling software PHREEQC (Parkhurst and Appelo, 1999). The model simulated simple advection with ion exchange. A 200 mm soil column was simulated with a CEC of 12 meq/100g (0.607 meq/L). A dispersivity of 0.002 m and no diffusion coefficient were used. Selectivity coefficients for each ion with respect to sodium were determined for 3 fractions of solution composed of monovalent cations: 0.73 representing conditions near the front of the plume, 0.9 for the mid point of the plume, and 0.96 for the highest fraction of monovalent cations determined during the column study. Figure 4.52 indicates selectivity coefficients for potassium, calcium and magnesium with respect to sodium were relatively constant at 0.07, 0.06 and 0.1, respectively, while selectivity coefficients for ammonium were 0.9, 0.5 and 0.15, respectively, for the three fractions. Results of these simulations are shown in Figure 4.110 to 4.116.

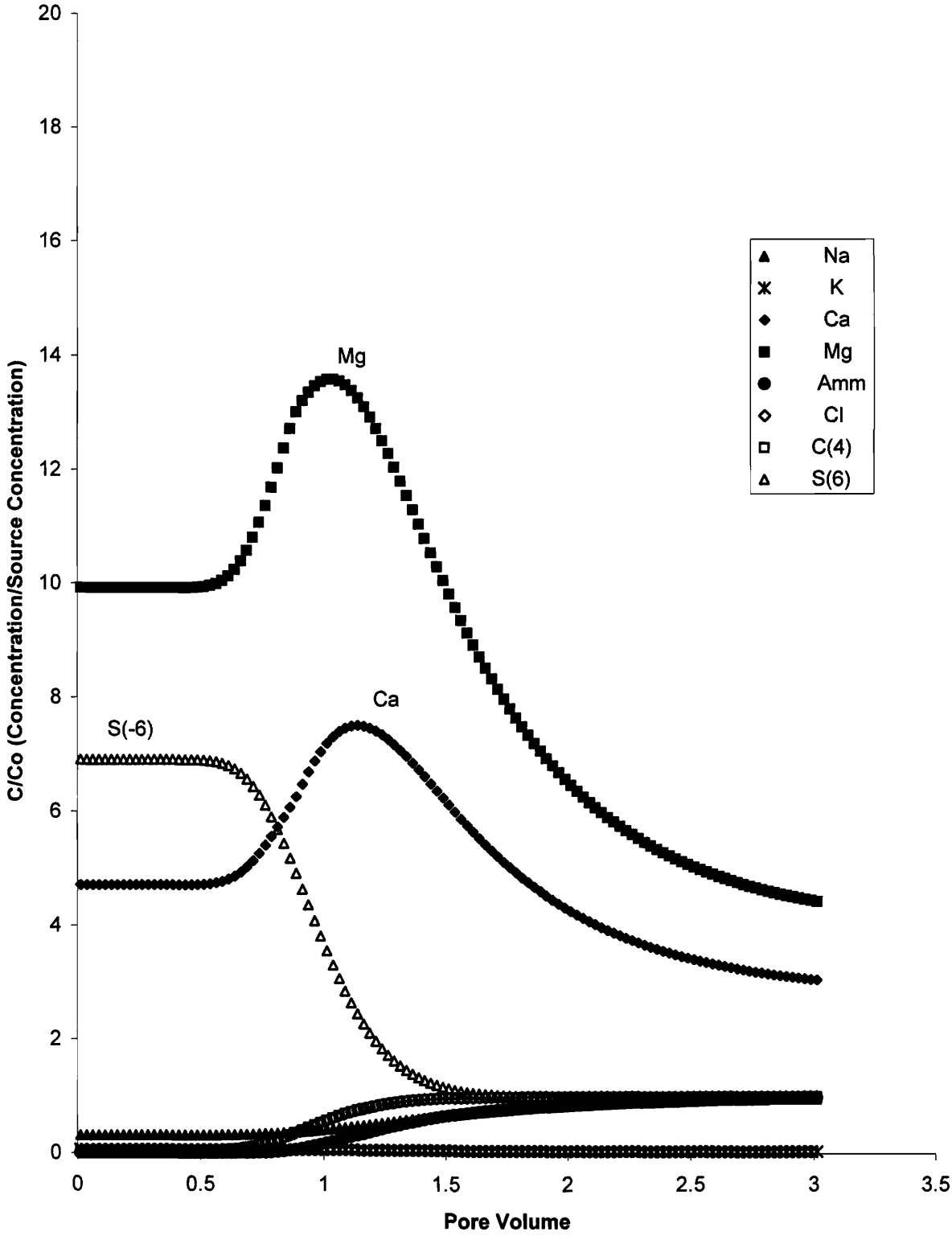

Figure 4.111: Column No. 1 PHREEQC model of breakthrough curves for a 200mm soil sample using selectivity coefficients determined for a ratio of monovalent to divalent cations in solution of 0.73 (near the front of the plume).

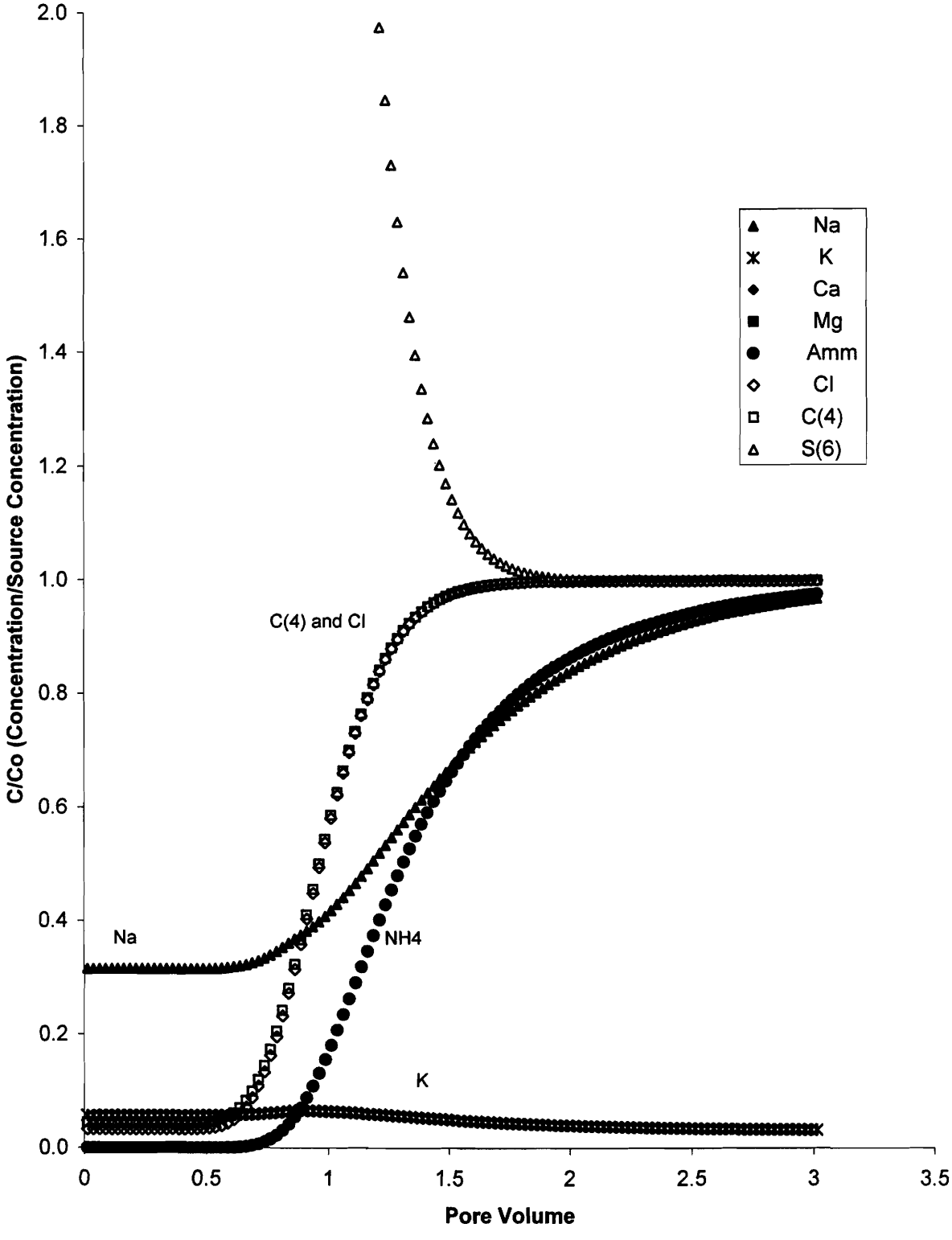

Figure 4.112 - Column No. 1 PHREEQC model of breakthrough curves for a 200mm soil sample using selectivity coefficients determined for a ratio of monovalent to divalent cations in solution of 0.73 (near the front of the plume).

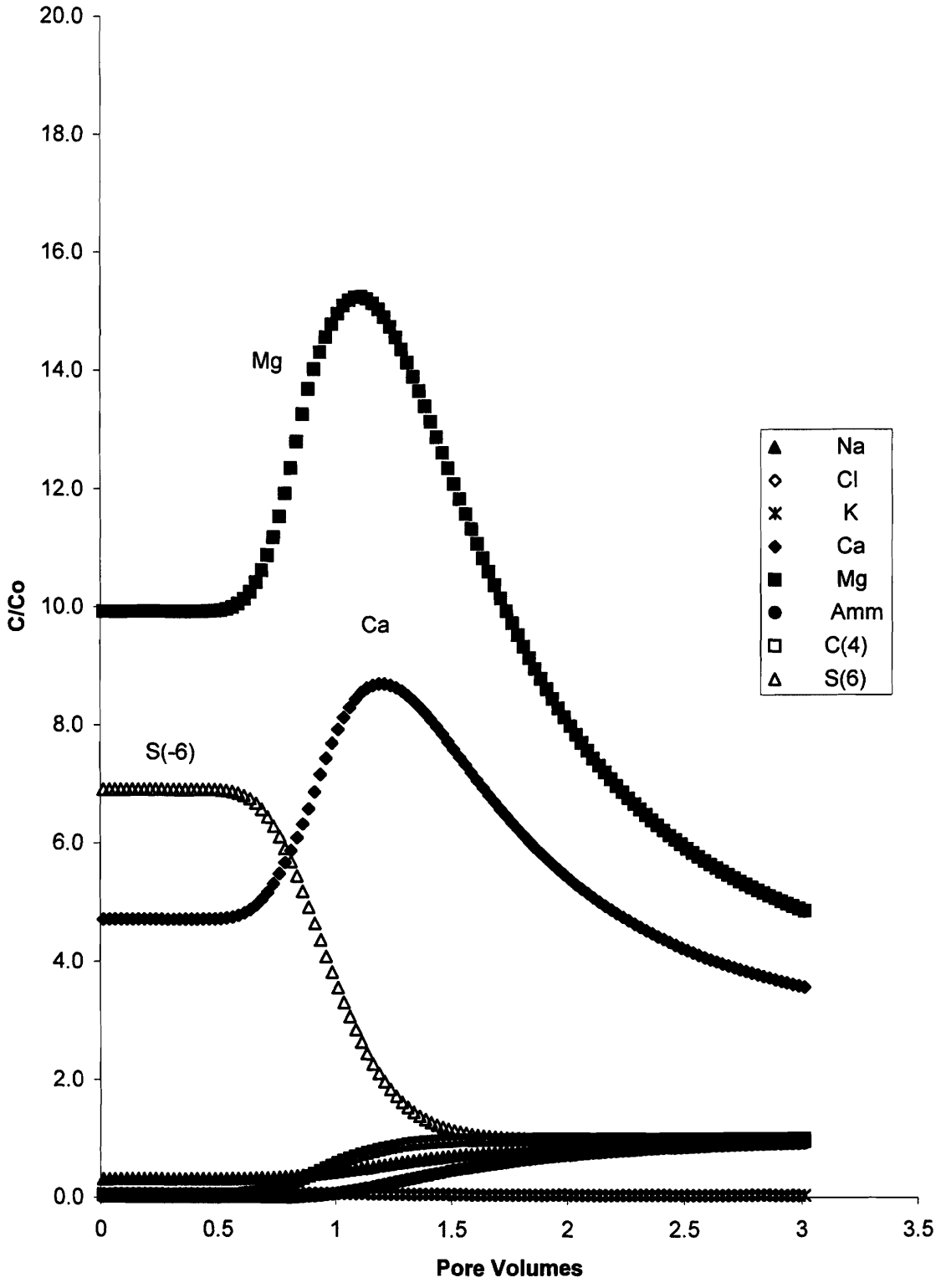

Figure 4.113: Column No. 1 PHREEQC simulation of breakthrough curves for a 200 mm thick soil sample using selectivity coefficients determined for a ratio of monovalent to divalent cations in solution of 0.9.

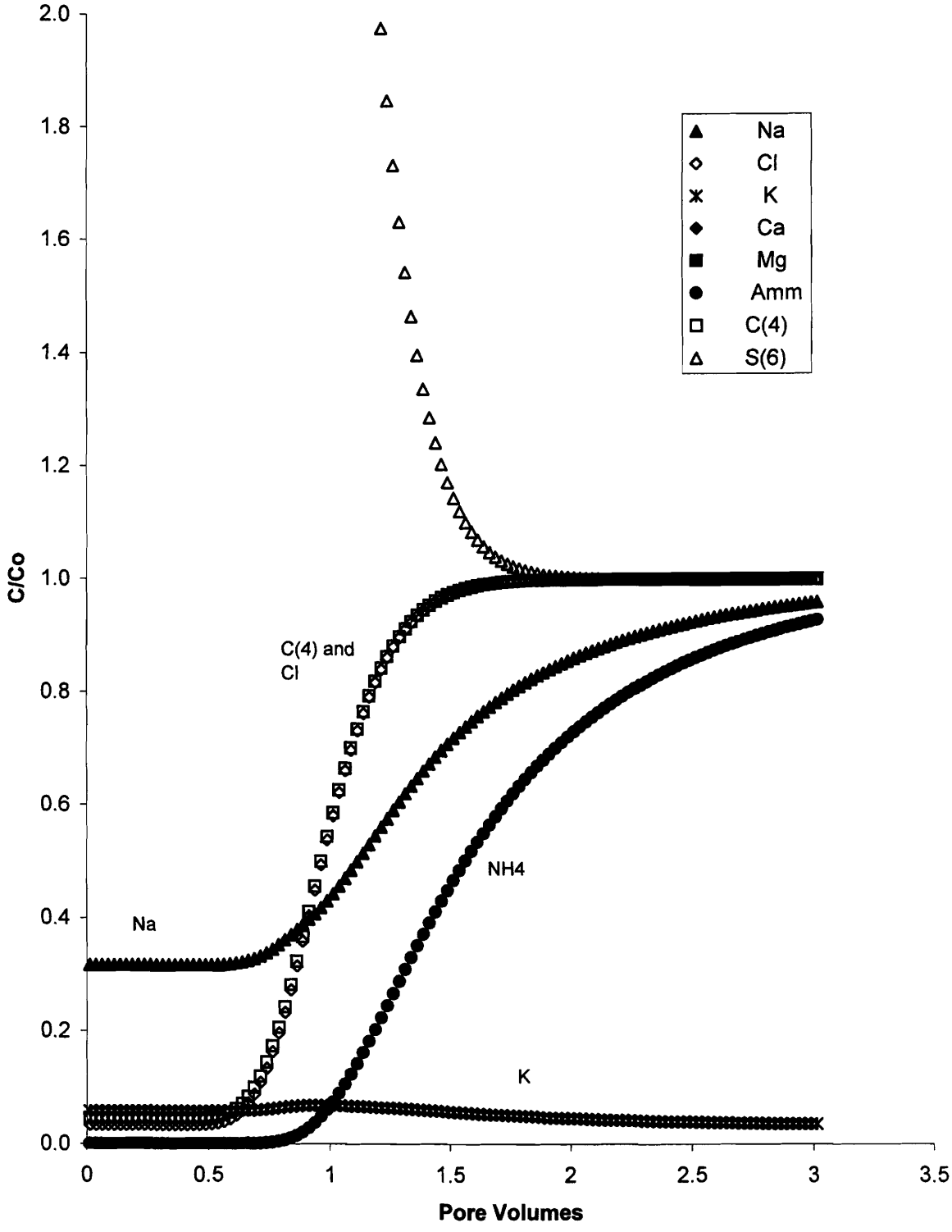

Figure 4.114: Column No. 1 PRHEEQC simulation of breakthrough curves for a 200 mm soil sample using selectivity coefficients determined for a ratio of monovalent to divalent cation in solution of 0.9.

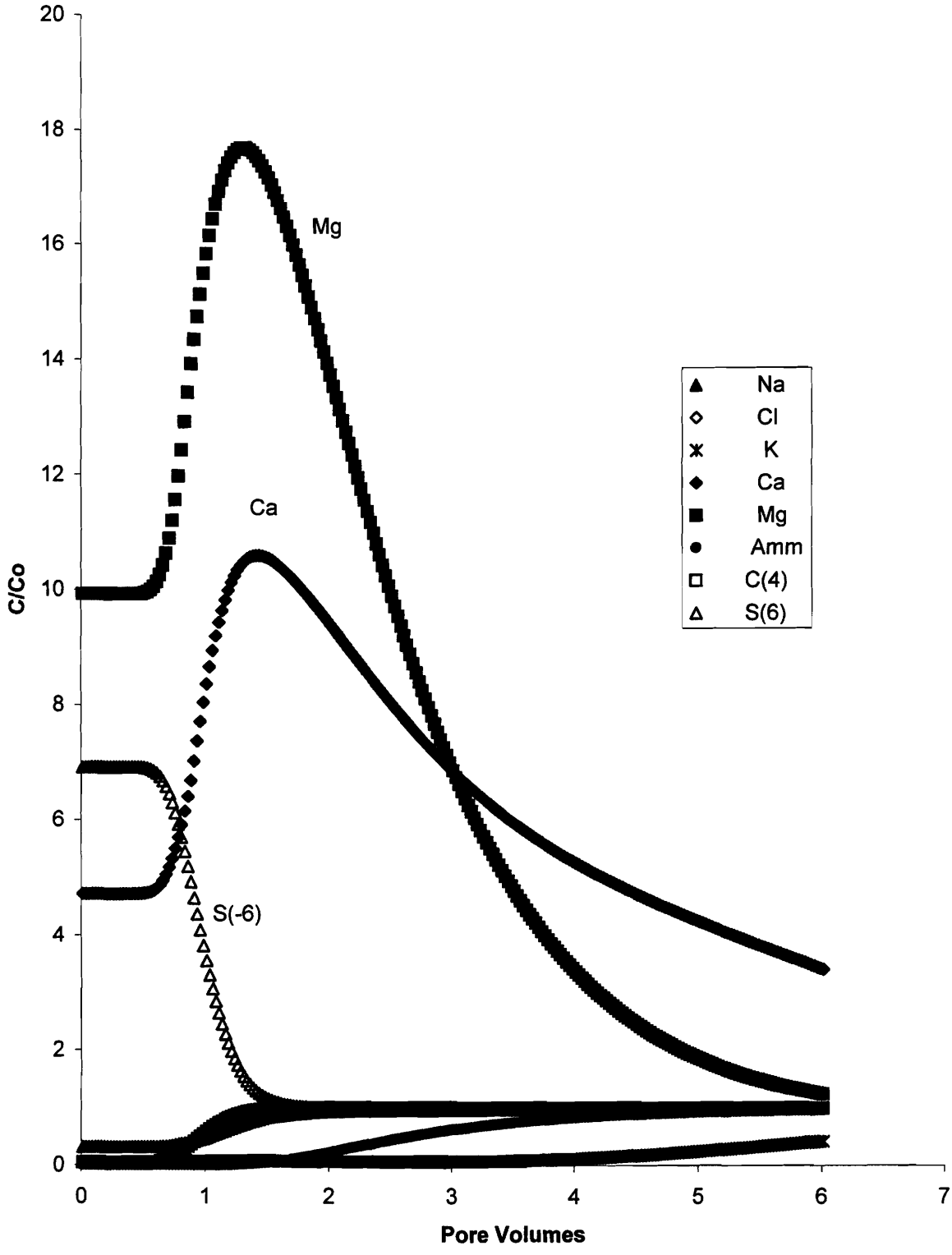

Figure 4.115: Column No 1 PHREEQC simulation of breakthroughcurves for a 200 mm soil sample using selectivity coefficients determined for a ratio of monovalent to divalent cations in solution of 0.96 (back of the plume).

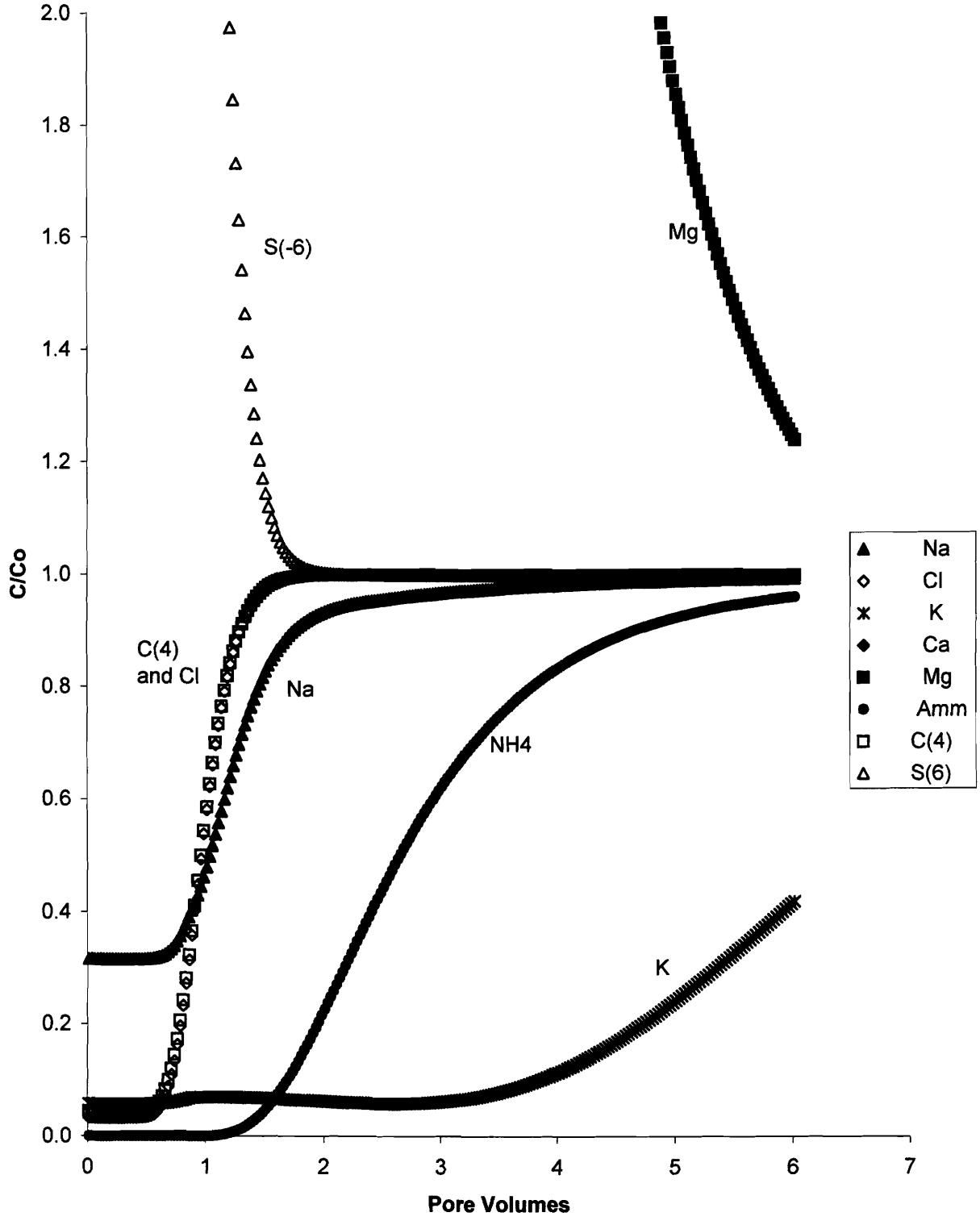

Figure 4.116: Column No. 1 PHREEQC simulation of breakthrough curves for a 200 mm of soil sample using selectivity coefficients determined for a ratio of monovalent to divalent cations in solution of 0.96 (back of the plume).

Figures 4.111, 4.113 and 4.115 show the reduction of sulphate in solution and the initial increase in magnesium and calcium. Calcium and magnesium initially had a relative concentration of 5 and 10 times that of the manure, respectively (Figure 4.111). At the lower fraction of monovalent cations, calcium and magnesium initially increased to a relative concentration of approximately 8 and 14, respectively (Figure 4.111). As the fraction of cations increases and the selectivity coefficient of ammonium decreases (i.e., ammonium selectivity increases), the concentrations of calcium and magnesium leaving the simulated column increase to a C/Co of approximately 10 and 18, respectively (Figure 4.115). This increase in calcium and magnesium within the first 1.5 pore volumes is followed by a decrease to concentrations lower than background. The higher relative increase in magnesium concentration confirms preference for exchange with calcium; this is most evident at the highest fraction of monovalent cations (highest ammonium selectivity) where relative magnesium concentrations decrease to levels below calcium, to close to source concentrations (C/Co=1; Figure 4.115). Relative calcium concentrations at the high fraction of monovalent cations remained near 4 even after 6 pore volumes had passed through the column.

The loss of calcium and magnesium is the result of exchange with potassium and ammonium in solution. Potassium is preferred on exchange sites throughout the range of monovalent to divalent cation ratios modeled. Potassium breakthrough at a concentration of C/Co=0.5 occurs at ~6 pore volumes (Figure 4.116), consistent with this study and the literature cited. Ammonium was only slightly attenuated at the lower fraction of monovalent cations achieving a relative concentration (C/Co) of 0.5 at ~1.3 and 1.5 pore volumes for cation ratios of 0.73 and 0.9, respectively (Figures 4.112 and 4.114). Ammonium attenuation at the highest fraction (0.96) resulted in a C/Co=0.5 at ~2.5 pore volumes, also consistent with this study and the literature.

Sodium started at a relative concentration (C/Co) of 0.3 and reached a concentration of 0.5 at ~1 pore volume for all three conditions modeled (Figures 4.112, 4.114 and 4.116). This is consistent with the laboratory and field findings of this study, however,

the sodium concentration did not reach a relative concentration of 1 until 3 pore volumes.

A simulation was also conducted to determine what may happen when the manure source is removed. A 200 mm soil sample was equilibrated with the manure solution, then the same simulation as above now conducted using the background soil solution as the source. The selectivity coefficients used were those determined for a ratio of monovalent to divalent cations in solution of 0.96 and therefore the results favour ammonium more than might be expected. The results (Figures 4.117 and 4.118) show initial removal of ammonium, potassium and sodium within the first 2 pore volumes and continued removal of ammonium over the next 4 pore volumes. This removal of ammonium coincides with an increase in magnesium concentration to C/Co=1 at approximately 6 pore volumes (Figure 4.118). This removal is significant as it demonstrates attenuation of ammonium is limited to the high monovalent cation concentration of the manure solution; ammonium will likely be released from the exchange complex by the natural soil solution in the event the manure storage is decommissioned. The stability of ammonium on the exchange complex and its removal by natural waters, in conjunction with changes in redox conditions following EMS decommissioning, warrants further study.

The simulations illustrate variable selectivity coefficients provide a more quantitative description of the transport of manure solutes. The next step in this research could be modification of current geochemical models to calculate selectivity coefficients at each advection step in the transport simulation.

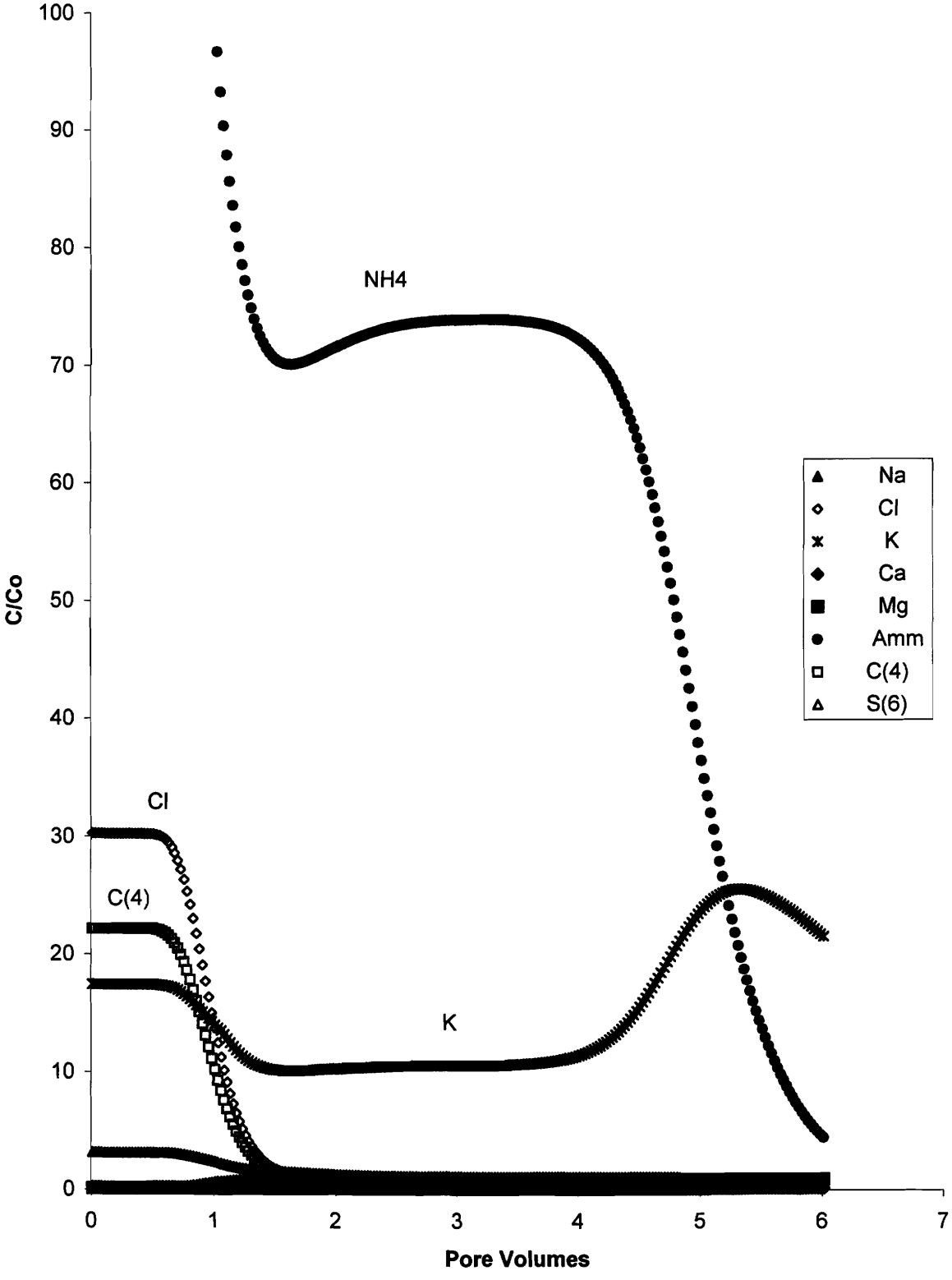

Figure 4.117: Column No. 1 PRHEEQC simulation of breakthrough curves for a fully contaminated 200mm thick soil sample subjected to a background groundwater using selectivity coefficients determined for the back of the plume.

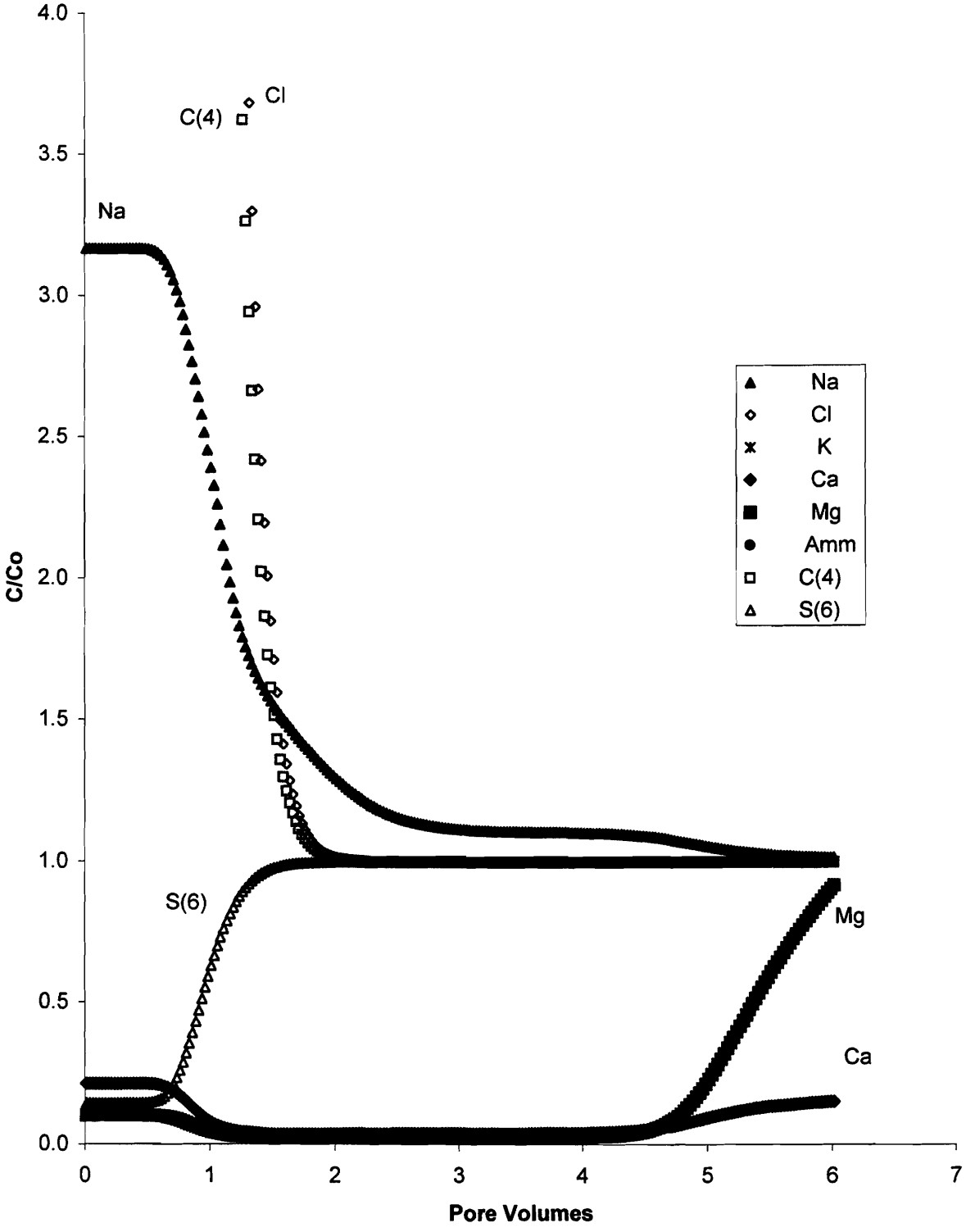

Figure 4.118: Column No. 1 PHREEQC simulation. of breakthrough curves for a fully contaminated 200mm thick soil sample subjected to background groundwater using selectivity coefficients determined for the back of the plume.

5 CONCLUSIONS AND IMPLICATIONS

The objectives of this research were to define the chemistry of the liquid portion of swine manure stored in earthen manure storages, characterize geochemical conditions within an EMS effluent plume and summarize factors controlling mobility of species of concern; and develop a method of establishing nitrogen mobility based on effluent and/or soil characteristics. These objectives were addressed through an integrated set of laboratory column and batch test experiments and detailed field monitoring.

EMS ponds contain a solution composed of, on a molar basis, 36% ammonium, 36% bicarbonate, 8% potassium, 6% chloride, 5% sodium plus sulphate, calcium, magnesium and other nutrients. Additionally, the solution also contains approximately 6,000 mg/L organic and 9,000 mg/L inorganic carbon and has a near neutral pH. As a result, the solution has a low Eh causing nitrogen to remain in the ammonium form.

Cation adsorption during transport from and EMS is variable due to variability in ion selectivity produce by factors such as ion concentrations in solution, total quantity of ions in solution, and proportion of each valence of ions in solution. The selectivity of ions by the exchange complex can also be affected by the quantity of higher valance cations already occupying exchange sites. This work has characterized the selectivity coefficients as a function of the ration of monovalent cations ions in solution and the quantity of calcium on soil exchange sites and illustrated the significance of the selectivity on contaminant transport from EMS.

Distribution and selectivity coefficients were determined in a laboratory column study. Selectivity coefficients of the ions varied as functions of several soil and solution characteristics. The highest correlation was obtained when plotting selectivity coefficients against the ratio of monovalent to divalent cations in solution and the

quantity of calcium on the exchange sites. Selectivity coefficients were determined to be within the range of published values with the exception of ammonium. Selectivity coefficients for calcium (0.05–0.4) and magnesium (0.07–0.5) with respect to sodium ranged from slightly lower to the same as values in the published literature. Calcium and magnesium were removed from soil exchange sites by the advancing contaminant plume containing relatively high concentrations of monovalent ions. Approximately 70% of the magnesium was replaced on exchange sites prior to replacement of calcium for both soils tested. Magnesium released into solution advanced near the front of the plume, and a portion of this magnesium replaced calcium on exchange sites causing a "hard water front" at the front of the plume. This hard water front was observed in the field investigation of a contaminant plume adjacent to an earthen hog manure storage. This front contained calcium and magnesium concentrations 4 to 263 times respectively their concentration in the EMS effluent and 7 and 29 times respectively their concentration in the background groundwater. These elevated levels of calcium and magnesium in front of the plume offer a method for contaminant plume detection in advance of detection of ammonium or potassium. Sodium did not appear able to preferentially replace other solution cations on soil exchange sites, resulting in sodium transporting similar to non reactive ions. This behaviour was observed in both the laboratory columns and the field investigation.

Potassium selectivity coefficients with respect to sodium determined for both soils tested agreed with values found in the literature for similar studies. Potassium appeared to be preferred on exchange sites for both soils tested. Distribution coefficients indicate potassium was able to replace ions on the exchange complex at low potassium concentrations. Distribution coefficients for potassium ranged from 1 to 3.5 L/kg which convert to retardation factors of 5 to 11 for the soil tested. Potassium's ability to replace ions on the exchange complex was highest at low potassium concentrations in solutions but decreased significantly as both potassium and the total monovalent ion concentrations increased. This would suggest potassium would be most attenuated at the front of a plume and less attenuated as concentrations increased causing a relatively sharp or abrupt potassium front. This was illustrated in results of the field study.

Selectivity coefficients for ammonium referenced to sodium were determined to be quite variable, ranging from 0.23 to 2.2. Distribution coefficients for ammonium were ranged from 0.08 to 0.4 L/kg which convert to retardation factors of 1.3 to 3.0 for the soil tested. The ability of ammonium to replace ions on the exchange sites was shown to be a function of the ratio of monovalent to divalent cations in solution rather than simply the concentration of ammonium in solution. Ammonium's ability to replace ions on the exchange sites increased with increasing ratio of monovalent to divalent cations in solution, becoming significant above a ratio of 0.9. This should result in relatively abrupt ammonium seepage fronts, as was demonstrated in the field study. This abrupt front has the potential to impact groundwater resources as it could cause large fluxes of ammonium nitrogen over short periods of time. That is to say, ammonium breakthrough into an aquifer would be attenuated but occur suddenly when the front reached the aquifer.

Investigation of a contaminated plume in an unconfined aquifer indicated high organic carbon content and naturally low groundwater Eh resulting in the transport of nitrogen as ammonium with the exception of some nitrification and denitrification at the leading and upper edge of the plume. Retardation of ammonium and potassium along the centerline of the plume were 2 and 4 respectively. Attenuation of ammonium is consistent with laboratory findings; potassium attenuation in the field was slightly lower.

A preliminary simulation of advection and ion exchange using published selectivity coefficients underestimated magnesium stripping from exchange sites and overestimated ammonium attenuation. Simulations using selectivity coefficients determined in this study resulted in the observed preferential release of magnesium and the lower attenuation of ammonium.

5.1 Implications

The results of this work should provide the basis for an improved approached to predicting the impact of EMS on groundwater as it provide a clearer understanding of the chemistry of the EMS seepage and the attenuation factors limiting cation transport.

Transport of nitrogen in EMS effluent is primarily as ammonium. The retardation factor for ammonium was determined to be less than 3, an order of magnitude less than assumed in at least one geochemical transport model for landfill leachate (Erskine 2000). Therefore, nitrogen transport in EMS effluent plumes may be much greater than originally assumed by some regulators, developers and engineers. Furthermore, sorbed ammonium will likely release into solution once the source is removed and natural waters begins to leach the contaminated soil.

Modeling of cation transport in contaminant plumes may benefit from incorporation of variable selectivity coefficients although the selectivity functions would need to be determined for each situation and specific site soils. Once sufficient data is compiled, selectivity coefficient functions may be determinable for soils of similar characteristics.

Although modeling of the actual location of the ammonium front may need improvement, the hard water front produced by the ion exchange between the monovalent and divalent cations provides an opportunity for early detection of contaminant plumes. Any monitoring for EMS seepage should include a complete analysis of major and minor cations and anions.

5.2 Recommendations for further research

Additional data should be compiled regarding the chemistry of EMS effluent. This could be accomplished by asking any EMS sample analysis to include an analysis of a filtered sample for water chemistry. A database could then be compiled similar to those available for the typical fertilizer value of manures.

Selectivity coefficients for cations associated with contaminant transport of EMS effluent should be studied further. Better control of variables could be attained by use of exchange resins, source solutions with similar chemistry to manure, conducting experiments under constant environmental conditions and/or designing a batch test accounting for the changes in solution chemistry as a result of ion exchange. The most useful information would still be attained using soils similar to those found at waste containment sites.

Incorporation of variable selectivity of ions in transport models should improve the ability of these models to quantitatively predict transport distance of contaminants. Variable distribution coefficients should be considered in numerical transport models although functions for these coefficients will likely need to be determined for the site soils.

Continued investigation of the effluent plume at Site No. 1 and of other EMS effluent plumes would further characterize how EMS effluent reacts during contaminant transport. A recently decommissioned EMS should be instrumented to allow characterization of the effluent plume with time; the information gained would assist with the development of decommissioning strategies. This work is critical to our ability to protect groundwater resources both now, when new livestock facilities are being developed in the Prairies Provinces, and 25 to 50 years from now when current EMS are decommissioned.

6 LIST OF REFERENCES

Agricultural Operations Act (1995). Agricultural Operations Act - Intensive Livestock Provisions, Chapter A-12.1, Saskatchewan Agriculture Food and Rural Revitalization, Government of Saskatchewan, April 1995.

Anon, 1987. Sampling Guidelines for Groundwater Quality. Electr. Power Res. Rep. EPRI EA. September 1987. 72p.

Appelo, C.A.J. and Postma, D., 1996. Geochemistry, Groundwater And Pollution. A.A. Balkema, Rotterdam, Netherlands

ASTM D-4319, 2001, "Standard Test Method for Distribution Ratios by the Short Term Batch Method". ASTM International, 2001.

Austin, W.E. and J.H. Huddleston. 1999. "Variability of permanently installed platinum redox electrodes." Soil Sci. Soc. Am. J., 63:1757-1762.

Bailey, L. D. and E. G. Beauchamp. 1971. "Nitrate reduction and redox potentials measured with permanently and temporarily placed platinum electrodes in saturated soils." Canadian Journal of Soil Science, 51: 51-58.

Barrington, S.F., and C.A. Madramootoo, 1989. "Investigating seal formation from manure infiltration into soils." Trans. Amer. Soc. Agric. Eng. 32(2):851-856

Barrington, S.F., P.J. Jutras, and R.S. Broughton,1987a. "The sealing of soils by manure. Part I. Preliminary investigations" Can. Agric. Eng. 29(2):99-105

Barrington, S.F., P.J. Jutras, and R.S. Broughton,1987b. "The sealing of soils by manure. Part II Sealing Mechanisms." Can. Agric. Eng. 29(2):105-109

Barth, C.L. and J. Kroes. 1985. "Livestock lagoon sludge characterization." Agricultural Waste Utilization and Management: Proceedings of the Fifth International Symposium on Agricultural Wastes. Pp. 660-671.

Bayne, G.G., 1997. Nutrient values in Saskatchewan manure. Canadian Water Resources Association, Rural Water Quality Symposium. Winnipeg, Manitoba, March 25-26, 1997

Beekman, H. E., and Appelo, C. A. J. (1990). "Ion chromatography of fresh- and salt-water displacement: laboratory experiments and multicomponent transport modelling." *Journal Contam. Hydrol.*, 7, 21-37.

Berner, R.A., 1980. Early diagenesis: a theoretical approach. Princeton University Press, Princeton, N.J., USA. 241pp.

Betcher, R.N., 2000. Personal Communication. Miscellaneous data from manure sampling. Water Resources Division, Manitoba Natural Resources.

Bjerg, P.L. and Christensen, T.H., 1993. A field experiment on cation exchange-affected multicomponent solute transport in a sandy aquifer. Journal of Contaminant Hydrology, 12: 269-290.

Bjerg, P.L., Ammentorp, H.C. and Christensen, T.H., 1993. Model simulations of a field experiment on cation exchange-affected multicomponent solute transport in a sandy aquifer. Journal of Contaminant Hydrology, 12: 291-311.

Bjerg, P.L., Kirsten, R., Pedersen, J.K. and Christensen, T.H., 1995. Distribution of redox-sensitive groundwater quality parameters downgradient of a landfill (Grindsted, Denmark). Environmental Science and Technology, Vol. 29, No. 5: 1387-1394.

Blackwell, P.S. 1983. "Measurements of aeration in waterlogged soils: some improvement of techniques and their application to experiments using lysimeters." J. Soil Sci., 34:271-285.

Bockris, J.O. and F.L. Oldfield. 1955. "The oxidation-reduction reactions of hydrogen peroxide at inert metal electrodes and mercury cathodes." Trans. Faraday Soc., 51:249-259.

Bohn, H.L., 1969. "The emf of platinum electrodes in dilute solutions and its relation to soil pH." Soil Sci. Soc. Of Am. Proc., 33: 639-640.

Bolt, G.H., 1982. Theories of cation adsorption by soil constituents: Distribution equilibrium in electrostatic fields. Soil Chemistry B. Physico-Chemical Models, G.H. Bolt (Ed.), Developments in Soil Science 5B, Elsevier Scientific Publishing Company, Amsterdam, The Netherlands: 47-76.

Bone, Larry I. 1986. Developing Guides For Sampling And Analysis of Groundwater. ASTM Special Technical Publication, Hazardous and Industrial Solid Waste Testing and Disposal, Sixth Volume. Papers Presented at the Third International Symposium on Industrial and Hazardous Waste and the Symposium on Environmental Test Method Development. 1986 Alexandria, Egypt and Colorado Springs, CO, USA. Sponsored by: ASTM, Philadelphia, PA, USA. p 337 - 342.

Booram, C.V., T.E. Hazen and R.J. Smith. 1975. "Trends and Variations in an anaerobic lagoon with recycling." Managing Livestock Wastes, pp.537-540.

Bornstein, J. and M. McGurik. 1978. "Modifications to a soil oxygen diffusion ratemeter." Soil Sci., 126(5): 280-284.

Boulding, Russell J., 1993. Subsurface Characterization and Monitoring techniques: A Desk Reference Guide. Volume II: Solids and Ground Water, Appendices A and B. EPA/625/R-93-003a. Center for Environmental Research and Information.

Bruggenwert, M. G. M., and Kamphorst, A. (1979). "Survey of Experimental Information on Cation Exchange in Soil Systems." Soil Chemistry B. Physico-Chemical Models, G. H. Bolt, ed., Elsevier Science Publishers B.V., Amsterdam, The Netherlands, 141-203.

Campbell, A. J., MacLeod, J. A. and Stewart, C., 1997. "Nutrient characterization of stored liquid hog manure." CSAE 39(1): 43-48.

Campbell, J.A. 1980. "Oxygen flux measurements in organic soil." Can. J. Soil Sci., 60:641-650.

Ceazan, M.L., Thruman, E.M. and Smith, R.L., 1989, Retardation of ammonium and potassium transport through a contaminated sand and gravel aquifer: The role of cation exchange. Environmental Science and Technology, Vol. 23, No. 11: 1402-1408.

Chang, A. C., Olmstead, W. R., Johanson, J. B. and Yamishita, G., 1974. "The sealing mechanisms of wastewater ponds." Journal of the Water Pollution Control Federation 46(7): 1715-1721.

Christensen, T.H., Bjerg, P.L. and Kjeldsen, P., 2000. Natural attenuation: A feasible approach to remediation of ground water pollution at landfills? Ground Water Monitoring and Remediation GWMR, Winter 2000: 69-77.

Christensen, T.H., Kjeldsen, P., Bjerg, P.L., Jensen, D.L., Christensen, J.B., Baun, A., Albrechtsen, H.J. and Heron, G., 2001. Biochemistry of landfill leachate plumes. Applied Geochemistry, 16: 659-718.

Ciravolo, T. G., Martens, D. C., Hallock, D. L., Collins, E. R., Kornegay, E. T. and Thomas, H. R., 1979. "Pollutant movement to shallow ground water tables from anaerobic swine waste lagoons." Journal of Environmental Quality 8(1): 126-130.

Clay, D.E., C. E. Clapp, J.A.E. Molina and D.R. Linden. 1990. "Soil tillage impact on the diurnal redox potential cycle." Soil Sci. Soc. Am. J., 54: 516-521.

Clothier, B.E., Sauer, T.J. and Green, S.R., 1988. The movement of ammonium nitrate into unsaturated soil during unsteady absorption. Soil Science Society of America Journal, 52: 340-345.

Cogger, C.G., P.E. Kennedy and D. Carlson. 1992. "Seasonally saturated soils in the Puget Lowland. II. Measuring and interpreting redox potentials." Soil Sci., 154(1): 50-58.

Culik, M.N., Doran, J.W. and Richards, K.A., 1982. Construction of soil thermocouples for the novice soil temperature. Journal of the Soil Science Society of America, v. 46 (4); 882-884.

Culley, J.L.B. and P.A. Phillips, 1982. "Sealing of soils by liquid cattle manure" Can. Agric. Eng. 24:87-89

Dance, J.T. and Reardon, E.J., 1983. Migration of contaminants in groundwater at a landfill: A Case Study, 5. Cation migration in the dispersion test. Journal of Hydrology, 63: 109-130.

Davis, S., Fairbank, W. and Weisheit, H., 1973. "Dairy waste ponds effectively self-sealing." Transactions of the ASAE 16: 69-71.

Desimone, L.A., Barlow, P.M. and Howes, B.L., 1996. A Nitrogen-Rich Septage-Effluent Plume in a Glacial Aquifer, Cape Cod, Massachusetts, February 1990 Through December 1992. U.S. Geological Survey Water-Supply Paper 2456. 89pp.

DeTar, W.R., 1979. "Infiltration of liquid dairy manure into soil." Trans. Amer. Soc. Agric. Eng. 22:520-558

Dirasin, H.A. 1968. "Electrode potentials - Significance in biological systems." Part 1: Water and sewage works., 115(1): 453-456.

Driscoll, Fletcher G., 1986. Groundwater and Wells. Second Edition. Johnson Filtration Systems Inc., St. Paul, Minnesota, USA.

Drommerhausen, D. J., Radcliffe, D. E., Brune, D. E. and Gunter, H. D., 1995. "Electromagnetic conductivity surveys of dairies for groundwater nitrate." Journal of Environmental Quality 24: 1083-1091.

Erskine, A.D., 2000. Transport of ammonium in aquifers: retardation and degradation. Quarterly Journal of Engineering Geology and Hydrogeology, 33: 161-170.

Farrell, R. E., G. D. W. Swerhone, and C. van Kessel. 1991. "Construction and evaluation of a reference electrode assembly for use in monitoring in situ soil redox potentials." Communications in Soil Science and Plant Analysis: 22(11&12), 1059-1068.

Farrer, D., 1997. Personal Communication. Director, Saskatchewan Agriculture, Food and Rural Revitalization, (SAFRR); Inspection and Regulatory Management Branch, Government of Saskatchewan.

Faulkner, S. P., W. H. Patrick, Jr., and R. P. Gambrell. 1989. "Field techniques for measuring wetland soil parameters." Soil Science Society of America Journal, 53: 883-890.

Fetter, C.W., 1977. Attenuation of Waste Water Elutriated Through Glacial Outwash. Ground Water, 15, No. 5: 365-371

Fetter, C.W., 1993. Contaminant Hydrogeology. Macmillan Publishing Company, New York, New York, USA. 458pp.

Filson, H. 1994. Split spoon sampling below to earthen manure storages. Personal communication. Prairie Farm Rehabilitation Administration, Geotechnical Division.

Fonstad, T. A. and Maule, C. P., 1995. Earthen hog manure lagoons. Part I: Flux reduction due to sealing. CSAE Paper No. 95-508, CSAE Annual Conference, July 1995.

Fonstad, T. A. and Maule, C. P., 1996. Solute migration beneath earthen hog manure storages in saskatchewan. ASAE International Meeting, Pheonix, Arizona. July, 1996.Paper Presentation, Pub. No.: CSAE Paper No. 962049

Fonstad, T. A., 1996. "Effect of Manure Ponding on Soil Hydraulic Properties". Masters of Science Thesis. Department of Agricultural and Bioresource Engineering, University of Saskatchewan. P: 73.

Fonstad, T.A., 2001. Final Progress Report ADF Project No. 97000061: Long Term Performance and Safety of Earthen Hog Manure Storages. Submitted to the Agricultural Development Fund, Saskatchewan Agriculture, Food and Rural Revitalization, (SAFRR), Government of Saskatchewan. October 2001.

Freeze, R.A. and Cherry, J.A., 1979. Groundwater. Prentice-Hall, Inc., Englewood Cliffs, New Jersey, USA. 604pp.

Gaines, G.L. and Thomas, H.C., 1953. Adsorption studies on clay minerals. II. A formation of the thermodynamics of exchange adsorption. Journal of Chemical Physics, 21: 714-718.

Gangbazo, G., D. Cluis and M. Vallidres, 1989. "Nitrogen seepage from earthen-built manure storage tanks." ASAE/CSAE Paper No. 892002, 1989 ASAE/CSAE International Summer Meeting.

GEONET Consulting Ltd., 2000. A Study of Solute Transport from Earthen Manure Storages. Prepared for a Tri-Provincial Committee on Site Characterization, Alberta Agriculture, Food and Rural Development, Manitoba Agriculture and Food, Saskatchewan Agriculture and Food. March 28, 2000: 33pp.

Gerald Bayne, G., 1997. Nutrient Values In Saskatchewan Manure. Canadian Water Resources Association, Rural Water Quality Symposium. Winnipeg, Manitoba, March 25-26, 1997

Goodall, D.C. and Quigley, R.M., 1977. Pollutant migration from two sanitary landfill sites near Sarnia, Ontario. Can. Geotech. J., Vol. 14: 223-236.

Gosselin, D.C., Ayers, J.K. and Zhang, Y.-K. 1994. Modeling concentration variations in high-capacity wells. Implications for ground water sampling. Water Resources Bulletin, Vol. 30, No. 4, July - August 1994. American Water Resources Assoc., Bethesda, MD, USA. p 613-622.

Grable, A.R. and E.G. Seimer. 1968. "Effects of bulk density, aggregate size, and soil water suction on oxygen diffusion, redox potentials, and elongation of corn roots." Soil Sci.Soc. of Am. Proc. 32:180-186.

Grove, D.B. and Wood, W.W., 1979. Prediction and field verification of subsurface-water quality changes during artificial recharge, Lubbock, Texas. Ground Water, Vol. 17, No. 3: 250-257.

Hart, S.A. and Turner, M.E., 1965. "Lagoons for livestock manure". Journal WPCF November, 1965. Vol. 37, No.11. P:1578-1596

Hartz, Rich. 1991. Groundwater sampling from low recharging wells. Water/Engineering and Management. Vol. 138, No. 10, October 1991. P 30-31.

Hendry, M.J., McCready, R.G.L., and Gould, W.D., 1984. Distribution, source and evolution of nitrate in a glacial till of southern Alberta, Canada. J. Hydrol., 70: 177-198.

Huffman, R. L. and Westerman, P. W., 1995. "Estimated seepage losses from established swine waste lagoons in the lower coastal plain of North Carolina." Transactions of the ASAE 38(2): 449-453.

Kerr, H.W., 1928. The nature of base exchange and soil acidity. Journal of the American Society of Agronomy, 20: 309-355.

Kjeldsen, P., 1993. Groundwater pollution source characterization of an old landfill. Journal of Hydrology, 142: 349-371.

Korom, S.F., 1992. Natural denitrification in the saturated zone: A review. Water Resour. Res., 28(6): 1657-1668.

Kreitler, C.W., and Jones, D.C., 1975. Natural soil nitrate: The cause of the nitrate contamination of ground water in Runnels County, Texas. Ground Water, 13(1): 53-61.

Krishnamoorthy, C. and Overstreet, R., 1949. Theory of ion exchange relationships. Soil Science, 68: 307-315.

Kroes, J., C.L. Barth and R.B. Dodd. 1987. "Sludge sampler for waste lagoons." ASAE, 3(2): 258-260.

Laak, R., 1970. "Influence of domestic wastewater pre-treatment on soil clogging." Journal Water Pollution Control Federation. 42: P. 1495 - 1500, August, 1970.

Langmuir, D., 1997. Aqueous Environmental Geochemistry. Prentice Hall, Upper Saddle River, New Jersey, USA.

Lo, K.V., 1977. "A study of the infiltration characteristics of dairy waste storage lagoons." CSAE Paper No. 77-208, CSAE Annual Meeting August, 1977.

Lorimor, J.C., K. Kohl and G. Wells, 1997. "Swine liquid manure nutrient concentrations field study results." ASAE Paper No. 972043, ASAE Annual International Meeting August, 1997.

Mansell, R.S., Bloom, S.A., Selim, H.M., and Rhue, R.D., 1988. Simulated transport of multiple cations in soil using variable selectivity coefficients. Science Society of America Journal, v 52, n 6, Nov-Dec, 1988; 1533-1540

Maulé, C. P. and T.A. Fonstad. 2000. Hydraulic Conductivity Reduction Due to Ponded Hog Manure. Canadian Agricultural Engineering. 42 (4): 157-163.

McBride, M.B., 1994. Environmental Chemistry of Soils. Oxford University Press, New York, New York, USA. 406pp.

McKnight, K., 2003. Regional Specialist, Saskatchewan Agriculture, Food and Rural Revitalization, (SAFRR); Inspection and Regulatory Management Branch, Government of Saskatchewan.

Meek, B. D., and L. B. Grass. 1975. "Redox potential in irrigated desert soils as an indicator of aeration status." Soil Science Society of America Proceedings: 39(5): 870-875.

MidWest Plan Service (MWPS), 2000. Manure Characteristics; Manure Management Systems Series. MidWest Plan Service, Iowa State University, Ames, Iowa. 22pp.

Miller, D.C., J.B. Robinson and R.W. Gillham, 1985. "Self-Sealing of Earthen Liquid Manure Storage Ponds. I. A Case Study." J. Environ. Qual. 14(4):533-538.

Miller, M. H., Robinson, J. B. and Gallagher, D. W., 1976. "Accumulation of nutrients in soil beneath hog manure lagoons." Journal of Environmental Quality 5(3): 279-282.

Moffitt, D. C., Rickman, J., McElroy, C., D.Hendriks and Logan, H., 1993. Do waste treatment lagoons leak? ASAE International Winter Meeting, ASAE. P:Paper No. 934526

Nicholson, R.V., Cherry, J.A. and Reardon, E.J., 1983. Migration of Contaminants in Groundwater at a Landfill: A Case Study, 6. Hydrogeochemistry. Journal of Hydrology, 63: 131-176.

Parkhurst, D.L. and Appelo, C.A.J., 1999. User's Guide To PHREEQC (Version 2)- A Computer Program for Speciation, Batch-Reaction, One-Dimensional Transport, and Inverse Geochemical Calculations. Water-Resources Investigations Report 99-4259. U.S. Department of the Interior, U.S. Geologic Survey, 312pp.

Patrick, W.H. and R.E. Henderson. 1981. "Reduction and oxidation cycles of manganese and iron in flooded soil and in water solution." Soil Sci. Soc. Am. J., 45:855-859.

Paul, E.A. and Clark, F.E., 1996. Soil Microbiology and Biochemistry, 2nd Ed. Academic Press, San Diego, California, USA.

Pohlmann, Karl F., Icopini, Gary A., McAuthur, Richard D., and Rosal, Charlita G., 1994. Evaluation of Sampling and Field-Filtration Methods for the Analysis of Trace Metals in Ground Water. EPA/600/R-94/119. Environmental Monitoring Systems Laboratory, U.S. EPA, Las Vegas, Nevada.

Puls, Robert W. and Barcelona, Michael J. 1989. Ground Water Sampling for Metals Analyses. EPA Superfund Groundwater Issue. EPA/540/4-89/001.

Reardon, E.J., Dance, J.T. and Lolcama, J.L., 1983. Field Determination of Cation Exchange Properties for Calcareous Sand. Ground Water, Vol. 21, No. 4: 421-428.

Richards, J.G., 1998. Minicosm scale investigations into natural biogeochemical processes in a sandy vadose zone. Masters Thesis, Department of Geological Sciences, University of Saskatchewan.

Rickman, Ron W., J. Letey, G. M. Aubertin, and L. H. Stolzy. 1968. "Platinum microelectrode poisoning factors." Soil Science of America Proceedings Vol. 32.

Rieck- Hinz, A.M., G.A. Miller and J.W. Schafer. 1996. "Nutrient content of dairy manure from three handling systems." J. Prod. Agric. 9(1): 82-85.

Ritter, W. F., Walpole, E. W. and Eastburn, R. P., 1980. An anaerobic lagoon for swine manure and its effect on the groundwater quality in sandy-loam soils. 4th International Symposium on Livestock Waste, ASAE. P:244-246

Robins, Gary A. and Martins-Hayden, James M. 1991. Mass balance evaluation of monitoring well purging Part 1. Thoeretical models and implications for representative sampling. Journal of Contaminant Hydrology, Vol. 8, No. 3-4, December 1991. P203-224.

Rowe, R.K., Booker, J.R. and Fraser, M.J., 1998. POLLUTEv6. Professional Version 6.3.5. Distributed by GAEA Environmental Engineering Ltd.

Rowsell, J.G., M.H. Miller, and P.H. Groenbelt, 1985. "Self-Sealing of Earthen Liquid Manure Ponds. II. Rate and Mechanisms of Sealing." J. Environ. Qual. 14(4):539-543.

Rubin, J. and James, R.V., 1973. Dispersion-Affected Transport of Reacting Solutes in Saturated Porous Media: Method Applied to Equilibrium-Controlled Exchange in Unidirectional Steady Water Flow. Water Resources Research, Vol. 9, No. 5: 1332-1356.

Saskatchewan Agriculture Food and Rural Revitalization (SAFRR), 1997. Manual for: Developing a Manure and Dead Animal Management Plan. Saskatchewan Agriculture Food and Rural Revitalization, Agricultural Operations Section, Livestock and Veterinary Operations, Government of Saskatchewan, Canada, October 1997, 11pp.

Shanklin, D.E., Sidle, W.C. and Ferguson, M.E. 1995. Micro-purge low-flow sampling of uranium-contaminated groundwater at the Fernald environmental management project. Ground Water Monitoring & Remediation, Vol. 15, No. 3, Summer 1995. Ground Water Publishing, Dublin, OH, USA. p 168- 176.

Skackelford, C.D. and Daniel, D.E., 1991. Diffusion in Saturated Soil. II: Results for Compacted Clay. Journal of Geotechnical Engineering, Vol. 117, No. 3: 485-506.

Sposito, G., 1979. Derivation of the Langmuir equation for ion exchange reactions in soils. Journal of the Soil Science Society of America, v. 43 (1); 197-198.

Stumm, W. and Morgan, J.J., 1981. Aquatic Chemistry: An introduction emphasizing chemical equilibria in natural waters. John Wiley and Sons, New York, New York, USA.

The Pollution (By Livestock) Control Act (1985), Saskatchewan Agriculture Food and Rural Revitalization, Government of Saskatchewan

Thornton, S.F., Lerner, D.N. and Tellam, J.H., 2001. Attenuation of landfill leachate by clay liner materials in laboratory columns: 2. Behaviour of inorganic contaminants. Waste Management and Research, 19: 70-88.

Thornton, S.T., Tellam, J.H. and Lerner, D.N., 2000. Attenuation of landfill leachate by UK Triassic sandstone aquifer materials; 1. Fate of inorganic pollutants in laboratory columns. Journal of Contaminant Hydrology, 43: 327-354.

Trudell, M.R., Gillham, R.W., and Cherry, J.A., 1986. An in-situ study of the occurrence and rate of denitrification in a shallow unconfined sand aquifer. J. Hydrol., 83: 251-268.

U.S Environmental Protection Agency (EPA). 1991. Handbook: Ground Water Volume II: Methodology. EPA/625/6-90/016b. Center for Environmental Research and Information.

U.S. Environmental Protection Agency (EPA). 1991. Compendium of ERT Groundwater Sampling Procedures. EPA/540/P-91/007. Environmental Response Team, Emergency Response Division. U.S. EPA. Office of Emergency and Remedial Response. Washington, D.C.

U.S. Environmental Protection Agency (EPA). 1995. Ground Water Sampling - A Workshop Summary. Dallas, Texas. November 30 - December 2, 1993. EPA/600/R-94/205. Robert S. Kerr Environmental Research Laboratory, U.S. EPA, Ada, Oklahoma.

UMA Engineering Ltd., 1995. Final Report: Preliminary Investigation of Earthen Manure Storages in Saskatchewan. Submitted to SPI Marketing for the Canada-Saskatchewan Green Plan Agreement on Agriulture.

Valocchi, A.J., Roberts, P.V., Parks, G.A. and Street, R.L., 1981. Simulation of the Transport of Ion-Exchanging Solutes Using Laboratory-Determined Chemical Parameter Values. Ground Water, Vol. 19, No. 6: 600-607.

Valocchi, A.J., Street, R.L. and Roberts, P.V., 1981. Transport of Ion-Exchanging Solutes in Groundwater: Chromatographic Theory and Field Simulation. Water Resources Research, Vol. 17, No. 5: 1517-1527.

Van Ommen, H.C., 1985. The "Mixing-Cell" Concept Applied to Transport of Non-Reactive and Reactive Components in Soils and Groundwater. Journal of Hydrology, 78: 201-213.

Vanselow, F.P., 1932. Equilibria of the base exchange reactions of bentonites, permutites, soil colloids and zeolites. Soil Science, 33: 95-113.

Westerman, P. W., Huffman, R. L. and Feng, J. S., 1993. "Swine lagoon seepage in sandy soil." Transactions of the ASAE 38(6): 1749-1760.

Westerman, P.W., R.L. Huffman and J.S. Feng, 1993. "Swine-Lagoon Seepage in Sandy Soil". ASAE Paper No. 932531. 1993 International Winter Meeting.

Whistler, F. D., J. C. Lance and R. S. Linebarger. 1974. "Redox potentials in soil columns intermittently flooded with sewage water." Journal of Environmental Quality, 3(1): 68-74.

White, G.N. and Zelazny, L.W., 1988. Analysis and implications of the edge structure of dioctahedral phyllosilicates. *Clays and Clay Minerals*, v 36, n 2, Apr, 1988, p 141-146

Wiklander, L., 1964. Cation and anion exchange phenomena. In Chemistry of the Soil, F.E. Bear (Ed.). Van Nostrand Reinhold Company, New York, New York. USA. P: 163-203

Appendix A

Water and Soil Analysis – Operating Procedure Summary

A - Water and Soil Analysis – Operating Procedure Summary

WATER ANALYSIS

Nitrate and Nitrite

Nitrate as nitrogen in water was found by colormetric determination with a continuous flow analyzer. The nitrate was reduced to nitrite with hydrazine sulphate. The nitrite was determined by diazotizing with sulphanilamide and coupling with N-(1-naphthyl)-ethylenediamine dihydrochloride to form a highly coloured azo dye which is measured colorimetrically at 529 nm in a fully automated system. Nitrite was analyzed without the reducing reagents and is determined using the above colorimetric technique. The reportable detection limit was 0.01 mg/L as N. Samples with concentrations above 2 mg/L must be diluted.

Chloride

Chloride was analyzed using the mercuric thiocyanate colorimetric method on the Cobas Fara II centrifugal analyzer. The thiocyanate ion (SCN-) was displaced from mercuric thiocyanate by chloride. The liberated thiocyanate ion reacted with ferric ion to form the coloured complex ferric thiocyanate. The concentration was measured by measuring the absorbance at 480 nm. The detection limit was 1 mg/L. Samples with concentrations greater than 500 mg/L must be diluted.

Sulfide

A silver/sulfide ion selective electrode was used to measure the potential of standard and sample solutions. A calibration curve was prepared and the sulfide concentration of the sample is read from the curve. The detection limit was 0.01 mg/L. Samples with concentrations greater than 100 mg/L must be diluted.

Ammonia

Ammonia was analyzed using a water automated colorimetric method. Ammonia reacts with hypochlorite and phenol in the presence of a catalyst to form idophenol, which gives the sample solution a blue color. The Cobas Fara II automated centrifugal analyzer measured the absorbance of light in the solution at 630 nm which was proportional to the concentration. The detection limit was 0.01 mg/L. Samples with concentrations greater than 2.0 mg/L must be diluted.

Organic Carbon

Organic carbon in water was analyzed using the Dohrmann Phoenix 8000 carbon analyzer. Aqueous samples were treated with phosphoric acid to release inorganic carbon as CO_2. The remaining organic carbon in the sample was reacted with sodium persulfate and UV light to release the organic carbon as CO_2. The CO_2 was measured with a non-dispersive infrared detector. The detection limit was 0.2 mg/L for both Total Organic Carbon and Dissolved Organic Carbon. Samples with concentrations greater than 20 mg/L must be diluted.

Calcium, Magnesium, Potassium, Sodium, and Sulfate

Several elements in aqueous solution were determined using Inductively Coupled Plasma Atomic Emission Spectroscopy (ICP-AES) using the TJA-IRIS Advantage Analyzer. The plasma was a stream of argon gas ionized by an applied radio frequency field. Sample aerosols were injected into the plasma which subjected the atoms to temperatures of 6000 to 10,000 K. The high temperature ionized a high percentage of atoms in the aerosol and reduced chemical interferences. The emission spectra of the ionized atoms were optically measured in a computer controlled spectrometer. The light emitted from the plasma was focused onto the entrance slit of an Echelle Optical System. A prism and diffraction grating disperse the light which was focused on a Charge Injection Device (CID) detector. The detector monitored all configured wavelengths in a computer-controlled environment.

Table A1: Upper detection limits of various cations.

Ion	Upper Limit (mg/L)
Calcium	50
Magnesium	100
Potassium	20
Sodium	15
Sulfate	300

Metals

Several elements in aqueous solution may be determined using Inductively Coupled Plasma Atomic Emission Spectroscopy (ICP-AES). The plasma was a stream of argon gas that was ionized by an applied radio frequency field. Sample aerosols were injected into the plasma which subjected the atoms to temperatures of 6000 to 10,000 K. The high temperature ionized a high percentage of atoms in the aerosol and reduced chemical interferences. The ionized atoms produced emission spectra which were optically measured in a computer controlled system.

Table A2: Upper detection limits of various metals.

Metal	Upper Limit (mg/L)	Metal	Upper Limit (mg/L)
Al	70	Mo	50
Ba	30	Ni	60
Be	10	P	50
B	100	Si	100
Cd	20	Ag	50
Cr	100	Sr	10
Co	100	Ti	30
Cu	60	V	100
Fe	50	Zn	30
Pb	35	Zr	70
Mn	30		

Table A3: Summary of detection limits (units are mg/L)

Inorganic Chemistry	Lower Limit	Upper Limit
Ca	0.1	50
Cl	1	500
Mg	0.1	100
K	0.1	20
Na	0.1	15
SO4	0.2	300
sulfide	0.01	100
Tot. Hardness	1	
Ammonia-N	0.01	2
Nitrite-N	0.01	2
Nitrite-N+Nitrate-N	0.01	2
Total organic carbon	0.2	20
Al	0.005	70
Ba	0.001	30
Be	0.001	10
B	0.002	100
Cd	0.001	20
Cr	0.001	100
Co	0.001	100
Cu	0.001	60
Fe	0.001	50
Pb	0.002	35
Mn	0.001	30
Mo	0.001	50
Ni	0.001	60
P	0.01	50
Si	0.01	100
Ag	0.001	50
Sr	0.001	10
Ti	0.001	30
V	0.001	100
Zn	0.005	30
Zr	0.001	70

Samples were diluted to concentrations below the upper detection limits prior to analysis. Detection limits and sample concentrations were multiplied by the dilution factor and reported as the sample concentration. In general, nitrogen species were the limiting factor for dilutions as the lower and upper detection limits are 0.01 and 2 mg/L.

Example:

Sample diluted by 100 yields:

Ion	Analysis result (mg/L)	Dilution
Ca	9.6	100
Mg	4.2	100
Na	10.4	100
K	10.2	100
NH4-N	1.27	1000
SO4	60	100
Cl	230	10

Reported values:

Ion	Concentration (mg/L)	Detection Limits (mg/L)
Ca	960	+/- 10
Mg	420	+/- 10
Na	1040	+/- 10
K	1020	+/- 10
NH4-N	1270	+/- 10
SO4	6000	+/- 20
Cl	2300	+/- 10

SOIL ANALYSIS

Ammonia

Ammonia was analyzed using the Technicon II Automated Analyzer and Technicon Industrial Method No. 325-7HW. The determination of ammonia was based on a colorimetric method in which an emerald-green color is formed by the reaction of ammonia, sodium salicylate, sodium nitroprusside and sodium hypochorite (chlorine source) in a buffered alkaline medium at a pH of 12.8-13.0. The ammonia-salicylate complex was read at 660 nm. The detection range was 0-2 mg/L.

Sulfate

Sulfate was extracted from the soil using the saturated paste extraction method. An automated turbidimetric method was used to analyze the soil extract. The apparatus used was the Technicon Autoanalyzer Colorimeter. The dection range was 0-15 mg/L sulfur.

Chloride

Chloride was extracted from the soil using the saturated paste extraction method. Chloride content of the soil extracts were determined using an Orion Ionanalyzer Chloride Ion Activity Electrode Model 94-17, in conjunction with an Orion Single Junction Reference Electrode, Model 90-01 and a Fisher Accumet pH Meter. The readings in millivolts were made by immersing the electrodes in the solution containing chloride. The detection range was from 0-80 mg/L.

Sodium, Potassium, Calcium, and Magnesium

These cations were analyzed using flame atomic absorption spectrometry (Perkin-Elmer 5100 Spectrometer). The technique was based on the principle that atoms of a particular element absorb light at a specific wavelength. The detection limit for sodium, potassium, calcium, and magnesium were 0.2 μg/L, 2 μg/L, 1 μg/L, and 0.1 μg/L, respectively.

Appendix B

Statistical significance of correlation coefficients for the column and batch studies

Comparison of modeled and experimental data was completed using the following correlation equation:

$$r = \frac{\Sigma(XY)}{\sqrt{\Sigma(X^2)\Sigma(Y^2)}}$$

where r = correlation coefficient

X = first variable to be compared

Y = second variable to be compared

Significance of the correlation was taken from Table A-11 in "Basic Statistical Methods for Engineers and Scientists 2nd Ed." By J.B. Kennedy and A.M. Neville and published by Harper and Row Publishers Inc., 1976.

Column and batch test results have common quantities of samples therefore statistical significance level will be the same for data for each column or bath test as follows:

Test	No. of samples	v	r at 1% level	r^2 at 1% level	r at 5% level	r^2 at 5% level
Column No. 1	21	19	0.549	0.30	0.433	0.19
Col No. 1 (ammonium)	6	4	0.917	0.84	0.811	0.66
Column No. 2	20	18	0.561	0.31	0.444	0.20
Batch tests	10	8	0.765	0.59	0.623	0.39